BROUARD CONSULTING

101 rue du Temple
75003 Paris – France
Tél. : +33 / (0)6 09 04 37 33
http://www.Brouard–Consulting.com
Contact@Brouard–Consulting.com

Over-pressured caverns and leakage mechanisms

—

Phase 2: Cavern scale

4 November 2019

TABLE OF CONTENTS

INTRODUCTION

Thousands of salt caverns have been leached out worldwide. Their volumes range from 10,000 m^3 to several millions m^3. Many of the caverns are used to store gas or oil. These caverns eventually will be abandoned. At that time, they will be filled with brine, and a cement plug will be set in the borehole, isolating a large "bubble" of brine — the long-term behaviour of which is the subject of this Report. The Solution Mining Research Institute (SMRI), which comprises most companies, consultants and academics interested in salt caverns, has set this topic at the centre of its research program for many years and supported several of the tests described in this paper.

There has been concern that, in a sealed and abandoned cavern, cavern brine pressure increases to geostatic pressure (and above), leading to fracture creation at the cavern roof, brine seepage to overlying strata, possible pollution of potable water and additional subsidence. One example of this is known at Bryan Mound (Louisiana) and another is suspected at Barradeel (the Netherlands).

On 28 May 2018, the Dutch Staatstoezicht op de Mijnen (State Supervision of Mines, SodM) issued a Request for proposal whose objective was "*to be able to predict the occurrence of cavern instability and uncontrolled subsidence (including sinkholes) and to define and supervise cavern risk management protocols ensuring that cavern instability and uncontrolled subsidence risks stay at acceptable levels during operation and after abandonment*."

In response a consortium, led by Brouard Consulting, proposed to perform a study divided in three parts:

- Microscale
- Cavern scale
- Salt-Dome scale

More specifically, the Cavern scale report was defined as follows:

"*This part will be performed mostly by B. Brouard and P. Berest, based on their experience attested by a large number of publications. The final synthesis will take into account the results obtained in the parts dedicated to microscale and dome scale.*

Compile, discuss and interpret the following data:

1. *How and why maximum admissible pressures are selected in brine production and hydrocarbon storage caverns*

2. *Loss of cavern integrity: what can be learned from accidents*

3. *Frac tests in salt formations. Why, in many cases, the vertical stress is the less compressive stress*

4. *Lessons learned from in situ tests at high pressure (Etzel, Etrez, Vauvert etc.)*

5. *Review of the various models proposed in the literature to describe the hydromechanical behavior of highly pressurized caverns*

6. *A tentative synthesis: factors of influence for the behavior of highly pressurized caverns"*

The Cavern scale Report can be found below.

1. STRESSES IN A SALT FORMATION

The objective of this study is to understand the conditions present such that a fracture can be created in a brine-production cavern after abandonment, when cavern pressure is close to geostatic pressure. Empirical lessons can be drawn from the experience gained when operating brine-production and hydrocarbon-storage caverns, as the issue of the maximum admissible fluid pressure is crucial in this context: brine or hydrocarbon caverns must remain tight; for this reason, for more than 50 years, industry has selected maximum admissible pressures to avoid any risk of fluid escape.

In brine production caverns or liquid/liquefied storage caverns (except in some cases that will be discussed later), cavern pressure results, on one hand, from the weight of the saturated brine column between ground level and cavern bottom and, on the other hand, from head losses when fluids are circulated in the well. Brine pressure, in most cases, is much smaller than lithostatic (or geostatic) pressure. In fact, in such caverns, pressure is high only during tightness tests, which last a few days, or when it is considered convenient to let pressure increase in the cavern during standstill periods (as is often the case in strategic oil storages).

The case of gas storage caverns is different. The amount of natural gas that can be stored in a salt cavern depends essentially on the values of the maximum and minimum pressures of the gas. More gas can be stored when the maximum admissible pressure is higher. For this reason, the issue of maximal fluid pressure is especially important in gas storage caverns, and abundant existing literature is dedicated mostly to this case.

1.1 Stresses in a salt formation

1.1.1 Virgin state of stress

Fluid pressure in a cavern should be compared to the in-situ stresses in the formation at cavern depth. A fundamental difference must be made between the "*virgin*" or "*primary*" state of stress (which existed before the cavern was created) and the "*secondary*" state of stresses (which results from cavern creation and operation). These two notions are especially different in the case of visco-plastic rocks, such as halite and other evaporites, as their behaviour is not reversible (over time, very different stress distributions in the rock mass can be associated to the *same* cavern pressure).

From Continuum Mechanics, it is known that at each point of a continuum (e.g. a rock mass), the state of stress can be represented by a tensor (a symmetric 3×3 matrix), or σ. There exist three types of orthogonal directions, called the "principal" (or "main") directions. When these directions are selected, the stress tensor is represented by a matrix whose non-diagonal elements are zero. The three diagonal elements are the "*principal*" stresses. When the vertical stress is principal, the two other principal stresses are horizontal. It is usual to note σ_v, the vertical stress, σ_H, the most compressive horizontal stress, and σ_h, the least compressive horizontal stress, respectively - i.e. $\sigma_H < \sigma_h < 0$ (compressive stresses are negative). In addition, the stress tensor must satisfy the

"*equilibrium*" condition, $div\ \sigma + \rho g = 0$, where ρ is the density of the rock, and g is the gravity acceleration. These properties are true whatever the body considered (gas, liquid, solid).

These conditions alone do not allow the stress tensor to be computed. In addition, a constitutive law for the rock mass, the history of the mechanical and thermal loadings (at geological scale) and boundary conditions must be specified. For a rock mass, this is the difficult part of the problem, as neither the constitutive law, nor the history and boundary conditions are perfectly known. In many cases, assumptions must be made.

1.1.2 The isotropic assumption

Most authors consider that rock salt behaves as a fluid when long periods of time (dozens of years or centuries, depending on the intensity of the deviatoric stress) are considered. In a fluid at rest, the stress distribution is simple: the three principal stresses are equal (the "*isotropic*" assumption): for example, "*In depth below 500 m isostatic stress condition can be assumed in salt rock formations due to the creeping behavior of salt rock*" (Klafki et al., 1998, p. 276). When the state of stress is isotropic, $\sigma_v = \sigma_H = \sigma_h < 0$, and their common value is $-P$, where P can be computed using the equilibrium equation: $dP/dz = \rho(P,T)g$, where z is oriented downward. When density is approximately constant, $P(z) = \overline{\rho} gz$, where $\overline{\rho}$ is the average density of the overburden. A more precise value is reached when integrating the equilibrium equation with respect to depth (see Section 1.2.1), where $\overline{\rho} g$ (in psi/ft or bar/m) is the geostatic gradient, or volumetric weight, having a typical value of 0.022-0.023 MPa/m, as, in many cases, rock density is $\rho = 2200 - 2300$ kg/m^3 and $g = 9.81$ m/s^2.

1.1.3 Actual state of stress in a salt formation

This simple assumption ($\sigma_v = \sigma_H = \sigma_h$), however, does not seem to be true in several cases. This issue is addressed in more details in the "Dome scale" report where it is proved that, for various reasons, a deviatoric stress as large as 1 MPa can exist in domal salt. This is a difficult question because, as will be seen, *in situ* stresses are difficult to measure. It is noticeable that, in the salt-mining literature, some authors believe that the state of stress is less likely to be isotropic in domal salt (because domes are the seat of long-term active flow, and equilibrium has not had enough time to be reached). Other authors believe that the opposite is true: the state of stress in bedded salt is more complex, as salt beds often are composed of many layers, among which are competent non-salt layers, which do not behave as a fluid.

1.1.4 A frequent assumption

In the following, it is accepted, at most authors do, that the vertical stress is principal and that it equals the weight of the overburden, $\sigma_v(z) = -\overline{\rho} gz$ ($z =$ depth, and $\overline{\rho} =$ average rock density between $z = 0$ and z). This assumption is reasonable, though it is not proven.

1.2 *In situ* stress measurement

1.2.1 Density-based assessment of in situ stresses

The simplest way to assess the vertical *in situ* stress ($\sigma_v < 0$) consists of assuming that this stress is principal all the way from ground level to the considered depth. Most often, rock density, $\rho = \rho(z)$, is well known through density logs performed when drilling a borehole. Under this assumption, the vertical stress at depth z is provided by an integration:

$$\sigma_v^{dens}(z) = -\int_0^z \rho(\zeta)\, g d\zeta \tag{1}$$

Note that this method says nothing about the two horizontal principal stresses, except when an isotropic state of stress is assumed: $\sigma_v(z) = \sigma_h(z) = \sigma_H(z)$.

1.2.2 Frac tests

A hydraulic (or pneumatic) frac test consists of isolating an interval in the open hole of the well - for instance, by using a straddle packer. The two ends of the packer are sealed to the rock formation. There is a water (or brine, or gas) outlet in the middle of the packer that allows fluid pressure in the packer to be applied to the salt wall of the isolated interval. In a salt formation, hydraulic and pneumatic tests are performed, in which the injected fluid is saturated brine or nitrogen, respectively. Fluid pressure in the packer is increased swiftly until the fracture breakdown pressure, P_c (see Figure 1), is reached; this is observed when the pressure-vs-injected fluid volume curve reaches a maximum followed by an abrupt pressure drop. The injection rate then is controlled in order that a plateau is reached and injected fluid pressure is constant (fracture propagation pressure). After some time, injection is stopped, and the flowrate vanishes (Figure 1). Several such “frac cycles” are performed. The re-frac pressure, P_r, is derived from the pressure-injected volume curve during re-frac. The shut-in pressure (P_{si}) is derived from the shut-in phase, as explained by Rummel (1996), during the last re-frac cycle (see Figure 1). It generally is assumed that hydraulic fractures propagate in the direction of least resistance (planes of weakness) or perpendicular to the least compressive stress. In the absence of weakness, the shut-in pressure is deemed to equal the least compressive stress at test depth in the rock mass. By definition, $\sigma_H \le \sigma_h < 0$; hence, $\sigma_V \le \sigma_H \le -P_{si} = \sigma_h < 0$ or $\sigma_h \le \sigma_H = -P_{si} < 0$. The second option (the least compressive stress is vertical) is considered generally as being less credible, and

$$\sigma_V \le \sigma_H \le -P_{si} = \sigma_h \tag{2}$$

(compressive stresses are negative).

In some cases, determining the fracture propagation pressure and the shut-in pressure is not straightforward (Guo et al., 1993, suggest eight different methods). The facture breakdown pressure equals the minimum principal stress plus the so-called “tensile strength”, $T > 0$, which is somewhat

of a misnomer as, in fact, it is related to the toughness of the rock mass, $P_c = |\sigma_h| + T$. In the case of rock salt, the tensile strength often is considered to equal $T = 1 - 3$ MPa.

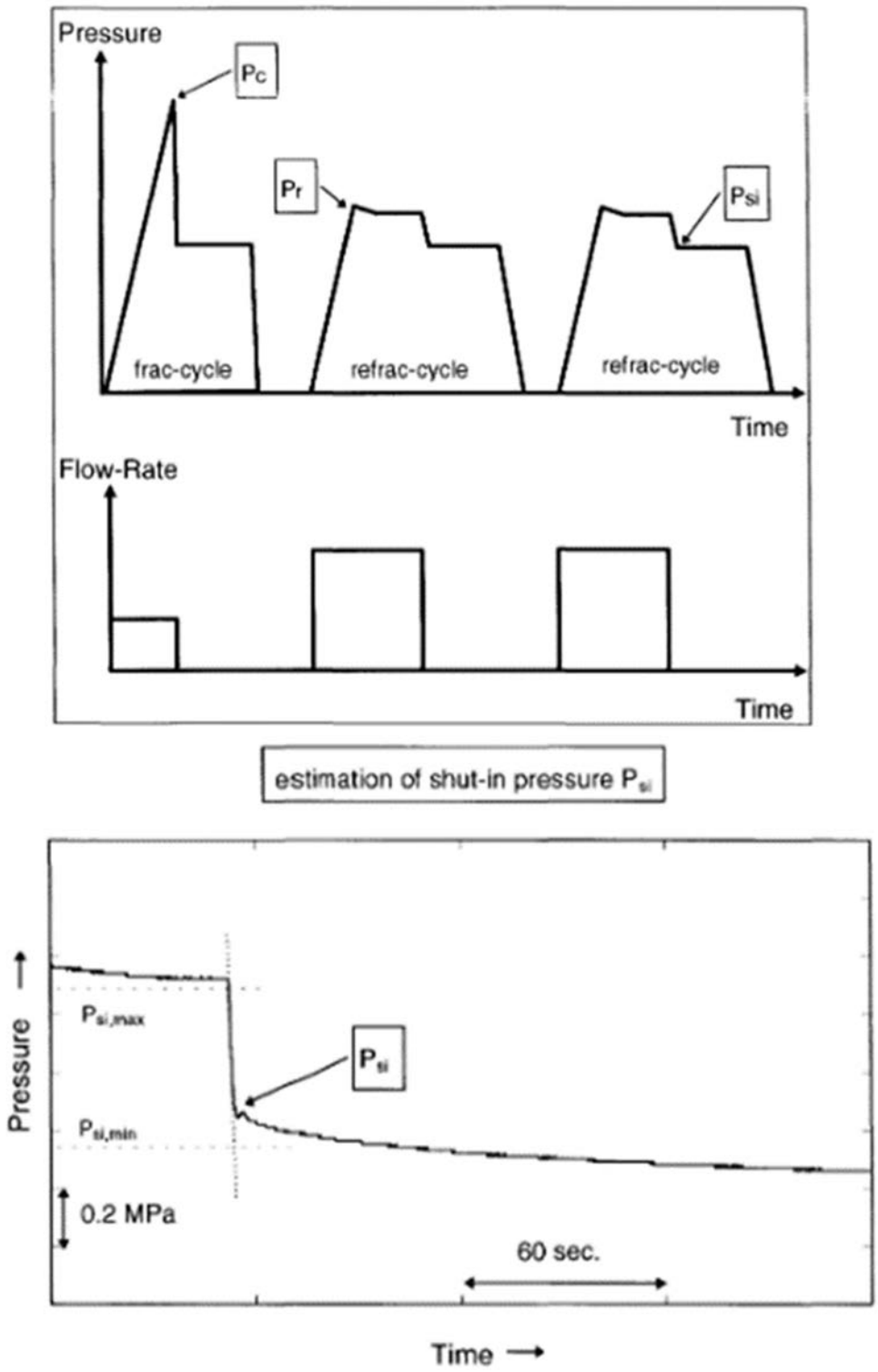

Figure 1 - Schematic frac-test procedure and determination of shut-in pressure (Rummel, 1996).

Note that the injection rate before the fracture breakdown pressure must be much larger than the infiltration rate in the rock mass to allow a rapid pressure increase – a condition that is not often met when a full-size cavern is considered. In addition, the notion of a "breakdown pressure" (the point

in the pressure-vs-time curve after which an abrupt pressure drop is observed) does not exist in a full-size cavern whose compressibility is larger than a borehole compressibility by three or four orders of magnitude (the amount of fluid seeping into the fracture is exceedingly small when compared to the volume of a full-size cavern).

1.2.3 Examples of frac tests in salt formations

Several examples are considered in the following.

Rummel et al. (1996) performed an extensive hydraulic fracturing program in Krummhörn K6, a 1815-m deep, 8-½" borehole drilled out in the Groothusen salt dome (Zechstein 2 salt). A double straddle packer was used, and 11 hydrofrac tests were carried out successively between 1300- and 1800-m depth (approximately). Each test included several re-frac cycles for reliable determination of the shut-in pressure. Rummel considers that "well documented" data were obtained. The shut-in pressure profile was $P_{si}\ \left[\text{MPa}\right] = 29.38 + 0.0194z\ \left[\text{m}\right]$, and the shut-in pressure gradient was 0.0221 MPa/m between 1300 and 1720 m (TVD), "*in good agreement with the vertical stress profile derived from various geophysical logs for the overburden density*" [p.1].

Schmidt (1993) describes pneumatic frac tests performed in the stratified salt deposits at Xanten and Epe (Germany). At Xanten, tests were performed in the 900- to 970-m deep Upper Werra salt (coarsely grained with intercalations of clay and anhydrite) and the 1029- to 1146-m deep Lower Werra salt (finely grained and pure). Fracture breakdown pressure in the Upper Werra salt (three tests performed) was reached at a 0.0255 ± 0.0001 MPa/m gradient; the shut-in pressure gradient was 0.0234 ± 0.0001 MPa/m. In the Lower Werra salt (four tests performed), the fracture breakdown gradient was 0.0226 ± 0.0002 MPa/m, and the shut-in pressure gradient was 0.02165 ± 0.00005 MPa/m (Schmidt explains the difference by the lower density of the potash-rich "Middle" Werra). At Epe, figures in the Upper Werra salt (2 tests) and in the Lower Werra salt (1 test) are almost identical, 0.025 ± 0.01 MPa/m (breakdown gradient) and 0.0242 ± 0.004 MPa/m (shut-in gradient), respectively. Here, again, the (relatively small) differences between tests results is related to different density distributions. Schmidt also mentions that, when designing a salt cavern, a difference must be made between the primary state of stress (before cavern creation) and the secondary state of stress (after cavern creation).

Staudtmeister and Schmidt (2000) performed tests in the Rüdersdorf K101 well in Germany, in which they discuss different methods used: four pneumatic tests and two hydraulic tests in the interval selected for future cavern emplacement, from 1280 m to 1600 m, and borehole gravimetry measurements (BHGM) down to 1280 m (location of the cavern roof). BHGMs consist of measuring the vertical gravity gradient at a given depth, which is related to the average density of the rock surrounding the well. BHGM densities are influenced by rock density changes far from the well, and a geological model of the salt formation must be built. Interestingly, Staudtmeister and Schmidt note that, based on the experience at Etzel, Krumhörn, Reckrod and Bemen Lesum, shut-in pressures during hydraulic measurements "*systematically lie 5% to 10% above the vertical primary stress component*" [p.334]. Pneumatic tests provided lower shut-in pressures. Conversely, uncertainties

affect density-based estimates of the vertical pressure, and upper and lower values were selected. Conclusions can be summarized as follows:

$$\min \sigma_v^{dens} < \max \sigma_v^{dens} \simeq P_{si}^{gas} \simeq 0.9 P_{si}^{liq} \tag{3}$$

Schreiner et al. (2004) consider that ''*under domal salt conditions … the three principal stresses are not equal … In a first assumption, the resulting pressure gradients should be significantly lower than in a bedded salt formation; i.e., in the order of 0.18 bar/m*''. However, "*testing of various salt dome locations of NE Germany … documented that the measured minimal stress values are significantly higher than the estimated lithostatic pressure*". Pneumatic tests were performed at depths 920 m to 1380 m; shut-in pressure was 1-1.5 MPa higher than the estimated lithostatic stress,

$$P_{si}^{gas} = \sigma_v^{dens} + 1 - 1.5 \text{ MPa} \tag{4}$$

The authors performed computations at geological time scales (> 1 Ma), taking into account salt rise and glaciation, and proved that the state of stress in the salt dome was almost isotropic, but higher than the lithostatic stress by 1-1.3 MPa.

According to Horvarth and Wille (2009), the weight of the overburden can be measured through "*density determination from rock samples, analysis of litho-density logs, hydraulic fracture tests and borehole gravity measurements … The pressure determined by fracture tests (the so-called "shut-in pressure*") *is thought to represent the [least-compressive] principal stress. However, fracture tests have been observed to provide formation pressure values about 5% higher [than other methods]*" [p. 84]. Also, as Klafki et al. (1998) note: "*in situ measured primary stresses are higher than calculated from rock densities*" [p. 276].

1.2.4 The role of secondary stress

The relations above, between the shut-in pressure and the least compressive stress ($P_{si} = \sigma_h$) is accepted by most authors when rock behaviour reasonably can be considered as elastic (i.e. reversible): when fluid pressure in the well is equal to the overburden pressure, the state of stress in the rock mass equals what it was ("virgin state of stress") before the well was drilled. This is incorrect in the case of rock salt. Consider the following sequence: the well is drilled out rapidly; the pressure drop in the wellbore is $\Delta P = P_\infty - P_i;$ the initial state of stresses is elastic:

$$\begin{cases} \sigma_{rr}^{ss} = -P_\infty + \Delta P \left(\dfrac{a}{r} \right)^2 \\ \sigma_{\varphi\varphi}^{ss} = -P_\infty - \Delta P \left(\dfrac{a}{r} \right)^2 \\ \sigma_{zz}^{ss} = -P_\infty \end{cases} \tag{5}$$

The wellbore then is kept open for several months. The Norton-Hoff law is assumed; when steady-state is reached, stresses distribution is

$$\begin{cases} \sigma_{rr}^{ss} = -P_{\infty} + \Delta P \left(\dfrac{a}{r} \right)^{2/n} \\ \sigma_{\varphi\varphi}^{ss} = -P_{\infty} + \left(1 - \dfrac{2}{n} \right) \Delta P \left(\dfrac{a}{r} \right)^{2/n} \\ \sigma_{zz}^{ss} = -P_{\infty} + \left(1 - \dfrac{1}{n} \right) \Delta P \left(\dfrac{a}{r} \right)^{2/n} \end{cases} \tag{6}$$

At this point, a frac test is performed, and pressure is increased abruptly to the geostatic pressure. The stresses distribution then is

$$\begin{cases} \sigma_{rr} = -P_{\infty} + \Delta P \left(\dfrac{a}{r} \right)^{2/n} - \Delta P \left(\dfrac{a}{r} \right)^{2} \\ \sigma_{\varphi\varphi} = -P_{\infty} + \left(1 - \dfrac{2}{n} \right) \Delta P \left(\dfrac{a}{r} \right)^{2/n} + \Delta P \left(\dfrac{a}{r} \right)^{2} \\ \sigma_{zz} = -P_{\infty} + \left(1 - \dfrac{1}{n} \right) \Delta P \left(\dfrac{a}{r} \right)^{2/n} \end{cases} \tag{7}$$

It is clear that, at the cavern wall, the two tangential effective stresses, $\sigma_{\varphi\varphi}^{eff}(a) = \sigma_{\varphi\varphi}(a) + P_{\infty}$ and $\sigma_{zz}^{eff}(a) = \sigma_{zz}(a) + P_{\infty}$, are tensile. In particular, after the pressure increase, the vertical stress at the wall of the open hole is less compressive than its virgin value (see, for instance, Wang et al., 2015) and, in a salt formation, **shut-in pressure should be significantly smaller than geostatic pressure**. This idea was mentioned first by Wawersik and Stone (1989), and a comprehensive discussion can be found in Brouard et al. (2007a) and Djizanne et al. (2012), leading to the conclusion that

$$P_{si} = \sigma_h^{\sec} < \sigma_h \tag{8}$$

It must be observed, however, that though this conclusion is perfectly correct from a mathematical perspective, low breakdown pressures have never been observed during actual frac tests.

1.2.5 A tentative conclusion

Lessons drawn from frac tests are equivocal; they are not fully consistent with what can be inferred from the salt constitutive law. In such a context, it seems reasonable to adopt the Horvarth and Wille (2009) conclusion that "*density logs have proved … to supply data of sufficient quality*" (p. 88).

A discussion on virgin-stress determination based on microstructure is provided in the micro-scale report (MaP, 2019, pp. 24-25).

2. MAXIMUM OPERATING PRESSURES IN SALT CAVERNS

2.1 Safety margins

When a well is filled with saturated brine and opened at ground level, brine pressure in the well is $P_b(z) = \rho_b g z$, and the halmostatic gradient is $\rho_g g = 0.12$ bar/m. More generally, when fluid pressure at depth H is P, the gradient at depth H is P/H. The pressure gradient often is computed at casing-shoe depth.

In a salt cavern, maximum fluid pressure must be smaller than the least compressive stress in the rock mass which, as explained in Chapter 1, Section 1.2, is taken to be equal to the vertical stress, which is assessed through density logs (and/or frac tests). However, some safety margin must be left. Besides unavoidable uncertainties when assessing the density-based vertical stress (see Section 1.2), there are three reasons for this, as follow.:

1. At the vicinity of a cavern, the east compressive secondary stress can be significantly smaller than the least compressive virgin stress.
2. The least compressive stress is not always the vertical stress — even if they often are equal.
3. The cement behind the last steel casing often is weaker than the rock mass itself.

2.2 A weak point: The cement

2.2.1 The cement

The cement between the steel casing and the rock mass is an engineered material, and its tightness basically depends on the quality of the cementing job. The cemented annular space includes two interfaces: that between the cement and the casing steel; and that between the cement and the rock mass. These interfaces are possible weak points, especially in gas storage caverns, because the cement shrinks and expands alternatively when large pressure swings are applied to the cavern gas. Most often, the cemented part of the well is weaker than the rock formation itself.

2.2.2 Factors important for cement quality

Cement integrity results from the properties of the rock mass, the quality of the cementing job, the well architecture (i.e. the number and the length of the cemented casings), the nature of the stored products, and the pressure and pressure changes of the stored fluids. Tight and plastic rock formations, such as salt and clay, can have a very favourable effect in that they naturally creep and tend to tighten around the well, improving the bonds between the cement and the casing, and between the cement and the rock formation (Bérest and Brouard, 2003).

Since the origin of oil drilling, progress has been made in cementing workmanship. In Texas, for example, Nicot (2009) mentions the following: use of centralizers (1930); calliper surveys (1940);

tagging of the cement plug, introduction of improved cement additives adapted to temperature, pressure and chemical specific conditions (1940); and improvement of the quality of material used in well construction. Nicot also outlines the promulgation by the Texas Railroad Commission, promulgation of specific plugging instructions (1934, 1967) in the Drinking Water Act, publication of API national standards (starting in 1953), and increased scrutiny by the State (after 1983). Effective tools allow assessment of the quality of the cement (CBL/VDL, high-frequency measurements, etc.). However, appraising the quality of a cement job is not easy. Experience proves that cement quality can be scattered. For salt cavern wells, with casing diameters larger than in oil fields, Kelly and Fleninken (1999) proposed the notion of a Cement Evaluation Logging Program to minimize uncertainties.

Gaseous products raise more difficult problems than do liquid products. On one hand, they are less viscous, and the gas flow-rate is faster; on the other hand, gases are much less dense than liquids. When a leak appears, gas pressure remains almost constant along the leak path, and gas pressure is able to fracture rock formations at shallow depth, where geostatic pressure is low (Figure 2).

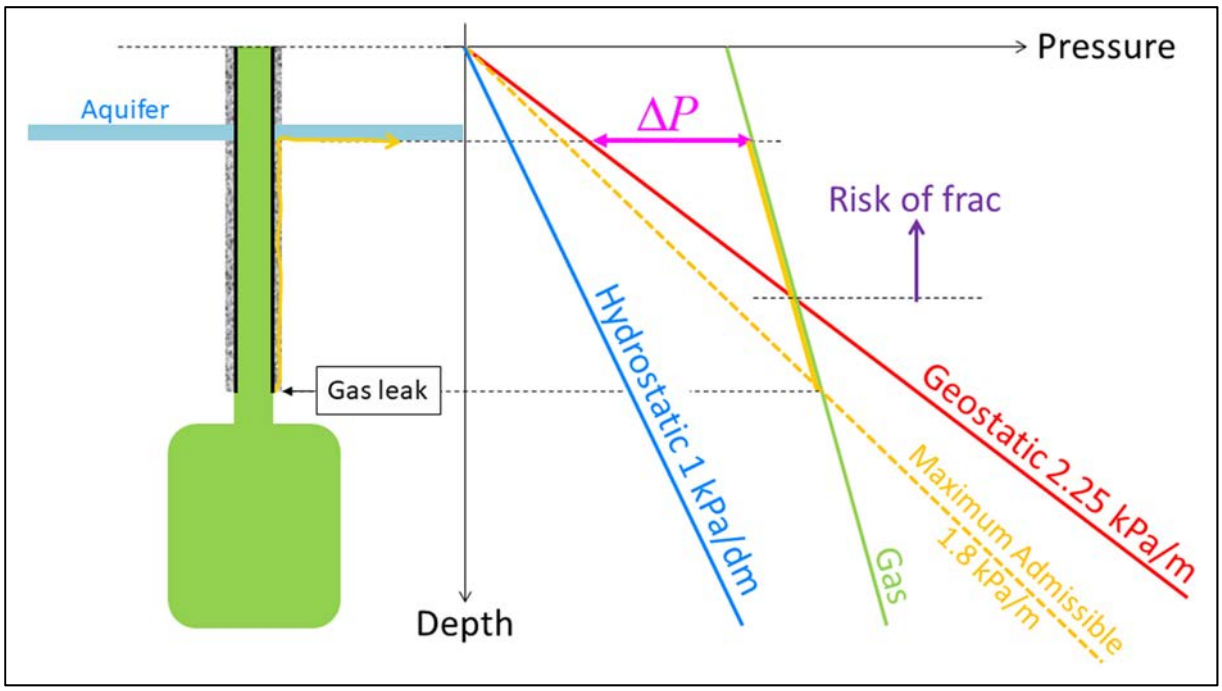

Figure 2 - Illustration of a gas leak. The gap between gas pressure and geostatic pressure decreases when gas rises in the cementation; it is positive at shallow depth.

Well architecture is also important. In Texas, for instance, two cemented casings must be anchored to the salt formation, as salt domes often are capped by a permeable zone (cap-rock), which is a weak point from the perspective of tightness (Figure 3). In Europe, the state of the art consists of equipping the wellbore with an inner tubing. A packer (sometimes two) is (are) placed at the bottom of the annular space, slightly above the casing shoe. The annular space typically is filled with non-corrosive water, and gas production is monitored at the top of the annular space. Such architecture minimizes the detrimental effects of large pressure and temperature swings on the cemented casing. However, uncertainties remain; for this reason, a margin of safety is needed.

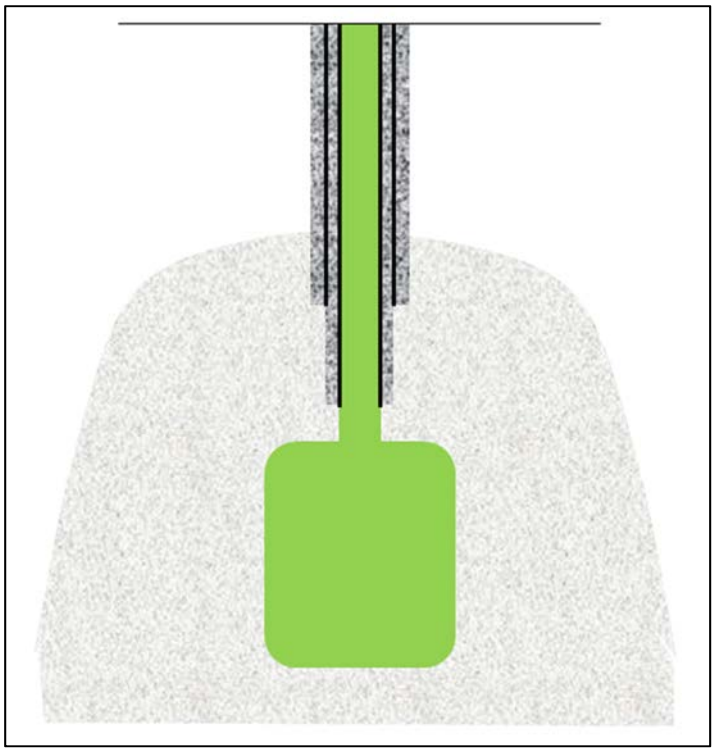

Figure 3 - Two cemented casings anchored to the salt formation.

2.3 The empirical approach: Pressure gradient

2.3.1 Margin of safety

The empirical, or pragmatic, approach consists of estimating the weight of the overburden at cavern-shoe depth using density logs (density-based vertical stress), assuming that it equals the vertical stress and selecting a maximum admissible pressure (80-85% of the vertical stress). This 15-20% margin of safety takes into account such factors as uncertainties, imperfectly known physical or mechanical processes, and possible cement weaknesses, as explained above.

This method is robust, as it is based on simple mechanical principles and reliable measurements (density logs). In addition, performing frac tests can be useful, as they provide the value (an upper bound, in fact) of the least compressive stress (shut-in pressure). The maximum operating pressure must be re-assessed in the (rare) case that the shut-in pressure is smaller than the vertical stress.

Research on cementation (its evolution with time, fracturing mechanisms, logs) must be fostered, but it is doubtful that this research affects, in the short term, the rule mentioned above, which relies primarily on experience.

2.3.2 Assessing rock-mass volumetric weight

The SI unit for rock density (ρ) is kg/m^3. The unit for volumetric weight, ρg, is MPa/m. Determining the actual density of the rock formations above the caverns is important in such a context. Pereira (2012) states that "*typical values of the overburden stress gradient may range from a low of 21.5 kPa/m (0.92 psi/foot) for a domal salt overlain by soft sediments, to a high of about 26 kPa/m (1.14 psi/foot) for a bedded salt largely overlain by dense limestone and anhydrite layers*" [p. 6-2] (see also Schreiner et al., 2010). Misinterpretation is possible, as explained by Rokahr et al. (2000). Before the Etzel test, described in Chapter 4, it was assumed that the lithostatic gradient was 0.0241 MPa/m (1.06 psi/ft). Additional investigations from a newly referenced borehole and three existing boreholes led to a revised value of 0.0204 to 0.0211 MPa/dm (0.9 to 0.93 psi/ft) — a significantly smaller figure. Lithodensity logs are convenient to use. Density measurements in the laboratory also can be used; they provide a lower bound of the in-situ rock density, which errs on the safe side.

2.3.3 Pressure gradient

Density, which is a site-specific notion, must be measured on a case-by-case basis. However, regulators often prefer rules that can be applied uniformly state-wide and that define a maximum allowable pressure gradient, $dP_{\max}/dz$ (e.g. in MPa/m, or psi/ft). This is the ratio between the maximum admissible pressure at the casing shoe and the casing-shoe depth. This pressure gradient must be smaller than the vertical pressure gradient (i.e. density-based vertical stress divided by depth). For example, a maximum pressure gradient of 0.018 MPa/m (0.8 psi/ft) is equivalent to 80% of a 0.0225 MPa/m (1 psi/ft) vertical pressure gradient based on an average $\rho = 2,295$ kg/m^3 overburden density.

This rule generally is accepted in the U.S. For instance, Texas Administrative Code § 3.97(k)(2) stipulates that "*The maximum operating pressure at the casing seat shall not exceed 0.85 psi/ft of depth*". In 2003, the Kansas Department of Health & Environment stated that "*The maximum allowable operating pressure for underground natural gas storage wells shall not exceed 0.75 psi/ft*", or 0.017 MPa/m (Poyer and Cochran, 2003, p. 199). In a report prepared for the SMRI, Pereira (2012) indicates that "*the maximum regulated pressure gradient is 0.9 psi/ft (0.0204 MPa/m) in Louisiana and Mississippi and 80% of fracture pressure or 0.8 psi/ft in Canada*". In France, Germany and the UK, the maximum admissible pressure is "*negotiated case by case*" [p. 6-14].

2.4 Typical values of maximum pressure in gas caverns

Most cavern designs meet this criterion (Table 1). Rummel et al. (1996) describe frac tests performed at Krummhörn, Germany, where three caverns had been leached out: casing-shoe depths were about 1500 m, and the selected maximum pressure was 27 MPa – an 0.018 MPa/m (0.8 psi/ft) gradient. Itsvan (1998) mentions a cavern under construction in Kansas in which the maximum gas-storage pressure was 1760 psi, a gradient of 0.88 psi/ft at 2000 ft. Bruno and Dusseault (2002) discussed the case of pressure limits for thin, bedded salt caverns: the maximum pressure for such caverns must not exceed the estimated fracture pressure for the weakest lithology (margins of safety not specified). Chabannes (2005) mentions a cavern at Egan (Jennings salt dome, Louisiana) in which

the maximum pressure gradient was 0.9 psi/ft. Colcombet et al. (2008) describe the Carriço Project, in which the maximum pressure was 18 MPa and the last cemented casing was around 1000 m (a 0.018-MPa/m gradient). Schweinsburg and Schneider (2010) present a cavern at Etzel, Germany, where the casing-shoe depth is 1150 m and the maximum gas pressure is 20 MPa — a 0.017 MPa /m (0.75 psi/ft) gradient. (More recently, 20.8 MPa was accepted.) Hoelen et al. (2010) dimensioned a four-cavern project at Zuidwending in the Netherlands. The caverns were to be operated between 9 MPa and 18 MPa, and the casing-shoe depth was 980-1028 m (an approximate gradient of 0.018 MPa/m). In China, Fansheng et al. (2010) indicate "*gas injection-production pressure is … 17 MPa to 32 MPa for gas storage constructed in about 2000 –m deep salt bed, and from 7 MPa to 17 MPa in about 1000-m deep salt bed*" (p. 190) — a maximum gradient of 0.016 to 0.0017-MPa/m. McLeod et al. (2011) describe a nine-cavern gas-storage facility at Aldbrough, Yorkshire, in which the casing-shoe depth was 1500 m and the maximum pressure was 27 MPa (a 0.015 MPa/m gradient). Bernhardt and Steijn (2013) discussed two cavern projects at Nüttermoor, Germany. There, the cavern-roof depths and maximum pressures at the casing shoe were 1020 m and 945 m, and 17 MPa and 16 MPa, respectively. In Germany, Wagler and Draijer (2013) discuss a nitrogen-storage project in which the last casing-shoe depth is 648.2 m. The maximum pressure initially considered was 12.2 MPa (a 0.018-MPa/m or 0.83 psi/ft gradient). Installing a new casing at a depth of 984 m led to a maximum pressure of 177 bars (a 0.018-MPa/m or 0.8 psi/ft gradient). Fawthrope et al. (2013) discuss construction of eight caverns at Holford, Cheshire, in which the casing-shoe depth was 550 m and the maximum pressure was 10 MPa, a 0.018 MPa/m gradient. In China, IRSM (Institute for Rock and Soil Mechanics, Wuhan) dimensioned new caverns, in which the gradient ranged from 0.016 MPa/m to 0.0188 MPa/m, with the smallest value associated with the deepest site.

Table 1 - Maximum gradients in selected sites.

Gas storage	Authors	CCS depth (m)	Pmax (MPa)	Maximum gradient (MPa/m)	Maximum gradient (psi/ft)
Aldbrough	Slingsby et al., 2011	1800	27	0.015	0.66
Carriço	Colcombet et al., 2008	1000	18	0.018	0.8
Etzel	Schweinsburg et al., 2010	1150	20	0.017	0.76
Holford	Fawthrop et al., 2013	≈ 550	10	0.018	0.8
Krummhörn	Rummel et al., 1996	≈1500	27	0.018	0.8
Nuttermoor	Bernhardt et al., 2013	≈ 1000	17	0.017	0.76
Teesside	Mullaly, 1982	≈ 350	4.5	0.013	0.58
Zuidwending	Hoelen et al., 2010	1000	18	0.018	0.8
Manosque	de Laguérie & Durup, 1994	1000	18	0.018	0.8
Stublach	Pellizzaro et al., 2011	≈ 550	10	0.018	0.8
Egan	Chabannes, 2005	1125	23	0.0204	0.9
Kansas	Itsvan, 1998	NA	12		
China	Fansheng et al., 2010	≈ 2000	17	0.016-0.017	0.72
Aldbrough	McLeod et al., 2011	≈1500	27	0.0155	0.66
Nüttermoor	Bernhardt et al., 2013	≈ 1020	17	0.017	0.8
Germany	Wagler et al., 2013	≈ 648	12.2	0.0188	0.83

Gas storage	Authors	CCS depth (m)	Pmax (MPa)	Maximum gradient (MPa/m)	Maximum gradient (psi/ft)
Torup	Johansen, 2010			0.0184	0.81
Huai'an	Zhao et al., 2013	1493	26.0	0.0175	0.77
Jintan (Xi-2#)	Yang et al., 2015	937	13.5 15.0	0.144 0.0160	0.64 0.7
Jintan (PetroChina)	Hongling Ma, Institute of Soil and Rock Mechanics, Wuhan, pers.com. (May 2018)	≈1000	17.0 18.0	0.0170 0.0180	0.76 0.8
Jintan (Sinopec)		900	17.0	0.0188	0.83
Qianjiang		1980	32.0	0.0160	0.7

2.5 Higher values of the maximum operating pressure

It is tempting to select a maximum operating pressure larger than those suggested above (80 to 85% of the overburden pressure) to increase the amount of gas that can be stored in the cavern. For instance, Igoshin et al. (2010) describe three gas-storage caverns under construction at Kaliningrad, Russia. The cavern volume is 400,000 m^3, and the maximum and minimum admissible cavern pressures are 18 MPa and 5.2 MPa, respectively. There, cavern depth is from 880 to 1020 m (casing-shoe depth not provided), making the gradient at the cavern top equal to 0.2 bar/m. Based on pneumatic tests, Schreiner et al. (2004) suggest a storage-pressure gradient of 0.19-0.205 bar/m or 0.84-0.91 psi/ft (around 85% of the geostatic pressure) for bedded salt formations and 0.18 bar/m in domal salt, as densities are lower.

The risk of a significant leak is greater when fluid pressure is higher, and that must be considered carefully. A high admissible pressure can be accepted when a large amount of information is available to increase confidence in the outcome.

For instance, Arnold et al. (2014) mentioned that: "*The storage site Bernburg is operated since the early 1970ies …the rock mechanical dimensioning of caverns has been developed and enhanced continuously using comprehensive investigations … the most recently approved rock mechanical dimensioning includes a Pmax of 100 bars casing shoe depth is 490 m. (gradient 2.04) ...*" [0.0204 MPa/m or 0.9 psi/ft] (p. 138). Johansen (2010) describes the Torup gas storage in Denmark. When the first caverns were created in 1981, the maximum pressure gradient was 0.0175 MPa/m (0.77 psi/ft). When the last cavern was leached out in 1992, the gradient was 0.0184 MPa/m (0.81 psi/ft). In these two cases, the increase in maximum admissible pressure was validated by the experience drawn from decades of satisfactory operation of existing caverns.

In our opinion, setting the maximum admissible pressure above the standard value (80 to 85% of the overburden weight) must be justified through a specific "*safety file*" that contains discussions of such topics as local sensitivity of the storage site (for instance, noting that a layer of salt or plastic clay

several hundreds of meters above the cavern roof is favourable, and a permeable cap rock within a small distance from the cavern roof is unfavourable), along with density files, results of the MITs, etc.

2.6 Brine production caverns

In most cases, liquid pressure in brine production caverns is much smaller than in gas storage caverns. At rest, brine production is halmostatic – i.e. at depth z (in m), it equals the weight, $\rho_b g z$, of a saturated brine column whose volumetric weight is $\rho_b g = 0.012$ MPa/m. During operation, pressures are higher than this figure because of head losses; however, they remain much lower than the geostatic pressure.

2.7 The case of Dutch caverns

In two sites in the Netherlands, Veendam and Frisia (Barradeel), in which creep-prone magnesium salts are leached out, brine pressures are higher than usual. These two cases are discussed in Sections 5.4 and 5.5.

2.8 The empirical approach: Tightness tests

Hundreds of natural gas caverns have been operated worldwide for decades. Only a small number of leaks are known (Réveillère et al., 2017). Most of them originate in roof collapse, or failure of a steel casing due to overstretching, shearing, corrosion milling or fatigue, rather than by the gas pressure itself. (Obviously, high gas pressures play a role.) Experience proves that the rule mentioned above is robust. However, it remains empirical, as it is based on the analysis of virgin stresses in the rock mass, a notion that implies some uncertainty, and it does not address the second problem mentioned in the introduction — i.e. cement tightness.

Cementing remains a difficult job, and it is recognized universally that a tightness test [Mechanical Integrity Test (MIT)] must be performed before commissioning a cavern. A tightness test consists of increasing cavern pressure to the maximum operating pressure (or slightly more) and monitoring cavern evolution. The best method consists of lowering a nitrogen column to develop a brine-nitrogen interface below the last casing shoe and monitoring the interface location over a couple of days: too fast an interface rise is a sign of poor tightness. Monitoring wellhead pressures during the test provides additional information. When the cavern neck is not consistent, lowering a light hydrocarbon column (instead of a nitrogen column) can provide good results. In some countries, tightness tests are performed periodically during the entire operating life of a cavern. Acceptance criteria have been proposed by Crotogino (1995) and Thiel (1993). In most cases, the results of the test performed before commissioning a cavern meet these criteria. When they do not, various techniques allow identification of the weak zones of the cement column and repair of the well before performing a second tightness test (see, for instance, McLeod et al., 2011).

2.9 Testing pressure

The testing pressure must be selected carefully. It must be equal to or larger than the maximum operating pressure (Figure 4). Many companies prefer that the testing pressure must equal the maximum operating pressure (Quintanilha de Menezes et al., 2001), as testing the well above the operating pressure can be harmful for future well integrity. Conversely, other companies prefer selecting a higher pressure, which provides additional confidence. One advantage of this second option is that, after several years of satisfactory operation, increasing maximum pressure is easier, as the cavern already has been tested for pressures higher than those used in operation.

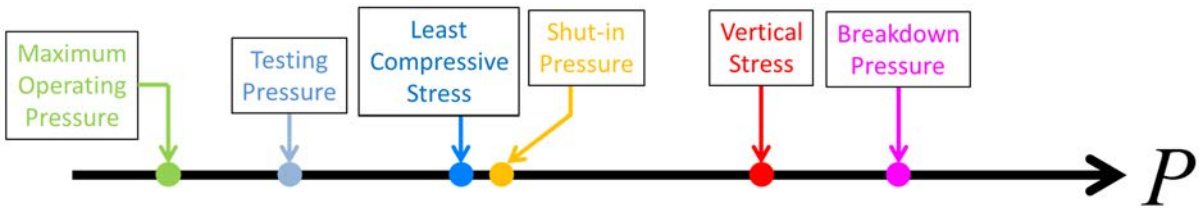

Figure 4 - The maximum operating pressure is smaller than the testing pressure, which is selected to be significantly smaller than the least compressive stress.

2.10 Recent research

The empirical approach includes a margin of safety that takes into account uncertainties and phenomena that are not well known. For instance, this approach relies on several assumptions: on one hand, during cavern operation and testing during wellbore drilling — even before fracking — salt permeability remains equal to its virgin or ‘’primary’’ value, which generally is very small; on the other hand, when cavern brine pressure is high, the state of stresses in the salt formation at the vicinity of the cavern walls is close to isotropic. Enough time has been given to “forget” the effects of the past history of cavern pressures. Several research projects, many supported by the SMRI, have led to a revision of these notions. They will be discussed in Chapter 4.

3. LOSS OF CAVERN INTEGRITY — WHAT CAN BE LEARNED FROM ACCIDENTS

Several cases in which salt caverns lose integrity are known. In most cases, a breach in the casing or cementation is the origin of the integrity loss. These cases are briefly discussed in Section 3.1. However, in this report, it is assumed that, before abandonment, the wellbore can be effectively and perennially sealed. (Several SMRI Reports and papers were dedicated to this issue). We mainly are interested in accidents in which a fracture was created at the cavern wall or roof rather than in the wellbore. It will be seen that, in many cases, it is difficult to know the exact origin of the integrity loss (a fracture, or a geologic heterogeneity in the salt formation).

3.1 Dewdney Field, Saskatchewan

This case was described by Coleman Hale et al. (2015).

3.1.1 Dewdney caverns evolution

The Dewdney field is located in Regina, Saskatchewan. The caverns are completed in the Prairie Evaporate Salt, an extensive bedded salt formation. At Dewdney Field, the salt interval top is 1575-m (5165-ft) deep and base is 1690-m (5540-ft) deep, generally. The upper 65 meters (215 ft) of the interval is composed of interbedded salt, potash and thin mudstone (clay) seams. Eight caverns were developed in the early 1970's. Three of them were used for natural gas storage. In 2015, four LPG storage caverns were active. They were operated by Spectra in compensated mode (brine is injected when products are withdrawn and cavern pressure does not vary much over time). The four active caverns have volumes ranging from 103,590 m^3 (652,000 bbls) to 149,862 m^3 (943,000 bbls) and maximum diameters range from 79.7 to 130.6 m (236 ft to 428 ft). Cavern roofs are generally flat, and the distance between cavern roof and last casing seat is small.

"*Throughout the operational history of the cavern field, this interbedded interval has proven to increase strain on the cemented production string of each cavern well. All of the wells have experienced some degree of cemented casing damage, and four of the eight wells have experienced severe casing separations within the interbedded interval*", p.1, Coleman Hale et al., 2015.

A good example is provided by Well 2, which was drilled in 1971 and used for LPG storage. In 2013, casing inspection logs found separated casing at 1602, 1613, 1621 and 1626.5 m. It was decided to install a liner and to drill a second wellbore entry (well 2A) to maintain fluid rates. Well 2A entry is 20 m (65 ft) to the east of Well 2. During Well 2A drilling, much information was gained on the state of Well 2 roof. Well 2A also provided an opportunity for the collection of formation cores and an updated set of wireline logs, which were analyzed by RESPEC. The salt is "hard" (very "slow creeping" according to Munson's classification, 1988). Potash creep rate is 10 times faster and intermediate between "hard" and "soft" salts. In addition, multiple horizontal mudstone (clay) seams, ranging from 3 to 21 cm in thickness (1.2 to 8.4 inches) were found. The clay is soft ("*it can be scratched with a knife*") and "*it was determined that the clay seams are a plane of weakness*" (Figure 3). During drilling, mud return was lost at 1602 m, where a clay seam exists, proving that a void or path existed with well 2. A Nitrogen test proved that void/path volume was 14.7 m^3. More generally, nitrogen

injections (during MIT) proved that horizontal fractures had been created in the mudstone seams (No cavern-to-cavern communication was detected). Void/path volumes ranged from 9.6 to 38.4 m^3 (60.4 to 241.5 bbls) and the radial extent can be at least 20 m away from the wellbore.

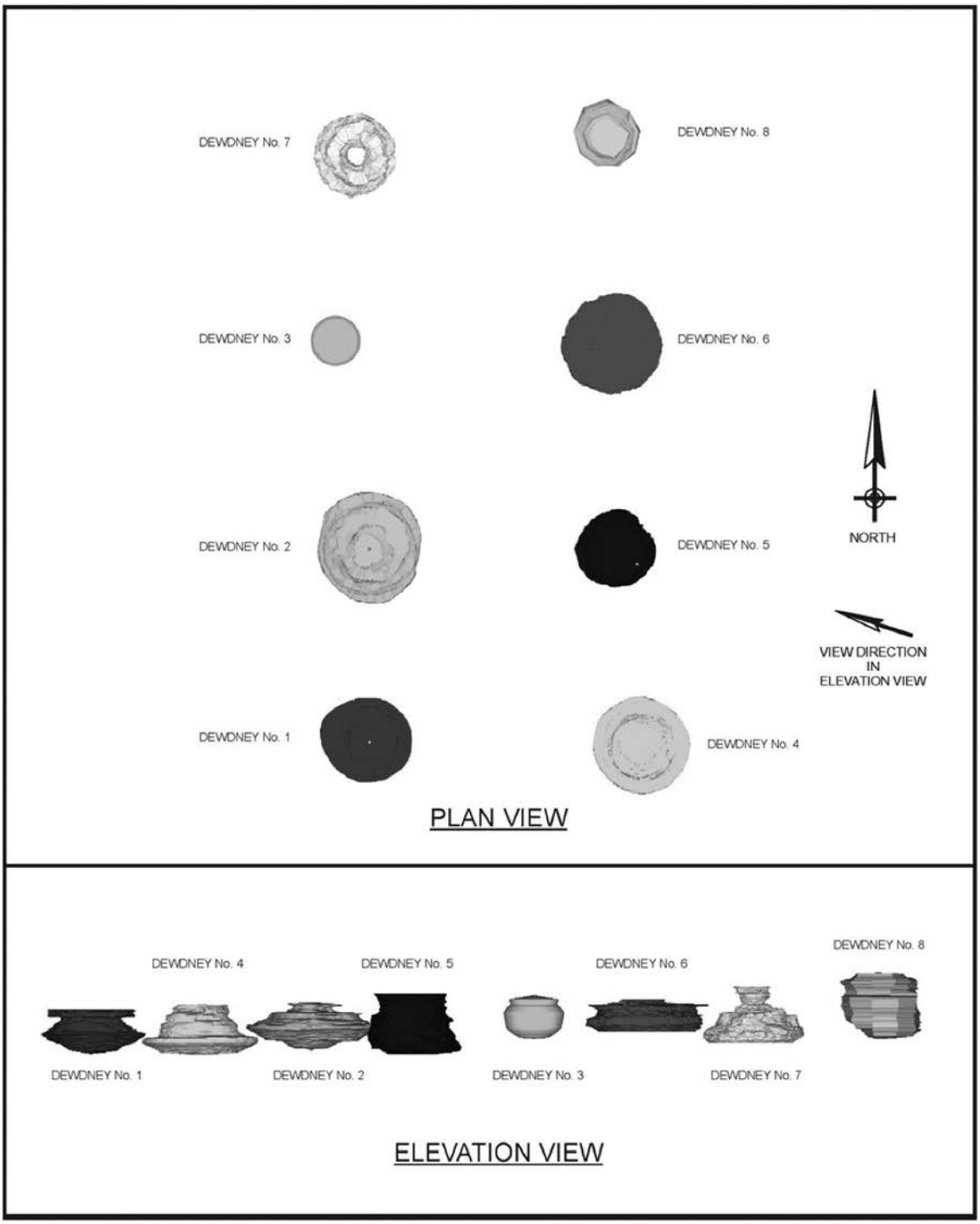

Figure 5 – Plan view and elevation view of the Dewdney cavern field (Coleman Hale et al, 2015).

3.1.2 RESPEC analysis

RESPEC analyzed vertical strains generated by 40-year long operation of several caverns. The steel casing was not explicitly modeled, displacements were assumed to be continuous at cement-casing-rock interfaces. The criterion for tensile failure was expressed in terms of a maximal strain of $\varepsilon = 3.2 \times 10^{-3}$. As a conclusion, overtime the vertical strain on the cemented casing exceeds the failure limit.

Casings failure have occurred approximately 30 to 35 years after well completion (and less for gas storage caverns operated between 0.15 psi/ft and 0.70 psi/ft [3.4 to 15.8 kPa/m]). Figure 4 shows a typical computation performed by RESPEC: at the bottom of the casing the 3.2 x 10^{-3} strain limit is exceeded before 5 years. The distances between the shoe seat and cavern roof or the maximum cavern diameter affect the magnitude of the vertical strain.

RESPEC concluded that caverns are stable (when operated according the brine-compensation method) but that the vertical strain on the cemented casings resulting from potash fast creep and mudstone poor tensile strength exceeds the casing strain limit. These effects are larger when the distances from the casing shoe to the top of the cavern and to the depth of maximal diameter are smaller. (such a geometry favors large strain rates in the salt roof).

3.1.3 A comment on vertical stresses above cavern roof

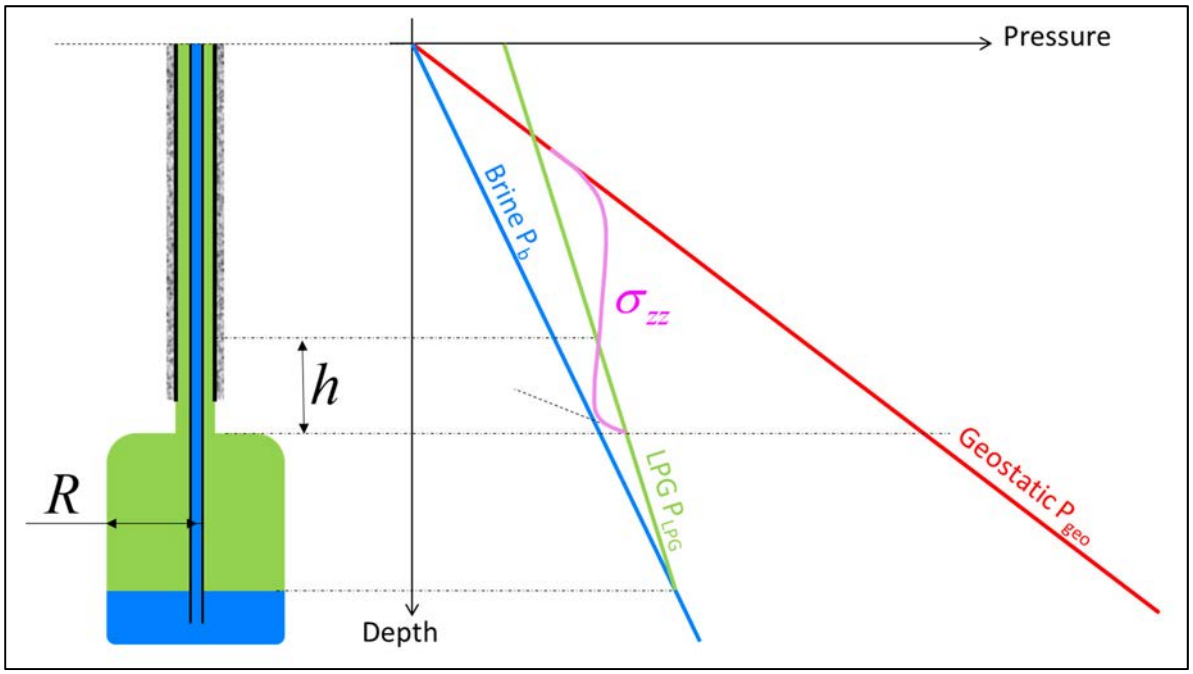

Figure 6 - Schematic profile of vertical stresses along the axis of symmetry above cavern roof.

Pressure distribution is represented on Figure 5. At cavern roof, the slope of the LPG pressure-vs-depth line is $dP_{LPG}/dz = 0.005$ MPa/m. (much smaller than the rock pressure-vs-depth line which is $dP_R/dz = 0.022$ MPa/m.) The vertical stress at cavern roof equals LPG pressure at the same depth. However, when the roof is flat, the vertical stress gradient above the cavern is

$d\sigma_{zz}/dz = -0.022$ MPa/m (compressive stresses are negative). There is a zone above the cavern roof such that LPG pressure is larger than the vertical stress; this zone is higher when cavern roof is larger; the risk of hydro-fracturing must be considered (this property results from mechanical equilibrium only). In other words, two scenarios must be considered, implying or not hydrofracturing:

1. layers above the roof bend and sag, ultimately leading to casing separation. LPG is in contact with the rock mass where the casing separated and hydro-fracturing of the mud layers take place

2. layers above the roof bend and sag, leading to tensile failure in the mud layers, further sagging and ultimately casing separation. LPG then can enter the voids created in the mud layers.

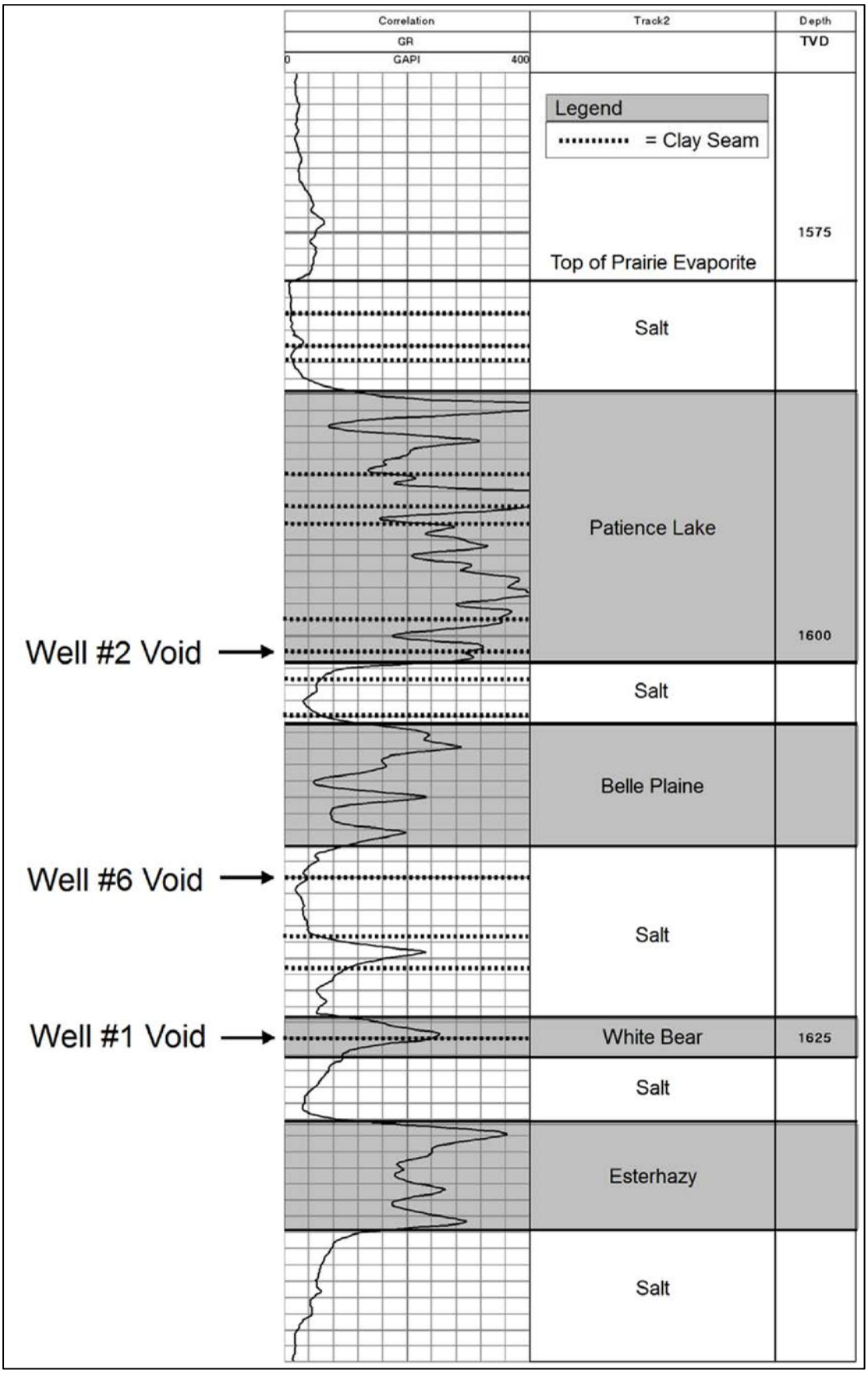

Figure 7 - General stratigraphic column of the Prairie evaporate at Dewdney Field (Coleman Hale et al., 2015).

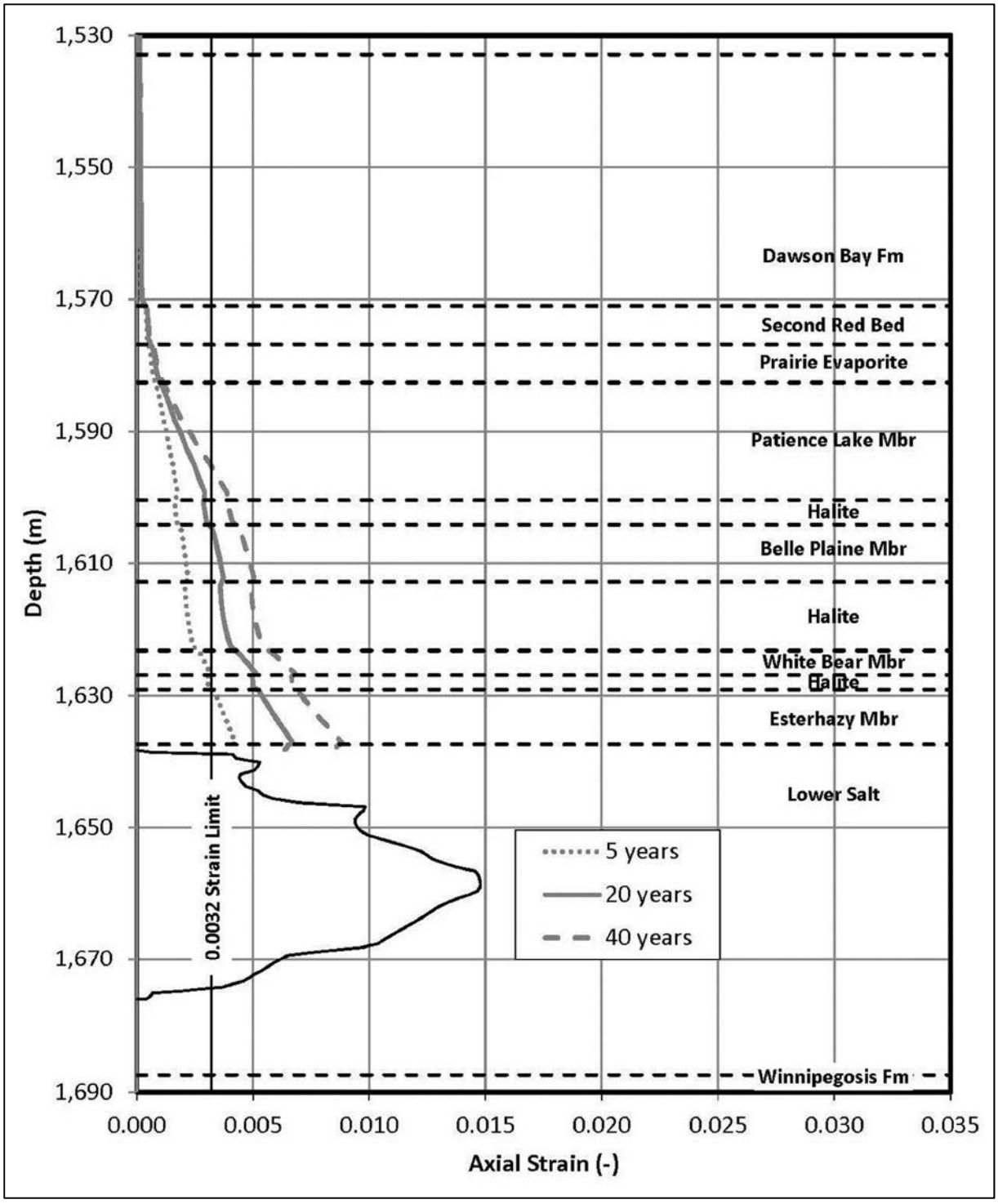

Figure 8 - General stratigraphic column of the Prairie evaporate at Dewdney Field (Coleman Hale et al., 2015).

3.2 Fracture following a breach in the casing and microfractures

Several salt caverns used for hydrocarbon storage experienced significant product losses or unexpected pressure drops that were provoked by a leak in the casing (Hutchinson, Kansas; Eminence, Louisiana; Boling and Mont Belvieu, Texas; Epe and Teutschental, Germany, etc.). A dozen such cases are described in Réveillère et al. (2017). It is likely that in several cases fracture took place. This is especially true when gas was stored (see Figure 9):

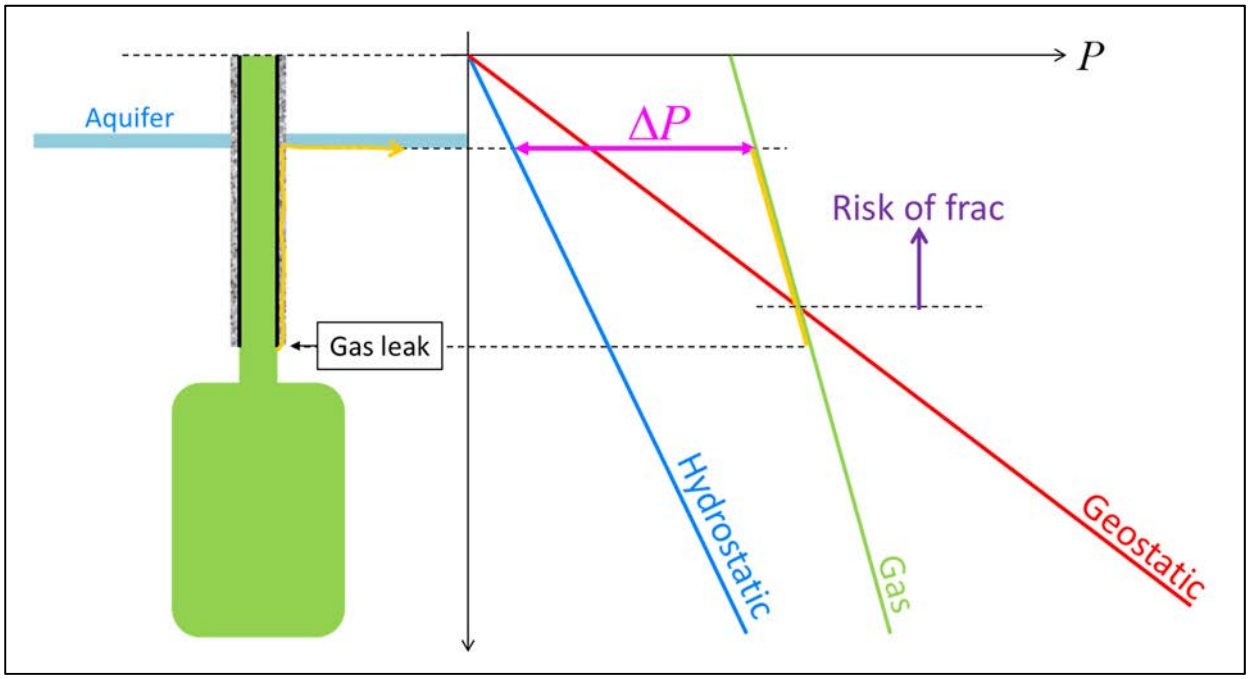

Figure 9 - Gas pressure distribution in the cementation of a leaky wellbore.

When a breach is created above the casing shoe, gas enters the cemented annulus and rises in the annulus. As gas density is much lower than rock density, gas pressure becomes higher than geostatic pressure, and a fracture becomes possible. Although no definite proof is available, there are indications that such a fracture occurred at Hutchinson, Kansas, for instance (Réveillère et al., 2017). These cases will not be discussed here, as the fracture did not occur in the salt formation itself.

It will be seen in Chapter 4 that micro-fractures or small fractures are likely to develop at the wall of caverns that experience large pressure increases. In many cases, such micro-fractures have no effect on cavern integrity, as their lengths are small: they cannot open into a permeable/porous reservoir (a "*receptor*") such that a steady flow can be created between the cavern and the receptor. Onset of such micro-fractures is difficult to detect, although a large number of micro-fractures increase cavern compressibility, a quantity which is relatively easy to measure.

For this reason, we will focus on cases that experience a pressure drop —a sign of the creation of a perennial hydraulic link between the cavern and a "receptor". Creation of a fracture can be the origin of such a link, other mechanisms often can be invoked.

An intermediate case must also be considered, when micro-fractures are created in the salt formation above the cavern roof, for instance after the casing was overstretched and broke. Such a case will be described in Section 3.3. Whether the fracture resulted from excessive brine pressure or from layers sagging in the overburden is not perfectly clear.

3.3 Regina South, Canada (1989)

Several roof falls are known to have occurred in salt caverns. The Regina South event is of special interest as it was accompanied by a large gas-pressure drop (Figure 10).

> "*The cavern roof depth was 5,363 ft … the roof salt thickness was 50 ft. … The maximum allowable wellhead pressure was set at 3,000 psig [a low maximum pressure for a gas cavern; at cavern roof, the maximum gradient was 0.127 bar/m, instead of 0.18 bar/m in most standard caverns]. The cavern was cycled once a year*." "*The final developed roof position was higher than originally planned and located in a structurally unstable area with many thin insoluble bands which threatened future stability. In July 1989, a 267-psig [18 bars] pressure drop occurred in this cavern following gas fill up to 3,000 psig [267 bars]. A rate of change in pressure decline from the pressure-vs.-time graphs used to monitor cavern operating condition suggested the cavern roof had a leak away from the well bore*" [Note that a block fall generates no pressure change when the cavern remains tight after the bock fall.]
>
> "*In September 1989, the cavern was gamma ray/neutron logged. An 8-16 ft [2.5-5 m] roof fall was indicated at the well bore area, and 60 ft [18 m] of new material lay in the cavern bottom, suggesting possible side-wall ledge falls."* (Crossley, 1998).

Gas is much more compressible than brine. A pressure drop such as noted above suggests an inventory loss by 267 psi/3000 psi = 9%. This is only possible when there is a porous and permeable layer (a "receptor") above the salt roof, which can accommodate a large volume of gas within a short period of time. It also must be mentioned that gas pressure was much lower than geostatic pressure when the pressure drop was observed. For this reason, it is extremely likely that the pressure drop did not originate in a frac: pressure gradient was low (0.0127 MPa/m).

In fact, roof failure results from a combination of three factors: low minimum pressure, relatively large roof span and, above all, poor mechanical quality of the roof, which comprises multiple interlayers. These three ingredients can be found in several other examples of roof failure, including, for example, Kiel, Germany (Baar, 1977, Figure 11), Jintan, China (Tongtao Wang, 2018), and Loop-Onehok, Texas (Istvan et al., 1998 and Johnson, 2003), see Figure 2. However, in these three cases, no gas pressure drop was observed as, opposite to the Melville case, the roof remained inside the salt formation.

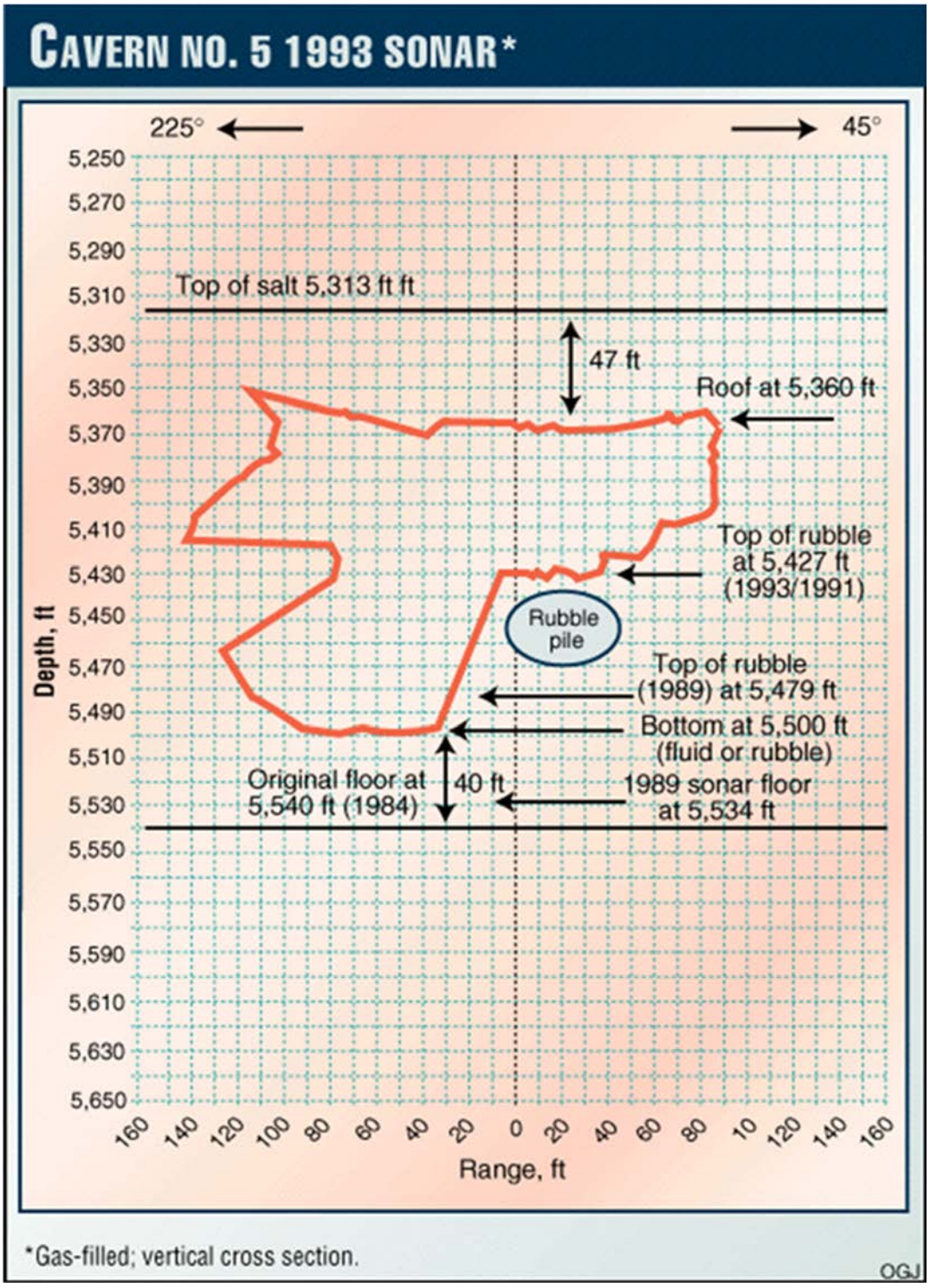

Figure 10 - Regina South No.5 cavern after the second roof fall, and rubble pile at the cavern bottom (Crossley, 1998).

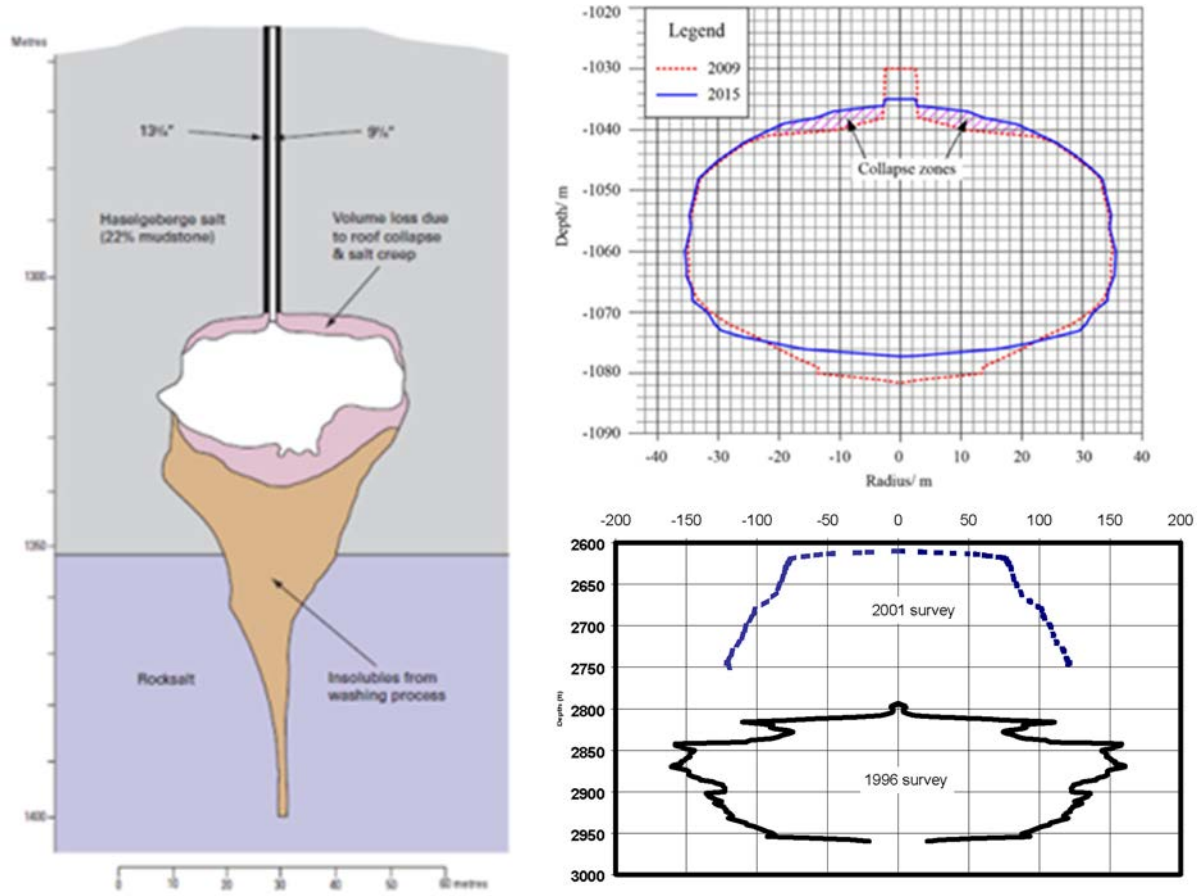

Figure 11 - Left: Kiel cavern, Germany – The horizontal line is the interface between the lower "pure" salt and the upper salt, whose insoluble content is much higher (British Geological Survey, 2008, after Baar, 1977). Top right: Jintan cavern, China (from Tongtao Wang, 2018). Bottom right: Loop-Onehok, Texas (Johnson, 2003).

3.4 Mineola, Texas (1995)

The Mineola Storage Terminal had two storage caverns near Mineola in East Texas. The wells originally were drilled as oil producers in the late 1950s. One of the two wells developed a casing leak. Breach depth was unknown. The "initial theory" (according to Gebhardt et al., 2001) was that injection of water had made the wall between the two caverns very thin. A leak was created when a workover [perhaps a Nitrogen MIT] was run on the second well. The pressure induced in the workover well caused the salt formation to fracture, and a pressure surge was transmitted to the second cavern, which caused a breach in its casing. Propane escaped through the surface soil to the atmosphere, collected in the low areas around the terminal and surrounding forest, and found an ignition source.

Note that Gebhardt and his colleagues are fire-killers rather than solution-miners. They speak of an "initial theory", which might be correct but which was not documented clearly enough when they prepared the paper (during an MIT, maximum testing pressure at cavern shoe depth is significantly smaller than geostatic pressure, and a fracture should not happen during an MIT).

3.5 Mont Belvieu, Texas (2014)

This case was described by Cartwright and Ratigan, 2005.

The Barbers Hill salt dome at Mont Belvieu, Texas, is the world's largest LPG storage facility (approximately 140 storage caverns). *Enterprise* operates several caverns in North, West and East Terminals. Well 16E is a brine production cavern. A diesel pad is used to control cavern roof leaching. In August 2014, diesel was added to the pad but "*a corresponding downward movement in the interface was not observed*", p.5. Various investigations were performed to determine the cause of the diesel blanket loss and the hydraulic integrity of the well and cavern. It was suspected that the cavern intersects a plane of preferred dissolution associated with a Boundary Shear Zone (25% of the caverns at Barbers Hill have intersected such planes). In such shear zones, salt porosity is significantly increased, allowing much faster dissolution. A detailed sonar survey was performed on September 9, 2004 after the two hanging strings had been removed, showing the existence of a plane of discontinuity, see Figure 12. An MIT was performed, beginning on October 10, 2004 at about 9:30 a.m., see Figure 14. Wellhead pressures in adjacent wells 1E, 2E and 11E (see Figure 13) were monitored with precision recorders. The test proved that wells 2E and 16E were hydraulically connected (2E wellhead pressure increased rapidly). Distance between 2E and 16E cavern walls is 300 ft (90 m).

At the beginning of the test, 16E wellhead pressure was 490 psi at production casing depth (1999 ft), or a 0.52 psi/ft + 490/1999 psi/ft = 0.765 psi/ft gradient (much smaller than geostatic gradient) This example proves that, in unfavorable geologic conditions, a hydraulic connection can be created between two adjacent caverns even when caverns pressures have remained relatively low during their operational life.

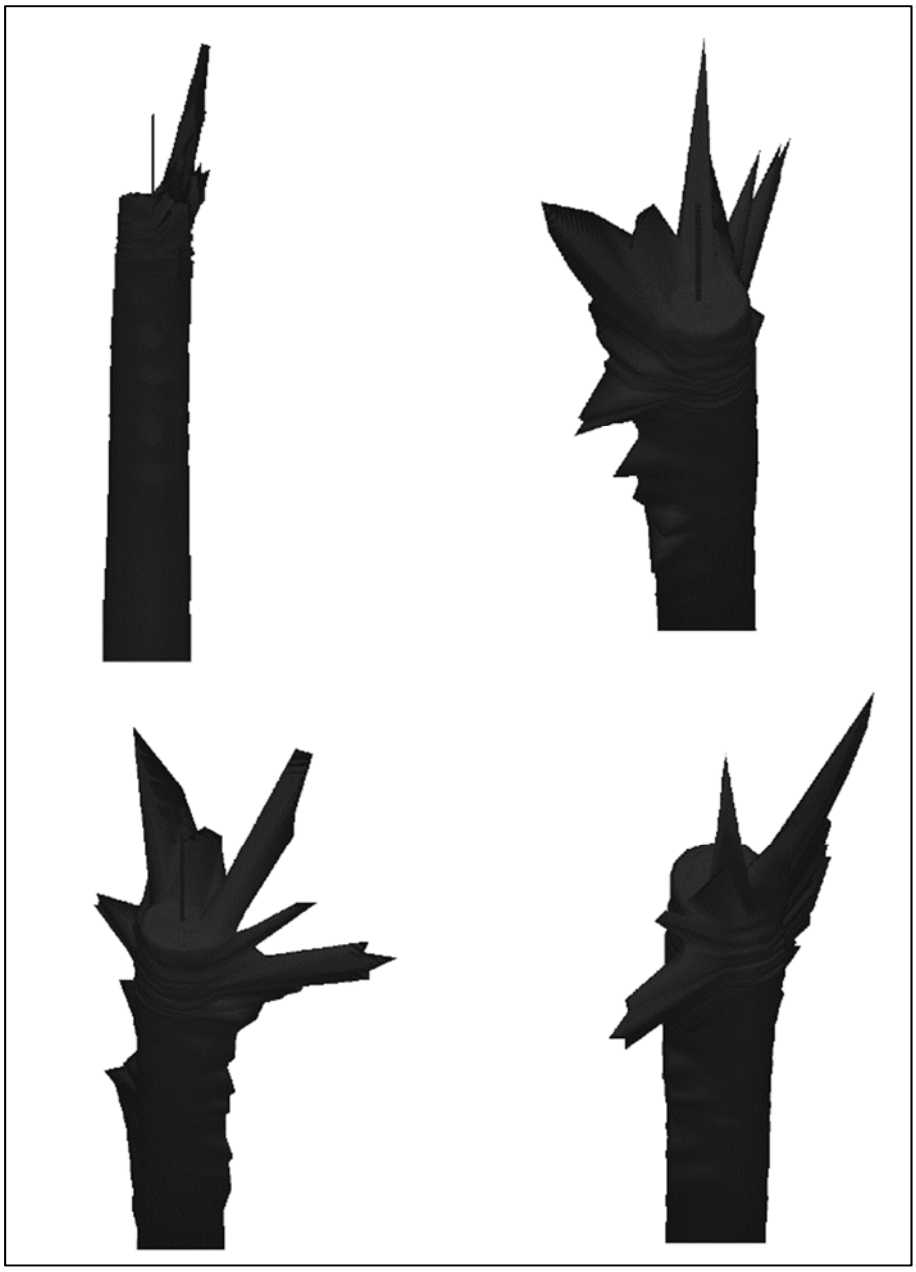

Figure 12 - Isometric illustrations in several directions of well 16E cavern roof area sonar surveys (Cartwright & Ratigan, 2005).

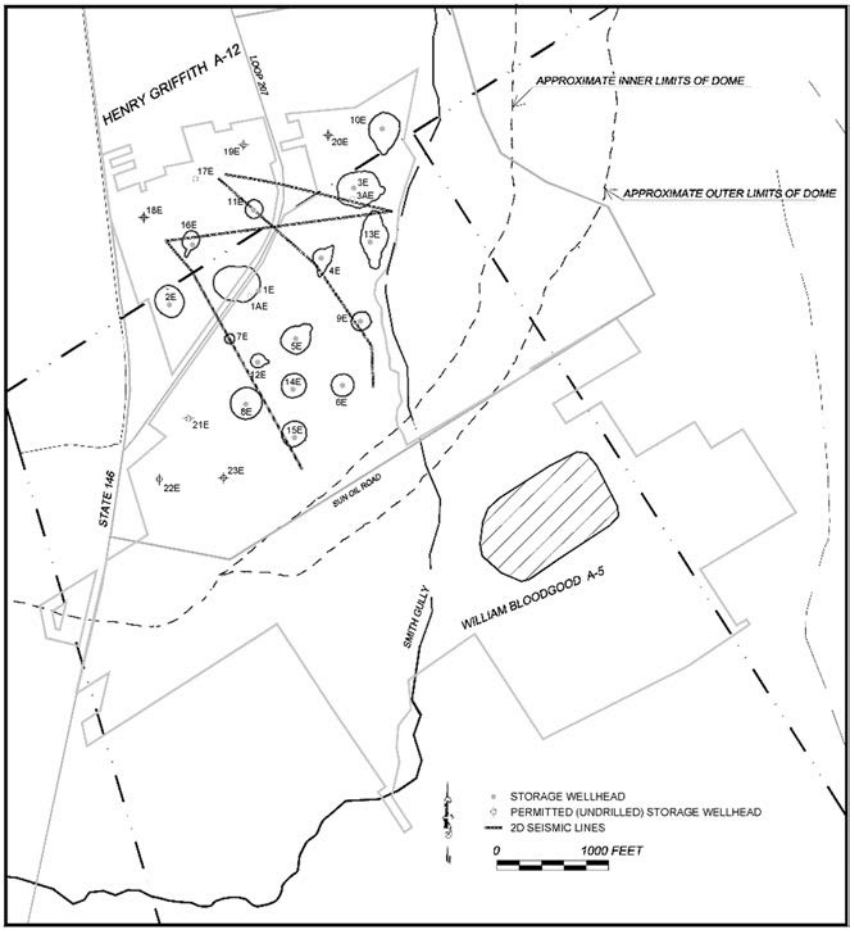

Figure 13 - Two-dimensional seismic survey area and line locations (Cartwright & Ratigan, 2005).

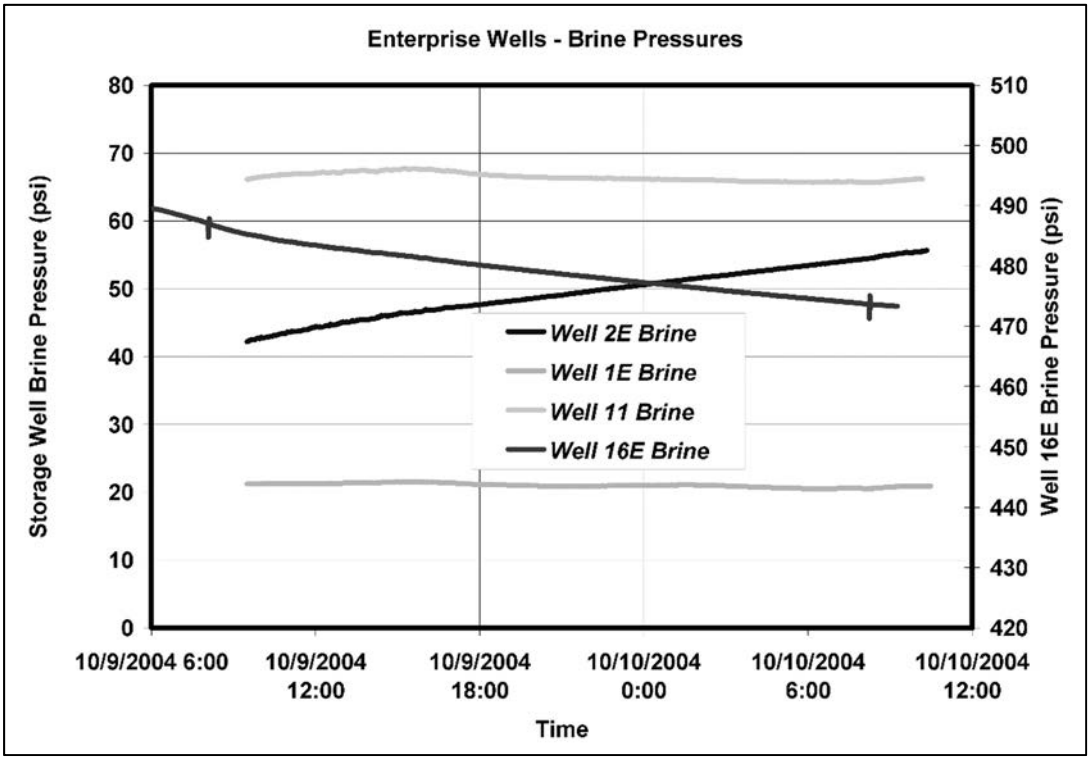

Figure 14 - Well brine pressures versus time during the observation period of the well 16E nitrogen/brine interface MIT (Cartwright & Ratigan, 2005).

3.6 Bayou Corne, Louisiana (2012)

On 3 August 2012, a sinkhole was discovered in the swamp near Bayou Corne in Assumption Parish, Louisiana (Bérest, 2017). Numerous gas bubbles had been observed as early as 31 May, and tremors had been felt since 8 June. The sinkhole was within a short distance from the footprint of the Napoleonville salt dome, where dozens of caverns had been leached out. It quickly was suspected that the sinkhole was related to Oxy3, an elongated axisymmetric cavern which, as established by a 2007 sonar survey, had a height of 2200 ft (670 m). The cavern radius was 100 ft (30 m) near the cavern roof at a 3395-ft (1050-m) depth; it was about 150 ft (45 m) at its widest point (near the cavern bottom; see Figure 15, which displays a conceptual model by CB&I and a recent geophysical interpretation by Kevin Hill). In 1982, when the well associated with the cavern was permitted, it was thought that the edge of the dome was at least 1000 ft (300 m) from the cavern. Vertical seismic profiles and more recent 3D seismic profiles showed that the salt wall between the dome edge and the cavern wall was much thinner than previously believed. In addition, a tightness test performed before abandoning the cavern in 2011 (at which time, the cavern volume was approximately 23 million bbls or 3.7 million m^3) proved that the cavern was not able to sustain high brine pressures — clear proof of existing leak pathways. It must also be mentioned that a severely depleted reservoir can be found at a depth larger than the cavern bottom. A complete picture of fluid pressures in the cavern and at the flank of the dome, as well as stresses in the cavern walls and in the sediments, is difficult to draw.

A relief well, Oxy3A, was spudded and re-entered the cavern on 24 September 2012. This allowed a sonar survey to be performed, wire-line bottom tags to be run and, when the well was shut in, wellhead pressure measurements taken. Measurements pointed to the fact that a plug of sediments, overlain by sludge (perhaps a mixture of oil and sediments) was slowly and consistently rising in the cavern as sediments entered the cavern and sinkhole size increased. Sediments flowed from the sinkhole to the cavern as a highly viscous material through a Disturbed Rock Zone (DRZ) along the dome edge. The breach in the salt wall is likely to have occurred in the lower part of the cavern, where salt-wall thickness was probably small.

It is also likely that, at the edge of the dome, a sheath composed of loose and soft sediments was formed during geological times (the product of early natural dissolution of the flank domes), allowing loose sediments to flow through the DRZ as through an hour glass of unusual size and shape, to the 23-million-bbls cavern until completely filled.

In this report, we mainly are interested in the origin of the creation of the breach: was a fracture involved? A clear answer is difficult. It seems that the cavern never experienced high pressures. However, structural interpretation of breach creation remains controversial.

During a trial (Judgement, 2017) following the sinkhole creation and growth, a tentative explanation was proposed: "*The Adams Hooker #1 well was spudded in 1986* … [it was operated] *as a depletion driven reservoir* [this reservoir is located along the flank of the dome below Oxy3 cavern bottom depth]. *Because a depletion driven reservoir does not refill the reservoir as it is depleted, the pressure in the Adams Hooker #1 reservoir continuously dropped as hydrocarbons were extracted from nearly 2781 psi in 1986 to 916 psi by 2000. Though no evidence indicates that this drop of pressure in itself*

initiated the OG3 cavern leak, the close proximity of the substantially low-pressure reservoir provided for an unreasonably dangerous condition once leaking [from Oxy3, also called OG3] *began. Once communication between the high pressure OG3 cavern and the low-pressure AH-1 reservoir initiated, the substantial pressure differential required a significant pressure drop in the OG3 cavern to achieve pressure equilibrium. Dr Nagel's unrebutted testimony establishes that this pressure loss was required to create the static stress change necessary to compromise the OG3 cavern wall."*

Adams Hooker #1 depletion may have played a role; however, many details are missing (reconciling fluid pressure distribution in the dome flank before and during sinkhole development with the explanation above is not an easy task).

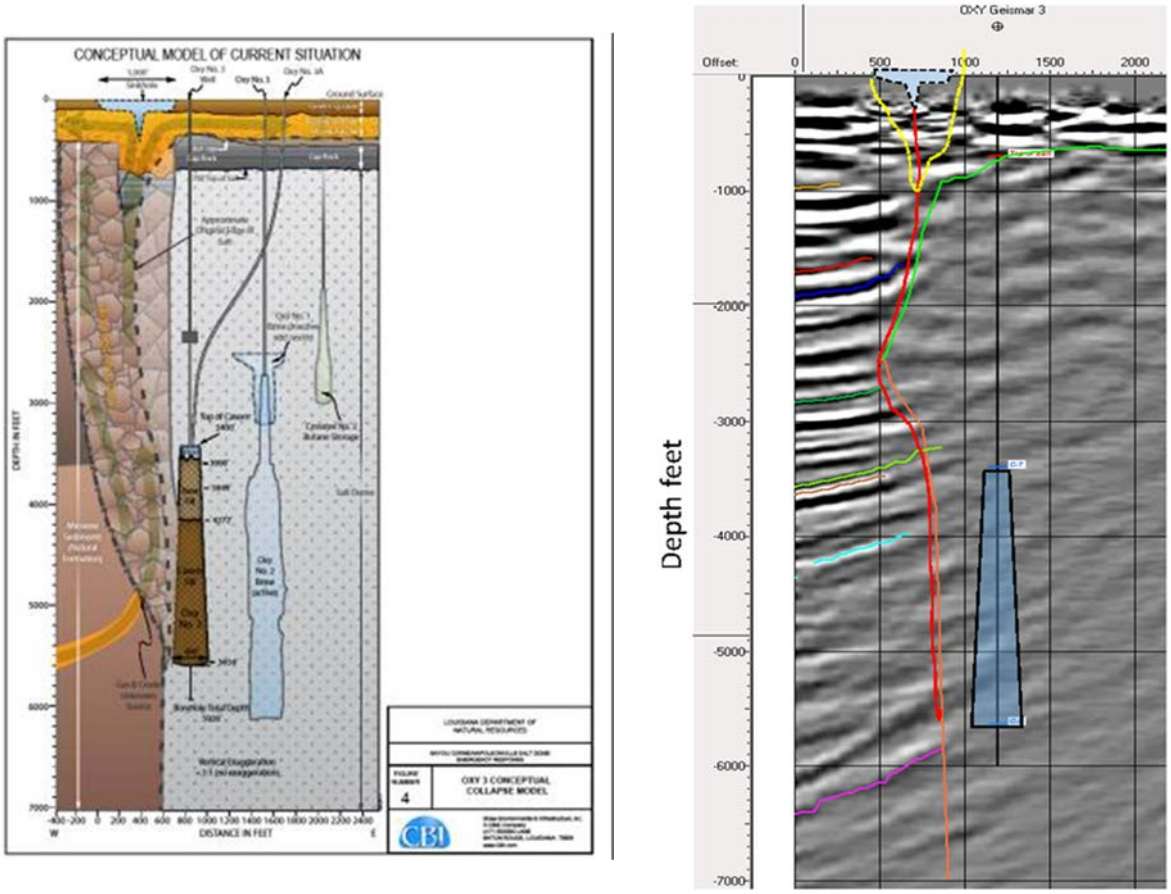

Figure 15 - Initial conceptual model of the Oxy3 cavern showing the sinkhole on the left, the flank of the salt dome, the 5000-ft (1600-m) deep breach, and the Oxy3 cavern, 90%-filled with sediments (Source: CB&I) and a recent interpretation (Kevin Hill, 2015, personal communication) on the right.

3.7 Spindletop, Texas (2001)

In the morning of 19 December 2001, one of the brine supply caverns operated by Texas Brine Company, LLC (TBC) at Spindletop, Texas, exhibited abnormally high wellhead pressure. TBC's Gladys City No. 2 offsets a gas-storage cavern operated by Centana Intrastate Pipeline, LLC – a subsidiary of Duke Energy Field Services, LP (Duke), see Figure 16. It quickly was determined that the cause of the elevated wellhead pressure on TBC's Gladys City No. 2 was the infiltration of natural gas into the brine cavern, although the wellheads of the Duke and TBC caverns are over 1500 ft (457 m) apart. Normal wellhead operating pressure on the TBC Gladys cavern was about 500 psi (34 bar), but had increased to approximately 1500 psi (103 bar) and continued to rise. The wellhead operating pressure of Duke's well at the time of the event was slightly over 3000 psi (207 bar). TBC began venting the outer, diesel-filled, annulus of its well, and Duke commenced reducing the pressure in its cavern by withdrawing gas. Wellhead operating pressure declined to just under 2400 psi (165 bar). These operations continued until 26 December 2001, when gas quit flaring at TBC's well.

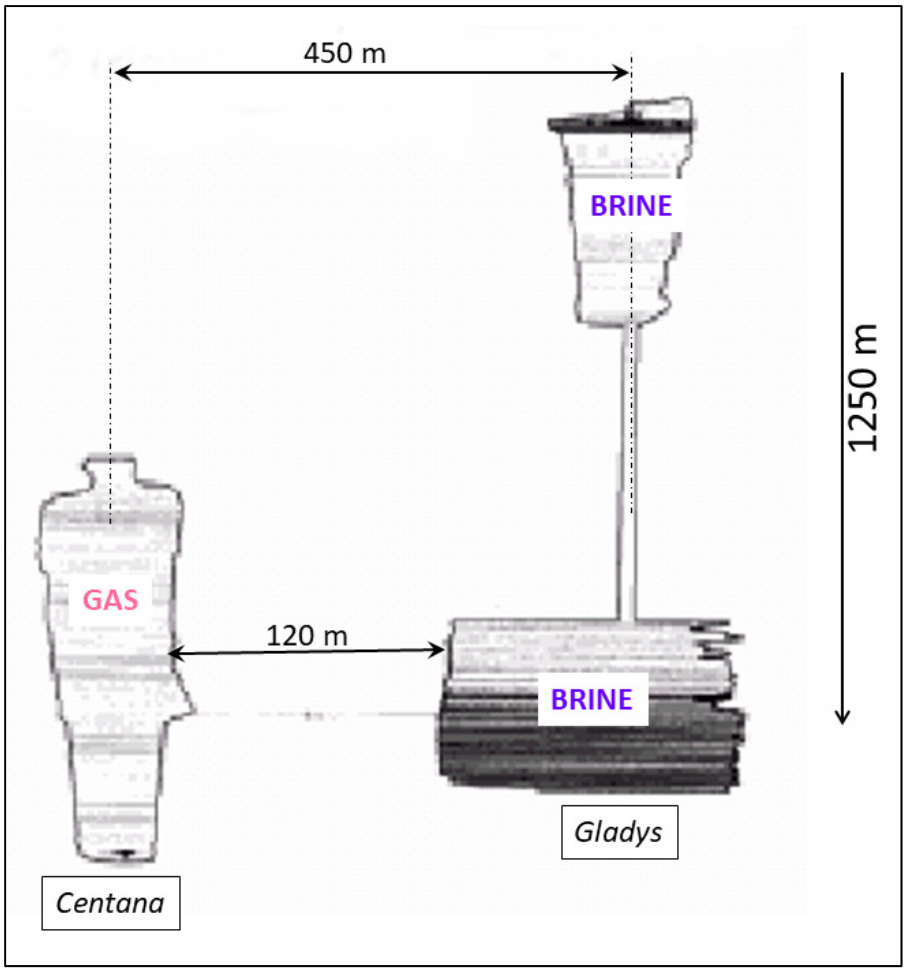

Figure 16 - Centana No.1 (left) and Gladys No.2 (right) (After Johnson, 2003).

Duke's Centana well was drilled in 1992, initially leached to a cavern capacity of approximately 1.8 million barrels, placed into gas storage service in 1992, and then enlarged to approximately 3.9 million barrels beginning in early 2000 through early 2001. A nitrogen/brine interface MIT was completed on 9 March 2001. Asymmetric growth occurred during enlargement. Figure 17 illustrates

this phenomenon. Sylvite (KCl) contamination of the salt was detected during enlargement. TBC's Gladys City No. 2 was drilled directionally in 1958. Although TBC had mined an interval at an elevation opposite the Duke cavern for many years, mining at that level had ceased prior to the creation of the Duke cavern and had since occurred at a shallow depth (Figure 16). Duke and TBC agreed to conduct pressure tests. A gas-pressure test commenced on 7 March 2002. A tracer gas was introduced. Approximately 705 MMscf was injected in two stages. In late April 2002, gas did begin infiltrating into TBC's cavern; a sample of the gas confirmed existence of the tracer gas.

TBC and Duke cooperated to re-enter and sonar the lower chamber of TBC's Gladys cavern. The process entailed landing a 7" casing string several feet into the base of the upper chamber and drilling through the intervening salt to the lower chamber.

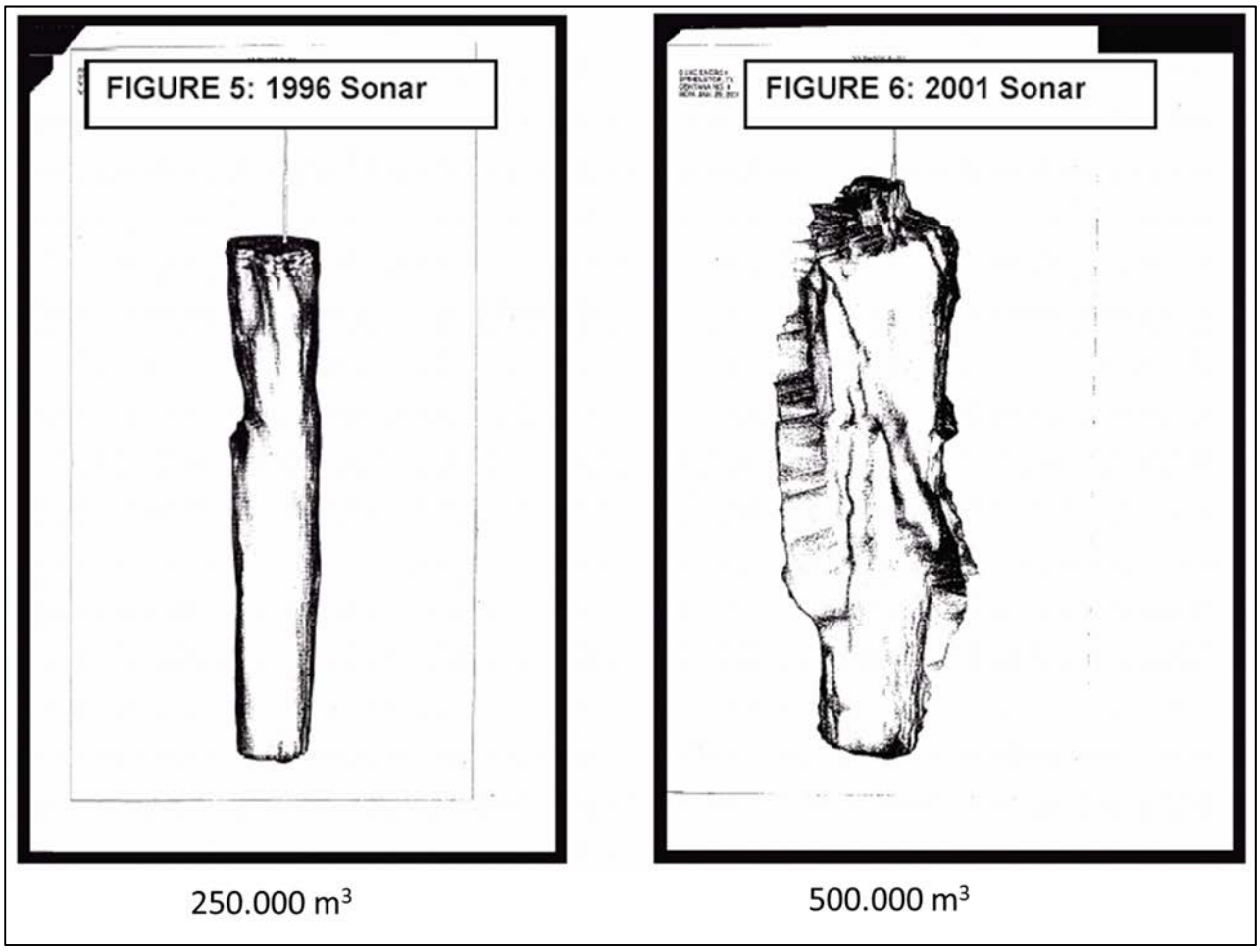

Figure 17 - Centana No.1 1996 (left) and 2001 (right) Sonars (Johnson, 2003).

The origin of the connection between the two caverns remain unclear "*It is now known that gas stored in the Centana No. 1 at a pressure of approximately 3000 psi (207 bar) will migrate through approximately 400 ft (122 m) of salt and enter the Gladys City n°2. It is unknown whether the gas is migrating through an induced fracture, a fault plane or a seam of porous and permeable salt intersecting both caverns at an unknown altitude*" (Johnson, 2003). It must be mentioned that, in principle, pressures in both caverns remained smaller than geostatic pressure during the entire operating life of the caverns.

3.8 Veendam, the Netherlands (2018)

Nedmag operates a magnesium chloride cavern field at Veendam (Figure 18 and Figure 19). The mining methods for its caverns were described in a paper by Fokker et al. (2004):

> "*The magnesium chloride mine operations of Nedmag Industries at Veendam have been the subject of earlier presentations at the SMRI. Magnesium chloride is extracted from several thick layers of carnallite and bischofite at a depth varying from 1300 to 1600 m. These layers are embedded in the upper part of a large halite deposit of the Zechstein III (Leine) evaporation cycle. Large-scale mining operation has begun in 1980 by creating separate caverns with a limited size and using an oil blanket roof control method. The separate caverns were kept at lithostatic pressure. In 1993 (test) and 1995 (final) Nedmag and government agencies (state and local) agreed to change the mining method drastically, by reducing the cavern pressures and allowing the Mg-salt to flow (squeeze) towards the caverns, to be solution mined. The recovery of especially the purest magnesium chloride-source (Bischofite) increased with probably an order of magnitude. The method of injection and production has changed over time, interconnecting 8 wells with an area of about 1 km.*"

It does not seem that the cavern field experienced any significant unexpected event until 20 April 2018, when wellhead pressure at TR-2, a shut-in well, abruptly dropped by 20-30 bars. This pressure drop propagated relatively rapidly to the other wells of the cluster, which, in 2018, were composed of 9 caverns, TR-1 to 8 and VE-4.

On April 20, at ≈ 3:14, wellhead pressure, which was 88 bars before the event, began decreasing rapidly in TR-2, a brine-filled well that had been inactive for a long time (Figure 20). This pressure drop was transmitted rapidly to the neighbouring TR-5 and TR-1 wells and, more slowly, to TR-7 and the other cluster wells. Such delays are not surprising: rather than a single cavern, the cluster is a labyrinth composed of many roughly permeable conduits. At 3:36, the TR-2 wellhead pressure was about stable at 65 bars, an overall drop by 88 – 65 = 23 bars in 22 minutes (Figure 20). Stabilization was reached more slowly in the other wells of the cluster.

Note that the trend is to admit that the steady-state creep-closure rate versus cavern pressure is linear when cavern pressure is close to geostatic pressure [Bérest et al. (2019a), and Bérest and Manivannan (2019b)].

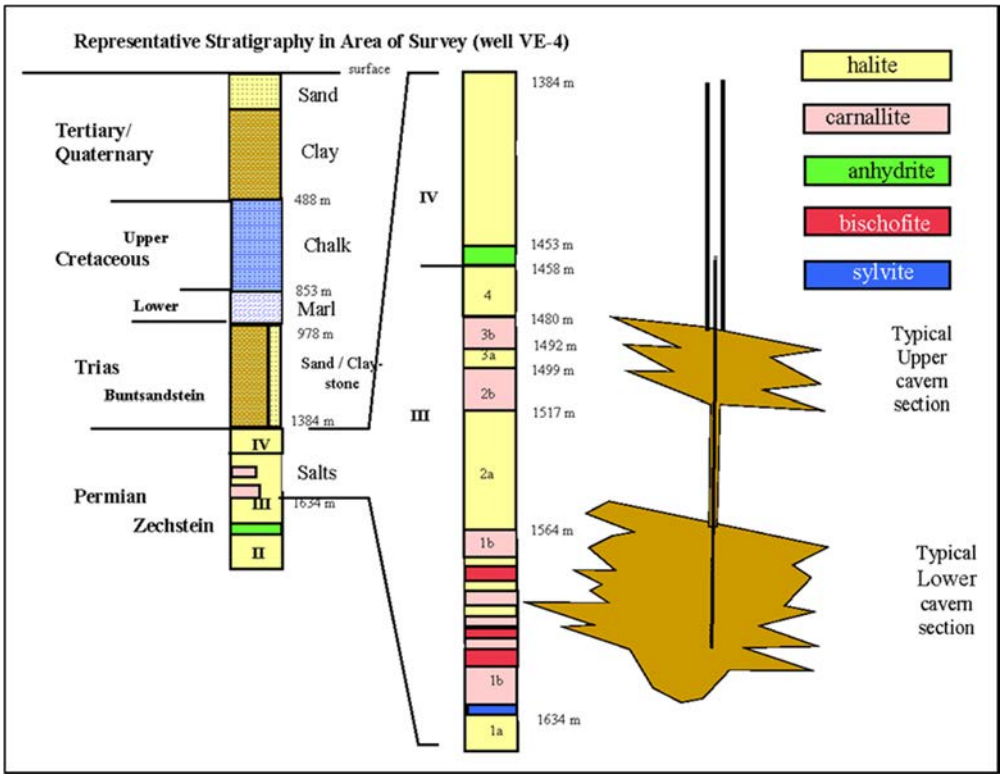

Figure 18 - Stratification of salts near Veendam, the Netherlands (Fokker et al., 2004).

Figure 19 - The Veendam cluster (Dienst ICT Uitvoering website).

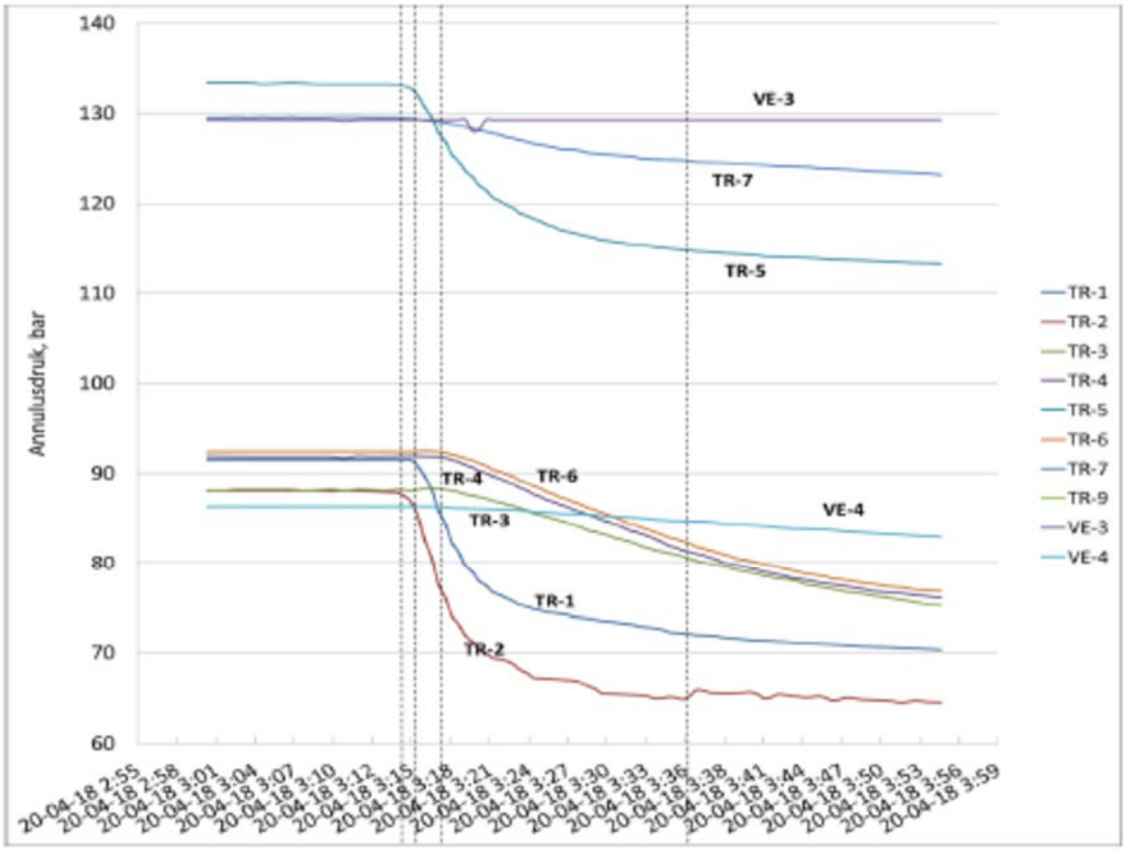

Figure 20 - The 20 April event (Dienst ICT Uitvoering website).

This event was unanticipated. A breach (roof fall or roof frac?) had been created at the roof of the cluster. It allowed brine seepage from the cluster. It is difficult to assess precisely the amount of brine that seeped from the cavern; it can be 1000 m^3 or several 10,000 m^3. It seems that the state of stress in the Bundsandstein layer (Figure 18) is strongly anisotropic (the horizontal stress is smaller than the vertical geostatic stress). Cavern pressure was 50 bars below geostatic on 20 April, which means that when a hydraulic connection is created between the cavern and the Bundsandstein layer, a fracture can be created in this layer, able to accommodate a large volume of brine (several thousand m^3). However, how the initial hydraulic connection through the salt roof was created remains open to discussion.

3.9 Clovelly salt dome, Louisiana (1992)

The Clovelly storage facility at the Louisiana Offshore Oil Port (LOOP) provides temporary storage for crude oil. In 1998, eight caverns had been constructed in a regular grid on 560-ft (171-m) centres. The caverns were constructed in a regular grid within the Clovelly dome (Figure 21). The dome has a top surface of approximately 200 acres (0.8 km²) at a depth of 1200 ft (370 m) below the surface. The vertical sides extend to a depth below 12,000 ft (3700 m). Cavern 14 is one of two caverns close to the south side of the salt dome (Figure 21). The caverns pass a mechanical integrity test (MIT), coincident with a sonar survey, every five years. The cavern is isolated with oil in place and pressured to approximately 600 psi (4 MPa). The test is successful when the pressure drop is smaller than 2 psi (13 kPa) in a 24-hour period.

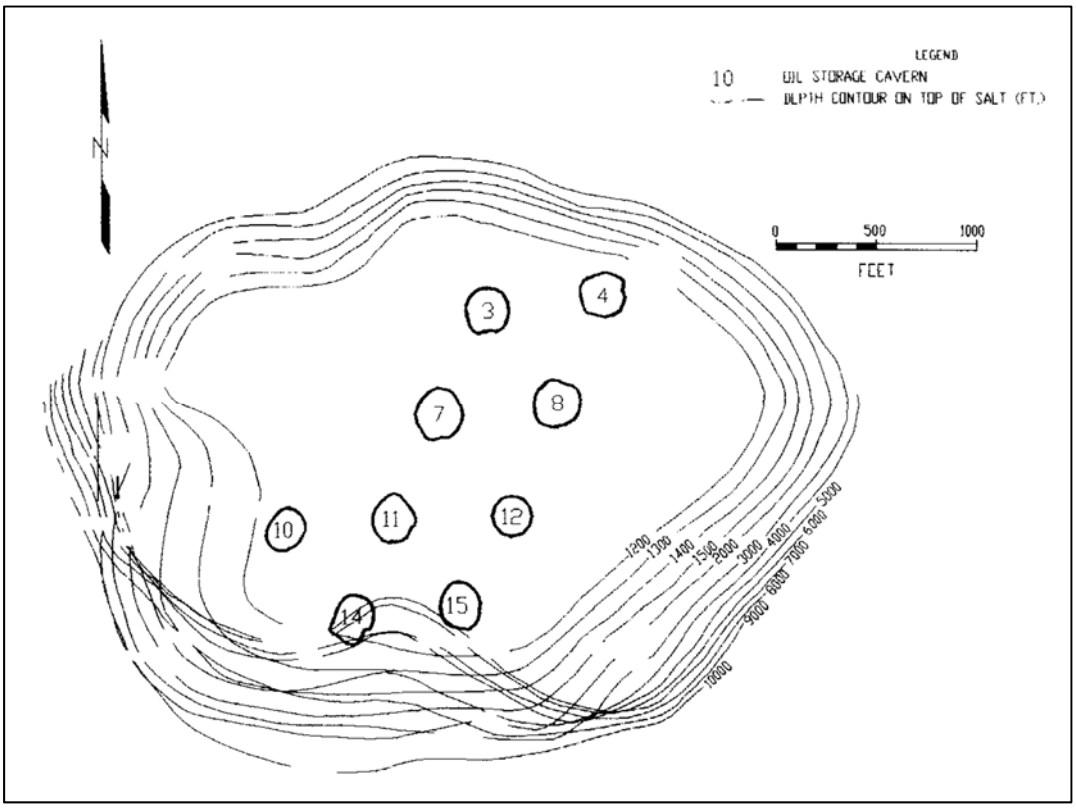

Figure 21 - Clovelly Salt Dome Contour Map. Depth contour on top of salt in ft (McCauley et al., 1998).

In 1992, during the third round of these tests, Cavern 14 failed to pass its MIT. Oil was removed immediately. No oil had been lost, suggesting that the leak was below the lowest brine/oil interface depth or that the leak was active only when cavern pressure was higher than during cavern operation. Interface tests were performed on each well. One oil/brine interface was lowered to 50 ft (15 m) below the casing shoe, and the cavern was pressurized. Density logs proved that the interfaces were stable, suggesting that the leak was below the interface depth. Prior sonar surveys in Cavern 14 had indicated an anomalous bulge approximately mid-way in the cavern at an approximate depth of 2000 ft (600 m) and oriented toward the south flank of the dome (Figure 22). A detailed survey defined the anomaly as a pronounced bulge with a flattened face, suggestive of an intersection with a wedge of extraneous material within the dome.

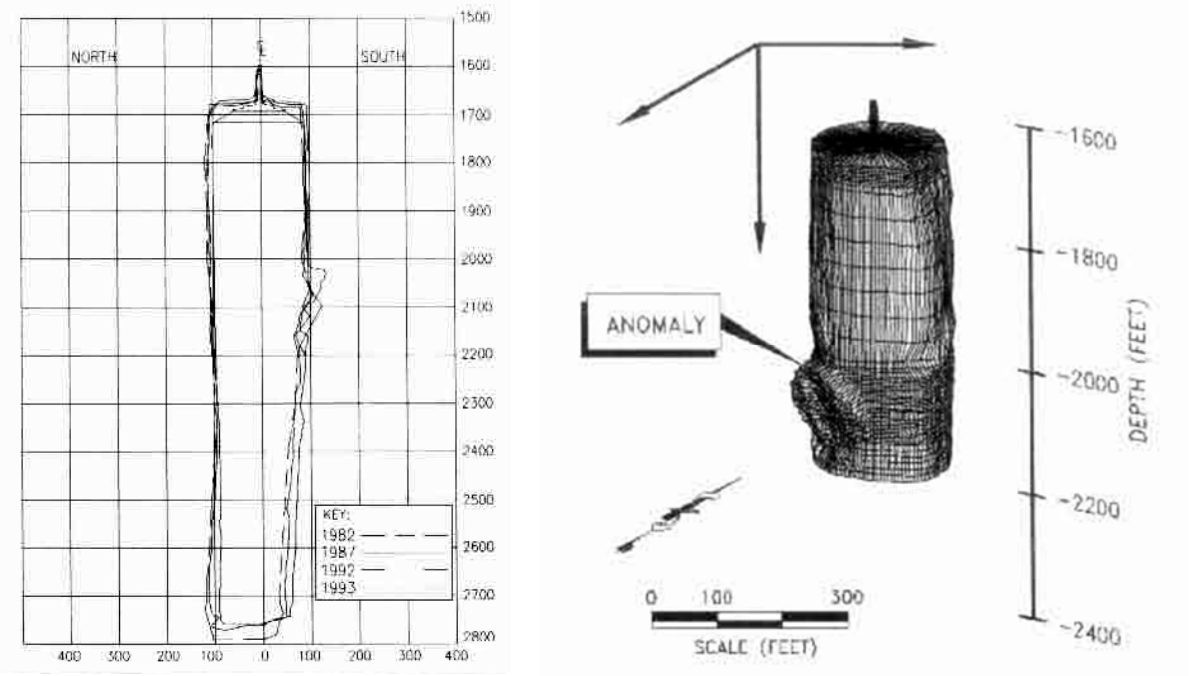

Figure 22 - Cavern 14 anomaly growth (left) and Detailed sonar survey showing anomaly interval (right) (McCauley et al., 1998).

A salt proximity survey was run from a depleted oil well located 3000 ft (900 m) south of Cavern 14. This survey revealed that a slight overhang existed on the south flank of the dome, but that Cavern 14 was at least 400 ft (120 m) from the edge of the salt. The cavern was left dormant. Brine level in the wells equalized about 300 ft (90 m) below the surface.

A bottom-hole pressure survey was conducted. The air/liquid interface was found at a depth of 500 ft (152 m). Below the interface and down to 750 ft, the pressure gradient was 0.37 psi/ft, suggesting the upper part of the well contained oil. Below 750 ft, the gradient was 0.52 psi/ft (the gradient of saturated brine). In the ground water surrounding the dome, the minimum gradient was that of fresh water, 0.433 psi/ft. As pressures must be equal at leak depth when equilibrium is reached, it was inferred that leak depth was approximately 2170 ft (661 m) or slightly deeper (water adjacent to the dome is brackish), which also is the bulge depth (the cavern roof is 1685-ft deep). The cavern was pressurized through carefully metered brine injections. During the 68-day testing period, various injection rates were used, including a 20-day shut-in period. Assuming that the leak was a linear function of the differential pressure, a simple model, consistent with the assumed leak depth, was fit against the results of the injection test. This analysis pointed to the following conclusion: it was considered highly likely that the brine leak was occurring into a sandstone layer at a depth of 2170 ft and that connection from the cavern to the exterior of the salt dome was through an "inhomogeneity‘’, physically and/or chemically different from the typical Clovelly domal salt, rather than through a fracture.

3.10 Conclusions

Several examples of pressure drops in a salt cavern were discussed. One incident (Regina South) originated from a roof fall; gas pressure was low, and fracture is highly unlikely. Two events (Bayou Corne, Clovelly) originate from the proximity of the cavern to the edge of a salt dome and the creation of a hydraulic link between the cavern and the dome flank. In the case of Clovelly, existence of a permeable layer - rather than a fracture – seems to be accepted. Two events (Mineola, Spindletop) possibly were created by a connection between neighbouring caverns. In the Mineola case, a hypothetical overpressure opened a fracture crossing through the salt wall between the two caverns; this assumption is not supported by many details. At Spindletop, probably the most puzzling case, the hydraulic connection might have been through a heterogeneity in the salt dome. In the case of the Veendam incident, creation of a fracture in the overlying Bundsandstein layer, where the state of stress is highly anisotropic, is likely. Creation of a fracture crossing the salt roof is still open to discussion.

In most cases, a definite conclusion is difficult to obtain.

4. A HISTORY OF THE ABANDONMENT PROBLEM

4.1 Executive Summary, Lessons learned from *in situ* tests

Prompted by increasing public concerns on the long-term consequences of opening underground works, and by several projects in which hazardous products were stored or disposed in salt caverns, the salt-cavern abandonment issue was raised in the 1980s (Figure 23).

The German approach

Wallner (1986, 1988) observed that, in a shut-in salt cavern, brine pressure increases as a cavern shrinks, a phenomenon called creep closure. Closure rate is slower when the gap between geostatic pressure and brine pressure is smaller, and closure rate in a tight shut-in cavern gets slower and slower. Mechanical equilibrium is reached when this gap ultimately vanishes. However, Wallner proved that, when equilibrium is reached, because of the difference in density between brine and rock, stresses at cavern wall cannot exactly equal the virgin geostatic stresses – in fact, at cavern top, tangential stresses are less compressive than brine pressure ("Wallner's margin"). In a porous and permeable rock, such a configuration would allow the onset of fractures. At that time, it often was believed that rock salt is perfectly tight: in a borehole excavated from a tight elastic rock mass, frac pressure is larger than twice the geostatic pressure. No frac can take place when brine pressure is only slightly larger than geostatic pressure.

However, rock salt behaviour is viscoplastic rather than elastic. At the wall of a cavern or a borehole excavated in a viscoplastic rock in which a constant pressure is applied, deviatoric stresses tend to decrease in the long term and the favourable "elastic" result mentioned above no longer holds. Wallner, studying the transient stress distribution in a viscoplastic rock mass (1986), proved that frac risk can be alleviated, provided that pressure increase rate is slow enough. An *in situ* test was designed and performed in a cavern at Etzel, Germany (1990-1992). Before the test, it was predicted that brine pressure could increase to a level significantly higher than geostatic pressure (typically, up to a gradient of 0.027 MPa/m, to be compared to the geostatic gradient which is 0.022 MPa/m, typically) without experiencing frac. Pressure was increased incrementally in the brine-filled cavern. In fact, salt permeability (i.e. the amount of brine entering the salt formation) increased significantly when cavern pressure was close, but lower than, the geostatic pressure at cavern depth. Djizanne et al. (2012) also observed that, during the Etzel test, cavern compressibility (the amount of brine to be injected in the cavern to increase its pressure by 1 MPa) increased long before cavern pressure is geostatic, suggesting that micro-factures or permeability increase had developed at the cavern wall.

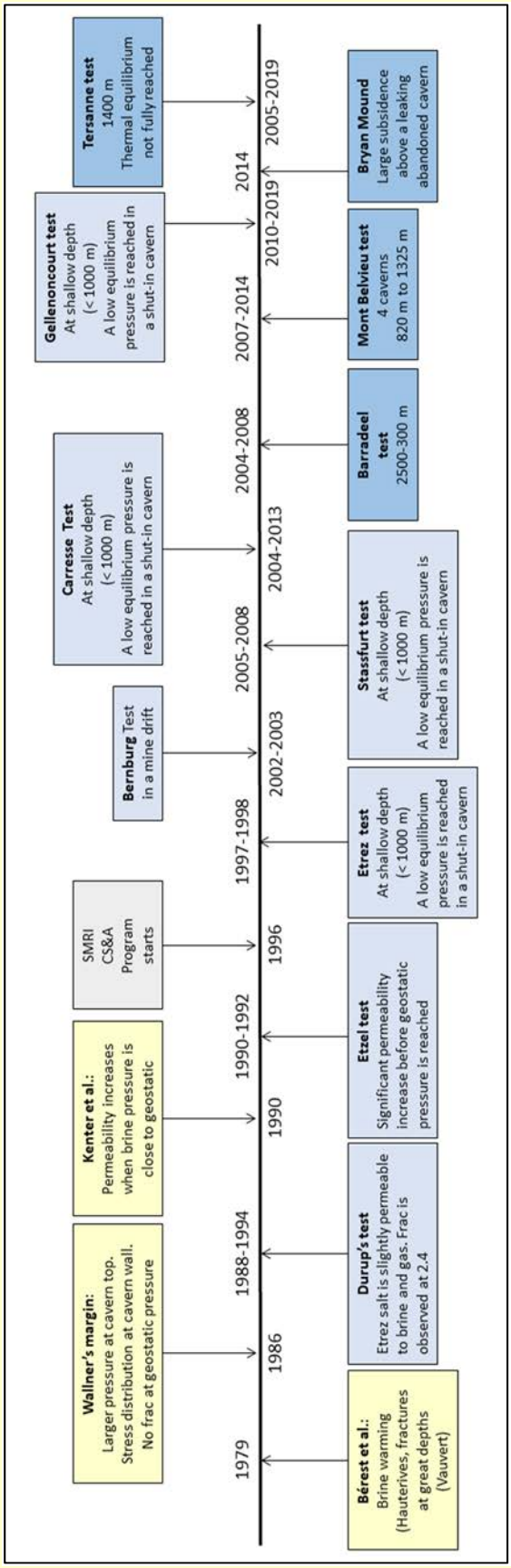

Figure 23 – Timeline of cavern-abandonment studies.

A Dutch point

In 1990, Kenter et al. published a paper describing tests performed at the laboratory on a mock-up simulating the roof of a salt cavern. Oil was used as a permeating fluid. When oil pressure was equal to, or slightly larger than, the consolidation pressure in the salt sample (which mimics the geostatic pressure), an increase of permeability by one order of magnitude was observed. These results were a breakthrough, as they proved that, from the point of view of micro-cracks opening, salt must be considered as a Terzaghi material – rather than a "tight" rock. These results were incorporated in a 1997 paper by Wallner and Paar, "*permeation seems to start when the fluid pressure equals the in-situ rock stress*".

The French approach

Bérest et al. (1979) observed that, when a cavern is shut-in, brine temperature often is significantly colder than rock mass temperature. Brine warms and thermal expansion takes place, a phenomenon that, together with cavern creep closure, leads to an increase in brine pressure. They noted that when caverns of the deep Vauvert brine field in France are shut-in, brine pressure increases rapidly. This pressure increase is generated first by creep closure. However, as cavern pressure increases, creep closure becomes much slower, and thermal expansion, a phenomenon that is independent of cavern pressure, takes the leading role. At Vauvert, pressure increase ultimately leads to the re-opening of hydraulic connections created before starting cavern leaching. Several years later, You et al. (1994) suggested that, before abandoning a Vauvert cavern, the temperature gap be smaller than 5 °C.

It has been said that rock salt used to be considered as "tight". Durup (1990 and 1994) performed permeability tests of brine and gas in a 1000-m deep borehole, EZ58, spudded in a bedded salt formation at Etrez, France. Fluid pressure was increased step-by-step; each step was 1-month long, and the duration of the tests was more than one year. Fracture was reached at a 0.024 MPa/m gradient; back-calculated salt permeability was approximately 6×10^{-10} m^2, (permeability increased when cavern pressure increased); and, as in Etzel, it was observed that borehole compressibility (i.e. borehole overall permeability) increased when pressure increased.
These results suggested that, when analysing pressure behaviour in a shut-in cavern, three main phenomena must be taken into account: brine thermal expansion, which is independent of cavern pressure; creep closure, which is a decreasing function of brine pressure; and brine permeation, which is an increasing function of brine pressure. In particular, when thermal expansion has become negligible, an equilibrium pressure, smaller than geostatic pressure, should exist such that the brine permeation rate exactly equals the cavern-closure rate (Bérest et al., 2001a). This notion remained to be proven in the field. In 1995, the Solution Mining Research Institute (SMRI) supported an abandonment test in EZ53, a 950-m deep cavern in Etrez, France. In this small and relatively old cavern, thermal equilibrium had been reached when the test began. Contrary to Wallner's initial views, primary permeability (i.e. the virgin permeability of the salt formation), which had been measured by Durup a few years before, was not considered as negligible. Based on a trial-and-error method, Bérest et al. (2001a) proved that an equilibrium pressure was reached

in the cavern such that brine permeation rate through the cavern walls exactly equalled the creep-closure rate. The equilibrium pressure was 63% of the geostatic pressure. In 2007, 13 years after the test started, cavern pressure was still the same as observed at the end of the test, 11 years before, proving that the notion of an equilibrium pressure is robust.

The SMRI Cavern Sealing and Abandonment Program

In 1996, the SMRI, which had supported the Durup tests in the EZ58 borehole and the Bérest et al. test in the EZ53 cavern, initiated a long-term program dedicated to abandonment issues. Thirteen research contracts were issued from 1996 to 2016, including literature reviews, laboratory tests, *in situ* tests, guidelines and syntheses. These efforts are described partially in the following.

Shallow Tests

Following the EZ53 test, several "trial-and-error" tests were performed (see Table 2). Their aim was to find the "equilibrium pressure" reached in a shut-in cavern.

Table 2 – Trial-and-error abandonment tests.

	Volume (m^3)	Depth[1] (m)	Idle Period[2] (yr)	Test duration (yr)	Halmostatic Pressure[3] (MPa)	Equilibrium Pressure (MPa)	Geostatic Pressure[4] (MPa)
Etrez EZ53	8000	950	25	13	11.4	13 ± 0.1	20.9
Bernburg	22	450	-	2	5.4	??[5]	9.9
Gellenoncourt SG13-14	140 000	250	30	7	3	3.55 ± 0.15	5.5
Stassfurt S102	13 500	43	30	4	5.2	8.25 ± 0.15	9.6
Carresse SPR2	9000	300	1	8	3.6	4.5[6]	6.6

1. Depth at which pressures are computed (casing shoe depth, or average depth)
2. Duration of the period before the test started during which small or no movement were performed
3. Based on a 0.012 MPa/m gradient
4. Based on a 0.022 MPa/m gradient
5. Steps too short to define equilibrium pressure precisely
6. Last step too short (brine still warming)

These tests and their interpretation by several different groups confirmed that brine pressure evolution in a shut-in cavern results from five main factors:

- **creep closure** (both transient and steady-state) whose influence, in general, is to increase cavern pressure. Creep closure is faster when brine pressure is lower.
- **brine warming**, a transient process that comes to an end after a period that is longer when the cavern is larger and whose influence, in general, is to increase cavern pressure.

- **brine permeation** through the cavern walls (Permeability can be "primary" (pre-existing) or "secondary" (resulting from cavern creation and operation). Permeation is faster when brine pressure is higher.
- **Additional dissolution** is a transient phenomenon (when brine is not fully saturated, additional dissolution takes place, ultimately leading in a cavern volume increase and pressure decrease).
- **Brine leaks** through the wellbore

When thermal equilibrium has been reached and the wellbore is tight, brine pressure reaches an equilibrium pressure, resulting from the opposite effects of creep closure and brine permeation. Equilibrium pressure significantly lower than geostatic pressure.

Deep tests

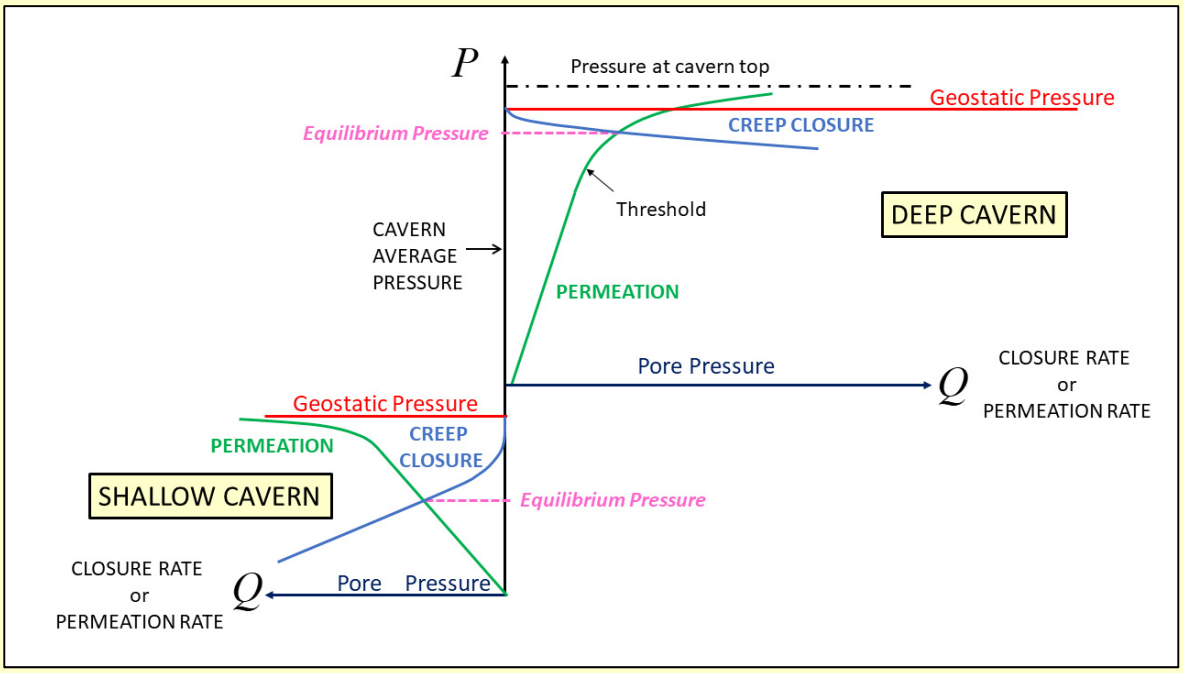

Figure 24 - Cavern pressure versus cavern closure rate and permeation rate. The difference between "pressure at cavern top" and "equilibrium pressure" is "Wallner's margin".

"Deep" caverns, however, raised a difficult problem; see Figure 24 ("deep" caverns are deeper than 1000 m; in fact, this limit is somewhat artificial, as creep ability and virgin permeability play a significant role and are site-dependent). Generally speaking, in a deeper cavern, one can expect that the cavern-closure rate is faster, as rock temperature and geostatic pressure are higher. It also can be suspected that permeability is smaller (however, when cavern pressure is higher than some "threshold", it is likely that rock permeability at cavern wall increases). These two reasons lead to an equilibrium pressure at cavern mid-depth much closer to geostatic pressure than that in a shallow cavern. Following Wallner's argument, see Section 4.2.1, it can be expected that, in an elongated cavern, brine pressure be higher than equilibrium pressure at cavern mid-depth.

However, it proved difficult to find deep testing caverns in which thermal equilibrium was reached. Pressure increase rate was governed at least partly by brine warming, a phenomenon whose influence was moot in the small and old “shallow” caverns in which the first series of tests had been performed. In that sense, the “deep” tests proved to be less conclusive than the “shallow” tests.

An abandonment test was supported by the SMRI at Mont Belvieu, Texas, on four relatively deep caverns. Shut-in tests were performed from 2007 to 2014. The pressure increase rate (due to brine warming and cavern creep closure) was high and, approximately after a 1-year long period, the maximum pressure allowed by the regulatory authorities (corresponding to a gradient of 0.8 psi per foot, or 0.018 MPa/m) was reached. Caverns were vented and a new testing phase began. Experimental determination of an equilibrium pressure (which might be suspected to be higher than 0.8 psi/ft) was impossible in such conditions (except through computations).

A shut-in test was performed in the Netherlands at Barradeel (2004-2008) in a 2500-3000-m cavern. During the first weeks, the pressure increase rate was extremely fast, a consequence of rapid creep closure. After this first period, brine warming, a slower phenomenon, began to be pre-eminent (this evolution is similar to what was observed at Vauvert, also a deep cavern). Some brine was injected in the cavern to increase cavern pressure. The increased pressure rate became exceedingly slow. Cavern compressibility was measured at different periods of the test. These measurements were very insightful. As at Etzel K-102 or Etrez EZ58, cavern compressibility increases significantly when the cavern is higher than a certain threshold. It is likely that micro-cracks open at cavern wall. At the end of the test, when cavern pressure is merely constant, it is reasonable to assume that a large amount of brine permeates into the rock mass.

It is extremely difficult to assess if this large brine permeation is due to the development of many micro-cracks whose lengths remain relatively small or to the development of a much smaller number of open fractures whose lengths are, say, several dozens of meters. Opposite to the case of a borehole, compressibility of a cavern is very large and the opening of a fracture (“breakdown”) does not lead to a large pressure drop. This difficulty raises the problem of a precise definition of a fracture, relevant for the abandonment issue. In the case of the Barradeel test, the definition provided by van Heekeren et al. (2009) is practical rather than theoretical: a fracture is a hydraulic link between the cavern and a porous-permeable layer allowing a large quantity of brine to flow from the cavern to the layer (what is known from the Veendam case suggests that such a link was created between the brine cavern and the overlying Bundsandstein layer, in which a fracture was created; there is no direct proof that a mechanical fracture was created through the salt roof, which may have fallen) . In such a sense, it was likely that no fracture was created at Barradeel [more recently, it is believed that the brine flow reached a neighbouring wellbore]. However, it is not impossible that fractures, in a mechanical sense (i.e. planar discontinuities in an initially continuous medium), were created, and their later evolution is difficult to predict.

4.2 The German approach

4.2.1 Wallner's conceptions

Several important notions were introduced by Langer et al. (1984) and Wallner (1986, modified later by Wallner and Paar 1997, see Section 4.3).

4.2.1.1 Long-term brine pressure distribution in a sealed cavern

After a brine-filled cavern is sealed (initial wellhead pressure is zero), a pressure increase is observed. Computations (taking into account cavern creep closure and cavern compressibility, see Section 5.7; rock is assumed to be perfectly tight) suggest that steady state is reached after a long period of time (cavern pressure remains constant and equal to geostatic [also called lithostatic] pressure, at least approximately). "*However, for this final situation, the internal fluid pressure is not in equilibrium with the rock stress. The fluid pressure at the top of the cavity exceeds the lithostatic stress at that depth by a substantial amount, at the bottom of the cavity the rock stress is higher than the fluid pressure*" (Wallner, 1986; see Figure 25). The origin of this effect is in the difference between brine density and rock density. For instance, the volumetric weight of brine and rock are 0.012 MPa/m and 0.022 MPa/m, respectively. When cavern height is h [in m], brine pressures at the cavern top and cavern bottom differ by 0.012 MPa/m × h; for geostatic pressure, the difference is 0.022 MPa/m × h. Brine pressure cannot equal geostatic pressure at any depth, and additional stresses are created; they are tensile in the cavern upper part, which slowly enlarges, and compressive in the cavern lower part, which slowly shrinks. The order of magnitude of the tensile stress is (0.022 MPa/m - 0.012 MPa/m) × h/2, or 0.5 MPa when cavern height is h = 100 m ("*Wallner's margin*").

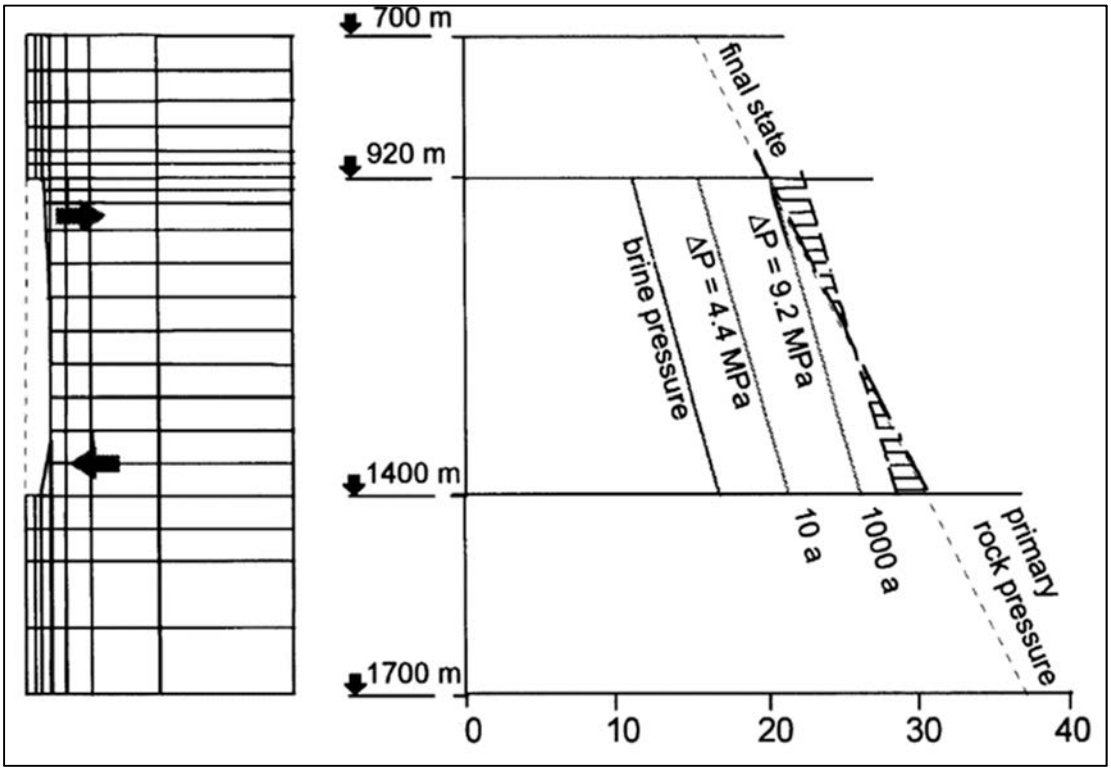

Figure 25 - Pressure build-up in a sealed cavity (Wallner, 1986).

4.2.1.2 Influence of pressure rise rate

In his 1986 paper, Wallner points out an important notion, discussed by Wawersik and Stone (1989) and which were discussed later by many authors: as salt behaviour is viscoplastic, rather than elastic, stress distribution in a borehole during a frac test is significantly different from what generally is assumed.

In Wallner's 1986 conception, salt is a perfectly tight rock, there is no "effective" stress (in Terzaghi's sense), and, in a vertical borehole of radius r_0, fracture is reached when fluid pressure is larger than

$$P_f = 3\sigma_h - \sigma_H + T \qquad T > 0 \text{ is small} \tag{9}$$

where T is the rock tensile strength, which typically is 1-2 MPa and often is assumed to be zero to be on the safe side, σ_h and σ_H are the two principal horizontal stresses (compressive stresses are positive). In the case of a formation in which the state of stress is isotropic (an assumption often made when a salt formation is concerned), $\sigma_h = \sigma_H = \bar{\sigma}$. When, in addition, rock behaviour is elastic, the condition can be written: $\sigma_\varphi > 2\bar{\sigma}$, where σ_φ is the hoop (or orthoradial) stress. This is illustrated by Figure 26 (from Wallner, 1986): wellbore pressure first is equal to $p_i = 0$, and hoop stress at the cavern wall is $\sigma_\varphi = 2\bar{\sigma}$. Pressure then is increased to $p_i = 2\bar{\sigma}$, and the hoop stress becomes $\sigma_\varphi = 0$ at the cavern wall, $r = r_0$. When $p_i > 2\bar{\sigma}$, the hoop stress is tensile and fracturing becomes possible. In fact, this prediction is overly optimistic, but it is consistent with the "perfectly tight" assumption.

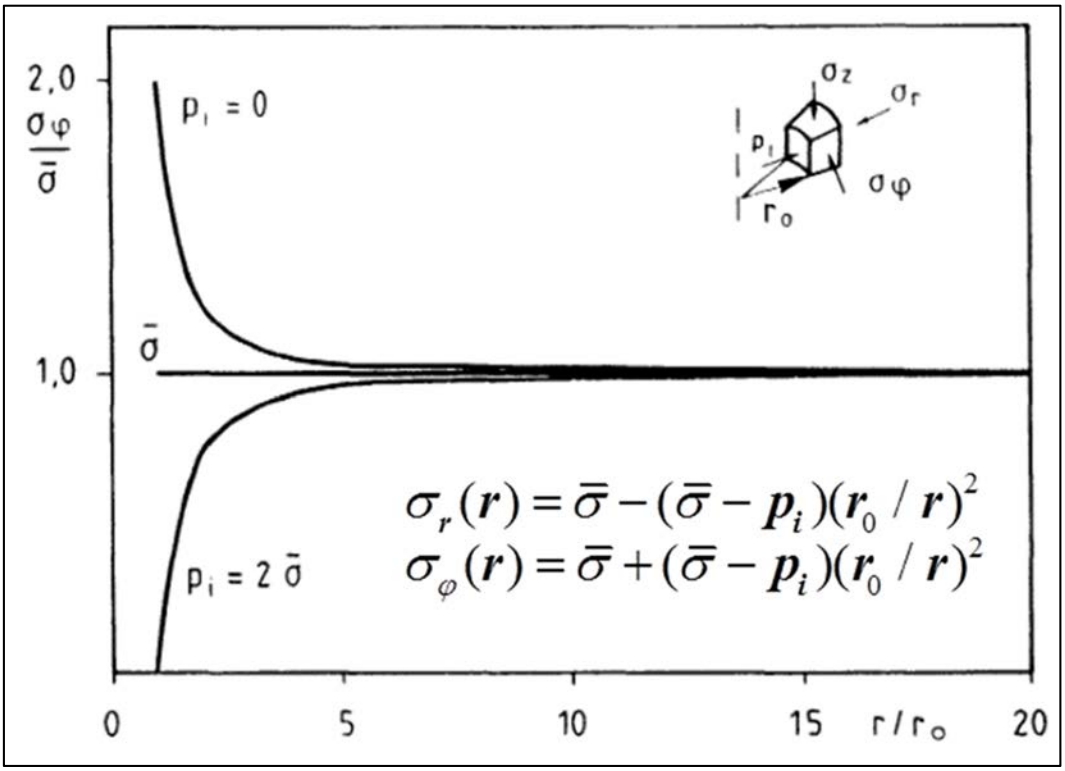

Figure 26 - Distribution of the hoop stress, σ_φ, when rock behaviour is elastic (Wallner, 1986).

Wallner's idea is that, in the case of a viscoplastic rock, stress distribution is time-dependent and can be more favourable from the perspective of fracture initiation (i.e. onset of tensile hoop stress at the open-hole wall). For instance, Wallner considers a borehole in which fluid pressure drops abruptly from $p_i = \bar{\sigma}$ to $p_i = 0$. Stress distribution is elastic at first; however, in sharp contrast with elastic behaviour, stress distribution slowly evolves and, after a long period of time ($t = \infty$), hoop stress distribution is as represented on Figure 27. The hoop stress after a long period of time is much less compressive than when the elastic solution is considered.

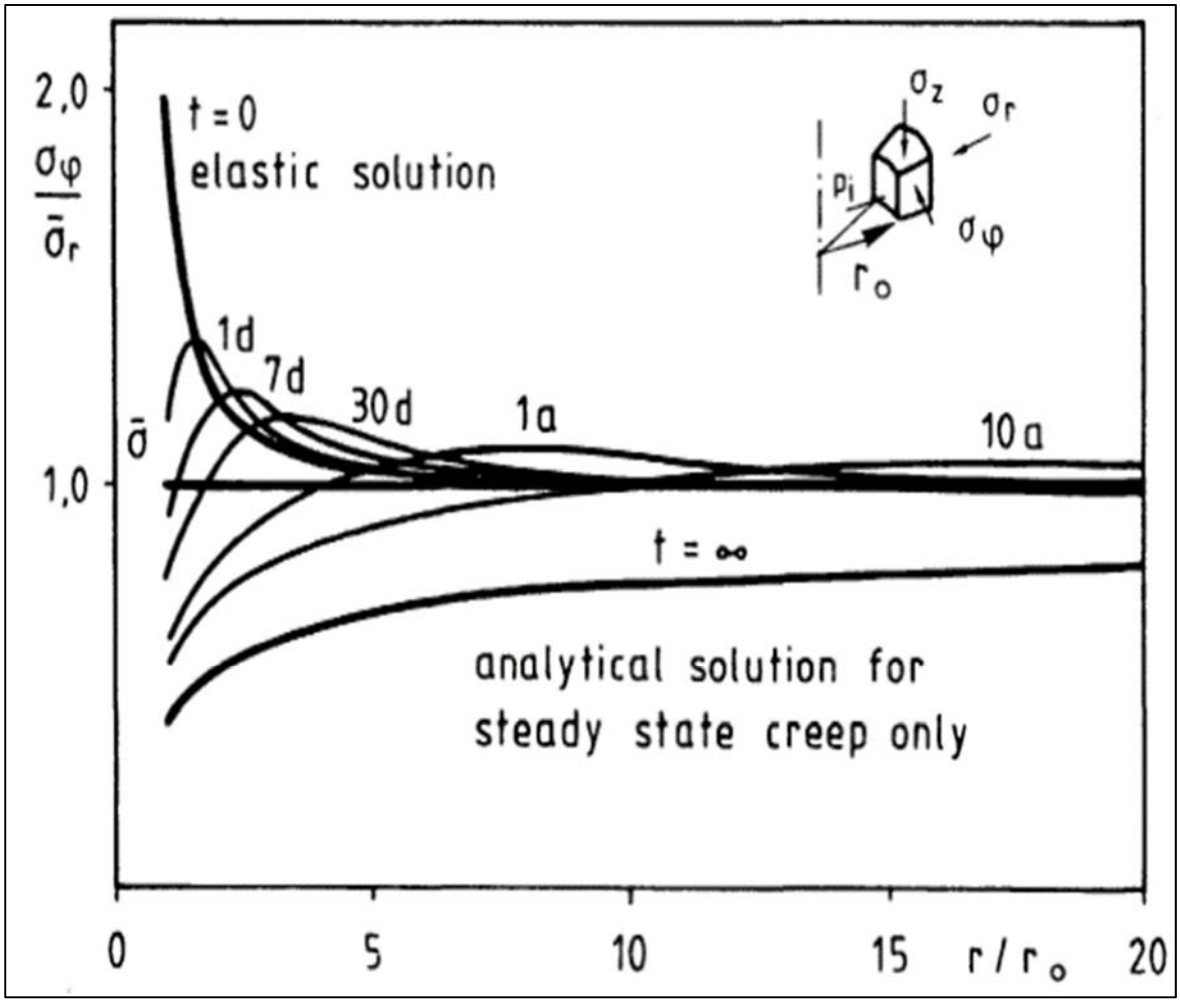

Figure 27 - Distribution of the hoop stress, $\sigma_\varphi = \sigma_\varphi(r,t)$, when $p_i(t<0) = \bar{\sigma}$ and $p_i(t>0) = 0$. Rock behaviour is viscoplastic (Norton-Hoff law, $\dot{\varepsilon} = \dot{\sigma}/E + A(T)\sigma^n$: $E = 24$ GPa, $\nu = 0.27$, $A = 0.18$ /day/MPa^n, $n = 5$) (Wallner, 1986).

Wallner (1986) draws on this idea and considers the following problem: At $t = 0$, borehole pressure abruptly drops to zero from $p_i = \bar{\sigma}$ to $p_i = 0$ (the elastic solution applies). Then, a slow brine-pressure increase is applied in the borehole. When the brine-pressure rate is slow enough, hoop stress is given enough time to redistribute and remains compressive, see Figure 28: initial brine pressure is zero; $\bar{\sigma} = 22$ MPa, and pressure increase rate is $\dot{p}_i = 1$ MPa/day. When $t = 44$ days,

$p_i = 44$ MPa $= 2\bar{\sigma}$. However, hoop stress at the cavern wall is compressive (and close to $\sigma_h = \sigma_H = \bar{\sigma}$) in sharp contrast with the elastic case.

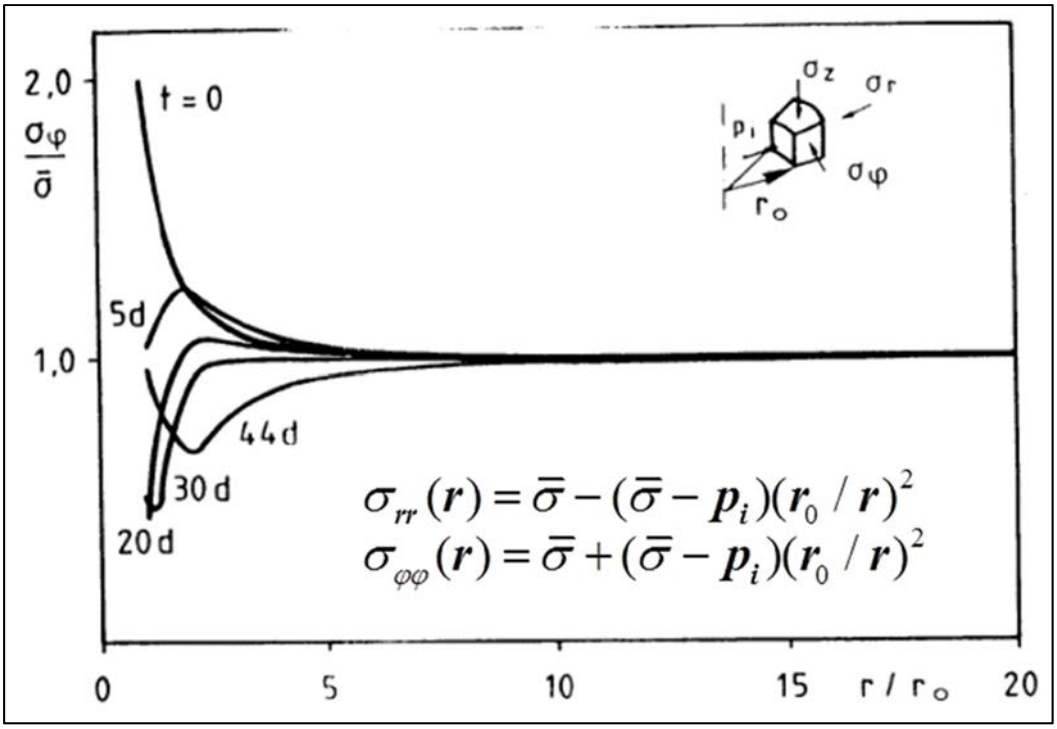

Figure 28 - Distribution of the hoop stress, $\sigma_\varphi = \sigma_\varphi(r,t)$, **when** $p_i(t<0) = \bar{\sigma}$, $p_i(0) = 0$, **and** $p_i(t>0) = \dot{p}_i t$. **Borehole depth is 1000 m,** $\bar{\sigma} = 22$ MPa, **rock behaviour is viscoplastic (Norton-Hoff law,** $\dot{\varepsilon} = \dot{\sigma}/E + A(T)\sigma^n$: $E = 24$ GPa, $\nu = 0.27$, $A = 0.18$ /day/MPa^n, $n = 5$**) (Wallner, 1986).**

When these results are transposed to a cavern (cavern shape is not an idealized cylinder, and numerical computations must be performed), they suggest that, in a shut-in cavern, whose pressure increases slowly enough, fracturing risk can be alleviated even when cavern fluid pressure is higher than geostatic pressure. Obviously, this notion must be discussed on a site-by-site basis: cavern depth, constitutive law, parameters of the constitutive law, fluid pressure increase rate and duration of the idle period before cavern shut-in (and cavern height, as discussed in Section 4.2.1) must be taken into account.

This is illustrated by Figure 29: different cavern depths and different values of the parameters of the constitutive law are considered, (1), (2), (3); the pressure rise rate for which hydrofracturing risk must be considered is discussed.

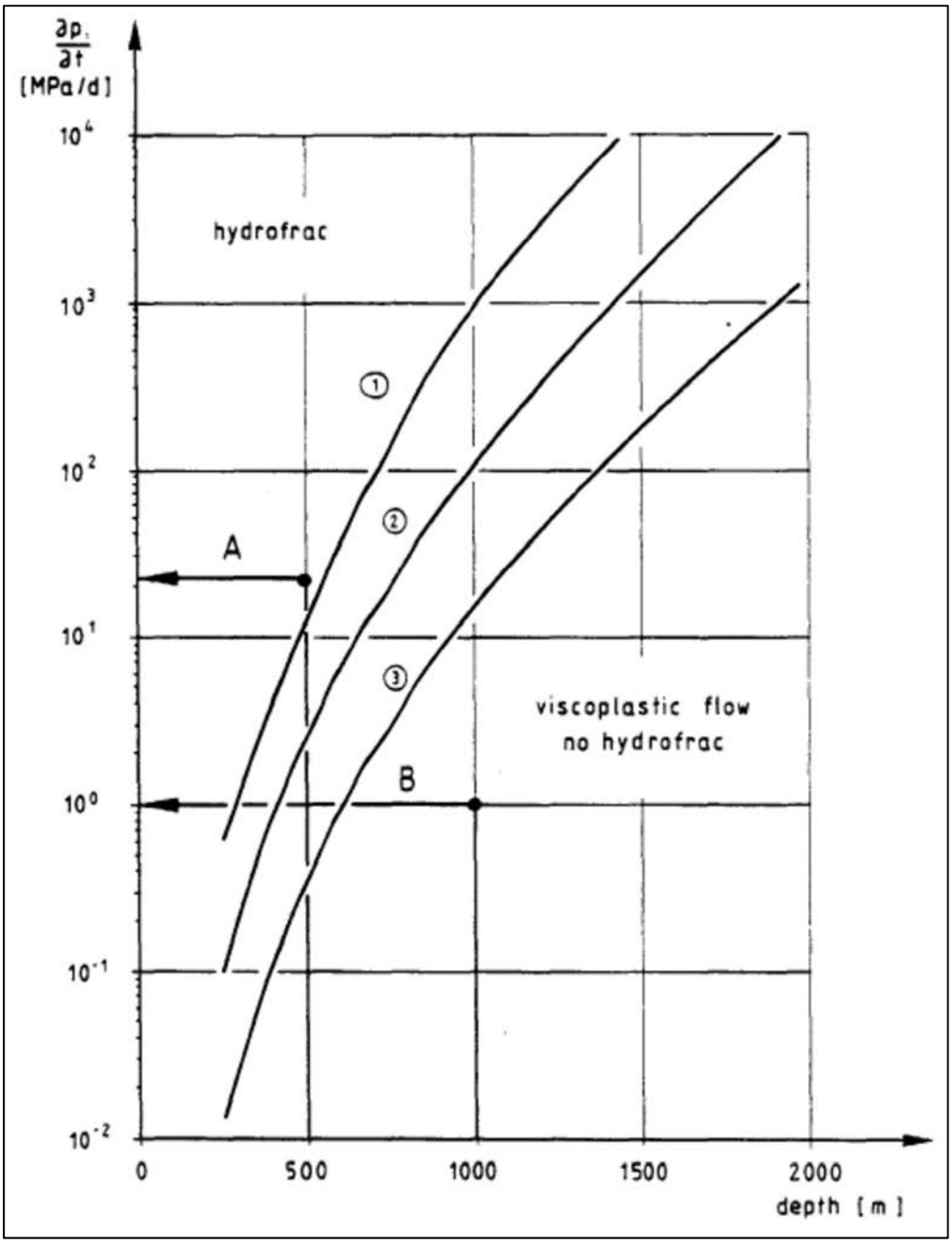

Figure 29 - Critical pressure increase rate in a cavern as a function of cavern depth. Different sets of parameters of the viscoplastic constitutive law are considered (1), (2), (3) (Wallner, 1986).

4.2.1.3 A comment on Wallner's conception

Wallner's conception is extremely important, as it inspired the design of the Etzel test. Taking into account the influence of time on stress distribution at the cavern wall was a brilliant idea, which later would be used by many authors. However, the notion of rock salt as a "tight rock" (fracturing can occur when $p_i = p_f > 3\sigma_h - \sigma_H + T$) will prove to be incorrect, as highlighted for instance by Kenter et al. (1990) and Fokker (1995), see below.

4.2.2 The Etzel abandonment test (1990-1992)

Cavern K-102 at Etzel (Germany) was solution-mined between 1974 and 1978 (Figure 30). Oil was stored until April 1983. Oil then was removed and, later, the cavern was filled with brine — except from a short period in August 1987. Cavern pressure certainly was not constant during the 1978-1990 period, and the cavern was vented periodically. A maximum brine-related head pressure of 6.95 MPa was reached at the end of February 1988; the associated gradient (at a given depth, liquid pressure divided by depth) at casing-shoe depth was about *G* = 0.0205 MPa/m. In April 1989, the Etzel K-102 cavern volume was *V* = 233,000 m^3. Casing-shoe depth was 827.7 m, cavern roof depth was 850 m, and cavern height was 622 m.

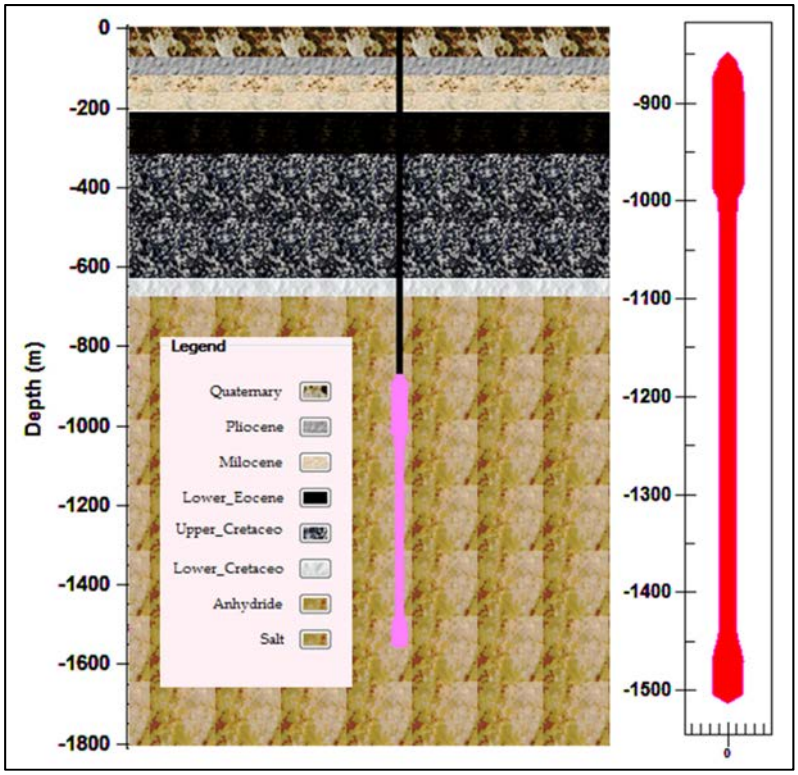

Figure 30 - Simplified geometry and stratigraphy of the Etzel K-102 Cavern (Djizanne et al., 2012).

In 1990, the Druckaufbautest Consortium decided to start a pressure build-up test in the Etzel K-102 cavern (Rokahr et al., 2000, from which the following description is drawn). The objective of the test was to obtain *in situ* data as a basis for defining a cavern abandonment procedure. At that time, the state of the art (see above, Section 4.2.1) was that cavern pressure could be increased to a high figure (a pressure gradient of *G* = 0.032 MPa/m at casing-shoe depth) provided that pressure build-up rate was slow enough.

The pressure gradient at casing-shoe depth was increased incrementally. The first step, at the end of which $G = 0.019$ MPa/m at casing-shoe depth, was reached after injecting approximately $\Delta V = 500$ m^3 in 45 days. At casing-shoe depth, cavern pressure increased by $\Delta P = 827.7 \times (0.019 - 0.012) = 5.79$ MPa (dot 1, Figure 31). The pressure-increase rate was slightly

faster than 0.1 MPa/day. The cavern compressibility coefficient during this period can be inferred to be $\beta = \Delta V / (V \Delta P) = 3.7 \times 10^{-4}$ /MPa (this figure is low).

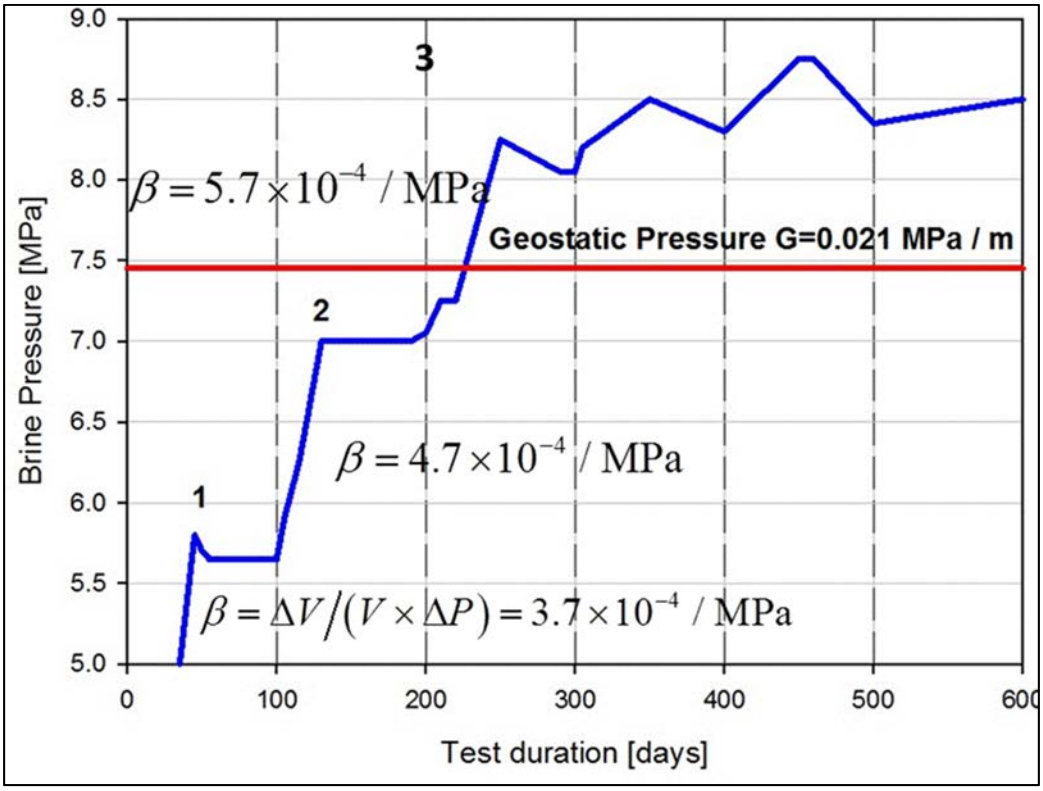

Figure 31 – Wellhead Pressure Evolution During the Etzel K-102 Test (Djizanne et al., 2012). Wellhead brine pressure is nil at the beginning of the test (day zero).

Cavern Compressibility

Cavern compressibility, or βV [in m^3/MPa], is the amount of brine [in m^3] to be injected in a cavern to increase its pressure by 1 MPa. In the case of a tight cavern, cavern compressibility can be computed using mass conservation, $d(\rho_b V) = \rho_b Q$; brine density is ρ_b, and Q_b is the injected-brine flowrate. Both brine and cavern are elastic bodies, and their densities or volumes vary when cavern pressure, p_i, changes; $\dot{\rho}_b = \rho_b^0 \beta_b \dot{p}_i$, where $\beta_b = 2.7 \times 10^{-4}$ /MPa is typical; and $\beta_c = \beta_c(E, \nu, \partial V)$, where E and ν are the elastic modulus and Poisson's ratio of the rock mass, respectively; ∂V is the cavern shape. In principle, $\beta = \beta_c + \beta_b$ does not depend on cavern pressure during a rapid injection. When β is not constant during an injection test, it means that the elastic assumption is not correct (i.e. "reverse" creep takes place, and cavern volume increases; however, this effect is small, Bérest et al., 2015) or that the cavern is no longer perfectly tight: some brine outflow through the cavern walls must be taken into account, see Section 4.7. Several tests described in this report suggest that the apparent compressibility increases significantly when cavern pressure is high.

The second step, at the end of which *G* = 0.0205 MPa/m, was reached after 134.4 m^3 were injected from day 100 to day 130 (approximately), dot 2 on Figure 31. The (apparent) compressibility coefficient during this step was $\beta = 4.7 \times 10^{-4}$ /MPa, a significant increase when compared to the first step. This result suggested that fractures or "secondary" permeability might have been created long before the geostatic gradient was reached. For this reason, the measured cavern compressibility is said to be "apparent": at low pressure, cavern compressibility reflects the elastic properties of cavern brine and rock mass (which depend on $E, \nu,$ and cavern shape). At high pressure (but lower than geostatic) apparent cavern compressibility reflects the elastic properties of cavern brine and rock mass plus the onset (or a large increase) of brine flow through the cavern walls. This notion is also evident during Durup's test (see Section 4.3.3).

During the third step, (apparent) compressibility consistently increased. After 7 weeks, 179.5 m^3 had been injected, and a gradient of G = 0.0219 MPa/m was reached. (The apparent compressibility coefficient was $\beta = 5.7 \times 10^{-4}$ /MPa, a sign of permeability change see Section 5.7.) After pumping stopped, cavern pressure consistently decreased. During the fourth step, a maximum gradient of *G* = 0.233 bar/m was reached; however, "*from this point on, the pressure in the cavern dropped gradually despite continued brine pumping*" (Rokahr et al., 2000, p. 92).

Before the test, it was believed that the geostatic (or lithostatic) gradient was $G_{geo} = 0.0241$ MPa/m, a high figure in the context of a salt formation. Well logs from existing and new boreholes were re-assessed and resulted in a revised figure of $G_{geo} = 0.024$ to 0.0211 MPa/m (this re-assessment proves that some uncertainty always exists when the value of the geostatic pressure is concerned). Opposite to what was believed before the test, although the pressure-increase rate was relatively slow, the cavern ceased to be perfectly tight before the cavern pressure equalled the geostatic pressure.

4.2.3 Consequences of the Etzel test

In conclusion, this test proves that salt permeability at the cavern wall can increase significantly even when cavern pressure is below geostatic. Interpretation of this test gave rise to an abundant literature (e.g. Rokahr et al., 2000; Lux et al., 2006; Djizanne et al., 2012), and most authors accepted that salt permeability at cavern wall increases when brine pressure is larger than the least compressive (tangential) stress at cavern wall. Such an idea, based on laboratory tests, had been suggested by Kenter et al. (1990), see Section 4.3. The Etzel test proved that this idea was still correct at cavern scale.

This test also proved that permeability increase started when the cavern pressure was significantly below geostatic. Djizanne et al. (2012) suggested that stress redistribution in the rock mass during the 1978-1900 period, when cavern pressure was relatively low, led to small tangential stresses at the cavern wall during the test (an idea reminiscent of Wallner's conception) and that the sequence (long low-pressure period in the cavern followed by swift pressure increase) can be at the origin of early microfracturing in a pressurized cavern.

4.3 A Dutch point

Wallner's ideas were based on the assumption that rock salt is completely impermeable to salt. In fact, as stated by Fokker (1995, p.46):

> *''… under this assumption, the elastic breakdown pressure in [a] borehole is theoretically more than twice the lithostatic pressure for an isotropic stress field ... However, elastic breakdown in never reached in rocksalt at this level. Various authors … have explained this discrepancy on the basis of the visco-elastic behavior of rock salt. … Although a creep related tangential stress drop without doubt occurs … it cannot explain the behavior observed in the laboratory and in the field*.''

Fokker mentions several laboratory or field tests that are not consistent with Wallner's assumption (including Durup's tests at EZ58, described in Section 4.4.3) and adds "*if … fluids are assumed to penetrate into the salt under certain … conditions and salt is treated as a Terzaghi material … the above laboratory and field observations can be properly and consistently explained*."

Fokker mentions earlier tests described in Kenter et al. (1990) that strongly support his views. A cylindrical sample is mounted in a high-pressure cell after being consolidated at isotropic stress (to heal microcracks opened during cutting and sampling). Oil is used as a testing fluid. Pressure is increased below the sample, and permeating oil is collected in a chamber above the sample. When fluid pressure is slightly larger than the consolidation pressure applied to the sample, an increase of permeability by one order of magnitude (from 0.1 to 1.5 µDarcy (10^{-19} to 1.5×10^{-18} m²) can be observed. It is interesting to notice that the "virgin" (after consolidation) permeability was small but non-zero. Permeation was through crystal boundaries. A large number of tests were performed; in particular, it was proved that the "virgin" permeability was a decreasing function of the consolidation time, suggesting that, when geological times are considered, consolidation can reduce salt permeability to extremely small values.

These results were a breakthrough; they proved that, from the point of view of micro-crack openings, salt should be considered as a Terzaghi material: a large permeability increase can be observed when the effective stress (the least compressive stress minus the applied fluid pressure at the salt wall) is negative – i.e. tensile. To a certain extent, they were able to explain the unexpected results of the Etzel test, as was mentioned by Wallner and Paar (1997).

Later tests confirmed these results. For instance, the SMRI supported permeability tests performed at Ecole Polytechnique on hollow spheres. A small cavity, volume 30 cm^3, is leached out at the centre of a carved salt sphere whose diameter is 25 cm. On the external radius, both a fluid pressure (which mimics pore pressure in the rock mass) and a radial stress (which mimics geostatic pressure) are applied. Internal pressure is increased incrementally. When internal pressure is slightly smaller than the "geostatic" stress, a drastic increase in permeability is observed (Bérest et al., 2000, 2001b).

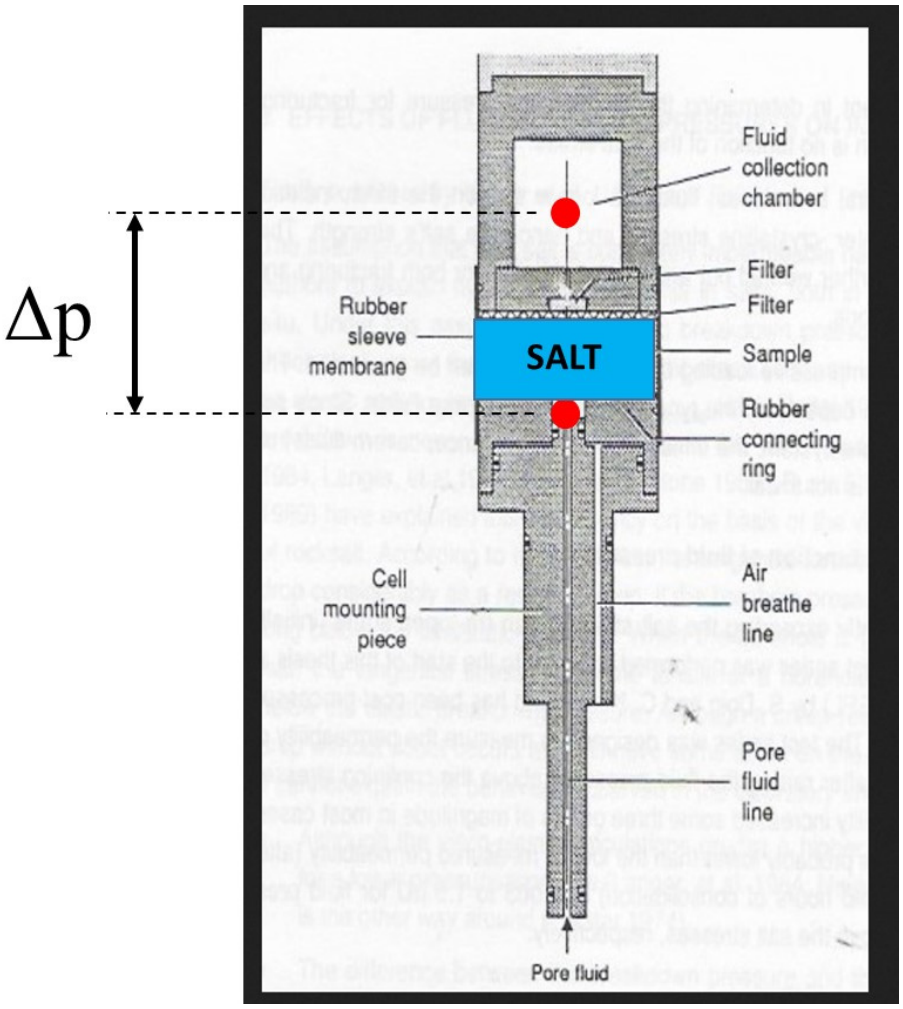

Figure 32.

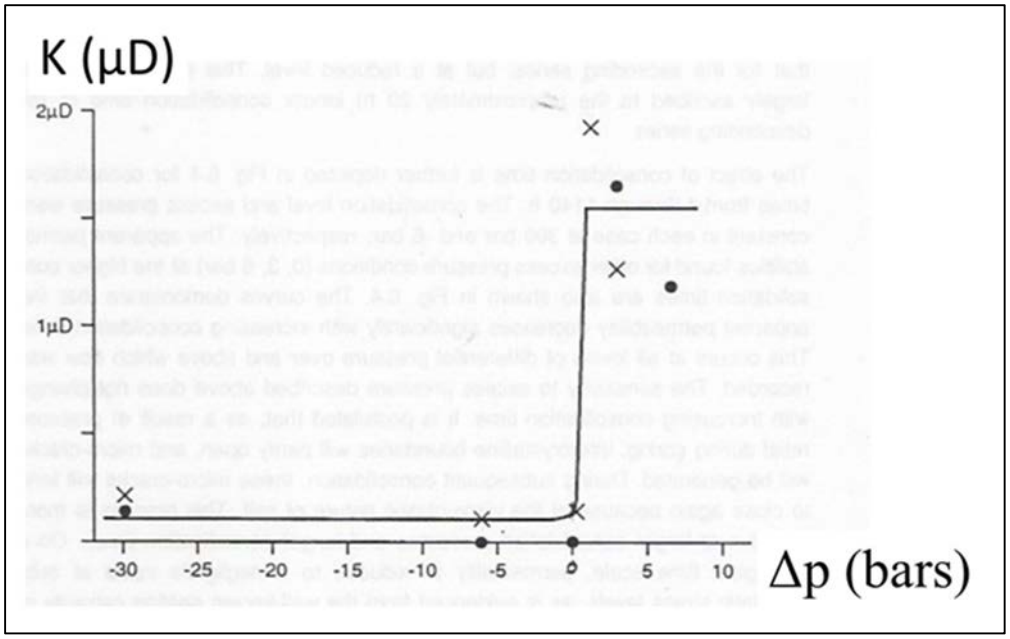

Figure 33 - Test set-up (left) and permeability as function of excess pressure (After Fokker, 1995)

4.4 The French Approach

4.4.1 Brine thermal expansion

In 1979, Bérest et al. discussed two notions that later would prove to be related closely to the abandonment issue: brine thermal expansion, and onset of fracture in a shut-in cavern. They discussed a pressure build-up observed after a two-well cavern was shut-in at Hauterives, France on 26 May 1975. Pressures are recorded at the wellheads of the two wellbores (Figure 34). A small leak was detected at day 90. Cavern depth is between 1550 m and 1650 m; the rock geothermal temperature at such a depth is 61°C; brine temperature when the cavern was shut-in was estimated to be 26 °C. The overall volume of the cavern was 430,000 m^3. Simple numerical computations were performed (a sphere whose volume is the same as the cavity's) and proved that a large part of the pressure rise could be explained by brine thermal expansion (the rest originates in cavern creep closure). They suggested a simple rule of thumb (see Section 5.4): a 1 °C brine temperature increase generates a brine pressure rise of 1 MPa in a tight shut-in cavern. An abundant literature has been dedicated to brine warming in a cavern (see, for instance, Karimi-Jafari et al., 2007), a notion that now is widely accepted. Wellhead pressure evolution in the Hauterives HA6-7 cavern were computed taking into account the effects of brine warming (Bérest et al., 2000b, Figure 35).

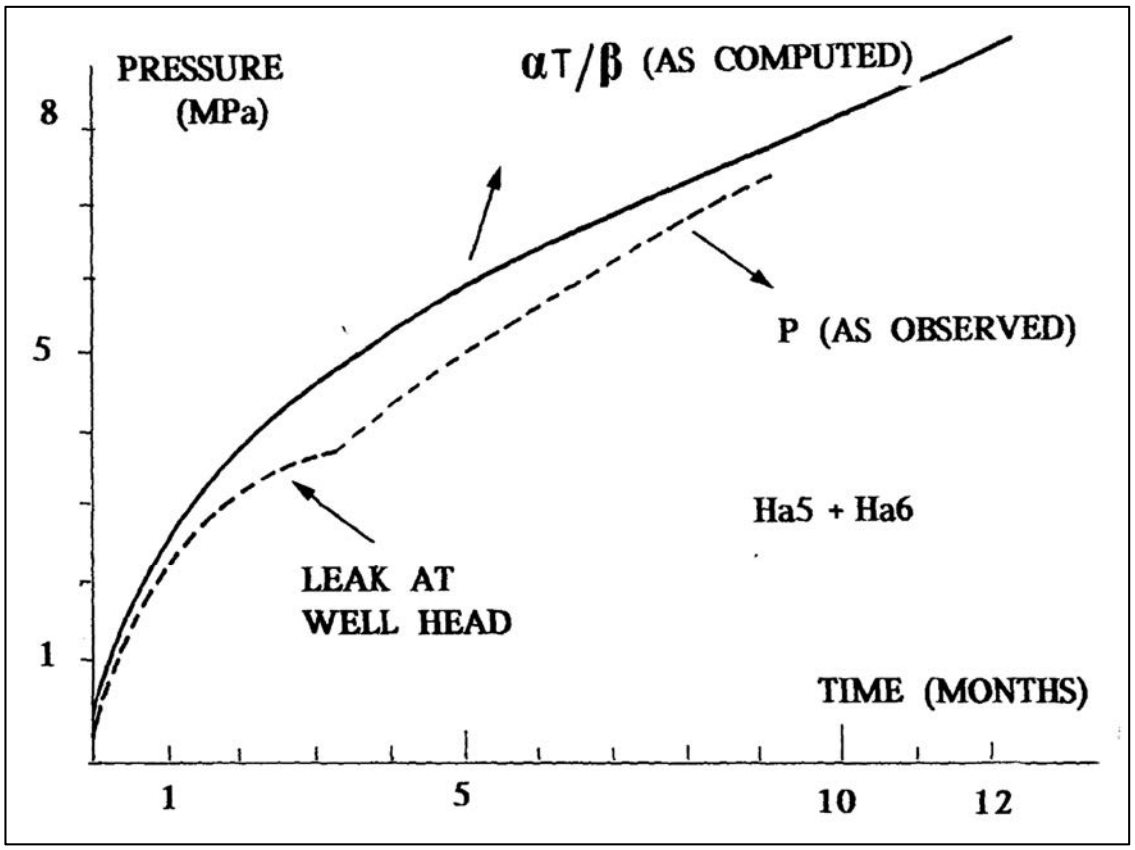

Figure 34 – Pressure build-up in a closed cavern at Hauterives (Bérest et al., 1979).

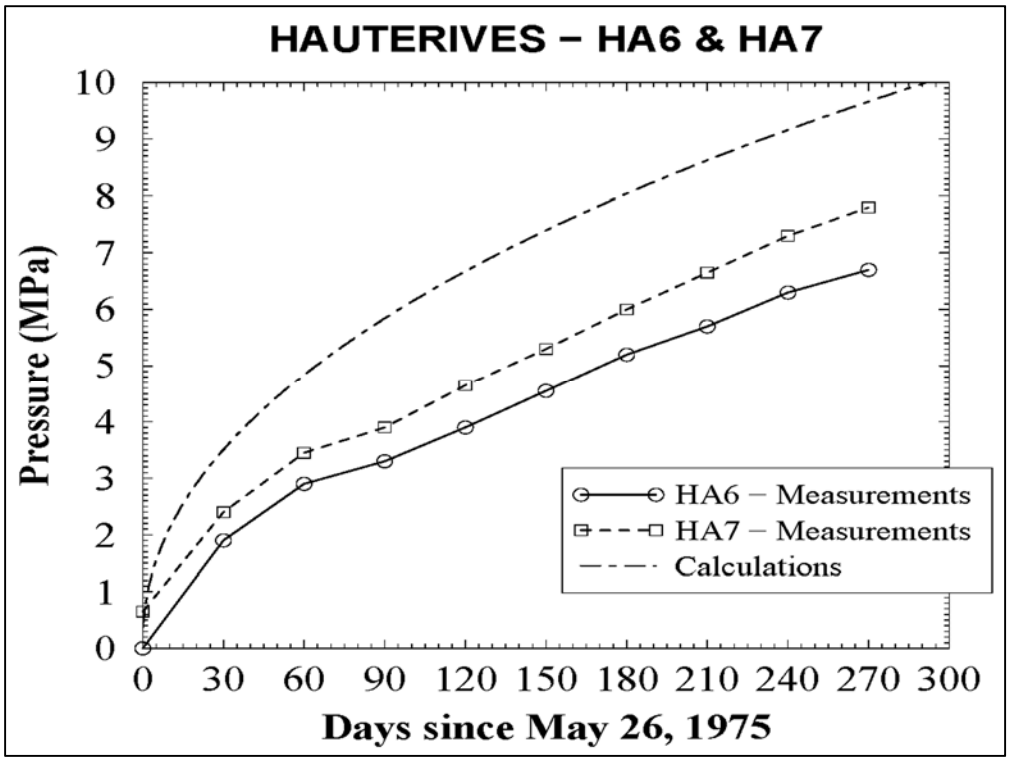

Figure 35 - Wellhead pressure evolution in the HA6-7 cavern and computed effects of brine warming (Bérest et al., 2000b).

Such a rule was adopted by You et al. (1994), who discussed abandonment of the Vauvert brine production field. They observed that two factors were responsible for pressure increase in a sealed cavern: creep closure, and brine warming. In their opinion, creep closure has a balancing effect in that it reverses when cavern pressure is larger than geostatic pressure. For this reason, they stated that a cavern can be abandoned when "*subsequent warming of the brine will be less than 5°C*" (p. 5). When this condition is not met, they propose that "*the time required for cavern pressure to reach geostatic pressure [due to the two factors mentioned above] will be such that the temperature at that time will be less than 5°C below geothermal*" (p.5).

4.4.2 The Vauvert (Parrapont) shut-in test (1978)

The Parrapont caverns at Vauvert near Nîmes in France were operated for brine production at a depth of 1800 m – 2300 m in the 1970s (caverns leached out recently in the Vauvert field are deeper). A hydraulic connection was created through hydro-fracturing between neighbouring wells; soft water was injected in one well, and brine was withdrawn from the other well. However, it was observed that the hydraulic connection closed when cavern pressure was low, a consequence of fast creep-closure rate. Figure 36 provides the results of a shut-in test performed in the 1970s (Bérest et al., 1979). The exact shapes of the caverns are unknown (sonar surveys could not be performed); however, it was known, for instance, that a total of 68,000 tons had been produced by the Pa1-Pa6 pair. A few days before the shut-in test, brine was still extracted from this pair of caverns.

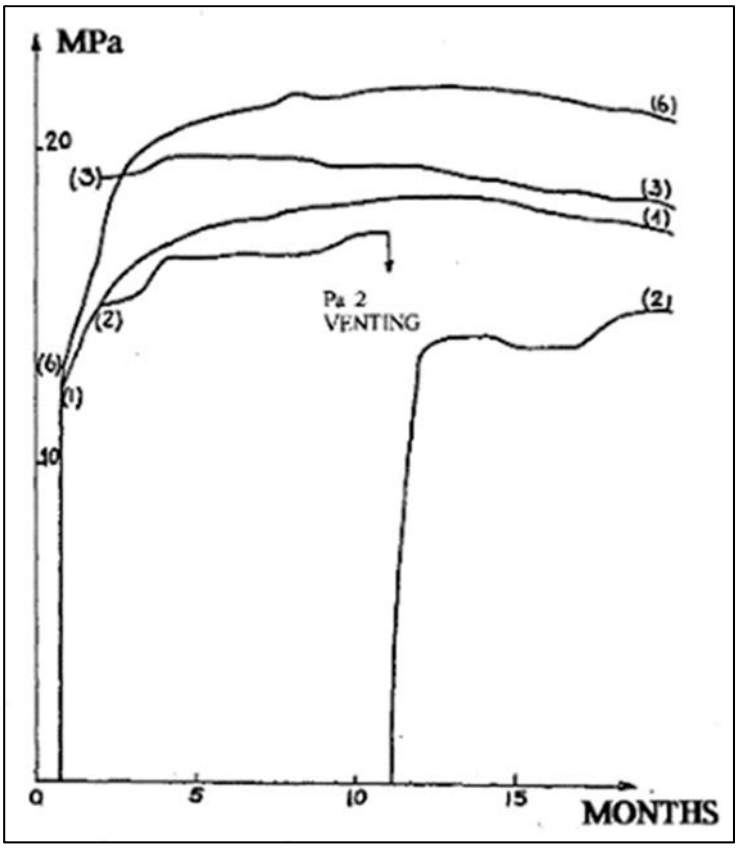

Figure 36 - Wellhead pressures evolutions in caverns Pa1, Pa2, Pa3 and Pa6 after caverns were shut-in (Bérest et al., 1979).

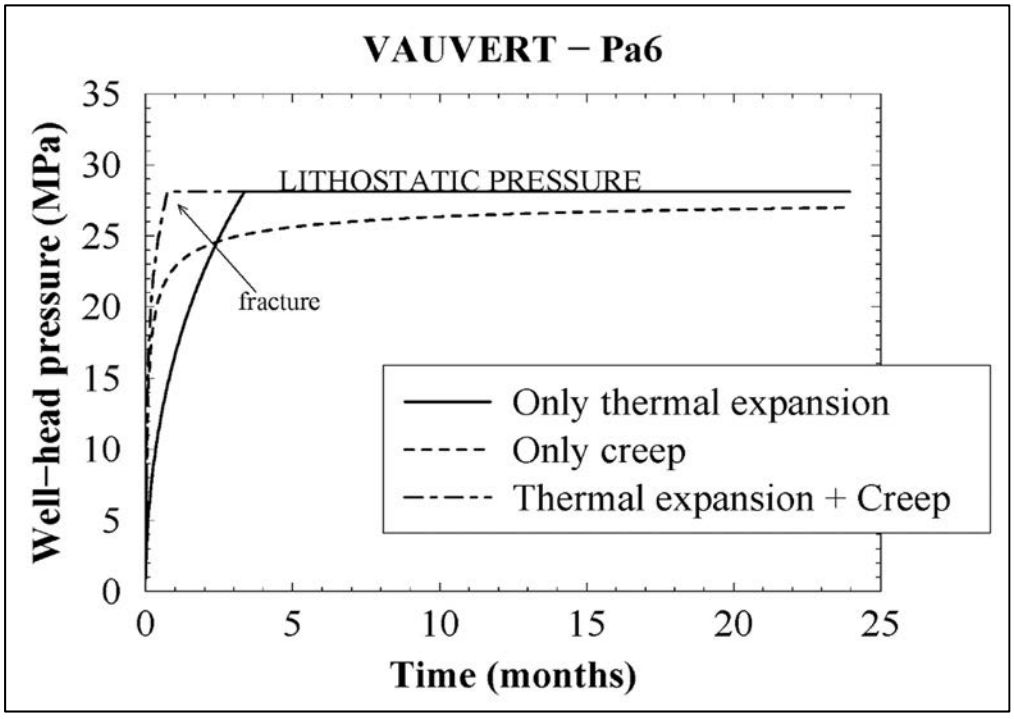

Figure 37 - Tentative interpretation of Pa6 pressure evolution (Bérest et al., 2000b).

Caverns Pa1, Pa2 and Pa6 are shut on the same day. When the shut-in test starts, cavern pressures are low, and the caverns are no longer connected: pressure evolutions are not parallel, clear proof of no connection. A tentative explanation of pressure evolution is as follows (Bérest et al., 2000b). Initial pressure increase is extremely fast over a couple of days; it is governed by creep closure (this cannot be explained by the effects of brine thermal expansion alone, which are much slower). However, as pressure builds up in the cavern, creep closure (a highly non-linear function of the gap between lithostatic pressure and cavern pressure) slows down dramatically, and brine warming becomes the governing phenomenon. Its effects are slower than those of creep closure, but they are independent of cavern pressure. After a couple of weeks, the hydraulic connection between Pa1 and Pa6 re-opens: pressure evolutions, which were independent, become almost perfectly parallel (wellhead pressures are not equal; an offset is observed, due to different compositions of the liquid columns in Pa1 and Pa6). Three or four months after the shut-in begins, the pressure-increase rate drops again. This is because the cavern is no longer tight (or because the hydraulic connection between Pa6 and the neighbouring Pa1 cavern enlarges, providing more room to accommodate brine thermal expansion). Wellhead pressure evolution in the Vauvert Pa6 cavern was computed taking into account the effects of brine warming and creep closure (Bérest et al., 2000b, Figure 37).

4.4.3 Durup's permeation tests at Etrez, France (1988-1989 and 1992-1994)

Salt permeability is a controversial issue – not only for scientific reasons, but also because several disposal projects in rock salt require a high tightness level. Obviously, salt permeability is exceedingly small in most cases (outstanding exceptions include shallow depth, anomalous zones at the interface between two splines in a salt dome, at the edge of a salt dome, etc.). However, a difficult issue is to define what is meant by "exceedingly small": does it mean $K = 10^{-21}$ m^2, or 10^{-18} m²?

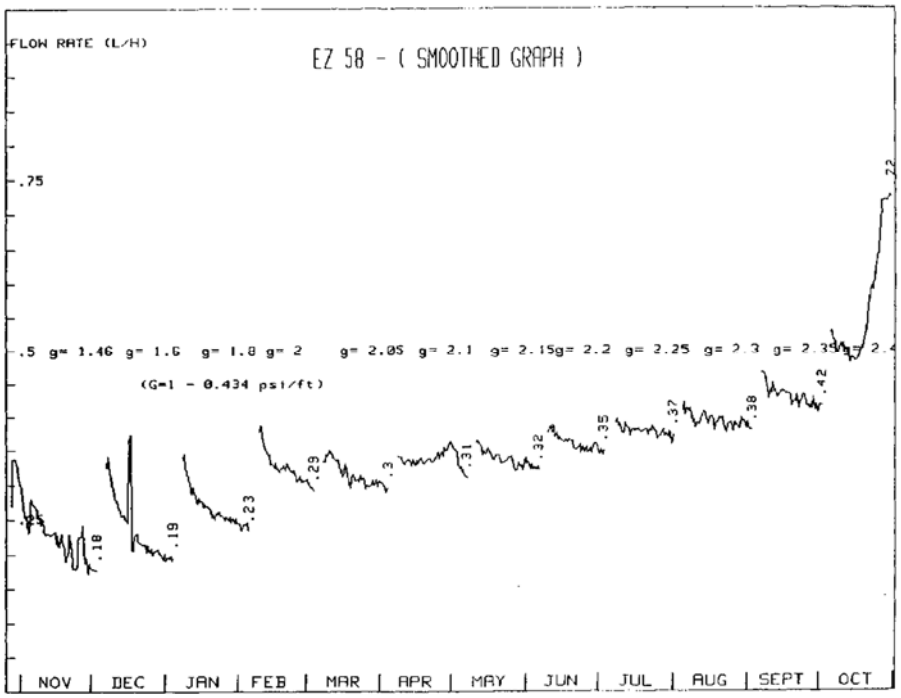

Figure 38 - Instantaneous injected flowrates as a function of time; g is the relative gradient during each step. Flowrate increases drastically when g = 2.4 (Durup, 1990).

Durup (1990 and 1994) performed long-term tests for tightness evaluations with brine and gas in the EZ58 borehole of the Etrez site in France, which had been drilled in May 1982. These tests were supported by the SMRI. EZ58 is a 1069-m deep well with an open hole that is 198-m high. Well completion included a 9-⅝" casing, whose depth is 870.8 m and an 898.7 m- long 5" string. The well was filled with brine, after which a light hydrocarbon column was lowered in the annular space to develop a brine-hydrocarbon interface at an initial depth of 898.7 m – i.e. below the casing shoe: hydrocarbon leaks through the casing or casing shoe can be distinguished from brine leaks through the open-hole walls (this "leak detection system" allows assessing the hydrocarbon leaks separately from the brine leaks and will be used often in later abandonment tests); and a casing packer was anchored at a depth of 864 m. (The advantage of setting a packer is that the open-hole volume is smaller and stiffer). Glycolated water was injected at the top of the brine column and, beginning on 26 October 1988, wellbore pressure was increased step by step from a *g* = 1.42 relative gradient (at casing-shoe depth) to a $g = 2.4$ relative gradient (the relative gradient equals the gradient (*G*, in MPa/m) divided by 0.0981). Each step lasted 30 days. Pressure was recorded twice a day through a pressure sensor at casing depth, after which glycolated water was injected at the wellhead to restore the testing pressure. The volume of injected water is deemed to equal the amount of brine that permeated through the open-hole walls in the interval of time between two consecutive pressure records (in fact, at the end of the test, the hydrocarbon-brine interface had risen by 3 m, an hydrocarbon volume change by 71.8 litres, a small quantity when compared to the cumulated injected water volume, which was 450 litres). The injected flowrate, (which increases when the difference between the relative gradient in the well and the relative gradient in the brine is larger – a feature that is consistent with Darcy's law) increases dramatically when the relative gradient reaches *g* = 2.4, a clear sign of a drastic permeability increase. The "*virgin*" permeability was back-calculated from the pressure evolution as $K = 6 \times 10^{-20}$ m^2.

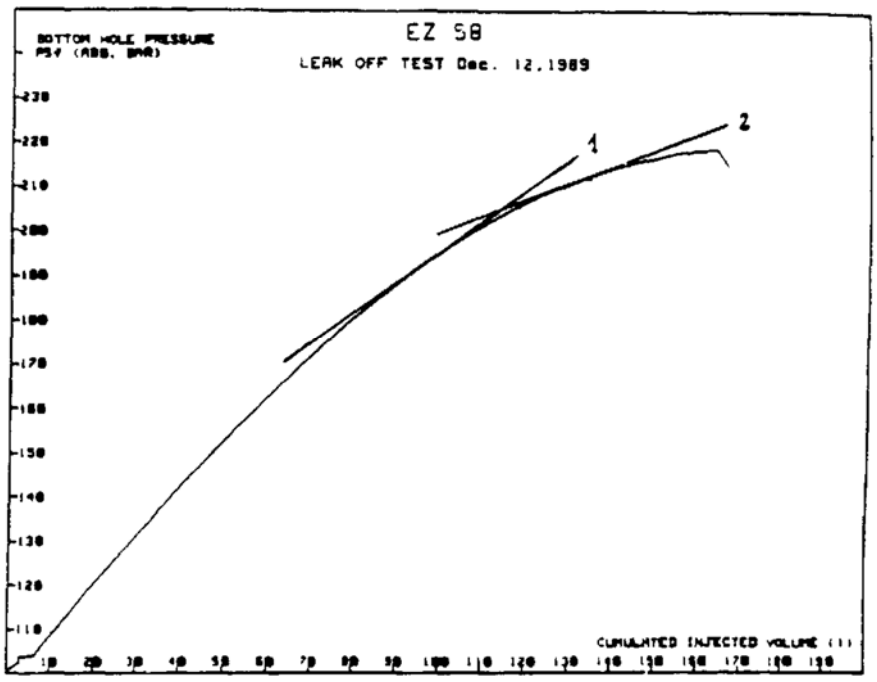

Figure 39 – Cumulated injected volume as a function of time during the test. Wellbore compressibility is the slope of this curve (Durup, 1994).

In fact, permeability increase was more gradual. Wellbore compressibility, or βV (the volume of fluid required to increase wellbore pressure by one pressure unit, see Section 4.2.2.) was computed. When pressure (at casing-shoe depth) increases from 14.5 MPa to 20.5 MPa, wellbore compressibility increased from 9.7 litres/MPa to 24 litres/MPa; and from 24 litres/MPa to 59 litres/MPa when pressure increased from 20.5 MPa to 21.8 MPa (see Figure 39). The "*threshold*" (see Section 5.4, Barradeel test, and Section 5.7), above which compressibility ceases to be constant is approximately 4.5 MPa.

After this test, wellbore pressure was released and, on 19 December 1989, a rapid injection test was performed, in which pressure was recorded every five minutes. After six hours, the maximum pressure reached during this test was 21.83 MPa at the casing shoe, a $g = 2.56$ gradient, which is not very different from what was observed during the "slow" one-year long test.

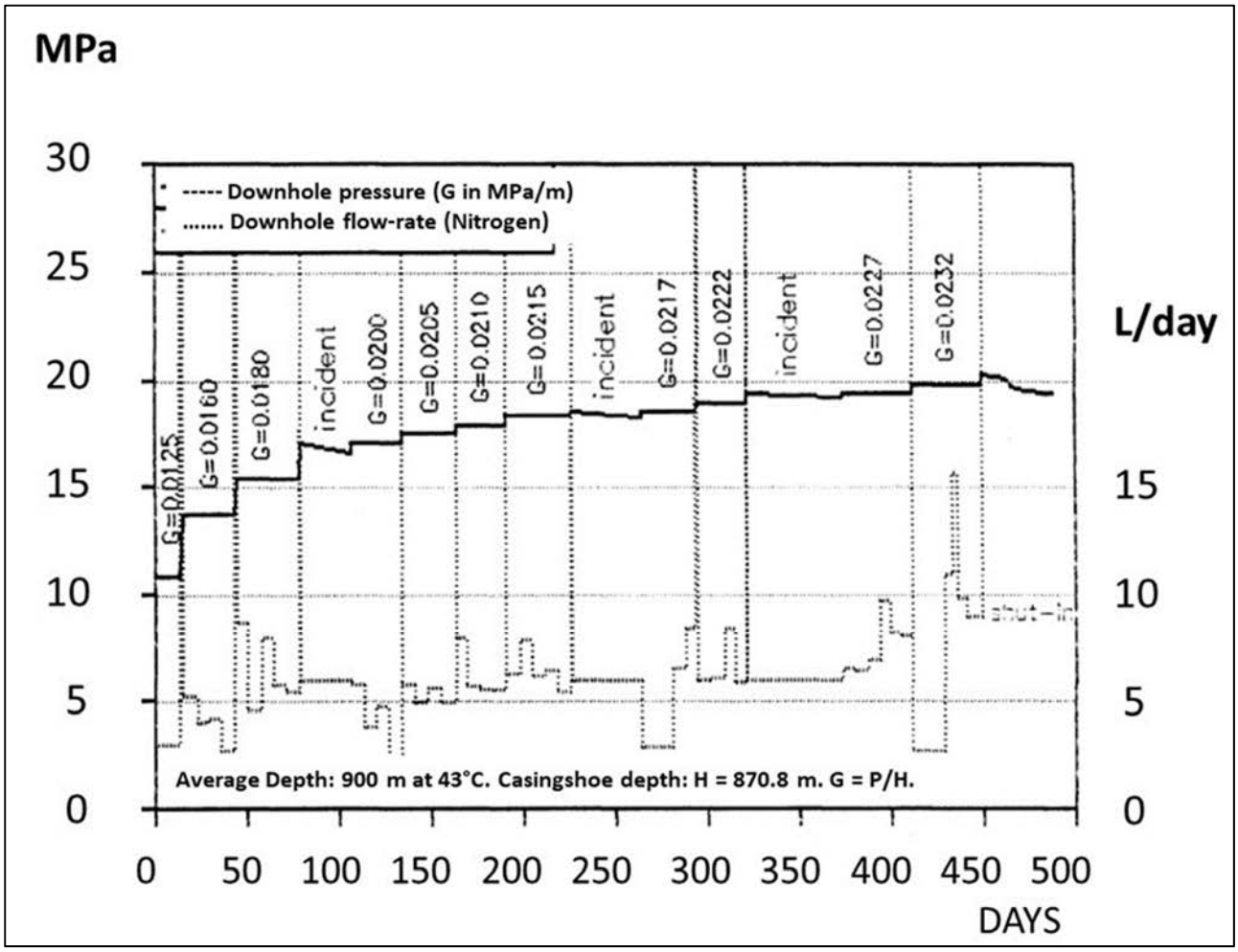

Figure 40 - The Etrez permeability test with gas (After Durup, 1994).

This test confirmed that Etrez salt was slightly permeable ($K = 6 \times 10^{-20}$ m^2) and that wellbore compressibility was a clear indicator, at least qualitatively, of wellbore permeability increase (a similar observation can be made when analysing the Etzel test, Section 4.2.2).

The same test was repeated with nitrogen (instead of brine) on the same EZ58 well (Durup, 1994). It might have been expected that, due to capillary forces and entrance pressure, no gas enters the brine-saturated formation at low pressure, but this prediction proved to be wrong. Gas pressure was increased incrementally over a 450-day-long test (Figure 40). The leak rate (litres/day, in downhole pressure and temperature conditions) was deemed equal to the amount of gas injected in the wellbore to restore testing pressure. Note that there were several "incidents" during which data were lost. The breakdown pressure, reached at the end of the test, was 0.0237 MPa/m, a value very close to the value reached during the brine test. The results of this test are not in full agreement with Fokker-Kenter's notion of a dramatic permeability increase before geostatic pressure is reached. (Only a small increase in injected gas rate can be observed when the gradient is larger than $G = 0.022$ MPa/m).

4.4.4 Equilibrium Pressure

From these findings (salt permeability is small, but not completely negligible; brine warming plays a significant role), it was inferred that three main phenomena govern pressure evolution in a sealed and abandoned cavern: brine thermal expansion; creep closure; and brine micro-permeation (two other phenomena are also important: additional dissolution – although this is a short-term transient phenomenon – and leaks through the casing and casing shoe – although the seal is a man-made device whose tightness cannot be assessed in a generic study).

In particular, when brine thermal expansion is completed fully, one can expect that an equilibrium pressure can be found when creep closure rate, which is a decreasing non-linear function of cavern pressure, and permeation rate through the cavern wall, which is an increasing function of cavern pressure (this function is likely to be linear in the low-pressure domain, and non-linear in the high pressure domain), exactly balance. In shallow caverns (less than 1000 m-deep), this "equilibrium" pressure should be relatively small (much smaller than geostatic pressure), alleviating any risk of fracturing (Bérest and Brouard, 1995). It was proposed that the SMRI perform a test with the objective of proving this notion.

4.4.5 The Etrez 53 (EZ53) test

An SMRI-supported abandonment test was performed from March 1997 to October 1998 in the small (8000 m^3), 950-m deep EZ53 cavern at Etrez, France (Bérest et al., 2001a). The EZ53 cavern was leached out from a Stampian bedded-salt formation at Etrez, France, where Storengy operates a gas-storage facility. Leaching was completed in 1982; in 1997, thermal equilibrium had been reached in this small cavern. Leaks through the casing during the test were feared (they must not be confused with permeation through the cavern walls), and a simple leak-detection system (described in Bérest et al., 2001; see also Section 4.4.3) was designed to assess well leaks. This system proved to be very effective, and leaks through the casing were exceedingly small.

The test consists of a *trial-and-error* process (Figure 41) that includes several phases. At the beginning of each phase, a specific initial pressure value is imposed through brine injection or withdrawal. When the pressure consistently increases (respectively, decreases) for a sufficiently long period of

time, it can be inferred that cavern pressure is lower (respectively, higher) than the equilibrium pressure. In such a case, a higher (respectively, lower) initial pressure is tried at the beginning of the next phase. One significant advantage of this method is that it provides both lower and upper bounds for the equilibrium pressure.

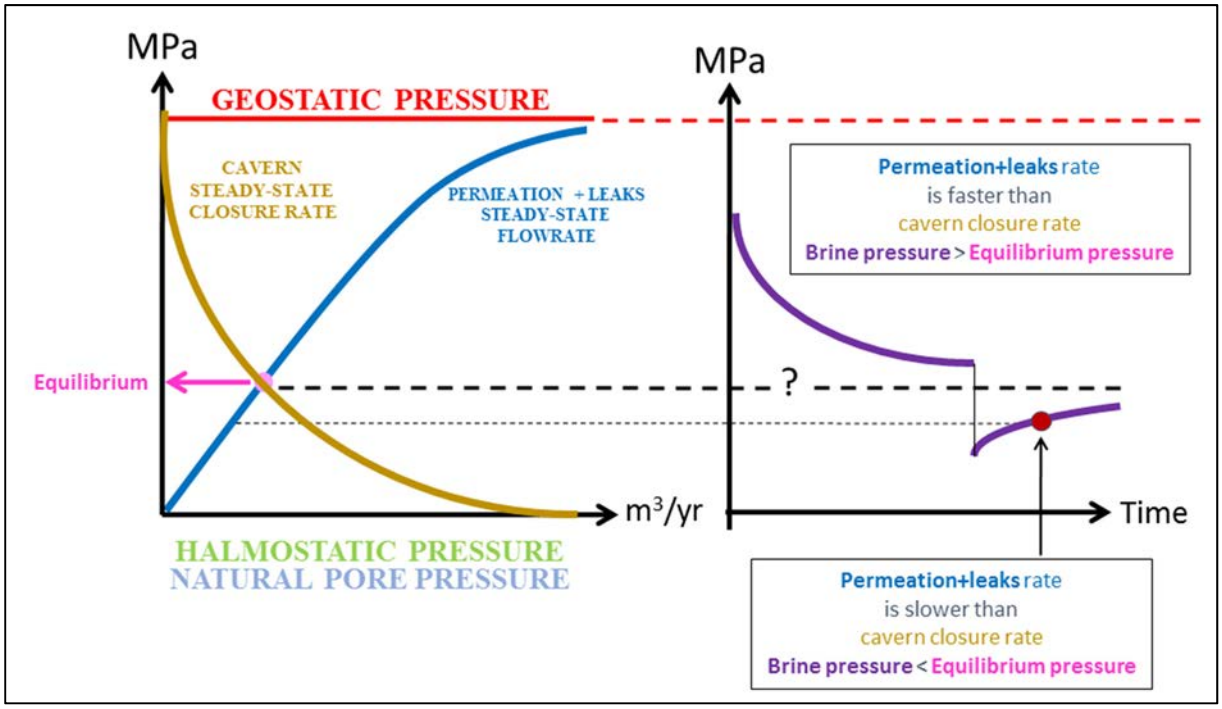

Figure 41 - Left: Equilibrium pressure. Right: The trial-and-error method.

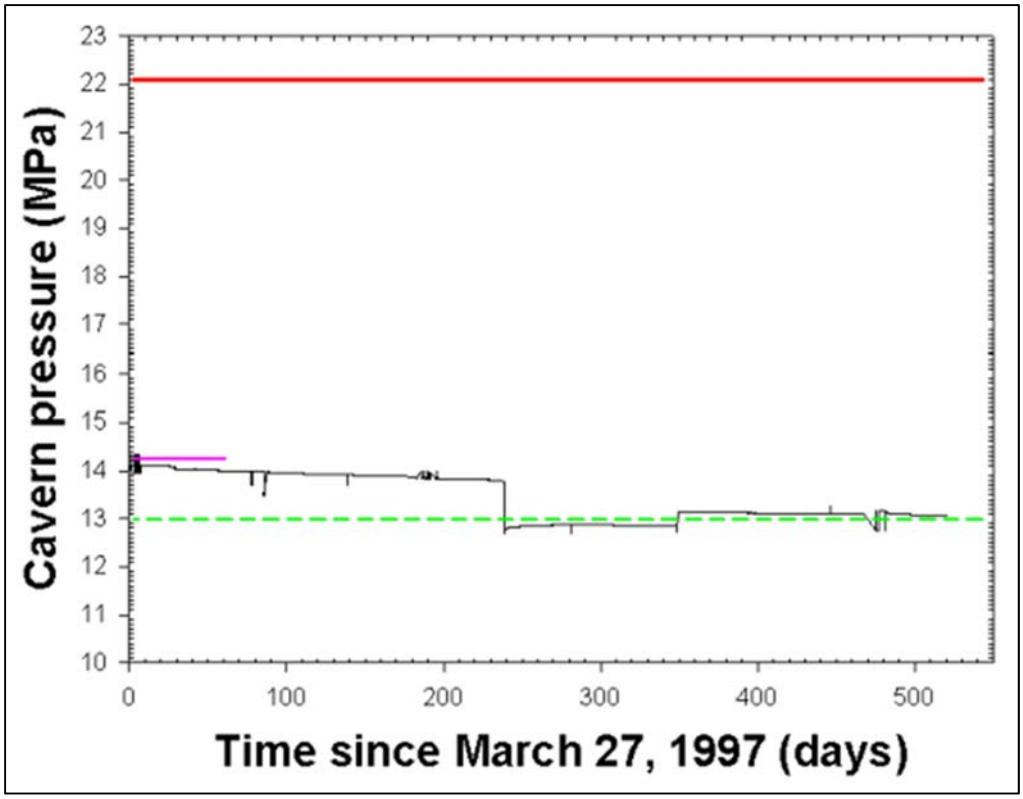

Figure 42 - Cavern pressure evolution from March 1997 to October 1998 (Bérest et al., 2001a).

The trial-and-error test began on 27 March1997 (day 1) and lasted for 540 days. Four initial pressures were tested successively (Figure 42). The test ran smoothly except for a small leak through the string at the wellhead from day 293 to day 315. At the end of the test, the cavern pressure at a depth of $H = 950$ m was $p_i = 13.1$ MPa, much smaller than the lithostatic pressure, $P_\infty = 21$ MPa, and larger than the halmostatic pressure, $P_h = 11.2$ MPa. This "equilibrium pressure" is reached when the effects of creep closure (which makes pressure increase) and the effects of brine permeation (which makes pressure decrease) are exactly equal (they were estimated to be 2.2 m^3/yr). It also was inferred that, at cavern scale, salt-formation permeability was $K = 2 \times 10^{-19}$ m^2. (Larger than what had been observed in the neighbouring EZ58 borehole, see Section 4.4.3; this is consistent with what is known from scale effect when permeability is concerned).

After the end of this test, no information on the period from October 1998 to April 2002 is available. On 24 May 2002, recording the central tubing pressure at the wellhead began again, and weekly recordings were performed (Figure 43). On 13 June 2002, a manometer was set at the wellhead on the annular space. Computed downhole pressures were close to the equilibrium pressure observed at the end of the first test.

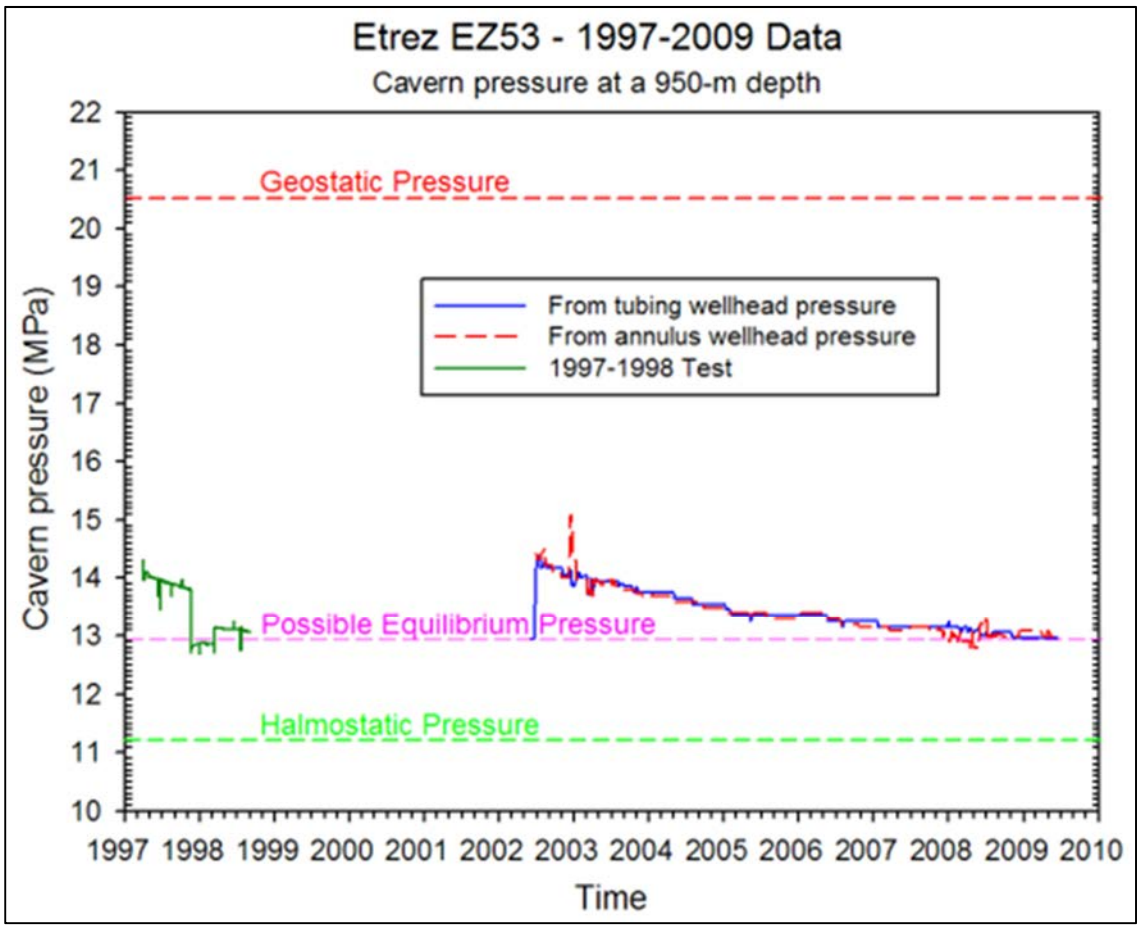

Figure 43 - Cavern pressure evolution during the 1997-2009 period (Bérest et al., 2013).

On 25 June 2002, fuel oil was withdrawn from the annular space, and brine was injected in the tubing. Cavern pressure increased. From March 2003 to 2007, pressure evolutions were smooth; both pressures (annular space and tubing) slowly decreased, as they did during the 1997-1998 test when

pressure conditions were similar, and the gap between these two pressures remained roughly constant (strongly suggesting that no oil leak took place). It can be concluded that, in 2009, the cavern equilibrium pressure at a 950-m depth was $P = 13 \pm 0.1$ MPa, a value that is consistent both with the value predicted at the end of the 1997-1998 test and with that observed until 2009, after the well was kept idle for many years.

4.5 The SMRI CS&A program

The SMRI had long recognized the complex issues associated with sealed and abandoned caverns (CS&A) and, in 1996, the SMRI initiated a long-term research program. In 2003, J. Ratigan, Program Manager, wrote a summary report from which are drawn the following excerpts.

"*following three succinct field tests performed in the late 1980s and early 1990s by Gaz de France and partially supported by the SMRI [Gaz de France, 1990, 1994; Berest et al., 1998]… the SMRI initiated a multi-project program focused on addressing the complex issues of sealing and abandonment of solution-mined cavern wells*" (Ratigan, 2003, p. 1).

In Table 3, Ratigan identifies the five processes influencing fluid pressure in a sealed cavern (see Section 4.4.4). He comments on the brine transport issue in the following terms:

> "*The nature of the cavern fluid transport from the cavern to the salt formation is perhaps the most significant and technically controversial issue in cavern sealing and abandonment*." (p.4). … "*Some cavern fluid will always permeate the salt in the cavern wall both before and after cavern sealing (unless the cavern fluid pressure is less than the pore pressure in the surrounding salt) … Whether or not a fracture or fractures develop depends on the rate of cavern fluid pressurization.''* "*…high rates of sealed cavern fluid pressure increases are generally the result of cavern fluid thermal expansion*."

Table 3 – Processes influencing pressure in a sealed cavern (Ratigan, 2003).

Process	Influence on Fluid Pressure	Time Scale
Salt creep	Monotonically *increases* cavern fluid pressure at a decreasing rate.	Majority of pressure *increase* occurs within tens of years after cavern sealing.[a]
Salt/cavern fluid heat transfer	Heating of the brine causes cavern fluid expansion and *increases* cavern fluid pressure at a decreasing rate.	Majority of pressure *increase* occurs within tens of years to many tens of years after cavern sealing.
Salt dissolution/cavern fluid saturation	Increases cavern volume and decreases fluid temperature, which in turn, causes a *decrease* in fluid pressure.	Majority of pressure *decrease* occurs within months after cavern sealing.
Cavern fluid transport into formation	Results in a cavern fluid pressure *decrease*.	May continue indefinitely.
Cavern fluid transport through sealing plug/ casing cement	Results in a cavern fluid pressure *decrease*.	May continue indefinitely.

(a) The rate of pressure increase on the cavern depth.

In this framework, before 2003, the SMRI CS&A issued six research contracts:

(1) preliminary literature review (KBB; Crotogino et al., 1997);

(2) wellbore casing-shoe laboratory test (RESPEC; Pfeifle et al., 2000);

(3) salt permeability testing program on hollow salt spheres (Ecole Polytechnique-LMS; Bérest et al., 2001b), see Section 2;

(4) interpretation and generalization of Ecole Polytechnique – LMS tests (Behr, 2001; Malinsky, 2001; Stormont, 2001);

(5) cavern modelling (IUB/KBB; Rokahr et al., 2002); and

(6) translation into English of the original Etzel test report (University of Hannover, Staudtmeister and Rokahr, 1998).

Ratigan's conclusions (p.20) are provided below.

"*The important operational observations and conclusions are stated below.*

• *In the absence of brine thermal expansion, the vast majority of solution-mined salt caverns can be sealed and abandoned without concern for salt fracture generation or significant brine migration from the cavern.*

• *Prior to cavern sealing, all caverns should be kept open as long as possible and practical to ensure a minimization of the temperature difference between the salt and the internal cavern brine. The time required for "minimization of the temperature difference" will depend on the cavern volume. Information from continuous well shut-*

in and bleed-off periods can contribute to the knowledge base necessary for safe and environmentally acceptable sealing.

• Casing shoe integrity tests should be performed prior to sealing to ensure this potential pathway has maintained integrity comparable to that required during the cavern operational history.

• Tall caverns and/or caverns that must be sealed before thermal equilibrium is approached require a case-by-case evaluation of sealing strategy."

After 2003, six other research contracts were performed:

(1) a salt-cavern abandonment field test in Carresse, France (Brouard et al., 2006a);

(2) cavern well abandonment techniques (Crotogino and Kepplinger, 2006);

(3) Stassfurt shallow cavern abandonment field tests (Bannach and Klafki, 2009);

(4) synthesis of SMRI-sponsored shallow cavern abandonment tests (Duquesnoy, 2011);

(5) salt cavern abandonment field test at Carresse, Update of the SMRI Research Report 2006-1 (Brouard Consulting et al., 2011); and

(6) Cavern abandonment field tests in deep caverns (Enterprise Products Operating et al., 2009 and 2015).

The contracts included two new tests in shallow caverns (Carresse, France; Stassfurt, Germany), discussed in Sections 4.9 and 4.10, and various syntheses. It became progressively clear that the shallow cavern issue was well understood (in addition to the three tests supported by the SMRI, tests were performed at Bernburg, Germany and Gellenoncourt, France, see Sections 4.7 and 4.8, and led to similar conclusions). However, the deep cavern issue was more controversial. Cavern creep closure is faster in a deep cavern, and there are reasons to believe that permeability is even smaller than in a shallow cavern. One consequence is that equilibrium pressure, as defined above, is much closer to geostatic pressure. In such a context, issues such those at the temperature gap (between brine and geothermal temperature) or the excess pressure at cavern tops become more critical. For this reason, SMRI decided to support a field test at Mont Belvieu (Barbers' Hill) in a deep cavern (see Section 5.2).

4.6 TNO (the Netherlands), 2003, and IEG (France), 2004, reports

In 2003 and 2004, Best Practices Reports were issued in the Netherlands and in France. Both Reports are based on the significance for cavern abandonment of the three main factors listed in Ratigan's SMRI CS&A Program (see Section 4.5): creep closure, brine heating and brine permeation through the cavern walls. Both Reports emphasize the importance of "*adequate knowledge of the geological setting*" (TNO Report, p.5): for instance, brine leakage is not a major risk in some cases, when the natural ground water system above the salt formation is salt saturated. Long-term subsidence also is a site-specific risk; in most cases, it is a more severe concern in the Netherlands than in France. Both Reports highlight the significance of monitoring. The following excerpt from IEG Report epitomizes this concern.

"*After brining has been completed, the brine production fields must be monitored for a long-enough period to verify that unfavourable mechanical or hydrogeological change has not occurred and that the predictions performed before abandonment fit the observed changes. In the Netherlands, the monitoring period is 30 years. The IEG recommends that the monitoring period be at least 20 years. One important objective will be to verify that there is a good fit between predicted and observed changes. In many countries (the Netherlands, Spain and the USA's New York State, Tully brine field – see Briggs and Sanford, 2000), an abandonment plan is submitted to the mining authorities before brining is completed. This plan includes a prediction of the expected changes over 2 or 3 decades. An objective of the measurement program is to check that observed data fit these predictions. The plan may make a provision for re-evaluation of the measurement frequency, in one direction or the other, whenever the observed results suggest that it is needed. Parameters to be measured include surface levelling, which is an important parameter and relatively easy to measure … The IEG strongly recommends that such abandonment plans be made mandatory*

For stable caverns, it is generally accepted that, in a group of hydraulically connected caverns, at least one well must remain open (unplugged). This is necessary at least for two reasons. On one hand, cavern-brine warming must be expected, as the temperature of the injected water is in many cases significantly colder than the rock mass at cavern depth; this heating process will continue over a long period — especially when the cavern is large. Such warming, which is recorded through thermometers set inside the cavern, generates brine thermal expansion and pressure build-up in a closed cavern. From time to time, the cavern must be vented through the unplugged well to prevent too high a pressure build-up. The effects of this warming must disappear before the remaining open wells can be unplugged.

On the other hand, pressure and temperature changes, ground displacements, will be predicted through computations before abandonment. Measurements performed after abandonment will allow to validate these predictions. Changes in pressure build-up will result both from brine warming and cavern creep, and the respective parts taken by these two mechanisms must be assessed correctly. It is suggested that these measurements, which are extremely useful but indirect or global, be complemented by further measurements that will verify that no unexpected cavern change takes place. In the wells to be kept open will be performed sonar measurement and logs (such as the gamma-ray log) to provide local information. Companies also must keep informed of any technical advances that could help to confirm the long-term prediction and provide solid information should

claim classification be required. The abandonment plan must also define the monitoring of water-bearing strata near the caverns. Wells will be used to make piezometric recordings, and the water salt content as a function of depth will be measured periodically. Here, again, a prediction of the expected changes must be provided before brining is completed. For intensive brine fields, special attention must be paid to the hydrogeological parameters, as risk to groundwater flow is of utmost importance. The abandonment plan will describe site reclamation.

The experts ask themselves whether or not they should suggest how long a period of time predictions must consider. This question is related to the responsibility our societies accept toward future generations and, as such, is far beyond the scope of this report. The IEG tried to assess the credibility of long-term predictions. The IEG thinks that, based on a 20-30-year long monitoring period, quantitative predictions can be made for a one century-long period of time; and that qualitative predictions (the sense of the evolution of the main phenomena) can be made for a several-centuries long period of time." (Bérest et al., IEG Report, 2004, p. 16).

4.7 Other “shallow” tests

After the “shallow cavern” Etrez test (1996-1997), several similar tests following the trial-and-error method defined in Section 4.4.5, were performed at Carresse (France), Gellenoncourt (France) (see Figure 44) and Stassfurt (Germany), as well as at Bernburg (Germany) in a small cavern excavated from a mine drift. The Carresse and Stassfurt tests were supported by the SMRI. For various reasons, the system allowing the assessment of leak tests (which had been used at Etrez) could not be set up. In these caverns – except, to a certain extent, at Carresse – thermal equilibrium had been reached when the tests begin.

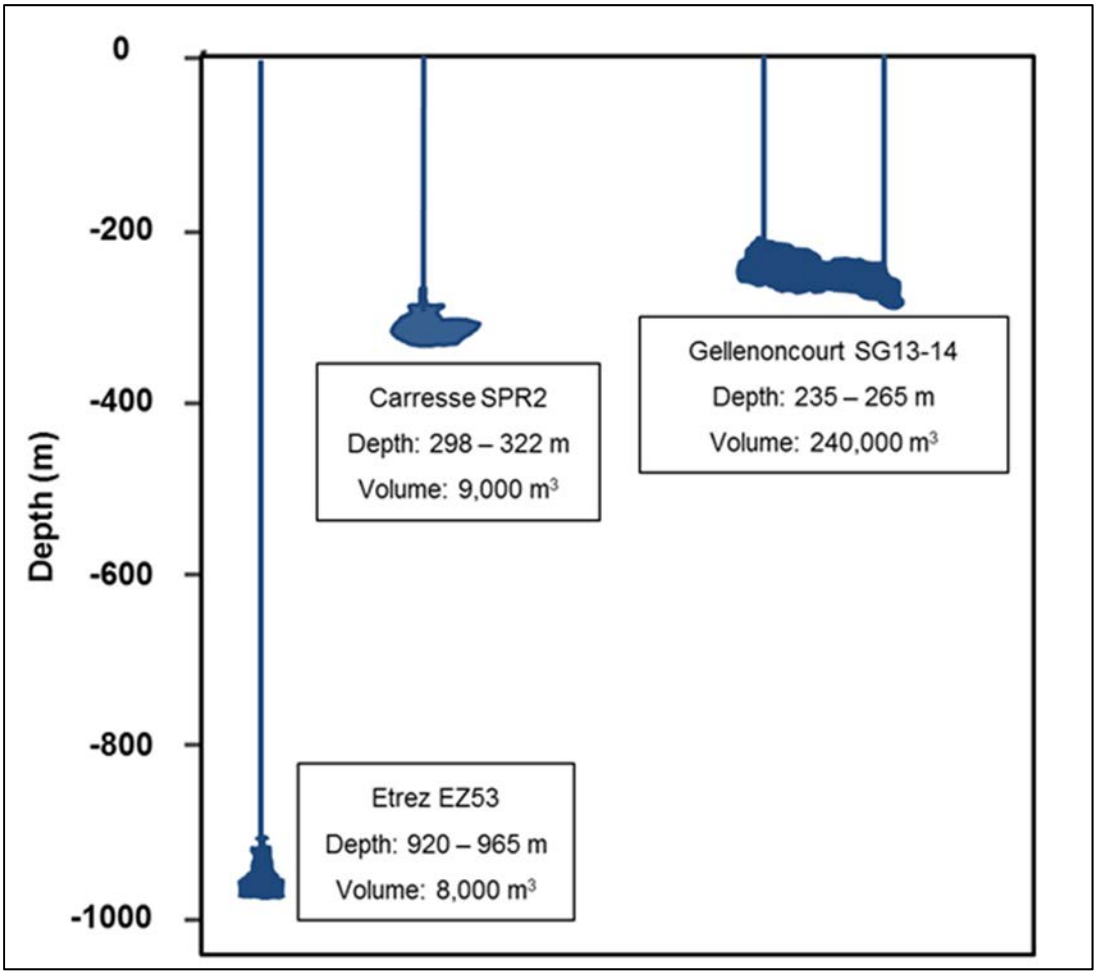

Figure 44 - Shape and depth of the EZ53, SPR2 and SG13-14 caverns.

4.8 The Bernburg Test (2001-2003)

A remarkable abandonment test in a small cavern leached out from a mine drift was described by Brückner et al. (2003), and Hiltscher and Zwätz (2003). In addition to this test, the project included creep and triaxial tests on salt samples, laboratory permeability tests, *in situ* stress measurements through hydrofracturing and preliminary tests in two 25-m long boreholes.

A 22-m^3 cavern had been leached out at a depth of 28 m beneath a 420-m drift of the Bernburg Mine in Germany (Figure 45, Figure 46 and Figure 47). In such a small cavern, thermal equilibrium is reached rapidly. The cavern was filled with brine, and seal tightness was checked through nitrogen leak tests. The testing program included a two-year multi-step ''shut-in" test. Results of this test are shown on Figure 42.

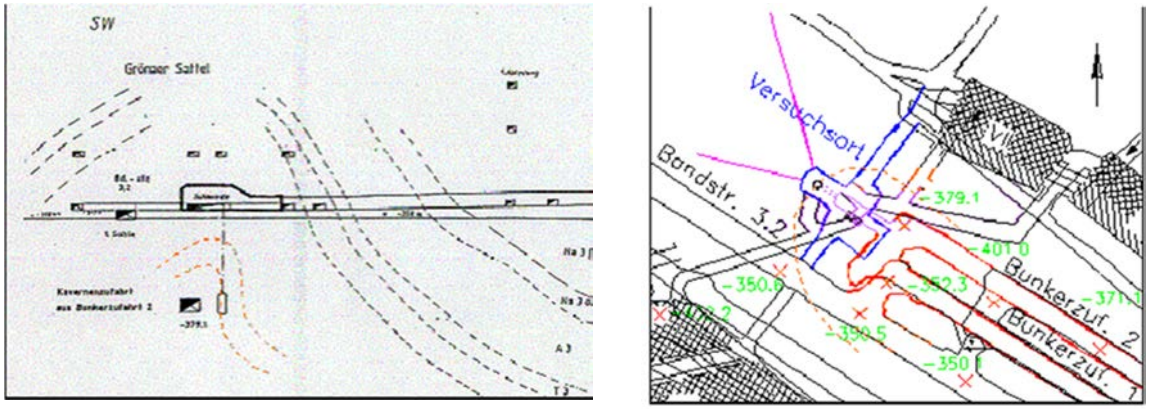

Figure 45 - Test area in the central part of the Grönaer anticline: (left) horizontal cross-section; (right) geological cross-section perpendicular to the fold axis.

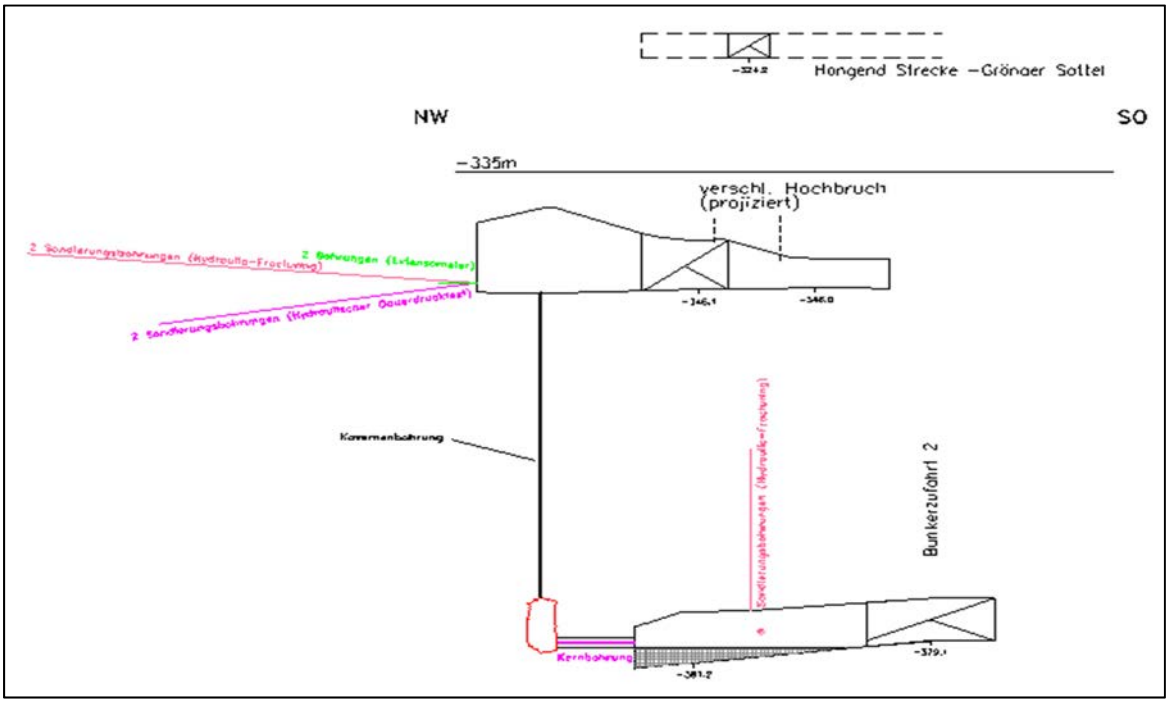

Figure 46 – Access to the test cavern (Hiltscher and Zwätz, 2003).

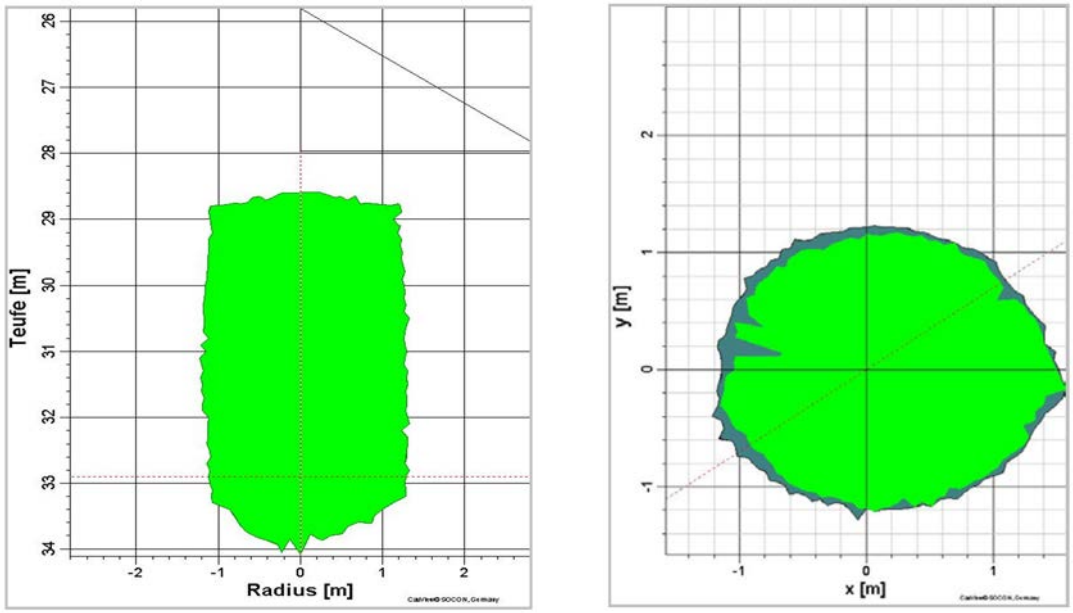

Figure 47 – Vertical and horizontal cross-sections of the test cavern (Hiltscher and Zwätz, 2003).

The following comments were made by Brückner et al. (2003, pp. 13-14).

- "*Starting in January 2002, in the first step, the cavern has been weakly pressurized up to a 10 bar well-head pressure with injection of 8.8 litres hydraulic oil. … the modulus of compression for the system brine-cavern could be determined to be in the range of 2.7 MPa,* [this is a misspelling; read 2.7 GPa, or β = 3.7 10^{-4}/MPa] *which is higher than in the bore holes. This value is combined with well-head pressure decay rates according to convergence rates between 0,03 and 0,06% per year. Generally, while manually pumping up the pressure increase in the cavern is directly proportional to the amount of oil injection resulting in a gradient of 1.22 bar per liter.* [or $\beta V = 0.82$ liter/bar]

- *After sealing the well at 10 bar we expected a slight pressure build up due to cavern convergence. Surprisingly, first we observed a slight pressure decrease comparable to the experiments in the bore holes which was confirmed after re-initialising the pressure again to 10 bars.* [This decrease might be due to various transient phenomena such as additional dissolution, reverse creep etc. see van Sambeek et al., 2005.]. *Then, after a transitional phase with a minimum of 9.1 bar reached after 3 weeks the well head pressure had started to increase with a progressive tendency. After 4 months observation time the well-head pressure was 12.3 bar, whereby from March with initially 2.6 mbar/d to May with finally 4.3 mbar/d the pressure build-up rate became nearly doubled*. [This is not easy to explain. The relatively complicated pressure history may be a factor].

- *In the next step the pressure was pumped up to 30 bar by injecting 14.2 l hydraulic oil. According to the first step, primary we observed a rapid pressure decay with degressive tendency until it became a minimum at around 28 bar which is followed by a 6 weeks phase*

of slight increase up to 28.2. The resulting pressure build up rate is 4 mbar/d, a value that is 10 times less than observed in the first step.

…

- *In the third step at an initial pressure of 50 bar a rapid pressure decrease has been observed which has been followed by a phase with degressive trend until a plateau of nearly constant pressure has been established at after two months. In the next step with a well-head pressure of 70 bar, 20.77 litres hydraulic oil were injected. After ten weeks the pressure has dropped down to 64.2 bar. The rate was degressive again and reached 12 mbar/d at the end of the period.*

- *In the fifth step a starting well-head pressure of 90 bar was planned, however, only 89 bar could be realized. Whereas in the lower pressure steps (< 80 bar) a nearly linear relationship between injected volume and pressure is observed, the necessary oil injection to reach higher pressures rises nearly exponentially up. [This observation suggests that microcracks open when the 8-MPa threshold is exceeded].*

- *After the cavern was tightly closed, the pressure dropped down to 82 bar only one day later. After a period of 3 month a well-head pressure of 78 bar has reached. The rate was 11 mbar/d at the end of the test.*

- *The next stage of the tests started with active depressurisation of the well-head pressure down to 50 bars. Importantly, after sealing again the pressure risen up to 60 bar, which is obviously to the reverse inflow of the fluid penetrated into the cavern wall under higher pressures*."

At the end of the test, 344 litres of oil had been injected to increase cavern pressure; 134 litres were recovered after the test.

During the first step, the creep-closure rate is faster than permeation rate, and brine pressure increases (Figure 48). This is still true during the second step (initial brine pressure was 30 bars), but pressure increase rate is slower. During the third step (50 bars), a plateau was reached after a few days. During the fourth and fifth steps (70 and 89 bars), brine pressure consistently decreases (for two months).

In our opinion, following the definitions coined during the Etrez test (see Section 3.5), the equilibrium pressure might be close to 50 bars (a longer test would have allowed a more precise assessment); lithostatic pressure was assessed to be 105 bars. This value (of the equilibrium pressure) is low when compared to other caverns. Note, however, that, in a homogeneous rock formation, cavern creep closure (in %/year, for instance) does not depend on cavern size. Permeation rate (in %/year) does. One consequence is that the equilibrium pressure is smaller in a smaller cavern.

Cavern apparent compressibility, βV, can be assessed when hydraulic oil is injected at the beginning of each step. From Brückner et al.'s paper and Figure 48, the following values can be computed:

- step 1, $\Delta V = 8.8$ litres, ΔP = 10 bars, βV = 0.88 litres/bar;

- step 2: ΔV = 14.2 litres, ΔP = 30 – 12.3 bars, βV = 0.80 litres/bar;
- step 4: ΔV = 20.77 litres, ΔP =70-47 bars, βV = 0.90 litres/bar; and
- step 5: "exponential" increase of apparent compressibility.

These features strongly suggest that, in addition to the "true" elastic compressibility, permeability increase (creation of micro-fractures) contributes to the as-measured, "apparent" compressibility. A tentative explanation of the initial compressibility decrease is provided in Section 5.7. They also confirm that cavern compressibility, as in the Etzel test (see Section 4.2.2), is a powerful tool for assessing damage at the cavern wall, see Section 4.7.

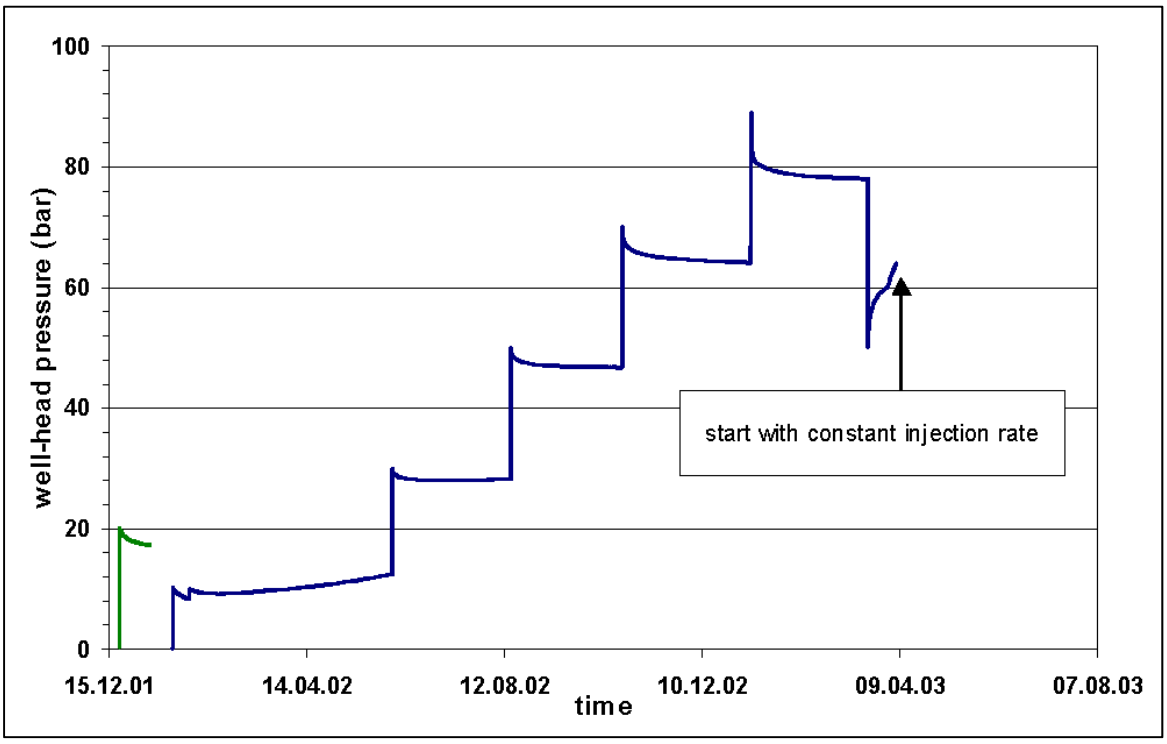

Figure 48 - Cavern pressure evolution during the Bernburg test (Brückner et al., 2003).

At the end of the test, an access to the cavern was opened (Figure 49), allowing visual inspection of the walls. According to Brückner et al. (2003):

- "*the most impressive feature is the occurrence of nearly vertical inclined anhydrite layers up to 10 cm thickness. They appear, as well as trans sections or as cover mainly on the wall surfaces in the north and south direction. The salt itself is visible free of disturbed zones or fractures and looks wet without local leakage*."

- *Focusing on the anhydrite structures, most of the primary material is found as detrital accumulation in the mud. The residual parts of anhydrite are forming internally complex folded skeletons rising up to 20 cm into the opening. Because the layers are internally broken and jointed, they are obviously not impeding the solution process as indicated by a nearly ideally cylinder geometry of the cavern. However, most important, visual inspection with UV-light gives indications that the permeation into the wall is*

preferentially concentrated on layers with anhydrite structures. Carefully inspection of the contour indicates, at least, three zones of fluid permeation into the wall:

- *Up to 30 cm pervasive solution front*
- *Up to 60 cm inhomogeneous fluid distribution with local spots and rims*
- *Up to 100 cm local 2D-spreading along anhydrite layers.*

- *In summary, our observations confirm that permeation processes in undisturbed salt are possible but they can be locally enhanced by internal anhydrite layers as major path ways. The extent of the observed permeation front corresponds very well to the results obtained by numerical modelling*."

According to Hiltscher and Zwätz (2003):

*"With the inspection of the cavern in presence of the responsible local mines authority it was stated that the border zone of Testcavern is stable and mechanically unstressed and can stand without additional support methods (*Figure 50*).*

Although the salt was expected to show no preconditions for solution transport, after entering the inner part, the most impressing feature is the occurrence of nearly vertical inclined anhydrite layers up to 10 cm thickness. They appear, as well as trans sections or as cover mainly on the wall surfaces in the north and south direction. The salt itself is visible free of disturbed zones or fractures and looks wet without local leakage."

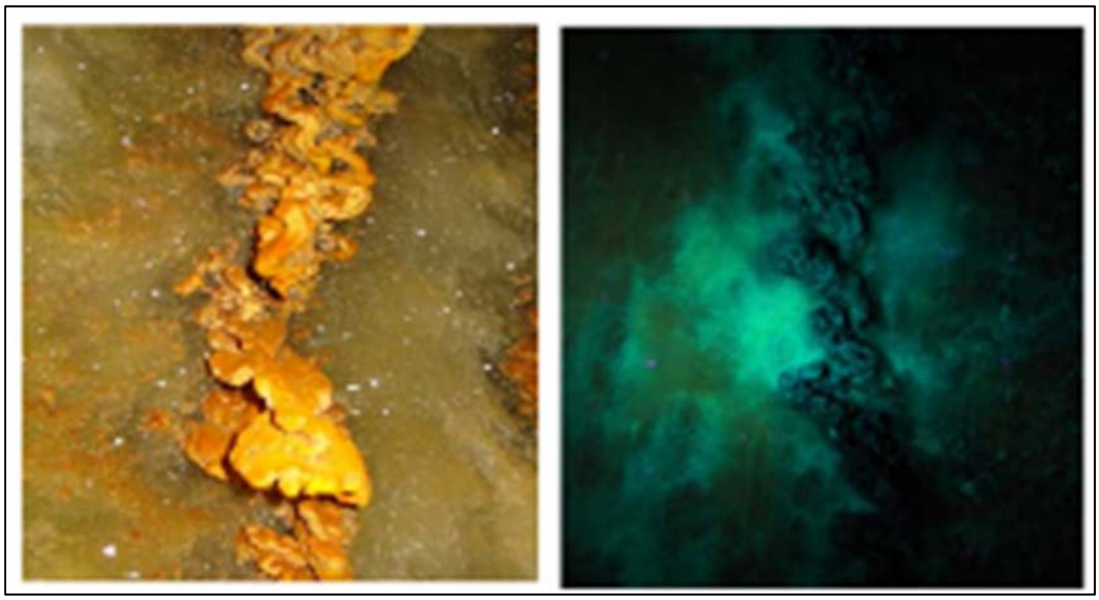

Figure 49 - Photographs of the cavern interior (a) and of the contour for visualization of permeation phenomena (b) (Brückner et al., 2003).

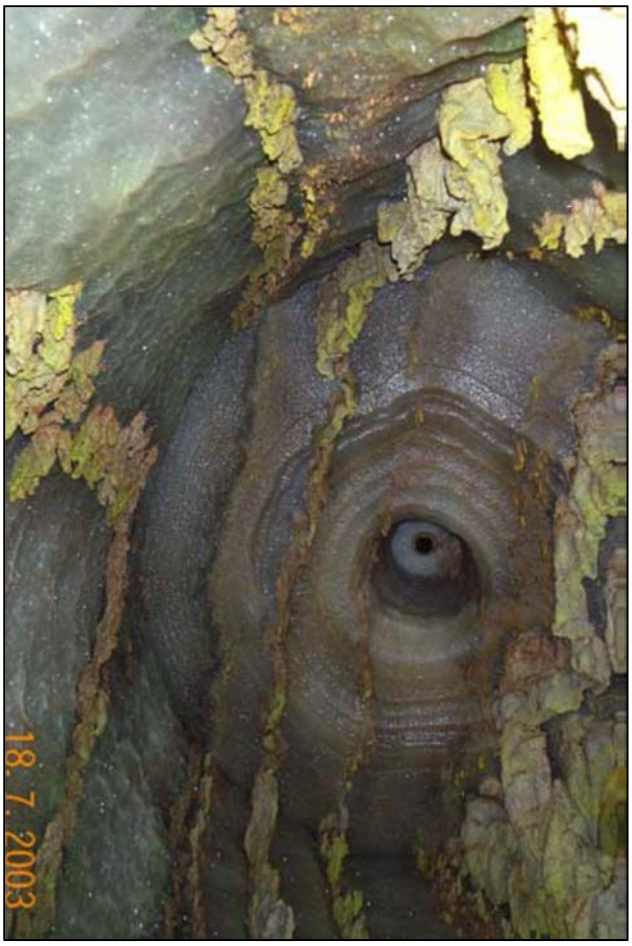

Figure 50 - Anhydrite bands in the roof of the cavern (Hiltscher and Zwätz, 2003).

4.9 Duquesnoy's 2011 Report to the SMRI

In 2011, A. Duquesnoy, based on the results of three SMRI-supported in situ tests and three other tests also described in this Report, proposed the following conclusions:

"*1. The three SMRI-financed field tests in shallow caverns show that, if cavern thermal equilibrium is (almost) reached, the long-term brine equilibrium pressure in the shallow caverns is well below lithostatic (= geostatic) pressure. More evidence for this conclusion is found in additional tests, such as the Carresse SPR3 creep test and the Bernburg shallow cavern pressure build-up test.*

2. The enclosed brine will slowly and gradually escape from the shallow caverns. For the small shallow caverns investigated, the calculated brine permeation varies between 0.6 and 1.4 m^3 per year. In the case of Stade-Süd larger shallow caverns have been abandoned, where also a brine permeation rate of some m^3/yr has been calculated, resulting in a brine penetration front reaching 10 m above cavern roof after 100 years.

3. The three SMRI-financed field tests have been executed in shallow small-volume caverns under laboratory-like conditions. Under these circumstances the validity of the SMRI concept of five factors governing pressure build-up has been shown. Furthermore, the results from the additionally reviewed tests in shallow caverns of Carresse and Bernburg are evidently supportive to the SMRI CS&A concept.

4. After any rapid cavern pressure build-up several transient phenomena are triggered. In that case application of (sophisticated) numerical models is needed to separately determine the effects of transient salt creep, brine permeation and additional salt dissolution on cavern pressure, because these are coupled processes.

5. Semi-analytical or 2D/3D-FEM numerical models are needed for predicting the combined long-term effects of salt creep, brine permeation and brine thermal expansion on cavern pressure development. In case of (almost) thermal equilibrium a conventional rock mechanical evaluation, applying well-known creep laws (NortonHoff, LUBBY2) and Darcy‟s flow law, is adequate enough. This type of modeling provides the long-term safety assessment normally required by mining authorities before granting permission for permanent cavern abandonment (Stade-Süd case, where also surface subsidence prediction and monitoring were obligatory).

In case of shallow cavern sealing and abandonment the following recommendations are relevant. The recommendations 1 to 4 are directly based on the results from the SMRI sponsored field tests. Recommendation 6 is given for the sake of completeness and might be relevant in exceptional cases only. It is based on the author's experience on abandoning shallow caverns in thinly bedded salts in The Netherlands. It should, furthermore, be noted that recommendation 6 does not apply to the many caverns dealt with in this report. Recommendation 7 is based on the author's general experience on official applications to mining authorities for definitely abandoning brine-filled caverns in the Netherlands, Germany and France:

1. Before permanently sealing a (shallow) cavern, an abandonment test should be performed. The test should consist of a sufficiently long observation period, during which one must try to assess separately the four processes (process 5: additional salt dissolution can be disregarded as it is a transient phenomenon) that govern long-term cavern pressure build-up. If more than one cavern at a cavern site has to be permanently abandoned, it should be checked whether the abandonment test results can be generalized.

2. During any cavern abandonment test a brine leak detection system should be installed in order to distinguish between brine migration into the salt rock and brine leaks through the casing shoe and wellbore.

3. If a shallow brine-filled cavern is at thermal equilibrium with the surrounding rock, the cavern can, in principal, be sealed and safely abandoned without delay. The tightness of the well must be proven; leaks through the casing and casing shoe have to be excluded. Furthermore, pay attention to the author's recommendations 6 and 7. This might imply that conventional numerical modeling is still needed to determine the long-term effects of salt creep and brine permeation on cavern pressure. Usually, before granting permission for permanent cavern abandonment mining authorities require this type of modeling with respect to a long-term safety assessment.

4. If thermal equilibrium is not yet reached, wait before sealing the cavern until the gap ΔT (°C) between brine temperature and formation temperature is smaller than β/α.(Plitho- Pbrine) ~ 0.01 H, where: β/α is close to 1 0C/MPa, Plitho = lithostatic pressure (MPa) at depth H, Pbrine= halmostatic pressure (MPa) at depth H, and H= casing shoe depth (m TV). The ratio β/α should be assessed for each specific cavern site. The temperature increase rate must be measured or computed. If after an observation period the gap ΔT is small enough, inject some extra brine in the cavern to obtain a brine pressure slightly higher than the anticipated/ calculated equilibrium pressure and seal the cavern. If the pressure rate is negative after some months, or less positive than expected from brine thermal expansion alone, and if the tightness of the well (casing and casing shoe) has been proven, the cavern can be safely abandoned without any risk for macro fractures or sudden, significant brine release into the salt roof and the overburden. In the case of large caverns the observation period after the extra brine injection, which causes a rapid cavern pressure increase, should preferably last about half a year. This longer time period is needed to ensure that transient phenomena, such as transient creep and additional salt dissolution that both cause a pressure decrease, have fainted away sufficiently and do not obscure the long-term pressure rate.

5. The SMRI Guidelines Manual (Research Project Report 2006-3) "Cavern Well Abandonment Techniques" represents a sound basis upon which companies should develop their own CS&A procedure for specific caverns, including a rock mechanical long-term stability analysis and surface monitoring.

6. Exceptionally, thus irrelevant for the many caverns reviewed in this report, a shallow cavern situated in thinly bedded salts and having a wide roof span with only a thin or absent salt roof layer starts (after an unknown period of time) migrating upward. This type of migration is the result of progressive roof deterioration mainly caused by rock mechanical overload and by brine affecting the overburden rock. This migration process may eventually cause a subsidence trough or even a sinkhole

at surface. This process could form a threat to public safety or contaminate drinkable-water producing sand(stone) layers above the cavern. Thus, in case of doubt on the long-term rock mechanical stability of the cavern roof, an inventory of the migrating potential of the cavern and related potential threats to the environment and third-party interests should be made before definitely sealing off the wellbore and abandoning the cavern. As long as the cavern is accessible effective mitigating measures can be taken such as filling the cavern with solid materials.
7. Mining authorities often require an answer to the following question before they decide to grant permission for permanent brine-filled cavern abandonment: "which brine volumes will eventually migrate where and at which times from the rock salt into water/brine bearing aquifers"? Related to this question is the need for a detailed geological analysis to show the presence of containment and confinement horizons in the overburden that prohibit aquifer contamination by expelled cavern brine. It is recommended that efforts of the SMRI research should now focus on these aspects of brine migration and containment, and on the development of a general methodology to tackle this question."

This Report, and the conclusions-recommendations copied above, prove that, when shallow cavern are concerned, a consensus has been reached in most of the research groups in Europe and the US. However, it is clear that Recommendation 4 must be used carefully (injecting some additional brine in the cavern to check that cavern pressure consistently decreases is safe only when the pressure level reached before injection is significantly smaller than geostatic pressure.)

4.10 The Gellenoncourt test (2010 – 2019)

The Gellenoncourt brine field, operated by Compagnie des Salins du Midi et Salines de l'Est (CSME) since 1965, is located at the eastern (and shallowest) edge of the Keuper bedded-salt formation of Lorraine-Champagne. The SG13 and SG14 7"-wells were drilled to a depth of 280-300 m in May 1975, and operated as brine-production wells from July 1976 to June 1977 (SG13), and from October 1978 to July 1980 (SG14). After some time, the two caverns coalesced, and SG13-SG14 now are connected by a large link; hydraulically, they can be considered as a single cavern (Figure 51). Cavern volume at the end of the mining operations were inferred from "mass balance" – i.e. from the cumulated amounts of injected water and withdrawn brine during mining operations - which suggests that the actual cavern volume might be as large as 140,000 m^3. The average cavern depth is 250 m.

The halmostatic pressure is $P_h = 2.97$ MPa, and the geostatic pressure is $P_\infty = 5.39$ MPa. At the beginning of the test, pressure evolution was very slow (Figure 52). In 2011, small amounts of brine were withdrawn periodically in order to reach equilibrium pressure more rapidly. Any pressure drop was followed by a transient period (several weeks) during which pressure increased before decreasing again (see EZ53 test, Section 4.4.5). Because it was observed that cavern pressure consistently decreased, it was decided, in Spring 2013, to lower the cavern pressure from $p_i = 3.79$ MPa to $p_i = 3.16$ MPa. After this pressure drop, cavern pressure consistently increased, proving that equilibrium pressure is smaller than 3.75 MPa and larger than 3.3 MPa.

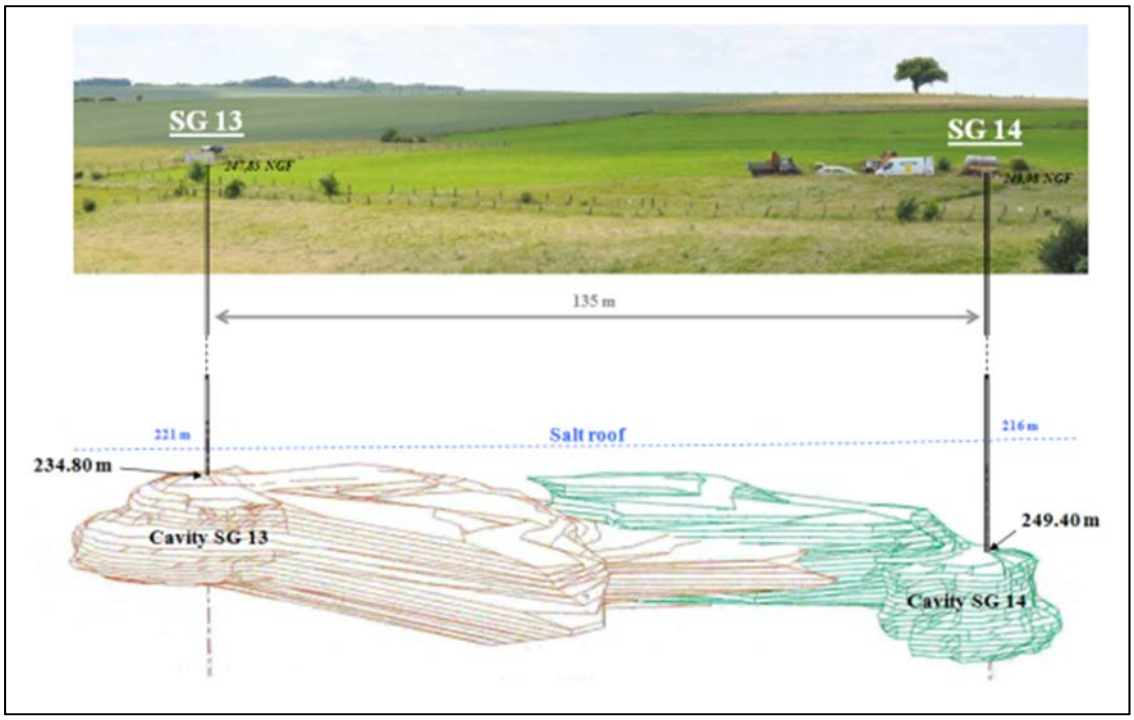

Figure 51 - 3D view of the SG13-SG14 cavern (Brouard et al., 2017).

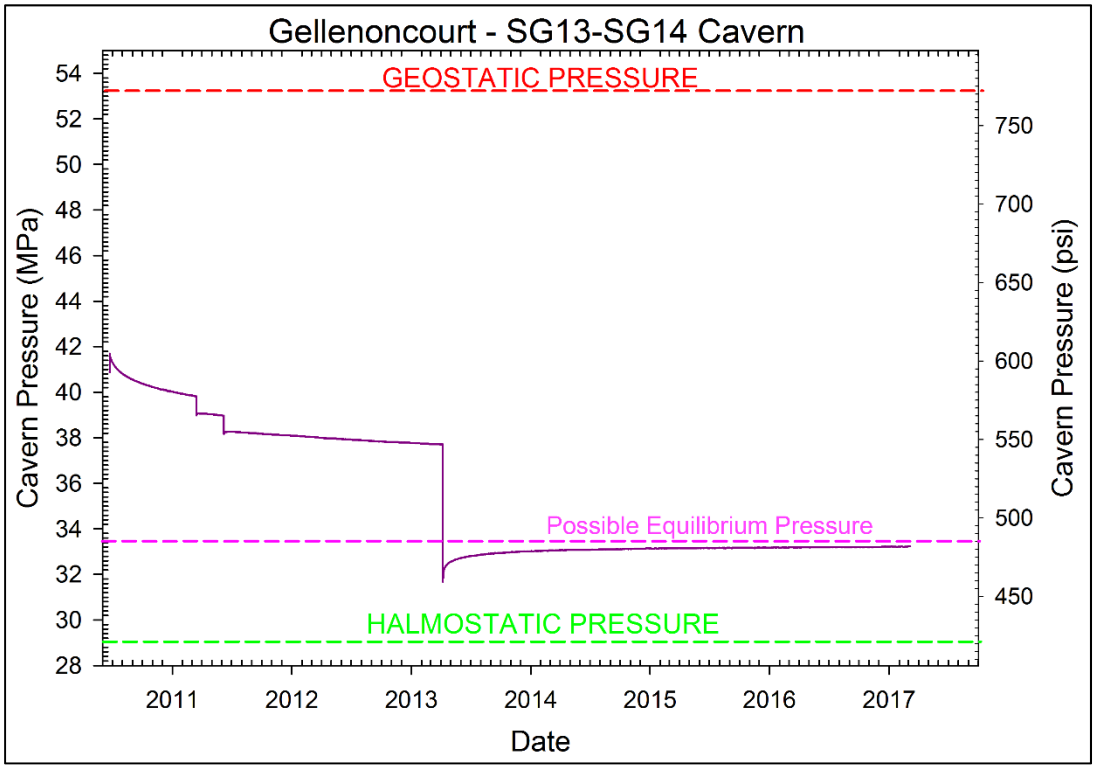

Figure 52 - Downhole-pressure evolution from 2010 to 2017 at a 250-m depth in the SG13-SG14 cavern. Pressure was adjusted several times through brine injection or withdrawal. Geostatic and halmostatic pressures were estimated to be 5.39 MPa and 2.97 MPa, respectively (Brouard et al. 2017).

4.11 The Stassfurt test (2005-2008)

The SMRI supported a test performed in the S101 and S102 caverns at Stassfurt (Germany). Test caverns S101 and S102 are represented on Figure 53. Their volume, height and roof depths are as follows: for S101, $V = 10{,}100$ m^3, $h = 60$ m and $H = 421$ m; for S102, $V = 13{,}600$ m^3, $h = 125$ m and $H = 436$ m. Average depths are 450 m and 500 m, respectively. When tests began, the caverns had been shut in for 30 years. In addition, they had been solution mined with warm water. It was highly likely that thermal equilibrium had been reached. As the wells were not equipped with a central tube, no leak-detection system (see Section 4.4.5) could be implemented. Based on reasonable analogies, leaks through the casing were believed to be small.

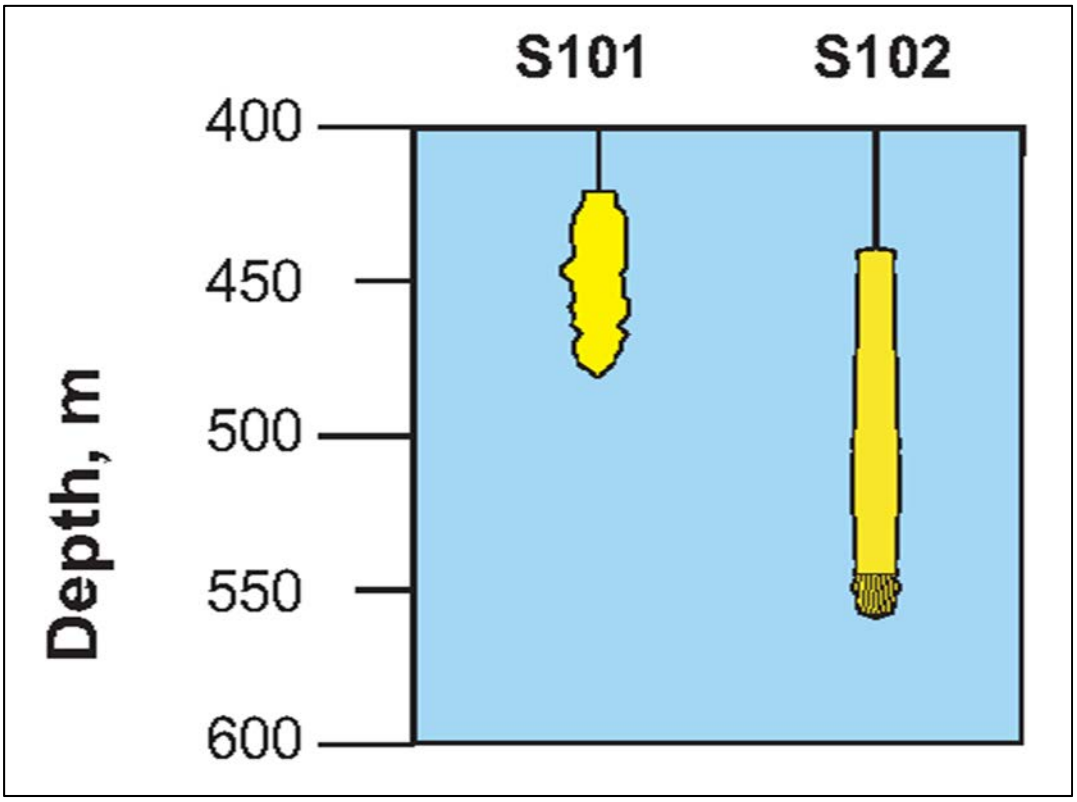

Figure 53 - Vertical cross-sections of caverns S101 and S102 of the Stassfurt brine field (Banach and Klafki, 2009).

Caverns had been shut-in in August and September 2001, respectively (Figure 54). The pressure-increase rate is slightly faster in S102 than in S101 (S102 is slightly deeper). Both rates slowly decrease with time. This is consistent with what is known from the mechanical behaviour of salt.

For S101, it was decided to let evolution continue; more accurate pressure sensors were set at the wellhead. Yearly fluctuations can be observed, due to seasonal temperature changes at ground level (see Figure 55).

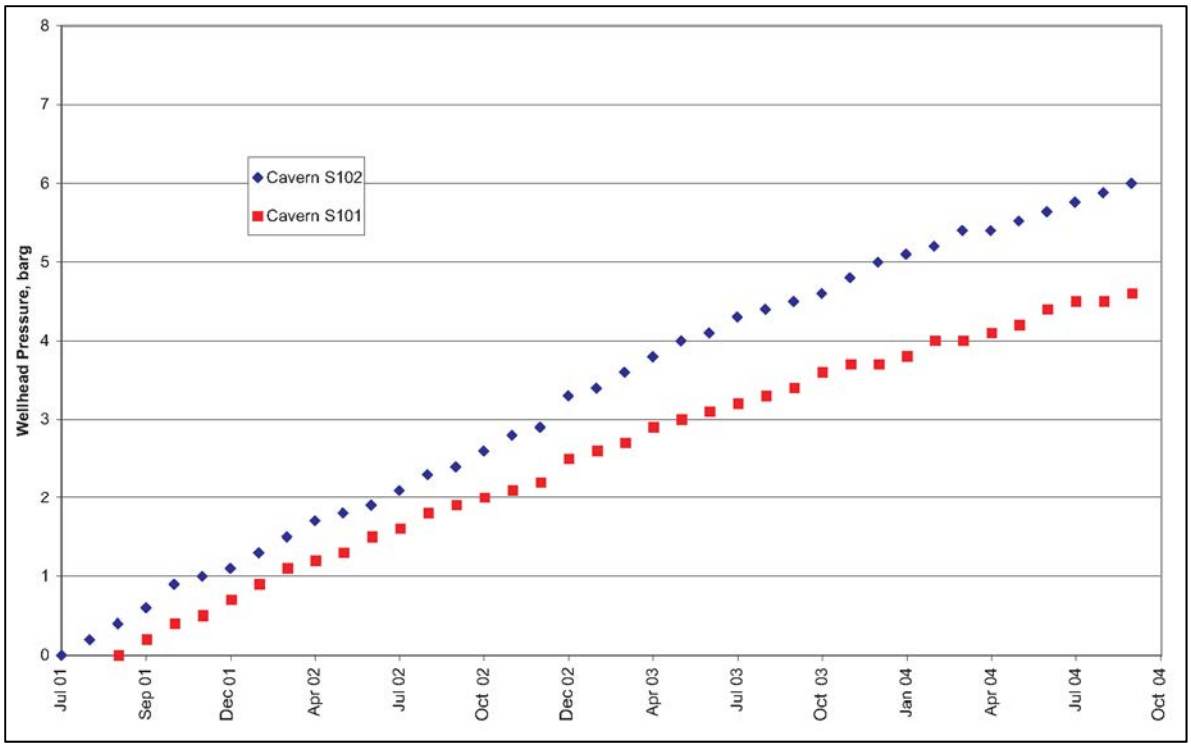

Figure 54 - S101 and S102 wellhead pressure evolutions before the abandonment test from July 2001 to October 2004 (Banach and Klafki, 2009).

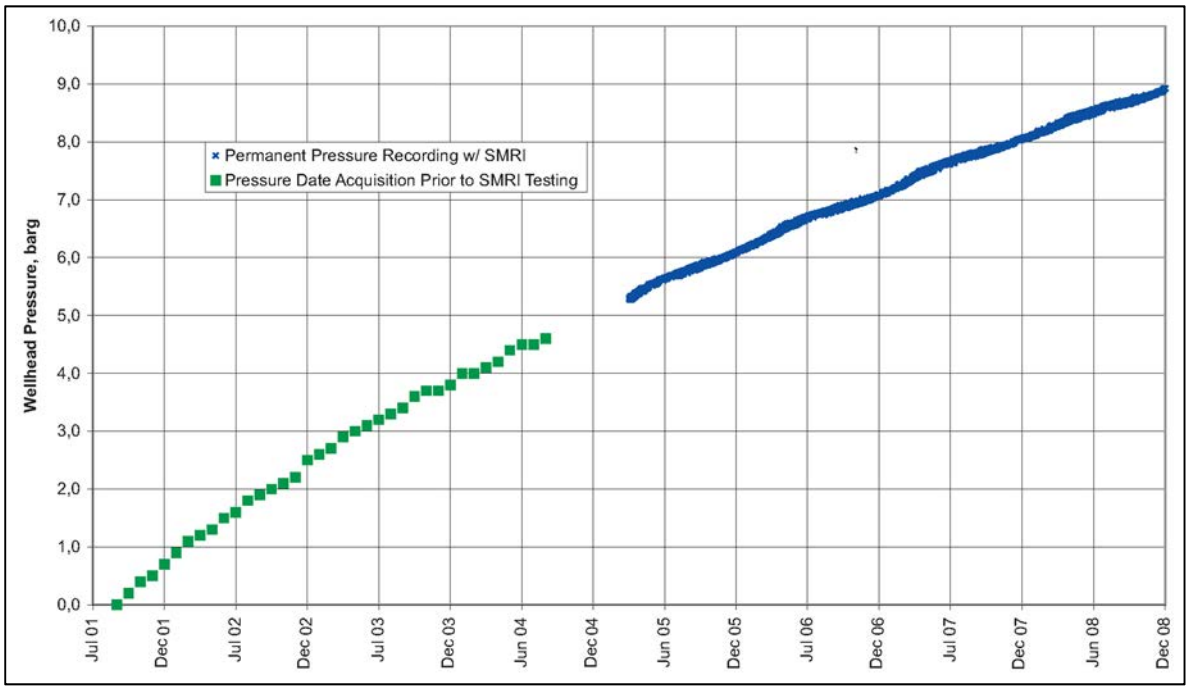

Figure 55 - S101 wellhead pressure evolution before (2001-2004) and during (2005-2008) the abandonment test (Banach and Klafki, 2009).

S102 was de-pressurized to atmospheric pressure. Sonar and temperature logs were performed. On 17 March 2005, S102 was pressurized again to 95% of the lithostatic pressure through brine injection (Figure 56). Wellhead pressure decreased first; however, after 10 months, it was almost perfectly constant. An abnormal pressure drop was observed on 7 November 2007. A small leak was identified at the casing-head housing and repaired. (This was not deliberate; however, the test became a *de facto* trial-and-error test; see Etrez EZ53, Section 4.4.5). After the repair, pressure increased again. This test strongly suggests that in this shallow cavern, in the long term, pressure will reach an equilibrium value that is significantly smaller (by 1.3 MPa) than lithostatic pressure at cavern depth.

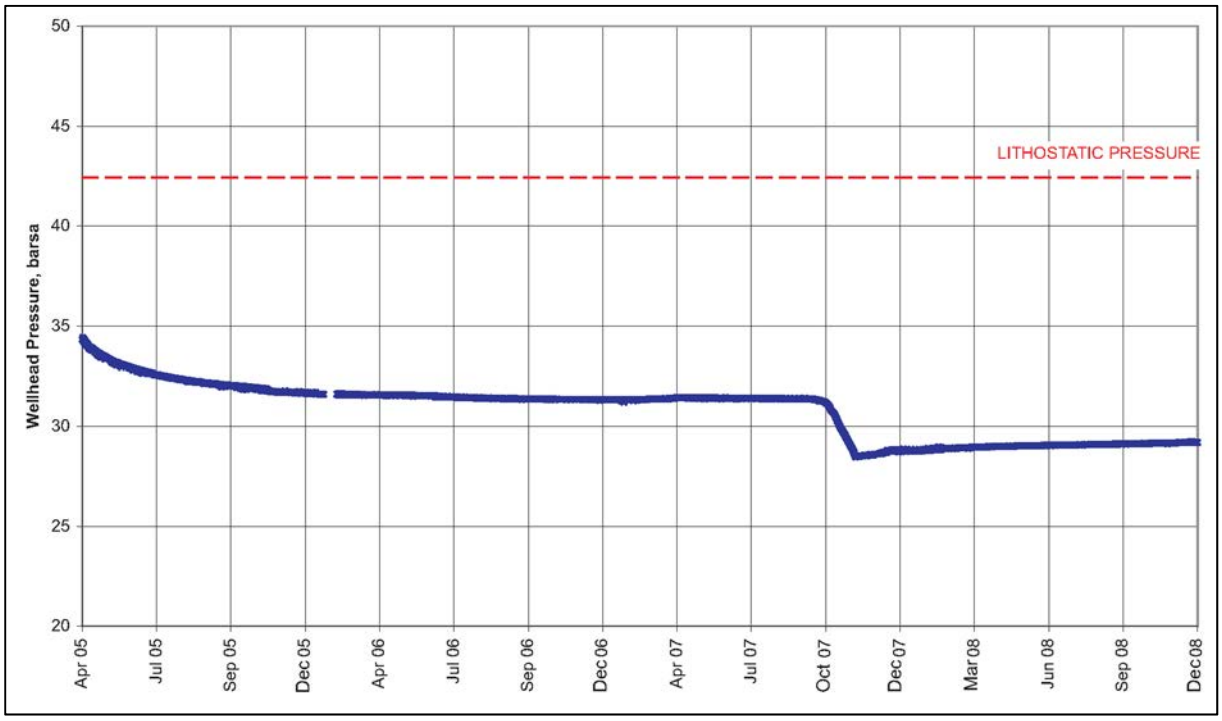

Figure 56 - S102 wellhead pressure evolution during the abandonment test (Banach and Klafki, 2009).

A model was built in which salt creep and brine permeation were included. In this model, permeability was able to increase. The main conclusions of the test are listed below.

- [Brine warming] For the test caverns at the Stassfurt salt, deposit salt/cavern fluid heat transfer can be excluded, proven by the congruent temperature profiles logged prior to testing and after test completion).

- [Additional dissolution] In terms of additional salt dissolution it has been identified that the increased leaching potential forced by the rapid pressure build-up will lead arithmetically to a comparable pressure fall-off, as expected from brine permeation at a transient rock stress state. However, this inherent ambiguity is limited to a rather short time period (days or weeks) after cavern pressurization and, therefore, does not affect the brine permeation process at the found equilibrium.

- [Creep closure] Salt creep has been analysed by history-matching the acquired pressure data applying rock mechanics models. Based on the analysis results, it becomes evident that cavern closure at the found equilibrium pressure is very low; thus, the respective brine flow rate that permeates the cavern wall must be equally small.

- [Creep closure] The performed rock mechanics modelling shows different rock-stress states around the cavern for the moment immediately after cavern pressurization compared to the found equilibrium pressure, which implies different salt permeabilities at the different rock-stress states. The measured pressure response at cavern S102, with gradually decreasing pressure fall-off rates for the first 10 months of the observation period, basically confirms the above-mentioned assumptions.

- [Permeation] The estimated salt permeability at the equilibrium pressure is equal to the often-applied initial permeability of $K_{ini} = 10^{-21}$ m^2, which indicates that the salt permeability does not necessarily need to be increased to reach a pressure equilibrium lower than the lithostatic pressure. For the transient rock-stress state, a raised permeability of $K_{ini} = 10^{-20}$ m^2 is estimated and is therefore approximately one order of magnitude higher than the initial estimate. Taking into account that, for the Stassfurt field test, the difference in cavern fluid pressure immediately after cavern pressurization compared to the found equilibrium is limited to $\Delta P = 6$ bar, the estimated permeability increase appears plausible.

A remarkable result of this test is that, in a small and shallow cavern, because creep closure is slow, even a small value of the permeability allows the system reaching a relatively low equilibrium pressure.

4.12 Bryan Mound (Louisiana)

This case was described by Sobolik and Lord (2014).

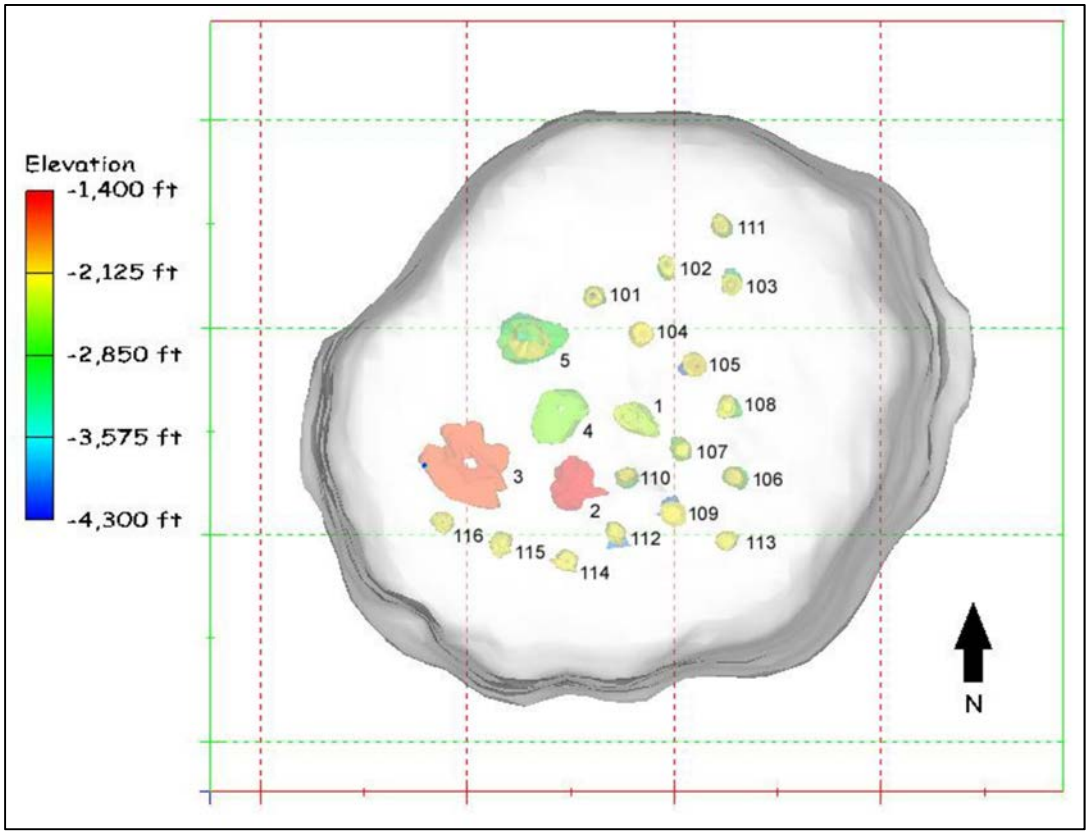

Figure 57 - Top view of the Bryan Mound salt dome and oil storage cavern model (610 m grid spacing). From Sobolik and Lord, 2014.

The Bryan Mound salt dome, located approximately 60 miles south of Houston, Texas, is a part of the Strategic Petroleum Reserve (SPR) operated by the US Department of Energy (DOE). It comprises of 20 storage caverns which, in 2014, held 43×10^6 m^3, or 226 MMbbls, of oil. Salt mechanical creep properties and levels of anhydrite impurities are highly heterogeneous and the dome includes several boundary shears zones and faults. Caprock was damaged in the early 20th century by sulphur mining.

Cavern 3, located in the southwestern quadrant of the dome (Figure 57), contains a volume of 1.02×10^6 m^3 based upon a 1979 sonar survey. The cavern's depth is at about 450 meters (1475 ft), only about 90 meters (300 ft) beneath the overlying caprock. The roof is highly irregular and the maximum diameter of the cavern (~410 m or 1345 ft) is the largest of any of the DOE-owned caverns. It was initially developed by Dow for brine production in the period 1942 to 1957. Due to its large roof span, it was shut down in 1957 and never used for storage purpose. Two years later, the pressure dropped, a clear evidence of a leak. Testing by Dow showed the well had hydraulic integrity, but not the cavern.

Subsidence rates have been recorded since December 1982. The subsidence rates between January 2007 to April 2009 are provided in Figure 58. They were highest above Cavern 3. The same trend can be observed from 2009 to 2013. Rates vary between 0.02 and 0.14 ft/yr (6 to 14 mm/yr). Various improvements, including additional monuments, a GPS and tiltmeter system were installed over Cavern 3. Numerical computations were performed; Cavern 3 was modeled as a slowly decreasing at a rate of 1.06 kPa/yr (0.15 psi/yr) beginning in late 2003.

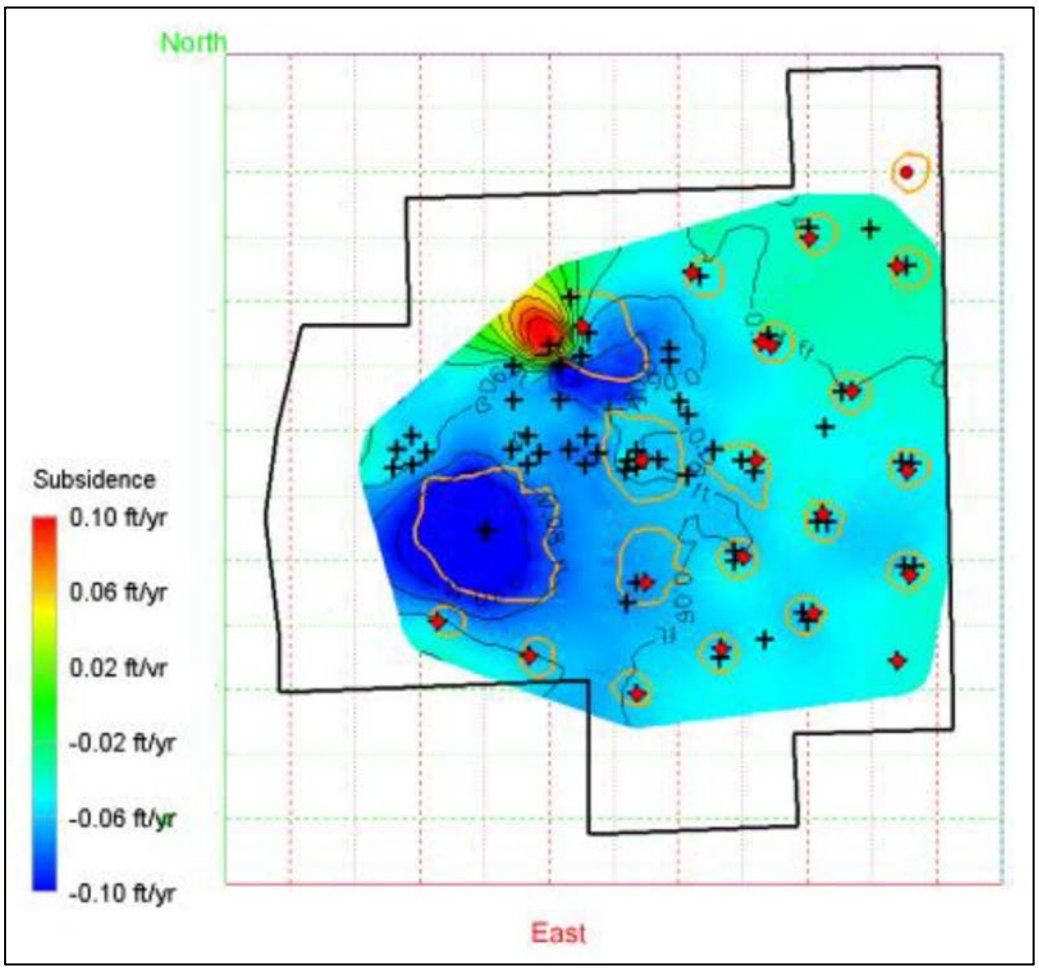

Figure 58 - Contour plot of subsidence rates (ft/yr) from January 2007 to April 2009. From Sobolik and Lord, 2014.

In principle, in a brine-filled shut-in cavern, brine pressure increases because of brine warming and creep closure, leading to slower closure rate. It is generally recognized that subsidence rate at ground level above a salt cavern is proportional to cavern closure rate. It results that subsidence rate above Cavern 3 should be slower than above the other caverns of the site which experience episodes during which cavern pressure is low (workovers). It is not, strongly suggesting that brine seepage from the cavern impedes pressure increase. It is generally assumed that the fluid loss would actually occur via a preferential path through the borehole to the caprock, damaged by earlier sulphur mining, into which the brine can flow.

4.13 The Carresse SPR2 test (2004-2013)

4.13.1 Test design

The SPR2 cavern is located in southwest France at Carresse, where Total operated a propane storage facility including three propane caverns and one brine cavern. SPR2 was leached out in the early 1960s in a diapiric structure of the Pyrenean foothills and used for storing liquid propane. It was decommissioned, and propane was withdrawn in 2002. SPR2 volume is $V \approx 9{,}000$ m^3 (see Figure 44, p.70). The salt formation contains relatively thin salt layers of Triassic age. The amount of insoluble materials, mainly clay and anhydrite, is relatively large (20% to 30%). Well completion includes a 286.6-m deep, 9-⅝" last-cemented casing and a 319.7-m deep 4" string. Cavern roof and bottom depths are 304.4 m and 321 m, respectively.

In this (approximately) 310-m deep cavern, the geostatic pressure is $P_\infty = 6.68$ MPa and the halmostatic pressure is $P_h = 3.64$ MPa. A trial-and-error test, supported by the SMRI, began in June 2004 on SPR2 (Brouard Consulting et al., 2006). The temperature increase rate of the brine was measured from October 2002 to January 2003; it was $\dot{T} = 0.66$ °C/yr. The gap between rock temperature and brine temperature was estimated to be 1.8 °C. It was suspected that some liquefied propane had remained trapped in the cavern. Géostock designed an innovative method consisting of lowering brine pressure below propane-vaporization pressure (de Laguérie et al., 2004) to allow propane vaporization in the traps. Detrapped propane was vented and flared. In June 2003, 22 metric tons of propane were released over 4 days. It is likely that propane vaporization slightly lowered cavern brine temperature. In April 2005 (one year after the beginning of the test), a leak-detection system was set in the well.

4.13.2 Test Results

At the beginning of the test (June 2004), cavern pressure was increased by 1.15 MPa through brine injection (A'-B' on Figure 59). During the course of the test, several pressure steps were achieved, through injection/withdrawal of green oil (C'-D', E'-F', G'-H'). As it was known that the cavern was not in thermal equilibrium with the rock mass, temperature evolution was computed based on earlier measurements, and the effect of brine warming was subtracted from the actual (as-measured) pressure evolution (see the green curve on Figure 59). This computation proved that inferring equilibrium pressure from test results is difficult when thermal equilibrium has not been reached. From 15 September2005 to mid-November 2005, pressure consistently decreased (a transient effect generated by "reverse" creep, transient permeation and additional dissolution, see Bérest et al., 2007). After December 2005, pressure increased again, and no additional injection/withdrawal was performed.

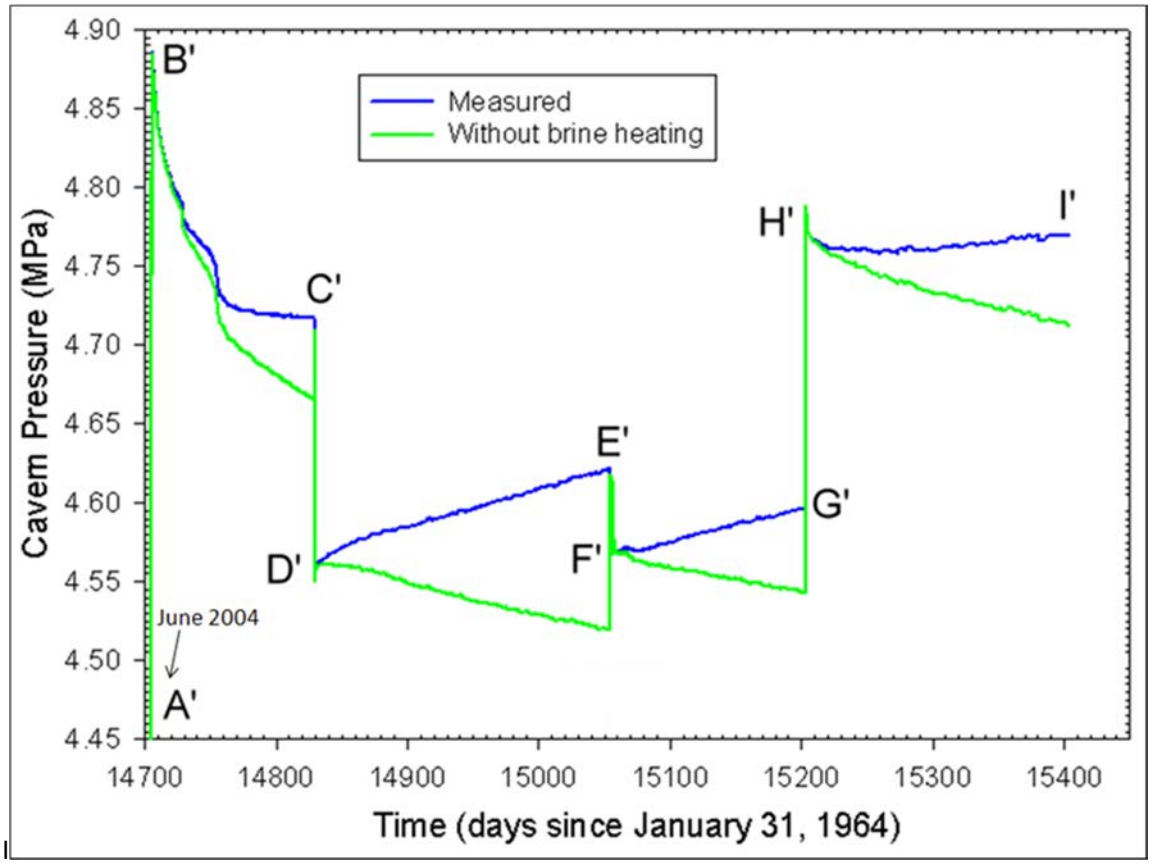

Figure 59 - SPR2 pressure evolution from June 2004 to April 2006 during the trial-and-error test (Brouard Consulting et al., 2006).

It was predicted at that time that the brine-temperature rate would decrease slowly and that thermal expansion would become small enough, after several years, to be unable to prevent cavern pressure drop.

4.13.3 Further evolution of cavern pressure from 2005 to 2013

Pressure evolution was recorded both in the annular space and in the central tubing from October 2005 (end of the trial-and-error test) to 2013 (see Figure 60). Pipes were removed at ground level in May 2010, leading to an increase in annular space pressure by 0.17 MPa, but this operation was not documented fully. It was expected that pressure reached a maximum after several years; in fact, the pressure increase rate consistently decreased but, eight years after the October 2005 injection, no maximum had been reached.

The difference between predicted and observed evolutions is relatively small (see Figure 61). In the framework of its Abandonment Research Program, the SMRI issued an RFP focused on obtaining a better explanation of this difference. The report by Brouard et al. (2010) considered several hypotheses and proved that the discrepancy could be explained by underestimating the geothermal temperature by 0.1 °C, a small figure. This example proves that brine warming can play a role even in a small cavern.

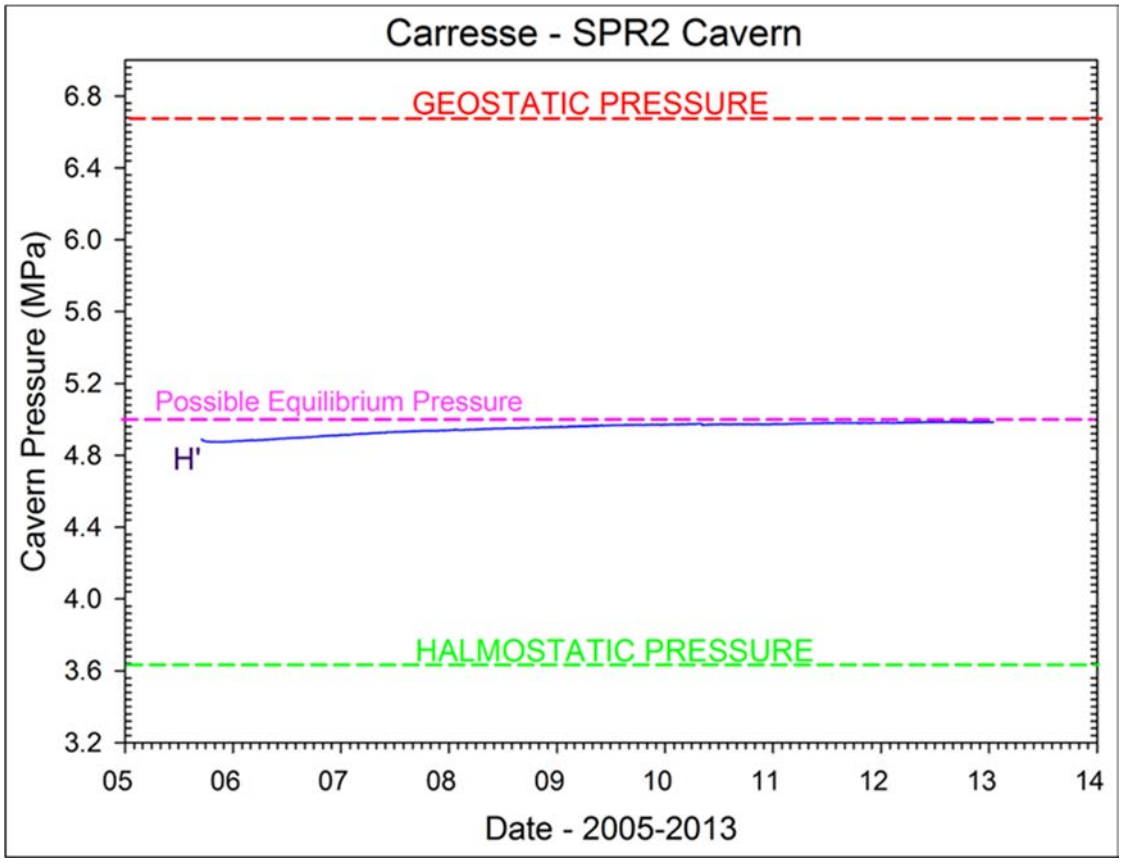

Figure 60 - SPR2 pressure evolution during the 2005-2013 period.

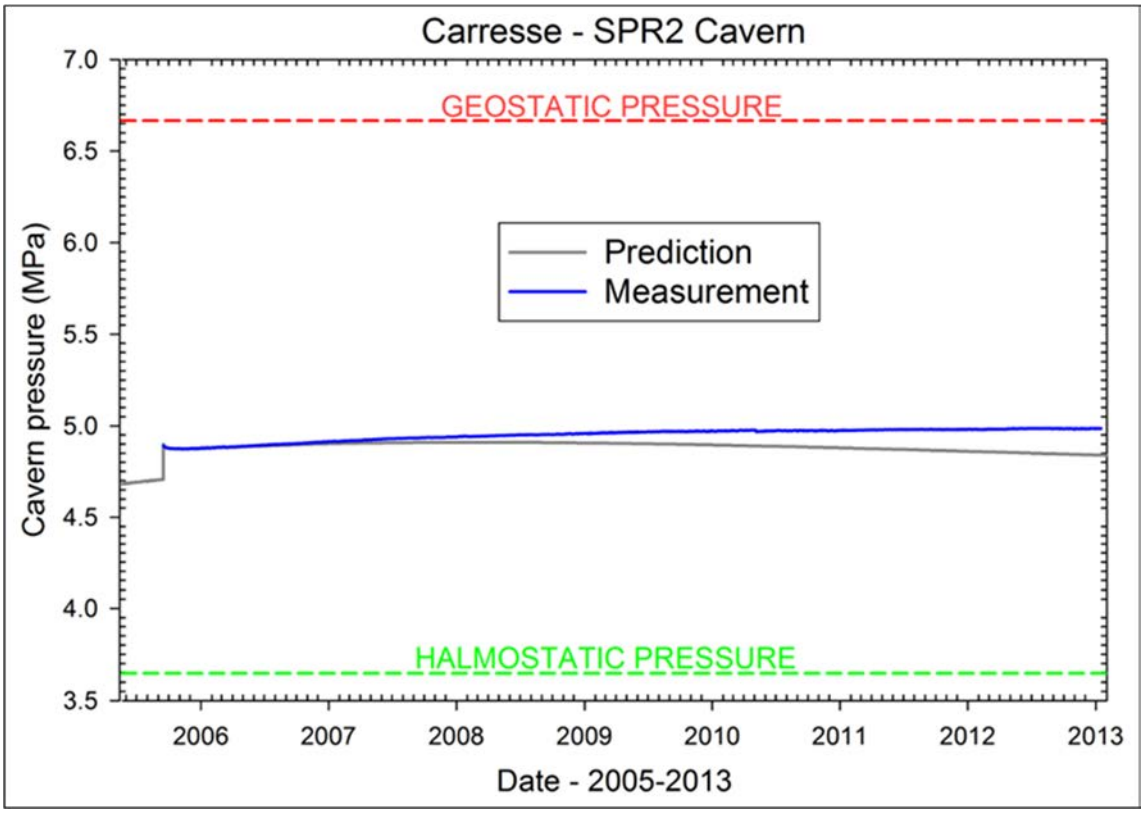

Figure 61 - SPR2 — Comparison between predicted cavern-pressure evolution and measured pressure (computed cavern pressures were predicted using the 2004-2006 test results).

4.14 The Matacães abandonment study (2018)

A brine field has been operated at Matacães in Portugal since 1954. Twenty-two caverns had been created for production of 19 million tons of salt. Salt production ended in 2014, and the operator asked Ineris, the French National Institute for Industrial Environment and Risks, to analyse the long-term behaviour of caverns after abandonment.

The approach adopted for this study is similar to the one proposed in Bérest et al. (2001a) and Thoraval et al. (2015). Three main phenomena were taken into account: cavern creep closure, whose rate is a decreasing function of cavern pressure; brine permeation through the cavern walls, which is an increasing function of cavern pressure; and brine warming, which is practically independent of cavern pressure and which vanishes after a time depending upon cavern size and shape. When brine warming can be disregarded, an equilibrium pressure can be found such that the brine-permeation rate exactly equals the cavern-convergence rate. The cavern is safe when this equilibrium pressure is significantly lower than lithostatic pressure.

An interesting feature of this particular site is that caverns vary considerably in depth and size, from $H = 289$ to 1200 m, and from $V = 15{,}000$ m^3 to 876,000 m^3.

Thoraval et al. (2018) focus on the investigation performed before an abandonment test. Temperature was measured in a couple of wells and have shown that equilibrium was not fully reached. Parameters of the creep law were fitted against the evolution of wellhead pressure during shut-in tests, and cavern compressibilities were measured to detect any possible hydraulic connection between the caverns. Computations proved that, even for the deepest cavern, equilibrium pressure remained below lithostatic pressure at the cavern roof. However, in some cases, due to the effects of brine warming, brine pressure can exceed lithostatic pressure during a transient period. At the date when the paper was presented (September 2018), an abandonment test was being planned for the near future.

4.15 Stade-Süd shallow cavern abandonment

The four brine-filled caverns that were to be abandoned at Stade-Süd (Brückner and Wekenborg, 2006) are situated in a dome-shaped anticline (Figure 62). One of the caverns is positioned somewhat deeper (its bottom at 1280 m), but the others are shallow (500-770 m, 600-680 m and 790-445 m). Their volumes range from 77,000 to 1,353,000 m^3. In 2004, compressibility tests were performed, yielding normal values of the compression modulus between $1/\beta = 2.4$ and 2.9 GPa, except for one cavern that produced small amounts of gas and yielded a modulus of 1 GPa only (compressibility factor of 10×10^{-5}/bar; the cavern compressibility factor, β (see Section 4.2.2), significantly increases when the cavern contains a small amount of gas (x in % volume), $\beta = \beta_c + \beta_b + x/P$). The German authorities required a numerical long-term safety assessment for the sealed and abandoned caverns. The rock mechanics model was fitted to the in-situ observations and resulted in prognoses for cavern convergence, pressure build-up and surface subsidence. The salt creep was described by the Norton-Hoff power law. The caverns were not yet in thermal equilibrium, but it was shown that thermal

brine expansion was insignificant compared to the effect of cavern convergence on the brine pressure build-up. The brine permeation was modelled by Darcy flow, using an initial salt permeability of 10^{-20} m² and a porosity of 0.3 %.

Modelling results (see Section 6.6) showed that brine penetrates the salt in the cavern-roof area with a rate of some m^3/yr (no numbers specified in the paper). According to computations, after 100 years, the brine has reached a level of 10 m above the cavern roof and about 50 m above the roof after 3000 years. The wells themselves were plugged and abandoned according to applicable mining regulations. This implied a special requirement for one cavern: to mill a 50-m-high window in the last cemented casing starting 40 m above the cavern roof, to underream the milled section to remove old cement and then to set a new tight cement plug.

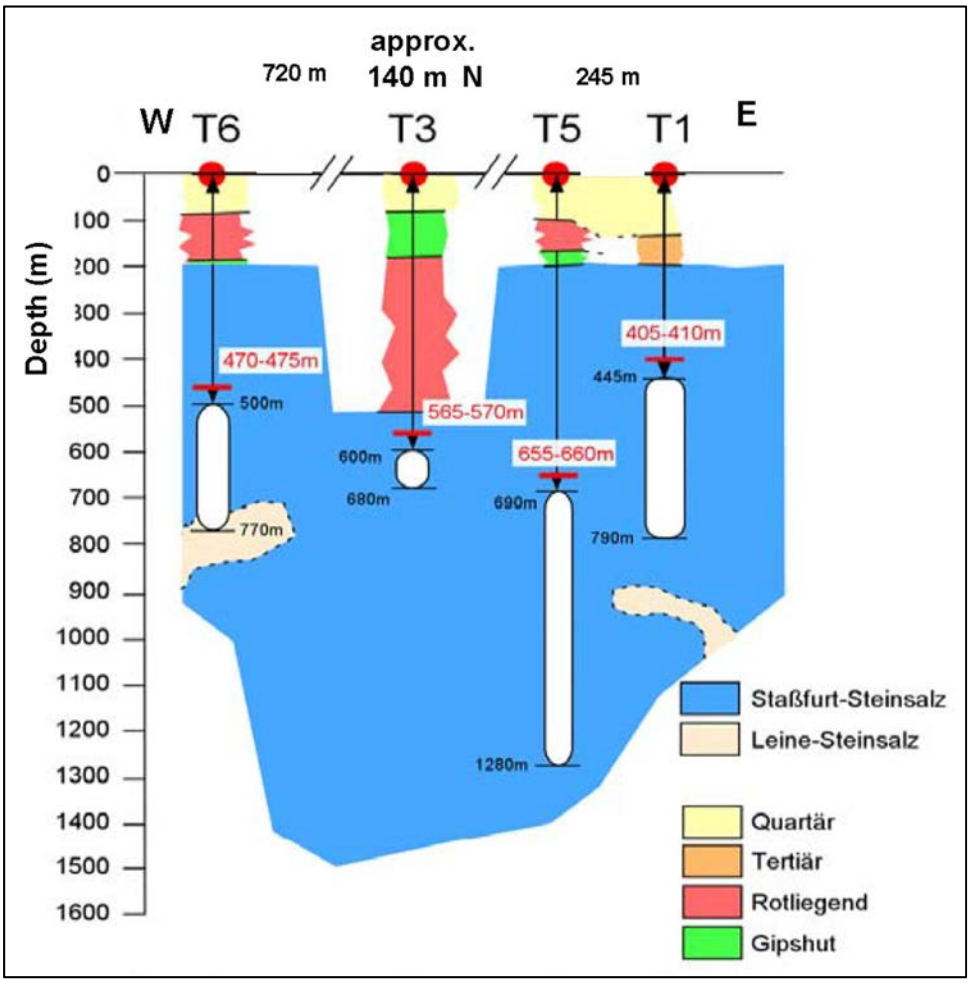

Figure 62 – Location of Stade-Süd caverns (Brückner and Wekenborg, 2006).

4.16 West Texas Salt Cavern Wells

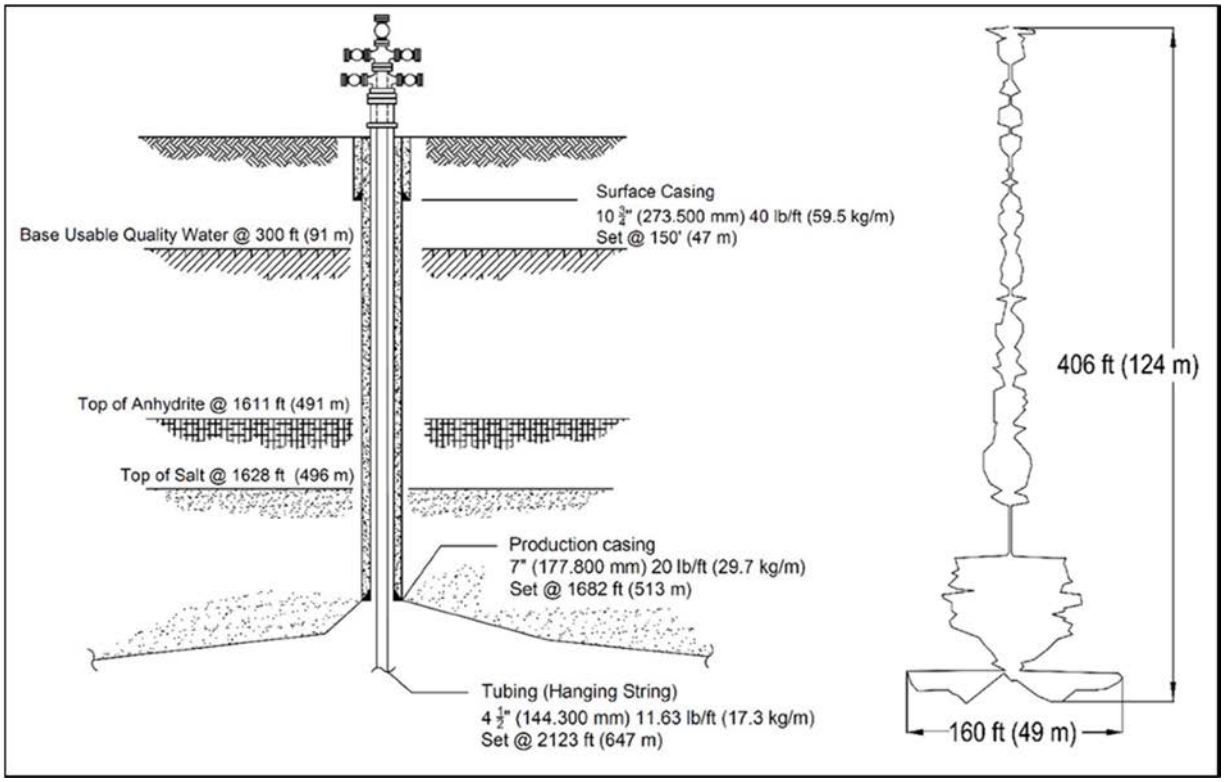

Figure 63 - Well completion (left) and Well No.1 shape and maximum dimensions (right).

A case study on the abandonment process of four solution-mined storage caverns developed in the Salado Formation of West Texas was presented by Schulte and Stilson (2019). The salt is found at depths of less than 2000 ft (600 m) and net thicknesses up to 700 ft (214 m). Salt beds are interbedded with mudstone and mud-salt beds, and anhydrite beds separate the salt-mudstone units. The cavern volumes are relatively small [50,000 barrels (US bbls) or 8,000 m^3], with Well No. 1 being the largest at 120,000 bbls (18,800 m^3). The caverns have no neck and the ratio diameter/height is high (see Figure 63). Analysis is performed within the SMRI theoretical framework: the authors mention the "*five primary phenomena resulting in pressure changes in a sealed or shut-in cavern that has been brine filled: (1) pressure gain due to cavern convergence or salt creep; (2) pressure gain due to cavern brine warming; (3) pressure loss due to brine loss casing or casing shoe leaks; (4) pressure loss due to salt dissolution to the cavern brine; and (5) pressure loss due to brine permeation into salt or non-salt members (Ratigan, 2003).*"

In fact, among the five phenomena mentioned above, the authors focus on casing leaks and brine warming, discussed below. [In these shallow caverns, creep closure is likely to be slow; the ratio between surface and volume is high, which means that permeation is likely to be effective; it is reasonable to assume that both contribute to a low equilibrium pressure, not analyzed in the paper]. Cement bond logs (CBLs) run on the cemented production casing (final or deep casing) strings to both the casing and the formation over the length of the wellbore. MITs were conducted at production casing shoe pressure gradients between 0.64 psi/ft (14.5 kPa/m) and 0.77 psi/ft (17.4 kPa/m). CBLs showed very good bonding.

The four caverns were removed from hydrocarbon storage service approximately two years prior to plugging. Pressure was measured over a period of seven months (including a bleed). Two wireline temperature logs, spaced by three months, were run. Over the three-month period, a warming trend of approximately 0.1 °F (0.06 °C) across the cavern interval was measured. The second temperature log for each well is presented in Figure 64. Figure 64 includes a temperature log (adjusted for comparison) from a nearby well, capturing the in-situ salt temperature gradient. Temperature gradient in the cavern is influenced by cavern shape (Figure 63): brine temperature increase is faster in the cavern parts whose radius is smaller (also clear in Figure 65). As a whole, temperature is close to equilibrium.

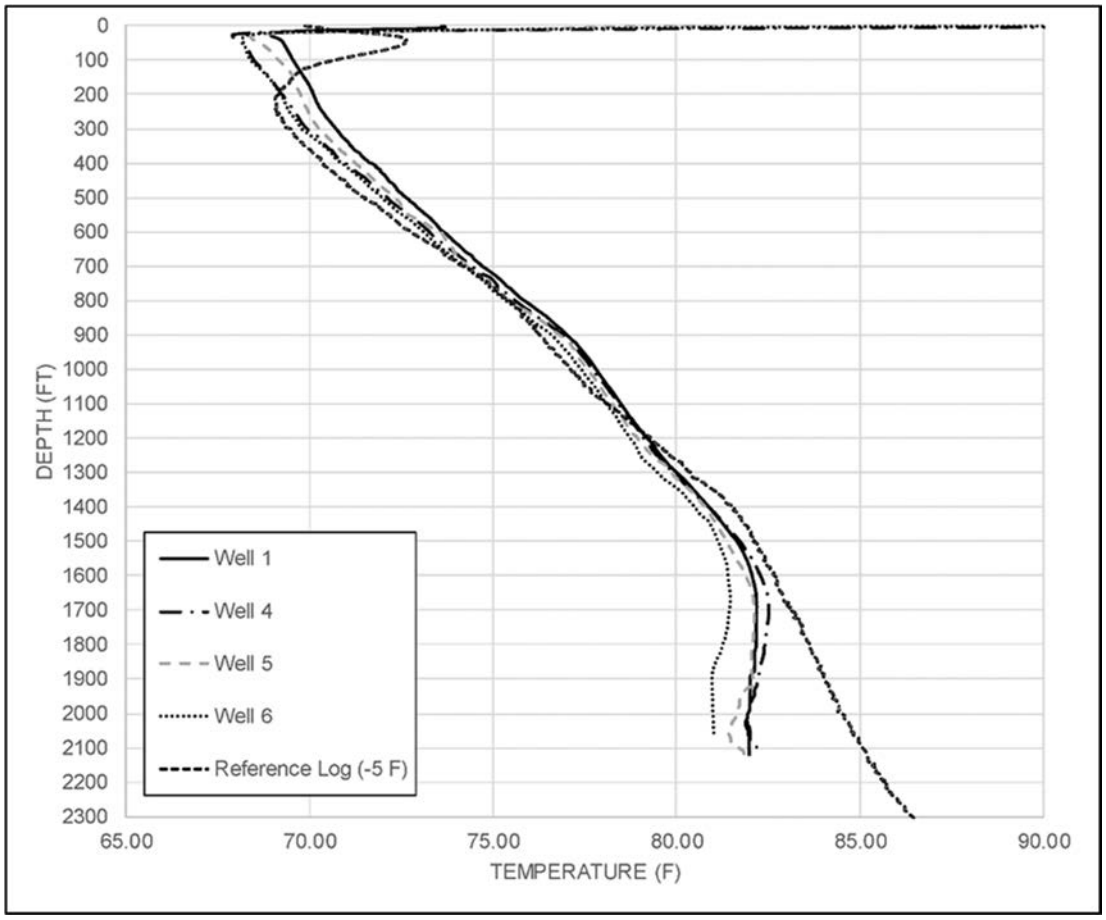

Figure 64 - Post operational cavern temperature (log 2) and reference temperature log.

Temperature evolution was modelled using SCTS (a specialized software) in order to assess the final cavern temperature and the resulting pressure increase (when permeation is neglected). For instance, the SCTS model of Well No. 1 predicts an increase in brine temperature of just 1°F (0.56 °C) over the next 50 years approaching a value of 83°F (28.3 °C). Assuming a coefficient of thermal expansion for brine of $\alpha = 0.00023$ per °F [the paper provides 0.000128 per °C as an equivalent; in fact, one must read 0.000414 per °C], a $\Delta T = 1$ °F (0.56 °C) increase in brine pressure will result in an (impeded) increase in brine volume of 0.023% and an ultimate pressure increase of $\Delta P = 43$ psi (296 kPa), when the cavern compressibility [i.e. βV] measured during the most recent MIT [i.e., $\Delta P = \alpha \Delta T / \beta$] is used. The authors mention that most recent MIT of Well 1 was performed at 350 psi (2.413 MPa) above brine pressure gradient (halmostatic pressure). Therefore, the ultimate

pressure of the cavern will be much less than the maximum pressure at which cavern tightness was demonstrated, thereby ensuring the long-term safety of cavern abandonment.

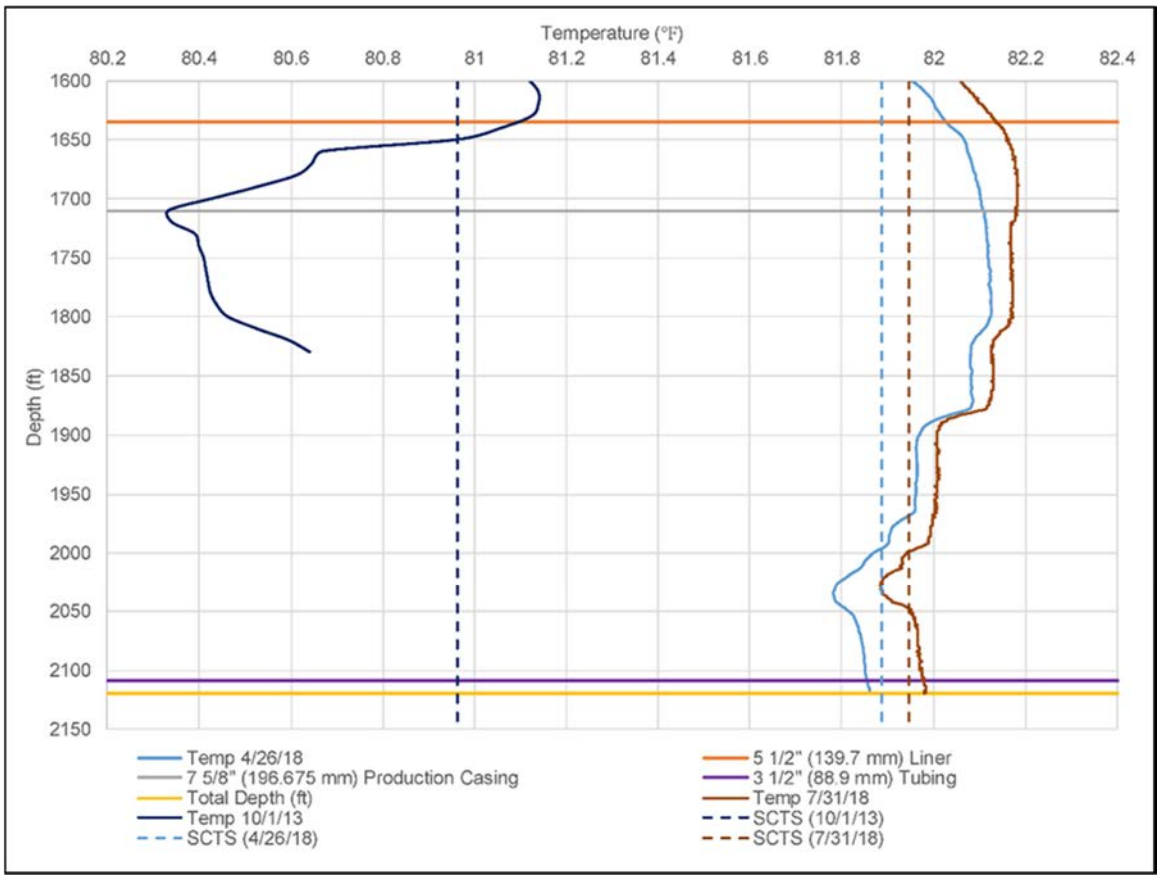

Figure 65 - Measured temperature vs. depth at three periods in time and SCTS predicted bulk temperature.

5. DEEP CAVERNS

5.1 A comment on tests performed in shallow caverns

The notion of an "equilibrium pressure", significantly smaller than geostatic pressure, is strongly supported by SMRI in situ tests performed in shallow caverns. However (see Table 4), some comments must be made. The caverns were "old" (the idle period before the test was long), except for Carresse SPR2, and "small" (except for Gellenoncourt SG13-14). As a consequence, thermal equilibrium between rock mass and cavern brine was almost perfectly achieved (except at Carresse SPR2). This would not be true in many large caverns (500,000 m^3).

Table 4 - Five tests performed in shallow caverns.

	Volume (m^3)	Depth[1] (m)	Idle Period[2] (yr)	Test Duration (yr)	Halmostatic Pressure[3] (MPa)	Equilibrium Pressure (MPa)	Geostatic Pressure[4] (MPa)
Etrez EZ53	8000	950	25	13	11.4	13 ± 0.1	20.9
Bernburg	22	450	-	2	5.4	??[5]	9.9
Gellenoncourt SG13-14	140 000	250	30	7	3	3.55 ± 0.15	5.5
Stassfurt S102	13 500	43	30	4	5.2	8.25 ± 0.15	9.6
Carresse SPR2	9000	300	1	8	3.6	4.5[6]	6.6

[1]Depth at which pressures are computed (casing shoe depth, or average depth)

[2]Duration of the period before the test started during which small or no movement were performed

[3]Based on a 0.012 MPa/m gradient

[4]Based on a 0.022 MPa/m gradient

[5]Steps too short to define equilibrium pressure precisely

[6]Last step too short (brine still warming)

These caverns are "shallow" (less than 1000 m deep) and the creep-closure rate is not extremely fast (when the wellbore was open, it was 3×10^{-4} /yr at EZ53, the deepest cavern in the series). A consequence of this is that equilibrium pressure, defined as the pressure for which the brine outflow rate equals the cavern-closure rate, is relatively low (significantly smaller than geostatic pressure). One can expect that in deeper caverns, closure rate is much faster, and permeability is likely to be smaller; both contribute to a much higher equilibrium pressure (the difference between geostatic pressure and equilibrium pressure is smaller than Wallner's margin, see Section 4.2.1). For this reason, tests in deep caverns were needed (Figure 66).

However, it proved difficult to find testing caverns in which thermal equilibrium was reached. Pressure increase rate was governed, at least partly, by brine warming, a phenomenon whose influence was moot in the small and old "shallow" caverns in which the first series of tests had been performed. In that sense, the "deep" tests proved to be less conclusive than the "shallow" tests.

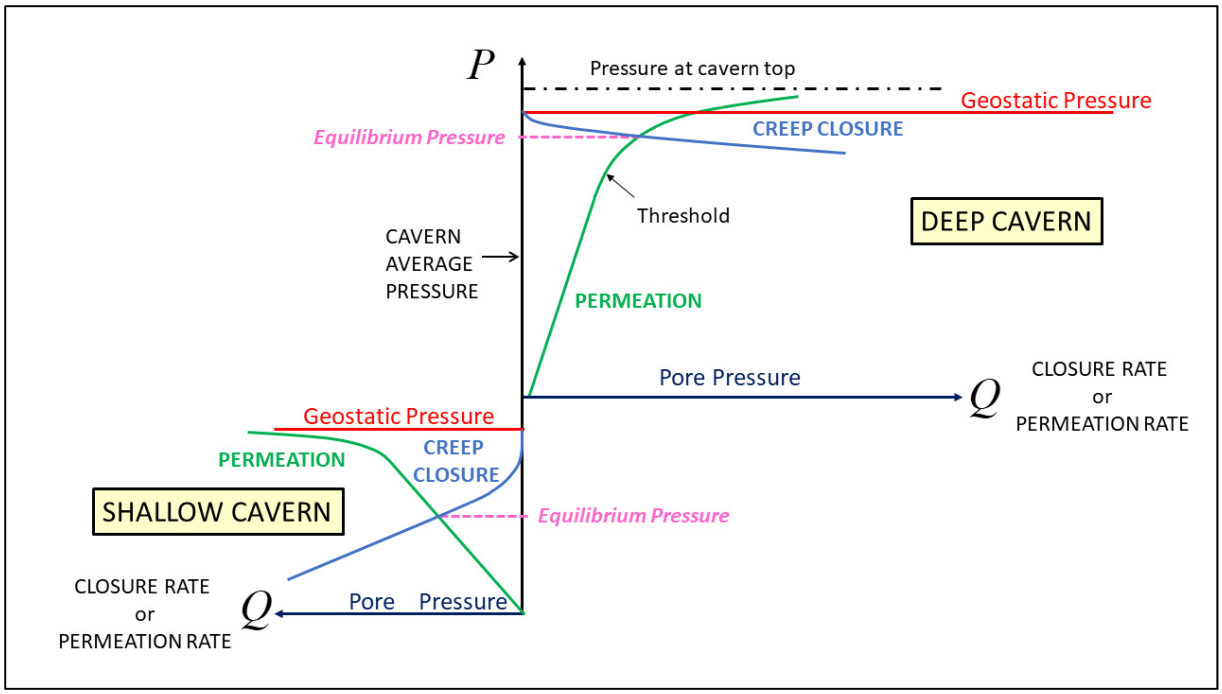

Figure 66 - Cavern pressure versus cavern closure rate and permeation rate.

5.2 Mont Belvieu (2007-2014)

In 2005, the SMRI supported three field projects in the framework of its Cavern Sealing and Abandonment program: Etrez and Carresse and Stassfurt, two “shallow” caverns. It was considered that, for many caverns, abandonment and sealing could be accomplished effectively provided the cavern temperature were reasonably near the geothermal temperature at cavern depth. This was especially true for shallow caverns (less than 1000-m deep) in which creep closure is relatively slow.

It was decided to perform a test in four “deep” caverns at Mont Belvieu, Texas, in the Barbers Hill salt dome. This facility is home to the largest underground LPG storage facility in the world (approximately 140 caverns). The field tests were performed in Wells No. 10W, No. 11W, No. 14W, and No. 15W2 (see Figure 67).

Wells No. 10 W and No. 15 W caverns have volumes slightly larger than 1 million barrels (160,000 m^3), and the Wells No. 11W and No. 14W caverns are essentially twice that size. The depths of the four caverns are between 2,700 ft (820 m) and 4,350 ft (1325 m). These caverns are close to the edge of the salt dome. When the test began in 2007, they had been quiescent (out of service) since 2003.

Diesel was injected in the annular space to a depth below the cemented casing shoe to form a “leak detection system” (see Section 4.4.5). Wellhead pressures were recorded hourly at ground level, both in the annulus and in the central tube. Evolution of the pressure differential (often called “delta” – a flat delta-vs-time curve suggests that no leak takes place from the casing) was computed to track interface displacements. This system was revealed to be not completely effective, as the brine-diesel interface sometimes moved downward, as hydrocarbons from the cavern moved to the annular space during the test.

In addition, two downhole pressure and temperature probes were fielded in Well No. 14W in 2008 and 2013. Their evolutions proved less smooth than expected. In addition, six temperature logs were run in three of the four wells and three logs in Well No. 14W. The test was eight-year long, from January 2007 to end of December 2014. Unfortunately, a fire occurred at the facility and normal operations were interrupted from January 2011 to early 2013 (pressures and temperatures were not recorded during this period.)

During the full duration of the test, cavern pressure increased consistently (but slowly and slowly). Regulations for maximum allowable pressures in Texas require that the pressure gradient at the last cemented casing shoe is less than 0.8 psi/ft. For this reason, wells were vented from time to time to keep cavern pressure below this limit. An example of pressure evolution is provided in Figure 69.

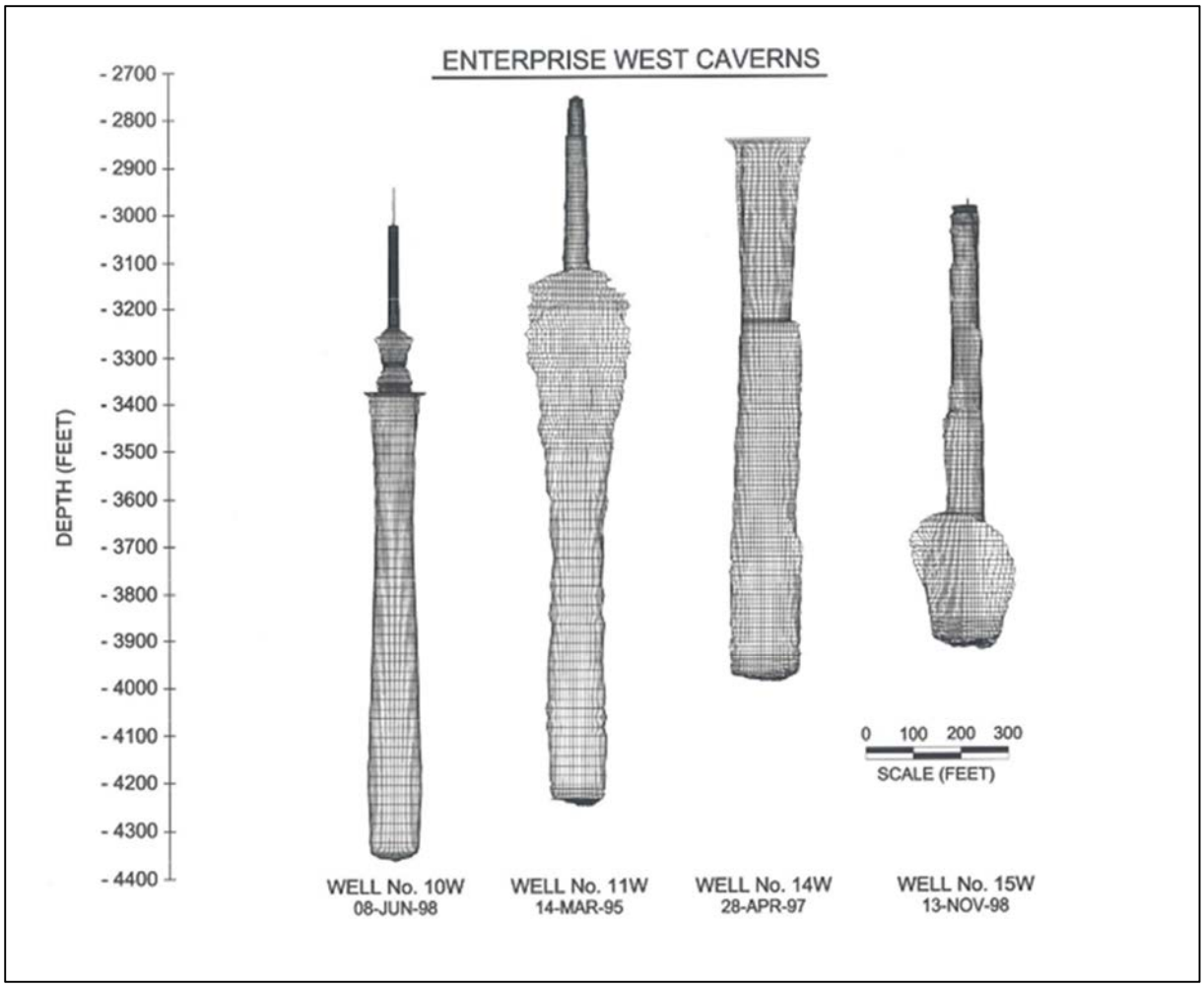

Figure 67 - Illustration of the Enterprise West Well Caverns and the four caverns selected for testing (Enterprise et al., 2015).

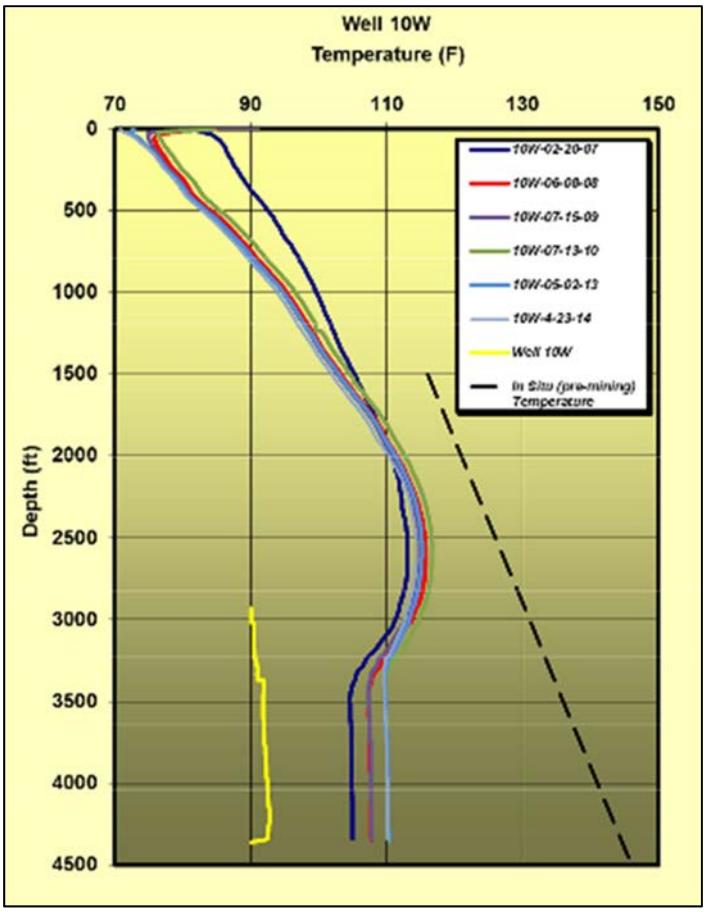

Figure 68 - Temperature logs in Enterprise Well n°10W (Enterprise et al., 2015).

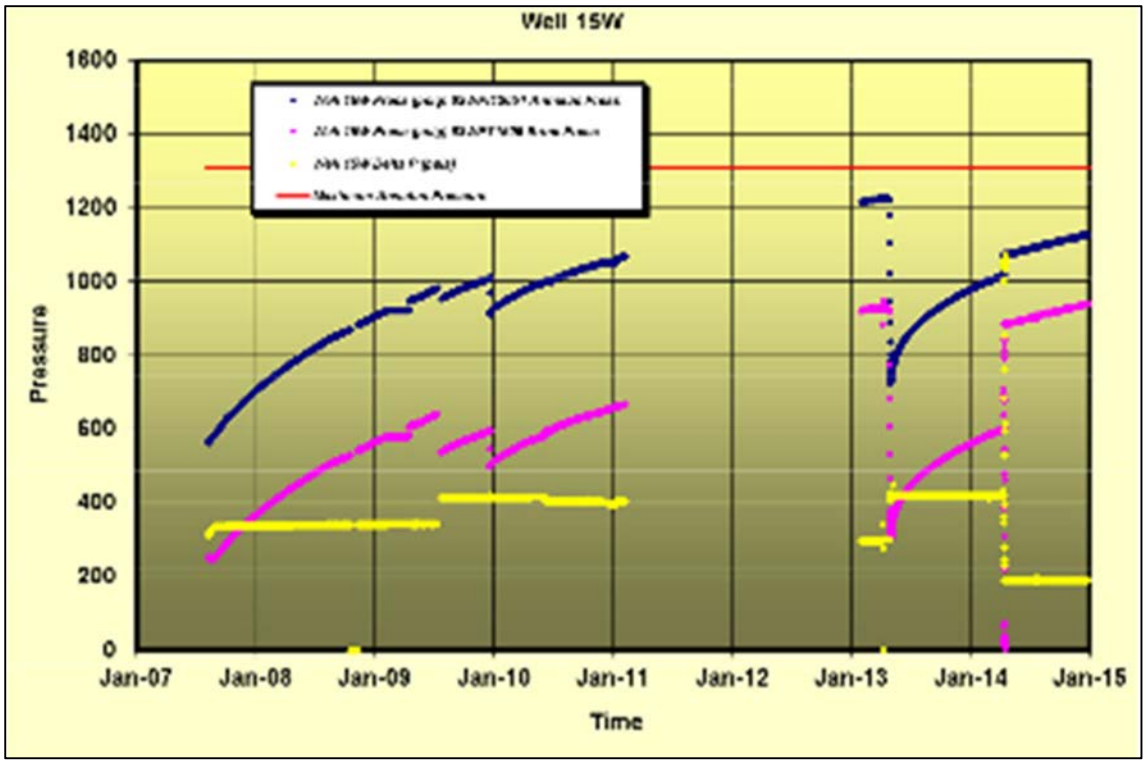

Figure 69 - Measured Wellhead Pressures and Differential ("Delta") for Well No. 15W (Enterprise et al., 2015).

Interpretation of the test was through numerical computations; creep closure (Munson-Dawson model) and heat transfer from the rock mass were taken into account. Creep closure appeared to be the most significant factor explaining cavern pressure increase. Smaller caverns experience a slightly more rapid temperature increase, as suggested by heat transfer equations. The difference between computed and observed pressure evolutions were deemed to reflect brine permeation to the rock mass, which is small. However, a pressure decline was observed in April 2013 on Well No. 15W.

This test was important for many reasons (it was the first "abandonment" test performed in the U.S., and advanced numerical computations were performed). However, for various reasons, it was not a "*breakthrough*". On one hand, heat transfer was still active, and equilibrium pressure could not be reached. On the other hand, it could be expected that equilibrium pressure would be higher than in shallow caverns; for safety reasons (which were reasonable), the regulatory authorities did not accept that cavern pressure at casing depth rises above 0.8 psi/ft – a gradient likely to be smaller than the equilibrium gradient.

5.3 The Tersanne (France) abandonment test (2005 – 2013)

Storengy operates a gas-storage field at Tersanne, France. Te02, the first cavern to be filled with gas in this site, was operated as a gas-storage cavern from 1970 to 2005. The cavern depth is 1400 m, and the initial volume of the cavern was 93,500 m^3. This cavern experienced large losses of volume, proving that Tersanne salt was creep-prone. It was re-brined in 1980 to perform a sonar survey, and a loss of 30% of volume was observed. It was refilled with gas and operated as a gas cavern again from 1982 to 2005, when Te02 was refilled with water "*in order to test the concept of cavern abandonment*" (Hévin et al., 2007). An additional loss of 30% was observed. Wellhead pressure was recorded at cavern mid-depth from 2005 to 2013 (Figure 70). Wellhead pressure consistently increased. From time to time, the cavern is vented to prevent too high a pressure rise.

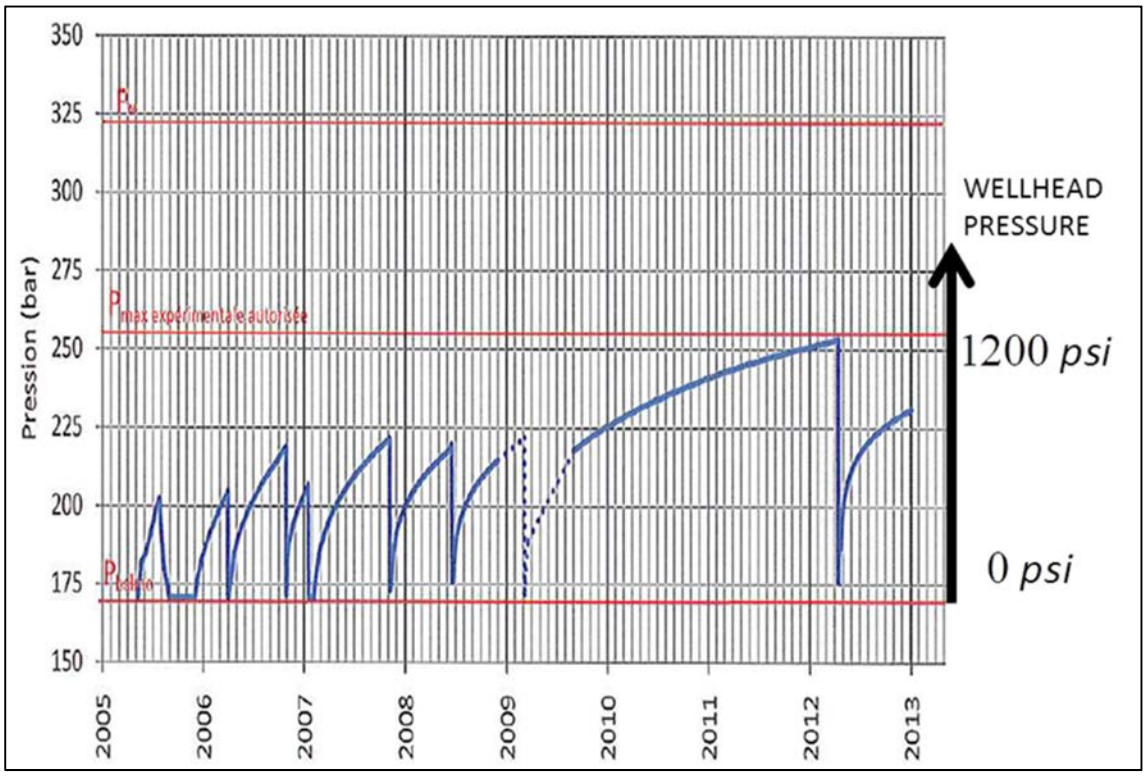

Figure 70 - Well Te02, Tersanne, France. Pressure evolution at cavern mid-depth from 2005 to 2012 (after Hévin et al., 2013).

Temperature also is measured at cavern mid depth (Figure 71). Temperature of the injected water was about 12 °C; when re-watering was completed, after one month, the cavern-brine temperature was 35 °C. In 2013, it was 62 °C. The rock temperature at cavern depth is 68 °C. In Hévin et al. (2013), cavern behaviour is modelled, taking into account creep closure, brine warming and permeation (a $K = 10^{-20}$ m^2 value was selected for computations, based on integrity tests performed in the wellbores of the Tersanne site before leaching began). Some gas remained trapped in the cavern, and cavern compressibility is higher than in most regular caverns (see Section 4.2.2). Brine warming explains a significant part of pressure increase.

As in the Mont Belvieu case discussed in Section 5.2, the existence of an equilibrium pressure is likely. However, experimental evidence is still out of reach, as thermal effects remain significant. This test is ongoing, and further results will be available in the near future.

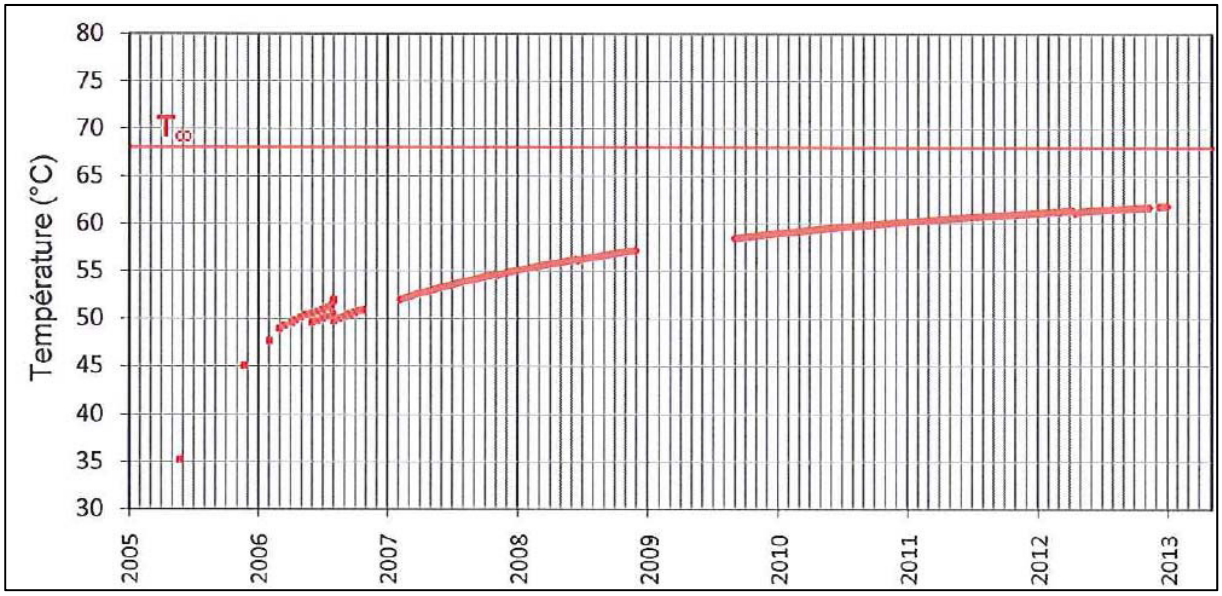

Figure 71 - Temperature evolution at cavern mid-depth (Hévin et al., 2013).

5.4 Barradeel (2004-2008)

An abandonment test on the BAS-2 cavern at Barradeel in the Netherlands was performed and described by van Heekeren et al. (2009). Salt is mined at a depth of 2500-3000 m (Figure 72). Salt is produced at "steady state"– i.e. cavern brine pressure is selected such that the cavern closure rate equals the salt production rate, and cavern pressure is constant during operation in this site, a somewhat unique mining method made possible by fast creep closure (de Lange et al., 2012). Maximum ground level subsidence allowed by the mining authorities was 35 cm, a value reached in the case of BAS-1 and BAS-2 in 2004. It was decided to shut-in BAS-1 and monitor its wellhead pressure.

Wellhead pressure from 01/01/04 to 01/10/08 (a 4-year-long test) is represented on Figure 73 (from van Heekeren et al., 2009). Origin and unit of pressures are not provided; however, Minkley et al. (2018b) redrew this picture, providing a pressure scale and a more precise cross-section of BA#2 (Figure 73, bottom). In particular, lithostatic (or geostatic) pressure is 55 MPa at a 2533-m depth (BAS-2 last cemented casing depth); this value, which is reasonable, is likely to be computed from some assessment of rock density above the cavern and cannot be considered as certain. [However, it is difficult to understand how, at the beginning of the test, cavern brine pressure can be zero at a 2553-m depth].

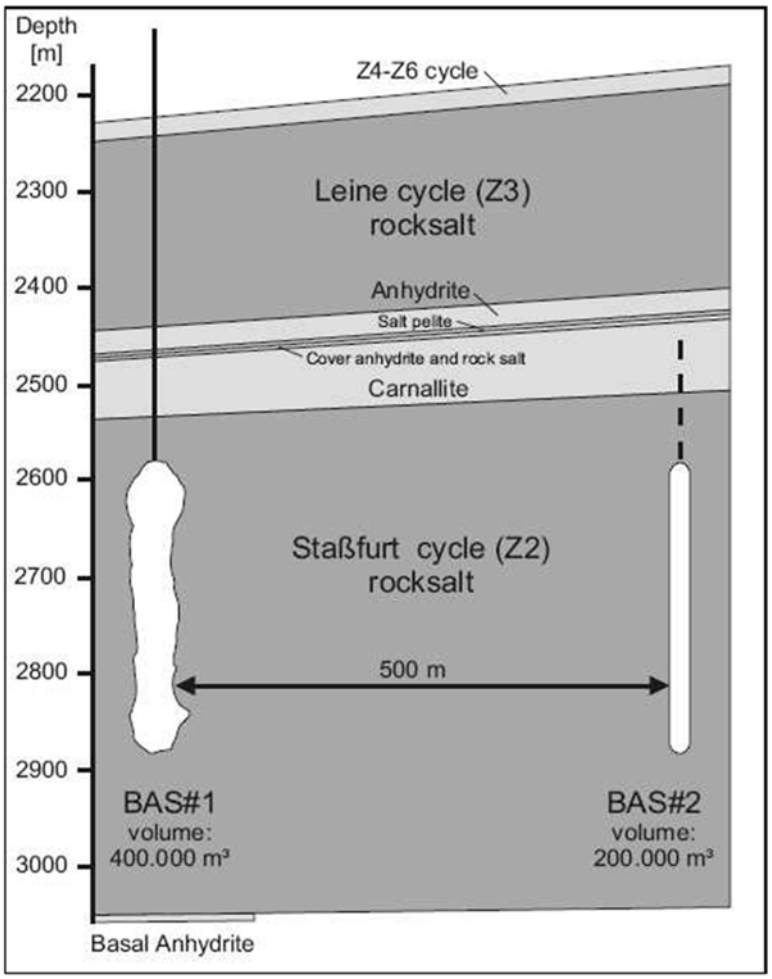

Figure 72 - Vertical cross-section of caverns BAS-1 and BAS-2 (van Heekeren et al., 2009).

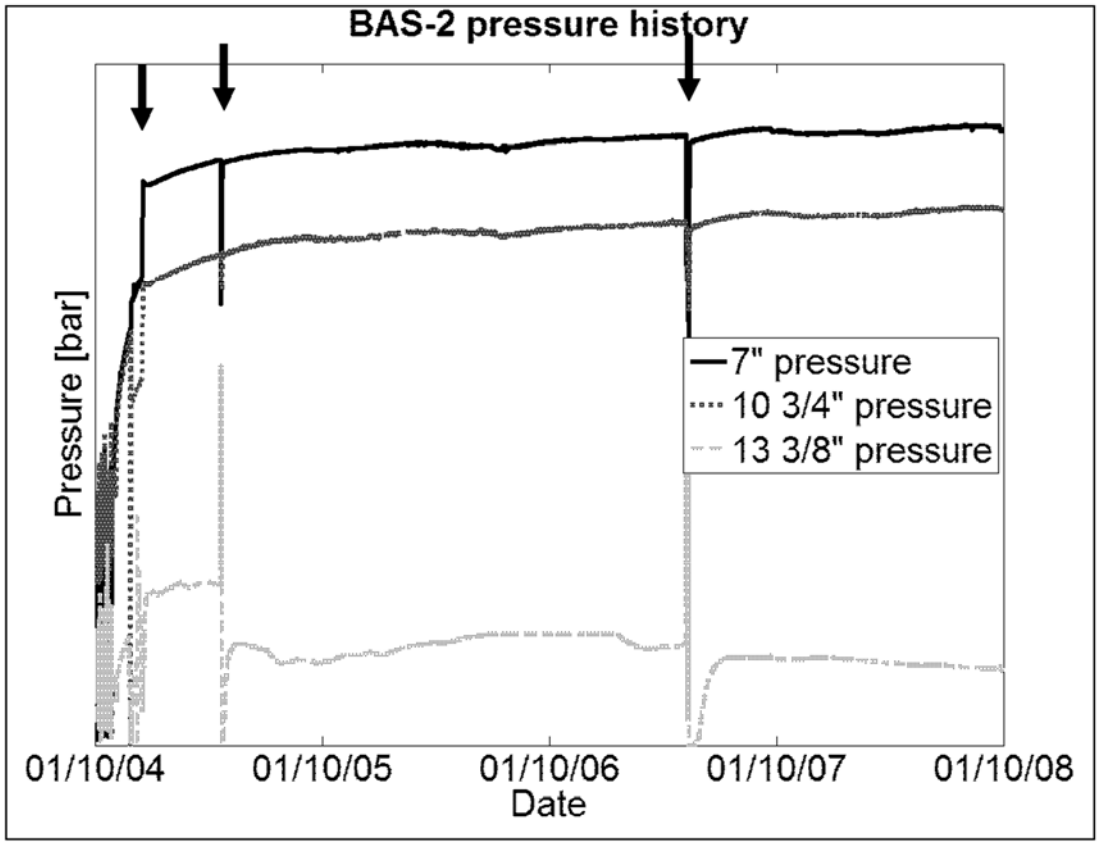

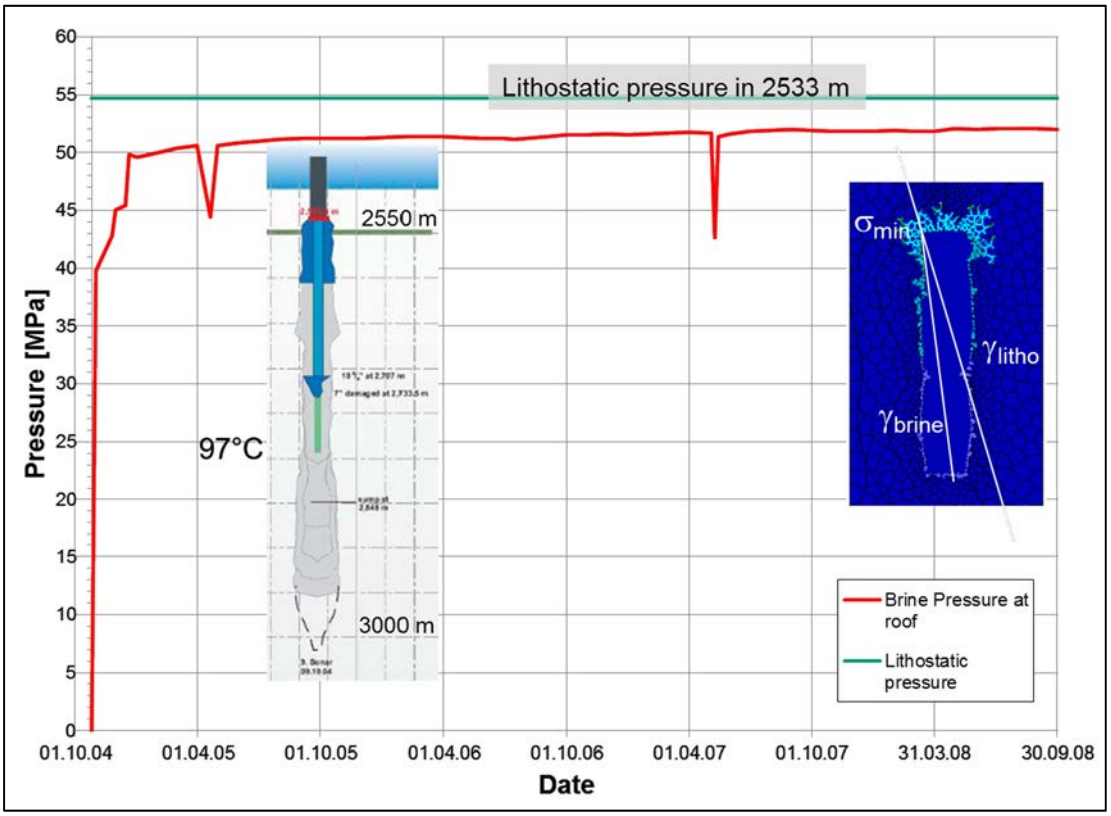

Figure 73 - Well-head pressure evolution according to van Heekeren et al., 2009 (above) and Minkley et al., 2018b (below).

A first phase can be observed during which the pressure-increase rate is extremely fast. After a few weeks, this rate slows down significantly. It was decided to inject some brine (first vertical arrow on Figure 73, above) to minimize creep closure. This move was successful, as the closure rate is much slower after this injection: four years later, the cumulated pressure increase is 0.2 MPa.

Cavern pressure evolution is reminiscent of what was observed at Vauvert (see Section 4.4.2). It is tempting to infer that creep closure was extremely active during the first phase and became much slower when cavern pressure became higher; the effects of brine thermal expansion become pre-eminent during the second phase. During the third phase, permeation, or flow through a fracture, prevents cavern pressure to rise anymore (or, at least, to rise significantly).

Van Heekeren et al. (2009) assume that pressure evolution results from five mechanisms: creep closure, brine warming, brine transport into the formation, salt dissolution, and leakage along the wellbore. This is similar to Bérest et al.'s analysis (2001a), and Sections 4.4.4 and 4.4.5. In this 203,000-m^3 elongated cavern, brine warming is fast. The geothermal rock temperature at cavern mid-depth seems to be 97 °C (Figure 73, bottom). In fact, after pressurization, brine temperature increased from 67 °C to 88 °C in four years (van Heekeren et al., 2009). A simple rule of thumb (Section 4.4.1) is as follows: in a shut-in tight cavern, a brine temperature increase of $\Delta T = 1$ °C generates a brine-pressure increase of 1 MPa: $\Delta P = \alpha \Delta T / \beta$; $\alpha = 4.4 \times 10^{-4}$ /°C, $\beta = 5.4 \times 10^{-4}$ /MPa (BAS-2 factor of compressibility value (β) was measured through venting-compression tests, see below). Pressure increase due to brine warming (after cavern pressurization) should have been $\Delta P = \alpha \Delta T / \beta = 8.6$ MPa. The observed pressure increase during this period was 0.2 MPa. Obviously, "something" happened after the end-of-2004 pressurization: a fracture opened or additional permeability was created. Whatever phenomenon took place, it was able to accommodate the brine-volume increase due to thermal dilatation, $\alpha V \Delta T = 1000$ m^3 of brine.

In their report, the authors claim that "*compression tests and the comprehensive model indicate that the cavern has been in a continuing permeating condition soon after shut-in and that the rate of fluid leak off stays below fracturing levels*" (Van Heekeren et al., 2009, p. 1) ("*compression tests*" are discussed below). In their view, permeation is through paths created during rock deformation, especially in the non-halitic rocks (4% of the total volume), or at cavern roof, when brine pressure is close to lithostatic pressure, following the mechanism suggested by Kenter (1990). It is essential for the discussion to assess the robustness of Van Heekeren arguments.

Van Heekeren et al. (2009) built a model that includes creep, brine expansion and permeation. Virgin permeability is exceedingly low (K = 10^{-22} m²), but it increases drastically when the difference between brine pressure is larger than the least compressive stress at cavern wall (how the increased permeability zone grows in the rock mass is not clear). They get a relatively good fit, although a couple of features of the as-observed evolution are not captured. However, this good agreement cannot be considered as definite proof of the absence of a fracture; to a certain extent, onset of fracture (when it does not open in a permeable layer) has the same effect as a more diffuse increase of permeability, as room is created to accommodate brine flowing out from the cavern, and more room is created when cavern pressure increases.

Additional evidence is based on “compression tests”. Four such tests were performed. They consist of withdrawing a small amount of brine to decrease cavern pressure and injecting a similar amount of brine to restore initial cavern pressure. During re-pressurization, injected volume is plotted against pressure change (the slope of this curve is the apparent compressibility or βV). These tests are extremely insightful, as they provide information on the cavern compressibility evolution, as was observed in Section 4.4.2 (Etzel), Section 4.4.3 (Durup’s tests at Etrez), and Section 4.7 (Bernburg).

Results of these tests are shown on Figure 74. Unfortunately, no scale is provided. At low pressure, apparent compressibility is a slowly increasing function of pressure; a pressure threshold can be observed, above which apparent compressibility drastically increases (such an effect also was observed during the in-situ tests mentioned above). This threshold seems to be significantly smaller than the virgin lithostatic pressure (however, remember that lithostatic pressure is roughly estimated). In fact, compressibility is smaller and smaller, and the threshold is higher and higher when later tests are considered. This threshold can have many origins, but the most likely explanation is that the brine outflow to the rock mass increases significantly when cavern pressure is higher than this threshold, see Section 5.7. The authors believe that this threshold (“leak-off point”) is associated with the “local” lithostatic stress (which we interpret as the tangential stress at the cavern wall, resulting from stress rearrangement during solution mining). This might be true. More on the Frisia test can be found in Section 5.6.

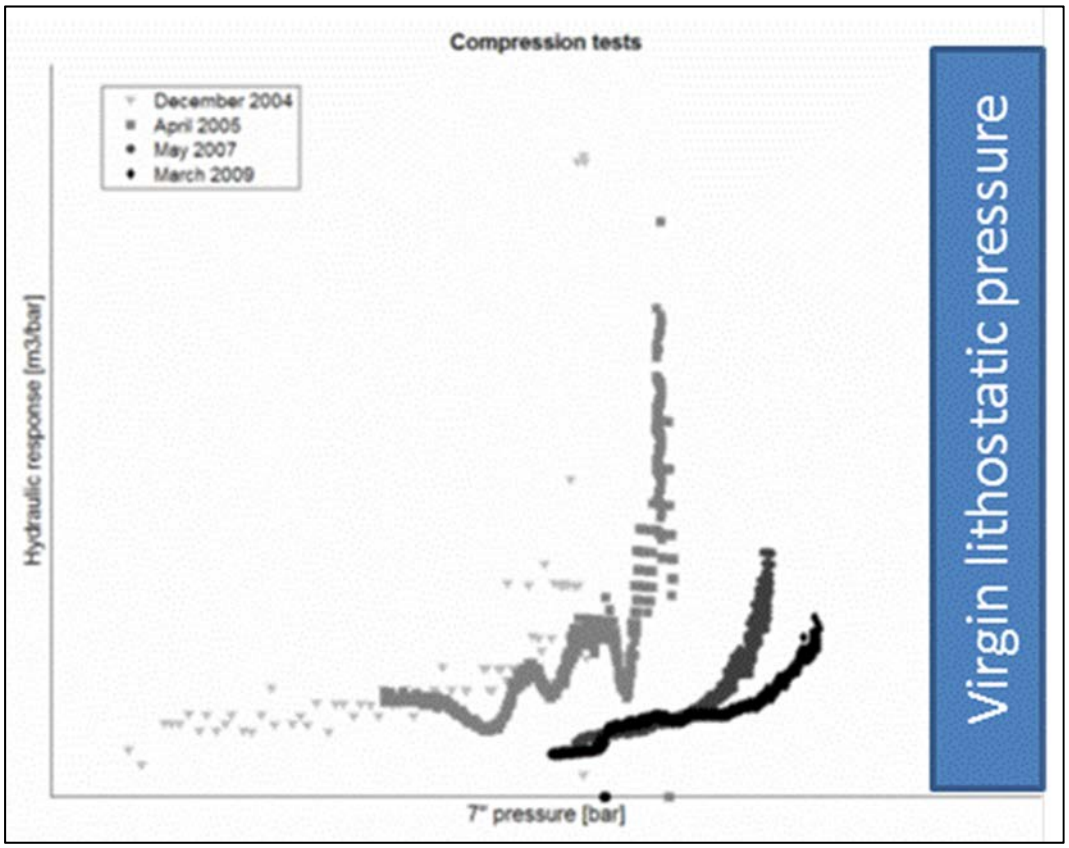

Figure 74 - Results of the four “compression” tests (Minkley et al., 2012).

5.5 The Veendam incident

Nedmag operates a magnesium chloride cavern field at Veendam, the Netherlands (Figure 75 and Figure 76). The mining methods were described in a paper by Fokker et al. (2004):

> "*The magnesium chloride mine operations of Nedmag Industries at Veendam have been the subject of earlier presentations at the SMRI. Magnesium chloride is extracted from several thick layers of carnallite and bischofite at a depth varying from 1300 to 1600 m. These layers are embedded in the upper part of a large halite deposit of the Zechstein III (Leine) evaporation cycle. Large-scale mining operation has begun in 1980 by creating separate caverns with a limited size and using an oil blanket roof control method. The separate caverns were kept at lithostatic pressure. In 1993 (test) and 1995 (final) Nedmag and government agencies (state and local) agreed to change the mining method drastically, by reducing the cavern pressures and allowing the Mg-salt to flow (squeeze) towards the caverns, to be solution mined. The recovery of especially the purest magnesium chloride-source (Bischofite) increased with probably an order of magnitude. The method of injection and production has changed over time, interconnecting 8 wells with an area of about 1 km*".

It does not seem that the cavern field experienced any significant unexpected event until 20 April 2018, when wellhead pressure at TR-2, a shut-in well, abruptly dropped by 20-30 bars. This pressure drop propagated fairly? rapidly to the other wells of the cluster, which, in 2018, comprised 9 caverns, TR-1 to 8 and VE-4, as explained below.

On 20 April, at 3:14 a.m., wellhead pressure, which was 88 bars before the event (Figure 77), began decreasing rapidly in TR-2, a brine-filled well that had been inactive for a long time (Figure 78). This pressure drop was transmitted rapidly to the neighbouring TR-5 and TR-1 wells and, more slowly, to TR-7 and the other wells of the cluster. Such delays are not surprising: rather than a single cavern, the cluster is a labyrinth composed of many more or less permeable conduits.

At 3:36 a.m., TR-2 wellhead pressure was more or less stable at 65 bars, an overall drop by 88 – 65 = 23 bars in 22 minutes (Figure 31). Stabilization was reached more slowly on the other wells of the cluster.

This event was unanticipated. A breach (roof fall or roof fracture?) had been created at the roof of the cluster that allowed brine seepage from the cluster. It is difficult to assess precisely the amount of brine that seeped from the cavern; it could be 1000 m^3 or several 10,000 m^3.

It seems that the state of stress in the Bundsandstein layer is strongly anisotropic (the horizontal stress is smaller than the geostatic stress). Cavern pressure was 50 bars below geostatic on 20 April (Figure 78), which means that if a hydraulic connection were created between the cavern and the Bundsandstein layer, a fracture could be created in this layer, able to accommodate a large volume of brine (several thousand m^3). However, how the initial hydraulic connection is created remains open to discussion.

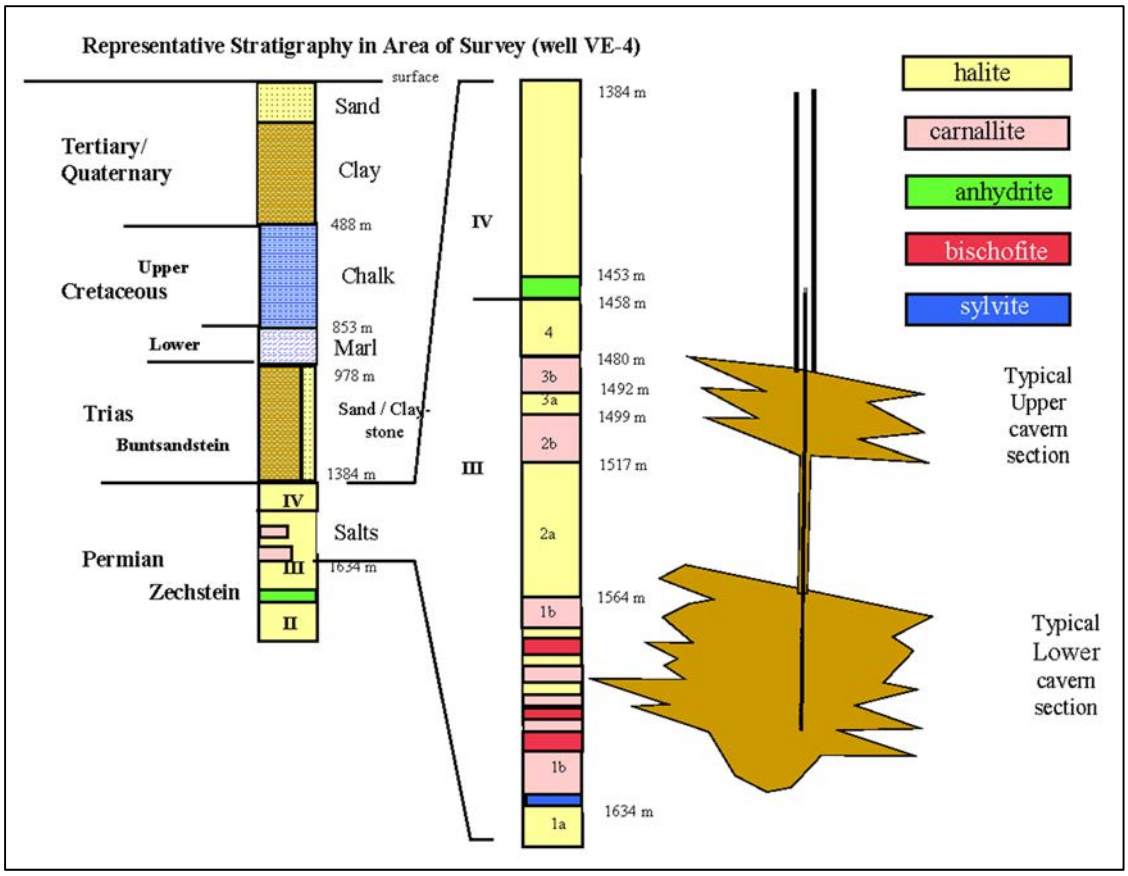

Figure 75 - Stratification of salts near Veendam the Netherlands (Fokker et al., 2004).

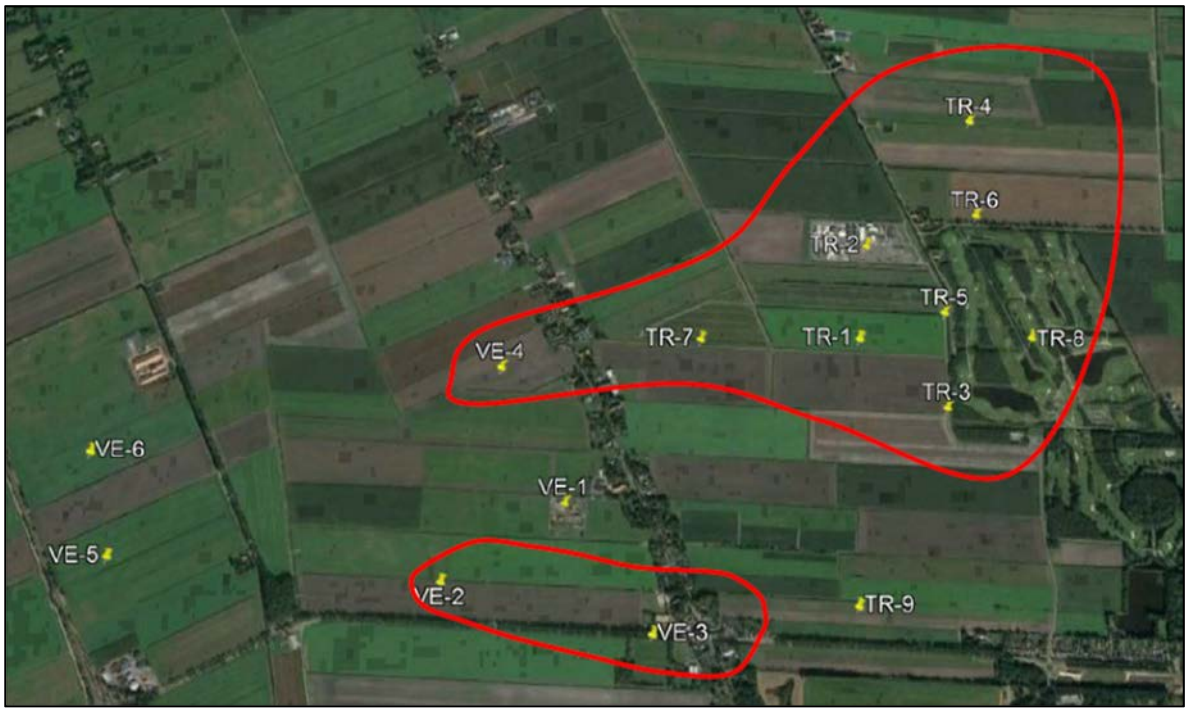

Figure 76 - The Veendam cluster (Dienst ICT Uitvoering website).

On 20 April, at 3:14 a.m., wellhead pressure, which was 88 bars before the event (Figure 77), began decreasing rapidly in TR-2, a brine-filled well that had been inactive for a long time (Figure 78). This pressure drop was transmitted rapidly to the neighbouring TR-5 and TR-1 wells and, more slowly, to TR-7 and the other wells of the cluster. Such delays are not surprising: rather than a single cavern, the cluster is a labyrinth composed of many more or less permeable conduits.

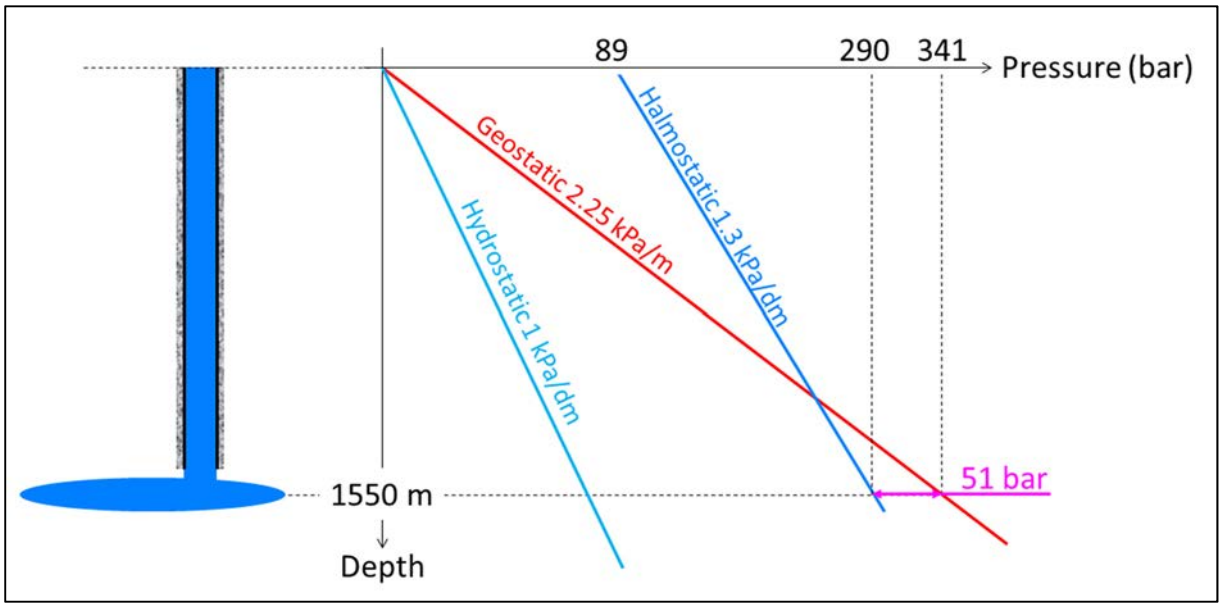

Figure 77 - Pressure distribution in Veendam wells (values are indicative).

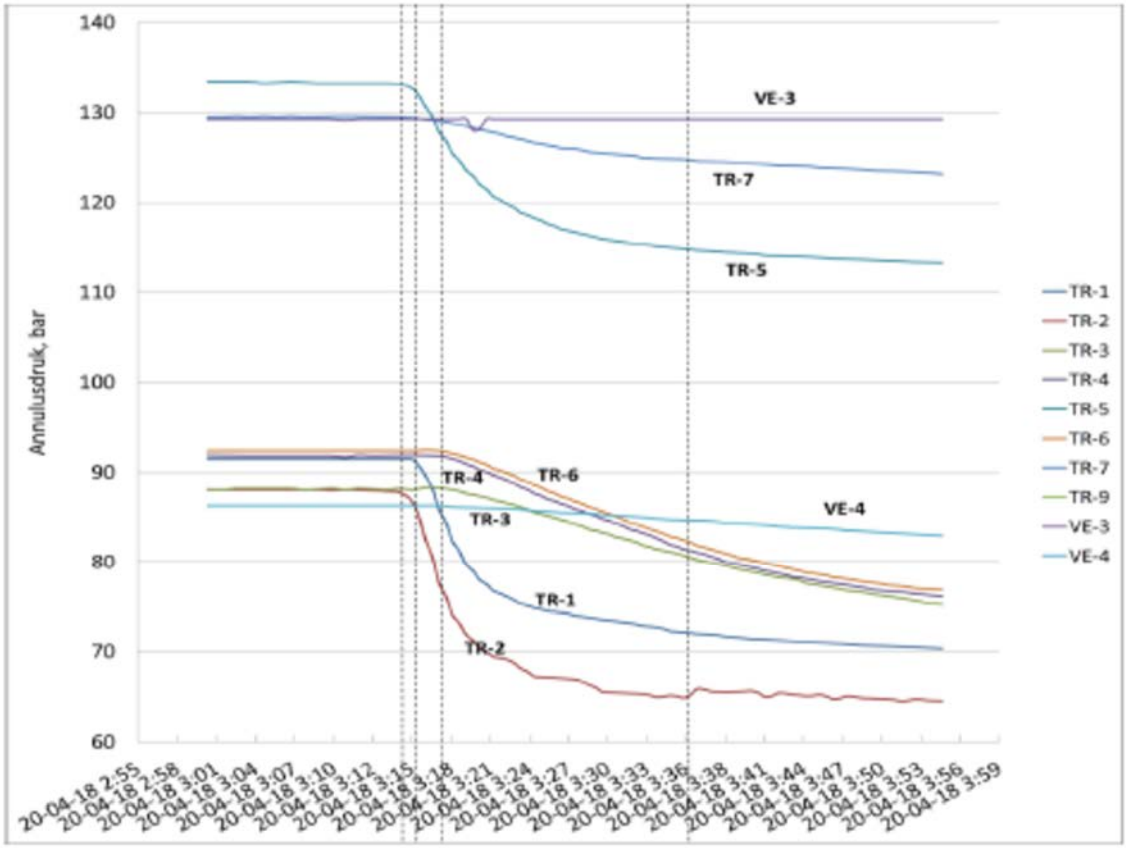

Figure 78 - The 20 April event (Dienst ICT Uitvoering website).

5.6 What is a fracture?

The formation of micro-fractures when cavern pressure is close enough to geostatic pressure can be considered a certainty. This is proved by the increase in the cavern compressibility (βV), which remains approximately constant until a threshold pressure (''leak-off pressure") is reached. However, this micro-fracking process is much smoother than what can be observed during a standard frac test. In a borehole, when the pressure breakdown is reached (onset of a fracture), borehole pressure abruptly drops. This is because a borehole is a very stiff cavity, and the volume of the brine that enters the fracture is not negligible when compared to the volume of the borehole. The same is not true in a full-size cavern whose volume is larger than a borehole volume by three orders of magnitude. This is a difficult point in any test of this kind. It is highly likely that, when cavern pressure increases, the number and length of these micro-fractures increase. It is not impossible that, after some time, localization takes place: most micro-fractures stop growing, a small number of the micro-fractures keep growing (their aperture and their length increase), leading to the formation of "fractures".

Van Heekeren et al. (2009) adopt a different point of view and a slightly different definition of a fracture. From Figure 73, Section 5.4, they infer that "*no permanent fracture to a more permeable layer are created because in that case a pressure drop would be expected*". In other words, fractures may have been created, but they are not able to generate a large brine flow to a permeable reservoir, as their lengths are too small. For instance, it is likely that a kind of "fracture" was opened at Veendam when a large and rapid pressure drop was observed (see Section 5.5). In fact, it is almost certain that a fracture was created at Veendam in the Bundtsandstein layer, a permeable layer whose bottom is 10-20 m above the roof of the shallowest cavern of the site. This fracture developed rapidly, as the state of stress in the Bundsandstein layer is anisotropic (the horizontal stress in this layer is much less compressive than brine pressure in the cavern). What exactly happened in the relatively thin salt layer between cavern roof and Bundsandstein bottom (fracture? roof collapse?) is less clear.

When the van Heekeren definition is accepted, the notion of a "frac" is somewhat blurred. A "frac" is not the opening of a discontinuity inside a previously continuous medium – that is a purely mechanical definition, independent of the scale of the phenomenon; a "frac" is the creation of a hydraulic link between a cavern and a porous-permeable layer allowing a large brine flowrate to be expelled from the cavern.

5.7 Cavern compressibility and Permeability increase

In Section 4.2.2, cavern compressibility or βV was defined as the ratio between the rate of injected volume in a cavern (Q_{inj}) and the resulting cavern pressure increase rate ($\dot{P}$) :

$$\beta V\dot{P} = Q_{inj} \tag{10}$$

V is the volume of the cavern and β is the factor of compressibility (in /MPa). The factor of compressibility is the sum of the brine factor of compressibility ($\beta_b = 2.7\times10^{-4}$/MPa) and the factor of compressibility of the cavern (the elastic ''box'' which contains the brine volume) or β_c. This factor depends on the elastic properties of the tock mass (*E*, *v*) and the shape of the cavern. For a typical cavern, $\beta_c = 1.3\times10^{-4}$/MPa and $\beta = \beta_b + \beta_c = 4\times10^{-4}$/MPa. In fact, the factor of compressibility is larger in a flat cavern or when gas is trapped in the cavern. Figure 79 is an example of a cavern compressibility measurement (Thiel, 1993). Cavern compressibility is $\beta V = 79.564$ m^3/MPa. Cavern volume is unknown. From Thiel's paper it can be inferred that casing shoe depth is 840 m, approximately, a depth at which halmostatic pressure is 10 MPa. When tubing pressure increases from 4.5 MPa to 5.1 MPa, the testing gradient increases from (10 + 4.5)/840 = 0.0172 MPa/m to 0.018 MPa/m. In this gradient range, the relation between injected volume and pressure increase is almost perfectly linear.

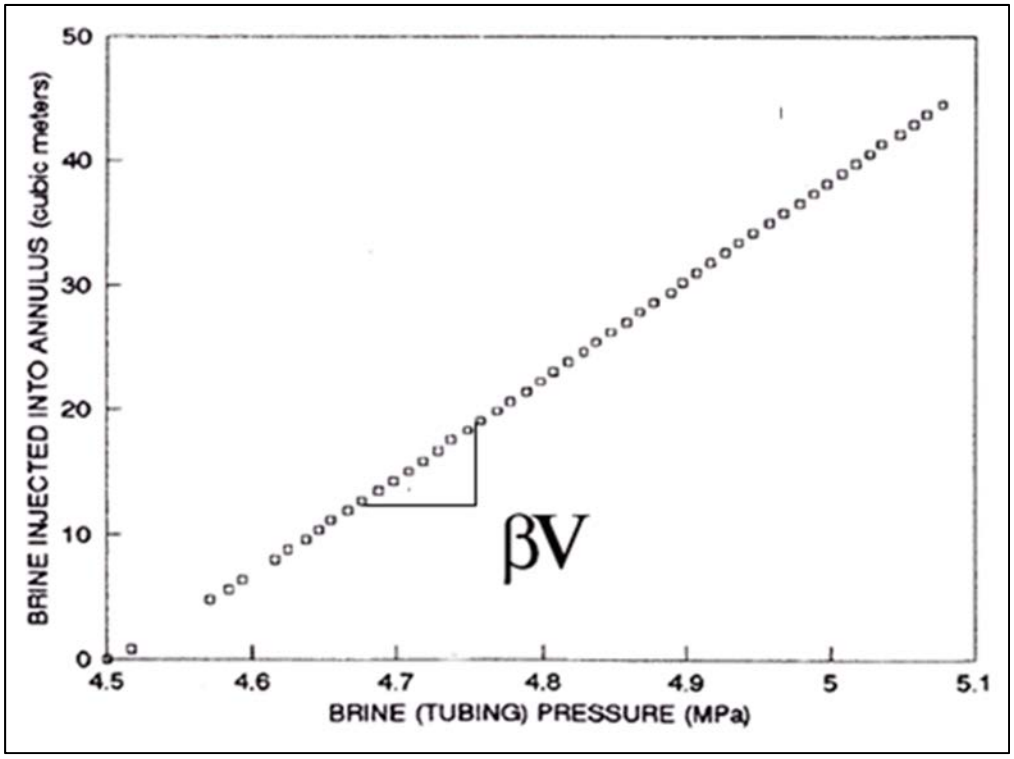

Figure 79 - A cavern compressibility measurement (After Thiel, 1993).

From a theoretical point of view, it can be predicted that the relation is not perfectly linear as, in addition to the elastic (instantaneous) response of the brine + cavern system, cavern or brine

experiences “reverse” creep or additional dissolution occur (Van Sambeek et al., 2007). These effects appear to be small in this context.

It was observed during the Etzel test (see Section 4.22) that the cavern compressibility factor or β increased significantly (Figure 80) when cavern pressure gradient increased from 0.019 MPa/m (it was 3.7×10^{-4} /MPa) to 0.0205 MPa/m (it was 4.7×10^{-4} /MPa) and above.

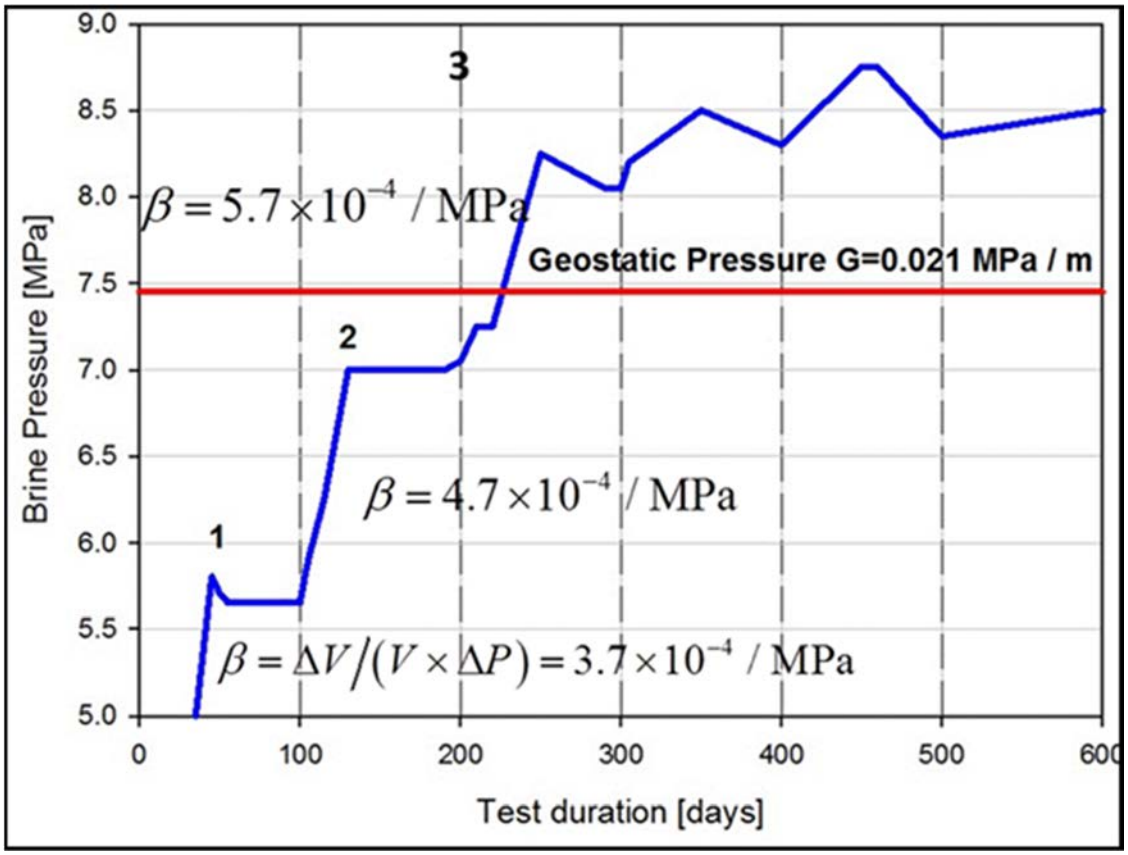

Figure 80 - Wellhead Pressure Evolution During the Etzel K-102 Test (Djizanne et al., 2012). Wellhead brine pressure is nil at the beginning of the test (day zero).

Similarly, Durup (see Section 4.4.3) performed a pressure build-up test in the EZ58 wellbore. (This wellbore had been pressurized to geostatic pressure in an earlier test). Open hole length was 198 m. The test was 6-hour long. On Figure 81, the pressure at well bottom depth (871 m) is plotted against the cumulated injected volume (wellbore compressibility or βV is the inverse of the slope of this curve). When pressure increases from 14.5 MPa to 20.5 MPa (from 0.017 MPa/m to 0.023 MPa/m at a 871 m depth), wellbore compressibility increased from $\beta V = 9.7$ Litres/MPa to $\beta V =$ 24 liters/MPa.

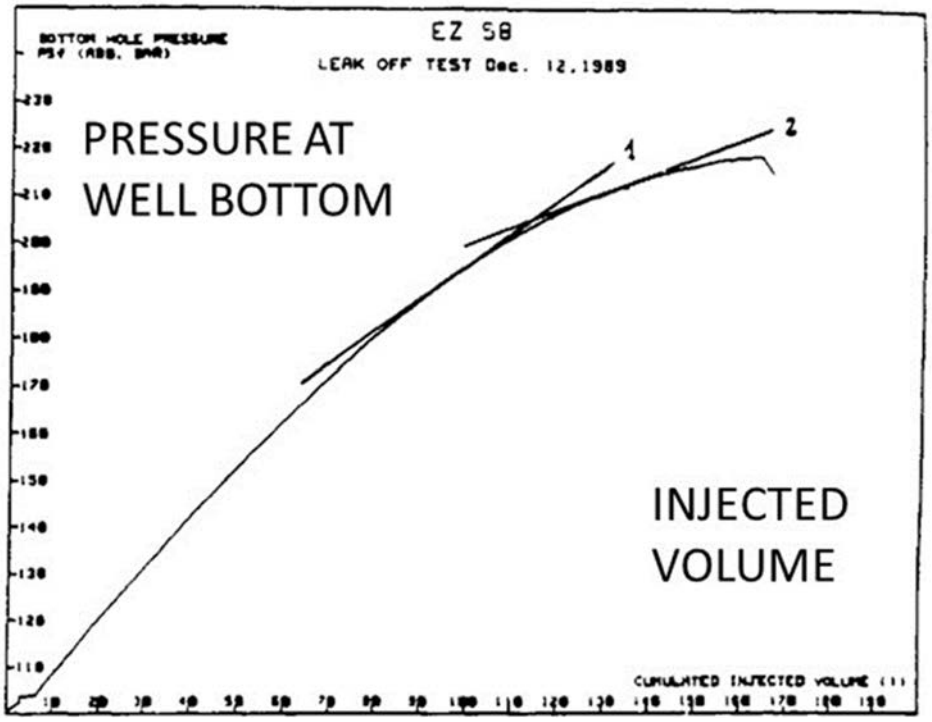

Figure 81 - Well bottom pressure as a function of injected volume (Durup, 1994).

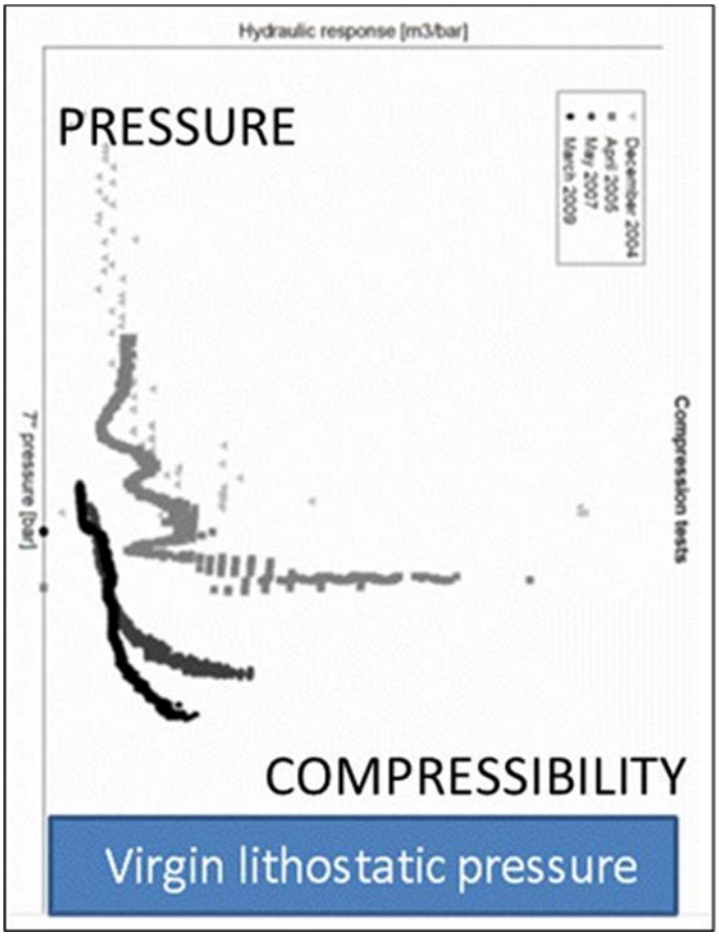

Figure 82 - Cavern compressibility (in m^3/bar) as a function of cavern pressure during four pressure build-up tests (Van Heekeren et al., 2009).

Van Heekeren et al. (see Section 5.4) measured cavern compressibility as a function of cavern pressure during four pressure build-up tests**.** Results of these tests are shown on Figure 82 (No scale is provided in the paper). At low pressure, apparent compressibility is a slowly increasing function of pressure; a pressure threshold can be observed, above which apparent compressibility drastically increases. This threshold seems to be significantly smaller than the virgin lithostatic pressure. In fact, compressibility is smaller and smaller, and the threshold is higher and higher when successive tests are considered.

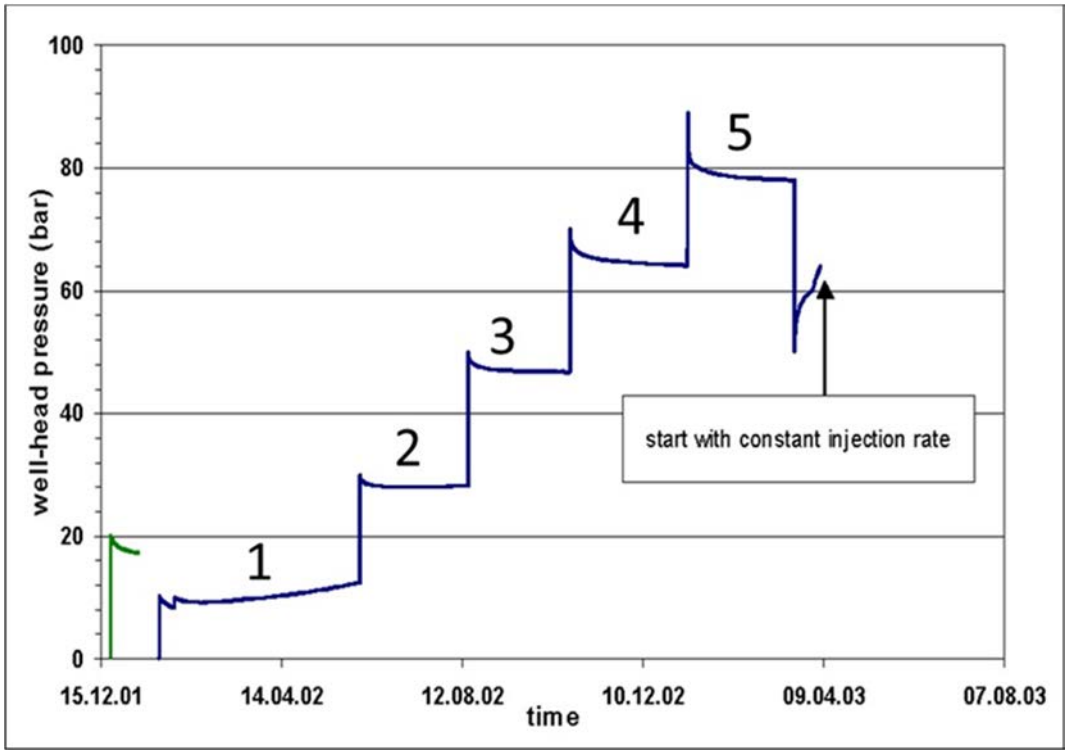

Figure 83 - Cavern pressure evolution during the Bernburg test (Brückner et al., 2003).

Brückner et al. (see Section 4.7) described a test performed in a 22 m^3 cavern leached out at a depth of 448 m from a drift at the Bernburg Mine. At the beginning of the test, 8.8 liters were injected in the cavern, pressure increased by 1 MPa, or $\beta V = 8.8$ liters/MPa ($\beta = 4 \times 10^{-4}$/MPa). During the second step (see Figure 83), pressure increased by $\Delta P = 3 - 1.23 = 1.77$ MPa when 14.2 liters were injected in the cavern (remarkably, the compressibility factor ***decreased*** to $\beta = 3.6 \times 10^{-4}$/MPa; we believe that a very small amount of air was trapped at cavern roof, drastically increasing initial compressibility. When the cavern contains a (volumetric) fraction of air $x = v/V$, its compressibility is $\beta + x/P$. For instance, $P = 1$ MPa, $x = 4 \times 10^{-5}$, the trapped-air volume is 0.88 liters, and cavern compressibility decreases when pressure increases). At the beginning of step 4, pressure increased from 4.7 MPa (a gradient of 4.7/448 = 1.05 MPa/m) to 7 MPa (a gradient of 1.56 MPa/m) when 20.77 liters were injected ($\beta = 4.1 \times 10^{-4}$/MPa). During the last step, pressure increased to 9 MPa (a 2.0 MPa/m gradient) and an "exponential" increase in compressibility was observed.

It is reasonable to assume that the increase in the apparent compressibility factor when cavern pressure is higher than a certain threshold (which is a site-specific notion; 0.018 MPa/m is probably

a typical value), significantly smaller than the geostatic pressure, results from the onset (or increase) of brine outflow from the cavern. Let Q_{out} be the brine outflow rate from the cavern, $\beta V\dot{P} = Q_{inj} - Q_{out}$, and the *apparent* compressibility (computed from as measured pressure rate and injected flow rate is:

$$\beta V\big|_{app}\,\dot{P} = \beta V\dot{P} + Q_{out} \tag{11}$$

Changes in cavern compressibility appear as a powerful tool for assessing « cavern » permeability evolution.

6. MODELING

This chapter is a review of the various models proposed in the literature to describe the hydromechanical behaviour of highly pressurized caverns

6.1 A sketch of the hydro-mechanical problem

A sketch of the hydromechanical problem is represented in Figure 84.

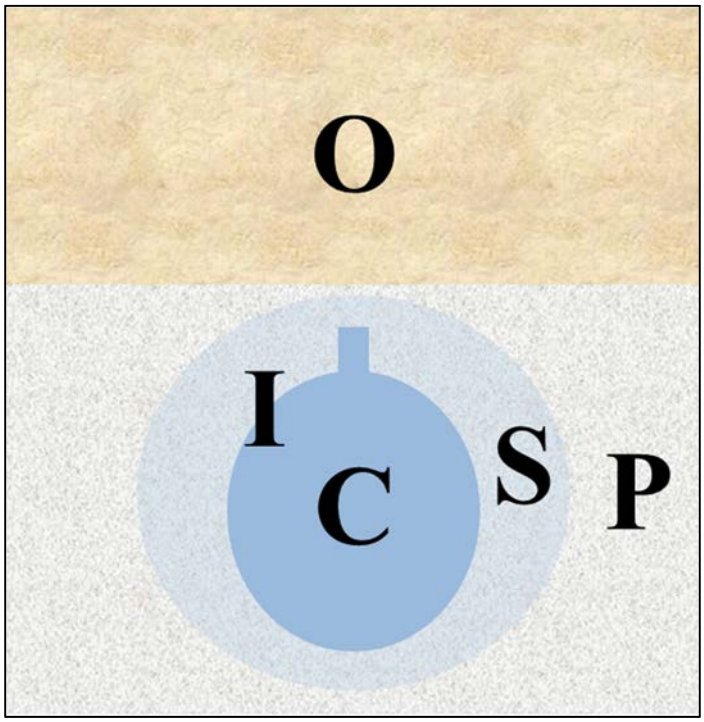

Figure 84 - A sketch of the cavern abandonment problem.

A cavern (**C**) was leached out from the salt formation; after abandonment, it is filled with brine. Its behaviour is characterized by a pressure, a temperature (say, at cavern mid-depth) and a state equation (a relation between cavern volume, temperature and pressure), typically

$$Q_{perm} / V = \alpha \dot{T} - \beta \dot{P} - \dot{\varepsilon}_{cr} \tag{12}$$

where Q_{perm} is the brine outflow through the cavern walls to the salt formation, V is the cavern volume, $\dot{\varepsilon}$ is the cavern-closure rate - (in general, $\dot{\varepsilon} < 0$, which is a non-linear function of the gap between the geostatic pressure (P_∞) and cavern pressure (P); α is the brine thermal expansion coefficient ($\alpha = 4 \times 10^{-4}$ /°C is typical); and β is the cavern factor of compressibility. Term β is the sum of the brine factor of compressibility (β_b) and the "hole" factor of compressibility, β_c, which is a function of the rock-mass elastic parameters and of cavern shape. Apparent cavern compressibility, βV^{app}, is easy to measure (it is the amount of brine that must be injected in a cavern to increase its pressure by a pressure unit). It is observed that apparent cavern compressibility increases when

cavern pressure increases; see, for instance, Sections 4.2.2. (Etzel test), 4.4.3 (Etrez 58 test) and 5.4 (Barradeel test). In fact, it is highly likely that the origin of this apparent factor of compressibility increase is the creation of permeable microfractures at cavern wall, which leads to an increase in brine outflow.

The abandonment problem consists of computing $T = T(t)$ and $P = P(t)$. The thermal problem [computation of $T = T\left(t\right)$] is weakly coupled. Temperature evolution results from heat transfer from the rock mass to the cavern ($\partial T_R / \partial t = k_{salt} \Delta T_R$) and boundary conditions at cavern wall, ($T_R = T$, $\rho_b C_P^b V \dot{T} = \int_{\partial\Omega} K_{salt} \partial T_{salt} / \partial n$ dA), neglecting thermomechanical coupling in the brine. Conversely, temperature changes play a significant mechanical role as they generate thermomechanical stresses in the rock mass; in addition, creep rate in the rock mass is a function of temperature. In sharp contrast, the poromechanical problem (evolution of stresses and pore pressure in the rock mass) is strongly coupled (stress changes generate permeability changes, and pore pressure changes generate effective stress changes).

In the virgin salt formation (**P**), deviatoric stresses are relatively small; no irreversible damage was created due to onset of dilation or of effective tensile stresses: generally, no coupling between mechanical behaviour and hydraulic behaviour is taken into account (no irreversible porosity-permeability change can take place). For some authors, fluid flow through the virgin rock formation is zero; for other authors, it can be described by the standard Darcy law. Thermal conductivity is constant.

In the damaged part of the salt formation (**S**), at the vicinity of the cavern walls, rock properties have changed significantly because of cavern creation and operation. Dilation appeared; dilation is an irreversible volume increase generated by onset of microfractures at the interface between grains when shear stresses are high when compared to mean pressure. Microfractures developed as the effective stress has experience tensile values (the effective stress equals the least compressive stress, which is negative, plus fluid pressure). These two processes often are called “damage”. In the context of cavern abandonment, damage is likely to originate in tensile effective stresses; however, dilation may have occurred during cavern operation, especially in a gas cavern when gas pressure is low. Damage leads to irreversible, or partially irreversible, changes of the mechanical and hydraulic properties of salt. Porosity increased because microfractures were created. When these microfractures are interconnected, permeability increases accordingly. Permeability increases are likely to be anisotropic (in the case of tensile effective stresses, microfractures open perpendicular to the least compressive stress; in the case of dilation, they open parallel to the most compressive stress). Permeability and mechanical behaviour are strongly coupled. Salt constitutive behaviour, which, in the primary (**P**) zone, was a function of the deviatoric stress, now depends only on the Terzaghi’ s or Biot’s effective stress [i.e. the actual stress plus a certain fraction of pore pressure, $\underline{\underline{\sigma}}_{eff} = \underline{\underline{\sigma}} + bP\underline{\underline{1}}$, Biot’s coefficient belongs to the $0 < b < 1$ range, and $b = 1$ is the Terzaghi’ s case; it is often accepted that microfracture at the cavern wall are created when one of the components of Terzaghi’ s effective stress is tensile, or larger than a small quantity, $T > 0$; however, in the rock mass, several authors assume that $b < 1$).] In most models, thermal conductivity in the damaged zone (**S**) is the same as in the virgin (**P**) zone.

Above the salt formation, the worst-case scenario consists of a porous-permeable aquifer layer (**O**) that must be protected from the intrusion of saturated brine. In the case of a salt dome, this layer can be located along the edge of the dome.

At the interface (**I**) between the primary (**P**) and secondary (**S**) zones, the constitutive law of the boundary must be specified - i.e. in each point of the boundary, a relation between, the rate of the boundary in the direction normal to the boundary on one hand, and some function of the state of stress at the boundary on the other. The simplest such constitutive law is a dilation criterion, e.g. $\sqrt{J_2} = a\left|I_1\right|$, or a tensile effective stress criterion, $\sigma^{lc} + P = T$, where σ^{lc} is the least compressive principal stress (note that the constitutive law does not depend on the boundary normal rate). However, less simple constitutive laws for the interface also are considered. The interface raises a difficult issue. It is likely that, at least in some cases, interface evolution is unstable (instead of a smooth evolution, localization takes place, in the form of a fracture or, more generally, of a thin elongated zone in which permeability is much larger than in most of the salt formation.) It is particularly the case when the interface moves upward as the brine-pressure gradient at rest is smaller than the vertical geostatic stress gradient (because brine is less dense than rock salt).

It is clear that a model describing *all* these effects requires several dozens of parameters; overall behaviour is nonlinear and, in some cases, localization can take place. Such highly sophisticated models have been developed for the nuclear waste disposal problem. In the case of salt caverns, more or less simplified models have been proposed by various authors. Some of them will be described in the following.

6.2 Rokahr et al. Model (1998)

Rokahr et al. (1998) discuss a criterion for the maximum acceptable pressure in a gas cavern. They state that fluid infiltration in the rock mass is possible when fluid pressure is larger than (or equal to) the least compressive tangential stress at cavern wall. "*A raised infiltration of storage medium is considered to start as soon as one component of the local principal stress state acting perpendicular to the spreading direction of the infiltration is lower in level than the internal cavern pressure acting at that point in time*.". However, it seems that the authors do not suggest a constitutive law to describe the poromechanical behaviour of the "secondary zone" (**S**) after the criterion is met at the cavern wall. They compare the least compressive stress to cavern gas pressure (in sharp contrast with brine, gas density is low or even negligible, and it is reasonable to assume that, after infiltration, gas pressure in the rock mass equals cavern gas pressure, at least when pressure losses are negligible) and suggest a simple criterion to define a secondary zone: gas pressure is smaller than the least compressive stress by a certain amount (e.g. 3 MPa). The primary, or "safety" zone, must be sufficiently large (the secondary zone must remain confined in the salt formation). Note that a consequence of this criterion is that a secondary zone exists above the cavern – although far from the cavern in most cases –because gas pressure is the same at any point and compressive stresses are small at shallow depth.

The authors consider a typical cavern (roof and bottom depths are 1000 m and 1400 m, respectively) in an isotropic salt formation and discuss the influence of a large number of parameters (depth,

weight of the overburden, roof shape, salt constitutive law, pressure history, etc.) on the size and location of the "barrier" at maximum operating pressure.

This paper is a remarkable first attempt to take into account experimental results, which were recent in 1998 (Kenter-Fokker lab tests, Etzel in situ test). However, the phenomenological description of the "damaged" or "secondary" zone is still simplistic (no change in permeability or constitutive law in this zone).

6.3 Lux et al. Model (2006)

Lux et al. (2006) discuss the possible creation of a "migration path" through the salt formation from the cavern to a permeable formation. The process comprises three phases: (1) cavern pressure build-up phase, in which there is a tight salt formation(2) an infiltration phase, during which permeability and additional porosity are created until the damaged zone reaches a permeable formation above the salt formation; and (3) a Darcy flow phase, during which brine flows from the cavern to the permeable formation through the newly created permeable zone in the salt formation.

Description of the second phase is especially important for this study. Infiltration starts when brine pressure is larger than the least compressive stress, LCS, (at the cavern wall), the difference between brine pressure and LCS being $\Delta\sigma_P$. Infiltration propagates in a direction perpendicular to the LCS. An empirical law describes the infiltration rate (which seems to be the normal rate to the boundary between the "infiltrated" and the "virgin" zones), as $\overline{v}_{\inf} = a\exp(b\Delta\sigma_P)$. In addition, a "secondary" porosity is created that can accommodate the brine permeating through the initially tight salt formation, $\phi^s = m\Delta\sigma_P + c$ (coefficients a,b,m and c are determined through permeation tests performed at the laboratory).

Note that such a "moving boundary" problem is correct when only one boundary condition is set on the moving boundary (separating the primary and secondary zones). The condition selected here is the boundary rate ($\overline{v}_{\inf} = a\exp(b\Delta\sigma_P)$) – i.e., there is no condition on $\Delta\sigma_P$ at the boundary, at least after a damaged zone appears.

Computations performed on a typical cavern prove that the process is slightly unstable in that the infiltration rate increase when the boundary rises (this is because rock stresses decrease faster than brine pressure when the boundary moves upward).

This model was one of the first attempts to describe propagation of a "damaged" zone through mathematical equations. However, it suffers from several flaws. In principle, the "impregnated" zone is filled with pressurized brine, and its poro-mechanical behaviour should be described ("effective" stress, Biot's coefficient etc.); when this description is performed, brine permeation through the damaged zone can be computed, and there is no need for an infiltration rate law, a purely empirical notion based on tests performed on small samples in the laboratory. It seems that, instead, brine pressure (or, more precisely, potential) in the damaged zone equals cavern brine potential.

In addition, the model does not seem to include the possible onset of localization (i.e. the creation of a thin zone in which damage takes place) and, as such, it cannot prove that a fracture cannot be created. This can be called the "fracture test": a numerical model predicting a smooth evolution is credible only when it is able to prove that, under certain circumstances, a fracture is created (for instance, when the pressure build-up rate in the cavern is extremely fast rather than relatively slow).

The authors revisit the Etzel field test and state that "*…the loss of integrity in the halite... took place at a gradient of approx....* $p_{FL}' = 0.210$ bar/m. . However, this statement does not consider the fact that cavern apparent compressibility (the amount of brine to be injected in a shut-in cavern to increase its pressure by 1 MPa) dramatically increases long before cavern pressure reaches the 0.210 bar/m level. In addition, they mention that *"… the fluid pressure strength level of the rock had been reached or clearly exceeded during this test. However, with respect to the type of failure, instead of the formation of singular macrofracs (also not excluded a priori) the failure took the form of fluid-pressure-induced zonal secondary migration paths consisting of microfissures*". However, the reason why macrofracking is not considered is not clearly explained.

6.4 Brouard et al. Model (2007b)

Brouard et al. (2007b) discuss the onset of tensile effective stresses in gas storage caverns. In this work, effective stresses are the sum of the actual (Cauchy) stresses plus fluid pressure in the rock mass. A conservative assumption consists of assuming that when one of the principal effective stresses is tensile (positive), micro-fracturing occurs, permeability increases and salt softens. Even if the vocabulary is slightly different, this notion is close to the approach of Rokahr et al. (1998), mentioned above. The authors focus on the influence of pressure history. They prove that when pressure is increased rapidly in a gas cavern after a long idle period, during which gas pressure was low and constant, onset of effective tensile stresses is extremely likely. This topic also was discussed by Wang et al. (2015) and Manivannan and Bérest (2019).

6.5 Wolters et al. Model (2012)

In Wolters et al. (2012), the same authors introduce several new ideas: damage (in the strictly mechanical sense) is described by a Kachanov-like model (damage generates evolutions of an internal parameter, *D*, that equals zero initially, and such that the constitutive law must be written for an "effective" stress, $\sigma/(1-D)$, rather than for the standard Cauchy stress, σ). In this model, healing/sealing is possible (for "sealing", newly generated permeability can vanish under the effect of stresses; for "healing", memory of damage vanishes, and the material becomes intact again). It seems that brine flow in the damaged zone (before its boundary reaches the permeable layer) is taken into account – an important difference to the former model.

Importantly, two models are proposed in this paper for the boundary (between the primary and secondary zones): the former model (MISES3-INFIL), in which the boundary normal rate is a function of $\Delta\sigma_p$; and a new model (FLAC3D-TOUGH2) in which the boundary condition is $\Delta\sigma_p = 0$. The stability of this type of problem (no infinite rate of the boundary) strongly depends on the loading parameter. When pressure is constant in the damaged zone, such a system often is unstable (a very

simple example is discussed, for example, in Bérest, 1998) and, for this reason, it is logical to describe pressure evolution in the damaged zone (a description that does not exist in the former model) and a secondary permeability is created in the damaged zone. In fact, the boundary rate is much slower when the latter model is selected; however, it is clear that these results depends strongly on the selected values of the parameters (there are four of them that describe the evolution of the secondary permeability).

6.6 Brückner and Wekenborg Model (2006)

Brückner and Wekenborg (2006) discussed the abandonment of four caverns at Stade-Süd, Germany. Three of them, T1, T3 and T6, are shallow (less than 800-m deep); T5's bottom is 1280-m deep. Field data were obtained from shut-in tests, temperature logs and compressibility tests.

The thermal model is as follows. Rock temperature distribution was fitted against an exponential law, $T_R - T_a = (T_r - T_b)\exp(-a/a_0)$, where a_0 is the radius of an equivalent cylinder; T_a is cavern temperature, T_R is the rock temperature at a distance *a* from the axis of symmetry, and T_b is the (fixed) rock temperature at a distance *b* from the axis of symmetry. Evolution of cavern brine temperature was inferred from this distribution through heat balance. Thermal expansion was computed from the following consideration: the flux of heat entering the cavern equals $\rho_b C_b V \dot{T}_a$, and it equals the heat lost by the rock mass, $\int \rho_R C_R \dot{T}_R \, d\Omega$; it is assumed that cavern thermal expansion equals cavern-brine thermal expansion minus rock mass contraction, $\alpha_b V\dot{T} - \alpha_R \int \dot{T}_R \, d\Omega$. This model is a little too simple. Rock temperature should be computed using Fourier's equation, $\partial T/\partial t = \Delta T$; in addition, cavern thermal expansion (as opposed to brine thermal expansion) is zero or very small (Karimi et al., 2007). The "expansion averaging" method leads to an underestimation of the effects of brine thermal expansion.

The poro-mechanical model is coupled. In the primary (**P**) zone, the Norton-Hoff law applies, $\dot{\varepsilon} = A_0 \exp(-Q/RT)\sigma^n$, in which permeation parameters are $\phi = 0.3\%$, and brine viscosity is $\mu = 1.8 \times 10^{-3}$ Pa.s. However, the primary zone is "dry" and each element of the mesh, beginning with the mesh elements at the cavern wall, is flooded by brine seeping from the cavern; seepage is described through Darcy's law. In a "wet" element (**S** zone), creep rate is faster (A_0 is multiplied by 5), and the constitutive law is written using effective stresses (rather than total stresses), which seem to be compared to a failure criterion. Stresses in the pillar around a cavern is compared to pillar strength. Caverns roofs are flat, and failure of elements is discussed. Model description is not fully comprehensive; for instance, interface (**I**) law (how a dilated zone increases) is not described fully. Note that by construction, localization is impossible (dilation zone growth is "mesh after mesh" and meshes are defined a priori.

6.7 Minkley et al. approach (2015)

From the same group, the approach of Minkley et al. (2015) is more sophisticated. An elasto-viscoplastic model is selected, and the flow rule is non-associated. The plasticity criterion also is a dilation criterion. A "softening" criterion is adopted – the criterion is a function of the cumulated plastic strain. It is significantly more severe than, for instance, Ratigan et al. (1991) criterion and leads to larger dilatant zone at cavern wall. The most original part is the coupled poromechanical model. In a gas cavern, the effective tensile stress criterion can be violated in two circumstances: (1) after a fast withdrawal, as high tensile thermoelastic stresses develop at cavern wall; and (2) during a fast injection, when gas pressure reaches high values. In the virgin state (**P**), salt is almost perfectly impermeable (values smaller than $K = 10^{-22}$ m were measured during tests in boreholes). However, high fluid pressures lead to opening of cracks at the grain boundaries, and progressive creation of discrete cracks ultimately lead to continuous paths for fluid flow when a percolation threshold is reached (in Minkley et al., 2018b, it is suggested that the percolation threshold can be written $P_c = f\left(\sigma_{\min} + \sigma_T\right)$, where P_c is the critical pressure, and σ_T is the tensile "strength". These paths are parallel to the least-compressive effective stress ($\sigma_{\min}$), as proved by laboratory tests. Permeability increases in the damaged zone, $KP = A\left(\sigma_{\min} + \sigma_T\right)^{\beta}$, hydraulic aperture of the grain boundaries is $w_{hyd} = \left(12K\right)^{1/2}$, and flow rate is computed following a cubic law. In this discontinuum-mechanical model, salt behaviour results from a standard elasto-viscoplastic behaviour of salt crystals, and the adhesive friction and gliding behaviour of grain boundaries, from which dilation appears. For numerical computations, salt crystals are mapped as polygonal bodies of different sizes and geometries. The case of cavern abandonment is especially important. Following Wallner's (1986) approach, in the final state, the average brine pressure in a cavern is close to geostatic pressure, and tensile effective stresses appear at the roof of the cavern. Micro-cracks open, and the percolation threshold is reached; brine flows upward in the micro-fractured zone above the cavern (in addition, dilatancy occurs at the cavern wall). In the case of a shallow cavern (the cavern top and bottom are 440 m and 600 m, respectively), the percolation zone has extended 80 m above the top of the cavern after 10,000 years.

Minkley et al.'s approach is probably the most advanced model in the literature dedicated to salt abandonment. However, extension of the percolation zone critically depends on the selected value of the percolation threshold (3 MPa). The percolation process is stable in the example provided (a shallow cavern); in a deeper cavern (say, 1500-m deep), the creep-closure rate can be expected to be faster by one of two orders of magnitude, as can a larger extent of the percolation zone. The stability of the process is difficult to discuss (as the percolation zone rises, the effective stress is more and more tensile in the upper part of this zone; growth rate of the zone depends critically on the ability of the brine outflow from the cavern to lower cavern pressure and increase in the cavern-closure rate.) In a deep cavern, it can be expected that the closure rate is fast, and brine pressure in the cavern and in the flow paths is not given enough time to release, allowing fast growth.

6.8 Thermal fractures

Fractures can be created at cavern wall when fluid pressure in the cavern is larger than the least compressive stress at cavern wall. Fractures can also be created when tensile thermal stresses generated by fluid cooling are larger than compressive stresses at cavern wall. An example of this, observed in a ventilation shaft of the Gorleben salt mine, was described by Wallner and Eickemeier (2001), Figure 85.

> "*During the cold season, temperatures in the shaft decreased by 20°C … within a time period of 80 days… horizontal and vertical fractures were detected by routine inspections in the shaft. Theses fractures had an average spacing of about 2.8 m. The fracture aperture amounted up to several mm."* (p. 365).

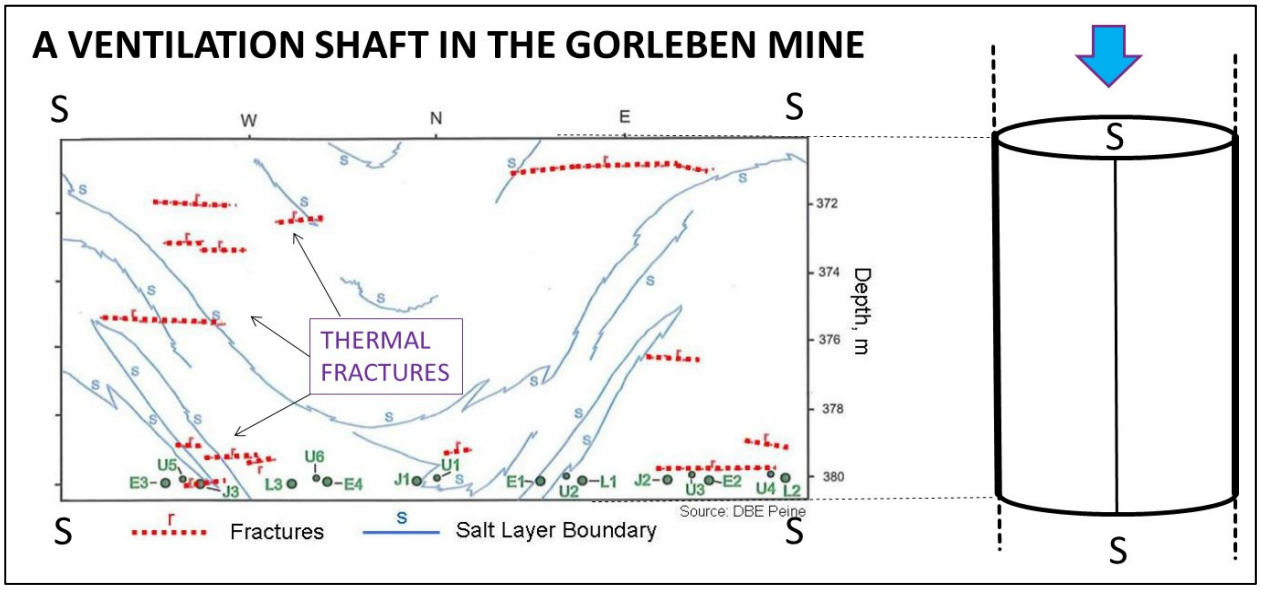

Figure 85 - Thermal fractures at the wall of a ventilation shaft (After Wallner and Eickemeier, 2001).

Modelling thermal fractures development is easier than hydraulic fracturing, as stress distribution in the rock mass is not modified by fluid penetration in the fractures (fracture aperture is thin and fluid in the fracture rapidly reaches thermal equilibrium with the rock mass).

In principle, Fracture Mechanics allows prediction of the aperture, depth and spacing of thermal fractures. This domain is still a matter of research. An example of this will be discussed below. However, a few partly empirical rules can be stated in the case that a wall is cooled down (Nemat-Nasser et al., 1978; Bahr et al., 2010):

i. Thermal fractures are perpendicular to the cavern wall. In a cylindrical well, fractures are mostly horizontal, because the least compressive stress is vertical.

ii. At the beginning of the cooling process, when the depth of penetration of temperature changes is shallow, stresses are tensile in a thin zone at the cavern wall, and many thermal micro-fractures appear at cavern wall. When cold temperatures penetrate deeper into the rock mass,

propagation of many fractures stops, and only a small number continue to develop (see Figure 86).

iii. Fracture depth approximately equals the depth of the zone in which tensile stresses are larger than rock tensile strength (assuming that this strength is zero is on the safe side). Obviously, the development of fractures modifies the state of stress in the vicinity of the fractures. The tensile stresses addressed here are those stresses computed with the assumption that no fracture exists.

iv. The ratio between fracture depth and fracture spacing is not very different from 1.

v. The ratio between the aperture of a fracture, o, and the spacing between two consecutive opened fractures, s, is: $o/s = -\alpha \delta T(a)$, where $\delta T(a) < 0$ is the temperature change at the cavern wall. (Bérest et al., 2016).

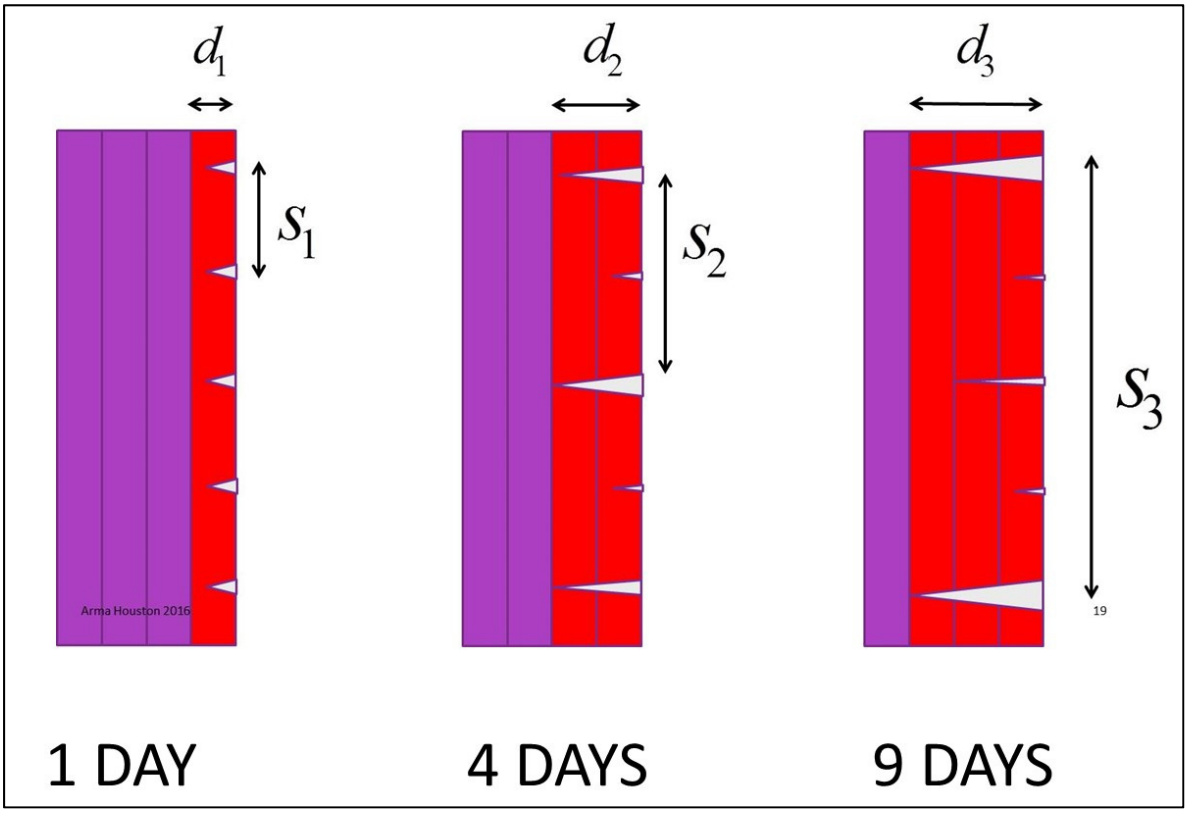

Figure 86 - Example of propagation of thermal fractures.

Computation requires advanced methods. This is illustrated on Figure 87, which represents the evolution of cracks in a cavern in which temperature was lowered by $\delta T = -40\ °C$ and kept constant for six months. (This is an unrealistic scenario; in an actual cavern, gas warming after gas withdrawal is fast.) Mechanical assumptions and details of the computations can be found in Sicsic et al. (2014). At the beginning of the process, crack length consistently increases as temperature changes penetrate deep into the rock mass. After 3 days, they are 1-m deep. After 7 days, of two neighbouring cracks, only one continues to grow. This crack selection, leading to periodic division by two of the number of active growing cracks, can be observed during the entire six-month period.

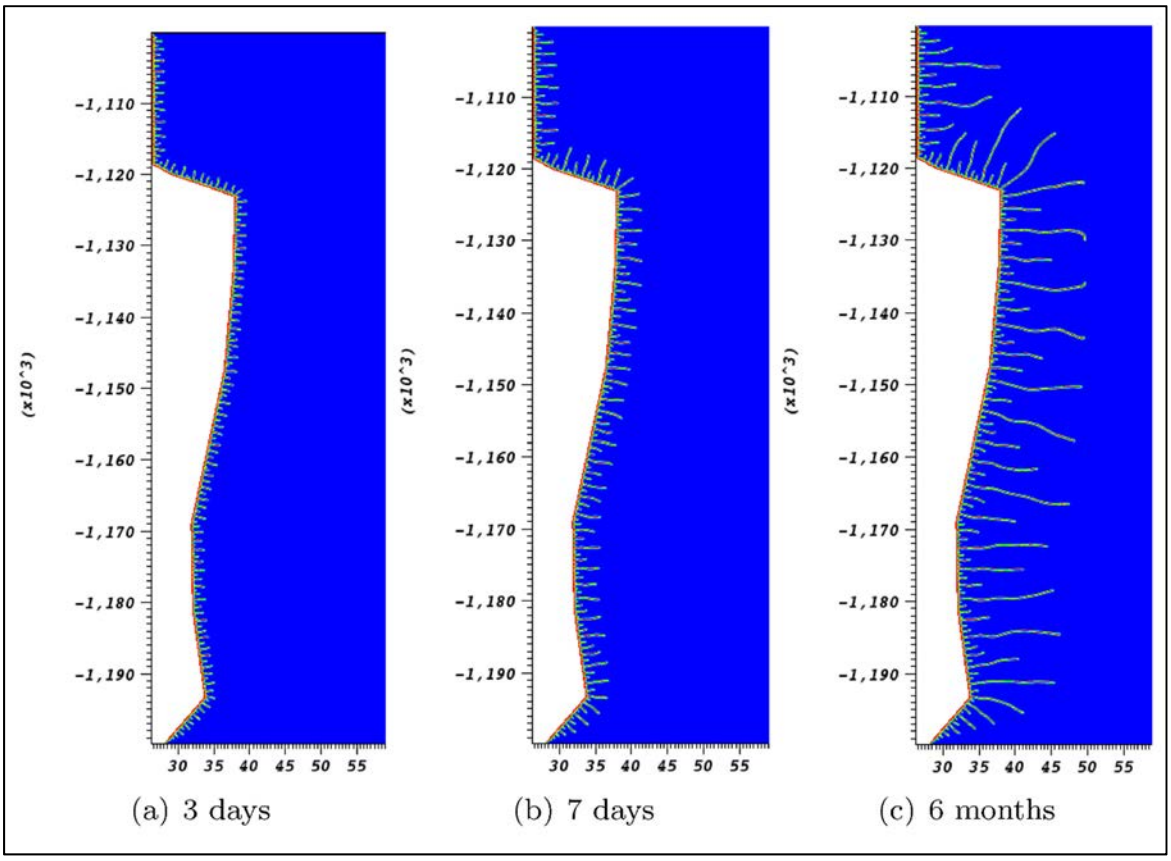

Figure 87 - Propagation of thermal cracks after 3 days, 7 days and 6 months when temperature in the cavern is kept low for 6 months (Sicsic and Bérest, 2014).

Even if the example above is relative to thermal fractures, it can be stated, as a general rule, that fracture propagation is an unstable process: growth of a smaller and smaller number of fractures is the process which minimizes the energy required for fracture propagation.

7. CONCLUSIONS AND RECOMMENDATIONS

7.1 Conclusions

[1] The state of stress in a salt formation can be assessed through density logs, frac tests and specialized logs. Interpretation of frac tests raises theoretical problems that have not been solved to date. Fracture tests seem to overestimate the actual stresses by 5-10%. It often is assumed that the state of stress is isotropic (exceptions clearly exist), and that, at a given depth, the geostatic pressure equals the weight of the overburden, $P_\infty = \gamma_R H$, where *H* is the cavern depth, and γ_R is the average volumetric weight of the overburden; $\gamma_R = 0.022 - 0.023$ MPa/m is typical. Density-based assessment of the vertical stress often is considered supplying data of sufficient quality.

[2] Thousands of caverns have been operated worldwide for brine production or for gas and liquid storage. In the case of gas or oil storage, for which safety and environmental protection concerns are especially important, companies select a maximum admissible pressure that is proportional to casing-shoe depth, $P_{\max} = \gamma_{\max} H$. In most cases, $\gamma_{\max}$ is close to 0.018 MPa/m. Maximum admissible pressure is significantly smaller than computed geostatic pressure. This large factor of safety ($\gamma_R / \gamma_{\max} = 120\%$) is dictated by experience and the special concerns mentioned above. The same maximum admissible pressure applies to brine caverns (in which high pressure is applied for short periods — e.g. when tightness tests are performed). However, a few exceptions can be found, notably at Veendam and Barradeel (in the Netherlands), where fast-creeping salts are leached out at depths larger than 2000 m and the operating pressure is closer to geostatic pressure.

[3] Several salt caverns used for hydrocarbon storage experienced product losses and unexpected pressure drops resulting from a casing leak (a dozen cases are known). They are not of direct interest for the present study, as it is assumed that wells will be plugged efficiently before abandonment (at Bryan Mound, poor plugging led to large subsidence). Leaks through cavern walls are much less frequent. The LOOP (oil storage, Clovelly Dome, Louisiana) and Bayou Corne (brine production, Napoleonville Dome, Louisiana) cases are explained by the proximity of the cavern to the flanks of the dome. The severe gas leak at Regina South (Canada) resulted from failure of a thin cavern roof that had poor mechanical qualities. The Mineola (Texas) case, which led to a propane blow-out, is poorly documented. The Spindletop case is puzzling: gas seeped from a gas cavern to a brine cavern, even though the cavern walls were 120-m apart. A horizontal discontinuity in salt composition is suspected, but evidence is scarce. The Veendam case (a severe pressure drop) seems to be related to high cavern pressure, a thin salt roof, and a strongly anisotropic state of stress in the overburden, where a fracture almost certainly developed after a connection was created with the cavern cluster through the salt roof. These examples outline the significance of the geological context and, more specifically, of the hydraulic and mechanical conditions at the boundary of the salt formation.

[4] Prompted by increasing public concerns in environmental protection and several projects in which hazardous products were disposed of in abandoned salt caverns, the abandonment issue was raised in the 1980s. From that time until now, advances have been considerable. In Germany, Wallner (1986) proved that, in the long term, brine overpressure develops at the cavern roof of a tight cavern (the "*Wallner's margin*"). At that time, rock salt was considered as perfectly tight and,

provided that the pressure build-up rate in the cavern was slow enough, it was expected that no fracturing would take place even when the cavern pressure became significantly higher than geostatic pressure (a gradient of $0.022 - 0.023$ MPa/m). In fact, the Etzel test (1990-1992) proved that the cavern ceased being tight when the pressure gradient in the cavern was as low as 0.019 MPa/m. The Kenter-Fokker tests performed at the laboratory in a mock-up cavern proved that a significant permeability increase was observed when the effective stress at cavern wall was tensile. In France, Bérest et al. (1979) highlighted the role of brine thermal expansion: years or decades are required before a brine cavern reaches thermal equilibrium with the rock mass — a serious concern when abandoning a cavern, as brine warming in a shut-in cavern typically leads to a pressure increase by 1 MPa/°C. The authors also showed that in a site where deep (2000 m) caverns had been linked by hydrofracturing, the pressure build-up rate is fast when caverns are shut in, leading to re-fracturing after a couple of months. Durup (1990 and 1994) performed long-term permeability tests in a 1000-m deep borehole in a bedded salt formation at Etrez; permeability to brine or gas was small but non-negligible.

A vast majority of authors agreed that evolution of a shut-in cavern is governed by three main phenomena: (1) brine warming, which is independent of cavern pressure; (2) creep closure, which is a decreasing (non-linear) function of cavern pressure and far-field stress field (whose possible anisotropy is important in this context); and (3) brine permeation through the cavern walls, which is an increasing function of cavern pressure. One consequence is that, at least when brine thermal expansion can be neglected and the wellbore is sealed efficiently, an equilibrium pressure is reached when the brine-outflow rate exactly balances the cavern-closure rate. In a shallow cavern (less than 1000-m deep; this figure is somewhat arbitrary), this equilibrium pressure is significantly lower than geostatic pressure, preventing any risk of fractures being created. Tests (several of which were sponsored by the Solution Mining Research Institute) were performed in France at Etrez, Carresse and Gellenoncourt, and, in Germany, at Bernburg and Stassfurt. These tests strongly supported these views. At Etrez, after an 18-month test, a low equilibrium pressure was reached. Fifteen years later, during a new shut-in test, the same equilibrium pressure was reached. It is accepted widely now that, provided thermal equilibrium is reached, shallow caverns can be abandoned safely.

These conclusions hold when the cavern is reasonably tight. At Brian Mound (Louisiana), subsidence was especially large above a large-diameter shallow cavern that did not have hydraulic integrity.

Several tests (Durup's tests at Etrez, the Etzel test and the Barradeel test, mentioned below) also proved that the *apparent* compressibility of a cavern or a wellbore (the volume of brine to be injected in a cavern to increase its pressure by a pressure unit) consistently increases when cavern pressure is larger than a certain threshold that is significantly smaller than geostatic pressure —evidence of an increase in cavern permeability.

In deeper caverns (more than 1000 m), creep closure is faster, and the equilibrium pressure is closer to the geostatic pressure. In many cases, the computed equilibrium pressure is larger than the maximum admissible pressure during operation (see above). The fracturing risk cannot be disregarded, especially when Wallner's margin and residual brine warming are taken into account. An 8-year-long test was performed in four caverns (more than 1000-m deep) at Mont Belvieu, Texas. Brine thermal expansion was still active, and drawing definite conclusions was difficult. At Tersanne,

France, a 1400-m deep cavern was shut in 14 years ago; here, again, brine warming is still active and, for safety reasons, the cavern must be vented from time to time: the computed equilibrium pressure is larger than the maximum pressure accepted by the mining authorities. Another test was performed in 2004-2008 at Barradeel, the Netherlands, in a 2500- to 3000-m deep cavern (BAS 2). Pressure increased rapidly in the shut-in cavern and reached a value close to geostatic, after which the pressure increase became very slow. It is highly likely that a significant volume of brine seeped to the rock mass. Issues changed accordingly: the question asked was not "*Can brine seep from the cavern?"* (it did) but, rather, "*Can a hydraulic connection be created between the cavern and a potable water reservoir*?" — a less demanding requirement.

[5] From a theoretical point of view, it is difficult to predict the effects on subsidence at ground level of a significant brine flow from a cavern to an overlying aquifer layer. The Bryan Mound and Veendam examples strongly suggest that subsidence increases.

[6] The Etzel test prompted several modelling attempts. It is now accepted widely that, after (or even slightly before) the effective tensile stress criterion is reached (one of the two tangential stress at cavern wall is less compressive than brine pressure), the porosity, permeability and mechanical behaviour of rock salt drastically change. As suggested by several authors (Karimi-Jafari et al., Djizanne et al., Smit et al.), these changes may take place long before cavern pressure reaches geostatic pressure, as, in a visco-plastic rock mass, tangential stresses at the cavern wall experience complicated evolutions. Much evidence is available from microscale studies (micro-fracturing takes place at grain boundaries). One must distinguish between a "primary" zone that did not experience damage and, closer to the cavern, a "secondary" zone, in which a strong hydro-mechanical coupling must be taken into account. Computing rock-mass evolution is difficult: the boundary between the primary and secondary zones is unknown *a priori*, and the constitutive law describing the poro-mechanical behaviour of the secondary zone involves many parameters whose acquisition at the laboratory requires considerable effort. The first models were quite simple; substantial advances were made, and sophisticated models are now available. Cavern compressibility has a stabilizing effect (any brine outflow leads to a decrease in cavern pressure); conversely, along an upward-oriented flow path, effective stresses tend to be more tensile at shallower depth — a possible cause of fast upward fracture growth. However, many difficulties remain. It is suspected that boundary evolution is not smooth and that localization/fracturing can take place. Field data are scarce. Despite considerable advances, solution of the evolution problem has not reached a fully stabilized state.

7.2 Recommendations

The case of large-diameter shallow caverns with no salt roof, which are prone to stoping and, ultimately, to creating a sinkhole, is not discussed here.

[1] When abandoning a cavern, the site-specific composition and sensitivity of the underground environment must be studied. Is subsidence a severe concern? Are potable water resources above or below the cavern field to be protected? Are they protected by a sufficient thickness of impermeable-ductile rocks? Are there large porous and permeable "receptors" able to accommodate large volumes of brine? Are they sensitive to hydro-fracturing when reached by highly

pressurized brine? Addressing this would require salt-dome scale numerical models that are coupled with poro-elasto-plastic model of the overburden to estimate the stress state and orientation at the salt-sediment interface, for reasonable variations in the material parameters.

[2] The thermal status of the cavern must be perfectly known. How large is the gap between brine temperature and rock temperature? How fast is the temperature change rate? How long is the waiting time needed to lower this gap to sufficiently small values?

[3] Information must be gathered on hydraulic (permeability) and mechanical (ability to creep) properties of the salt formation. Together with thermal properties, they allow building of a thermo-hydro-mechanical model able to predict the long-term behaviour of the shut-in cavern and cavern pressure evolution during the monitoring period (see below). This model should take uncertainties in rheological parameters into account. It is advisable to create dome-scale models that take the stress-state of the overburden into account, to monitor the expected stress evolution of the overburden along with the deformation of the cavity. A shut-in test should be performed before abandonment

[4] In shallow caverns (less than 1000 m), when thermal equilibrium is reached, several *in situ* tests performed in various geological conditions strongly suggest that, in the long term, an equilibrium pressure, significantly smaller than geostatic pressure, will be reached. Slow brine rates will permeate to the salt formation. Safe abandonment is possible. A monitoring period (several years and more) is needed before abandoning the cavern to verify that the actual cavern behaviour matches the behaviour predicted by computations.

[5] Deep caverns raise a more difficult problem, as the equilibrium pressure mentioned above is much closer from geostatic pressure. Taking into account Wallner's margin, the residual thermal gap (which is difficult to avoid in a very large cavern), and various uncertainties, it is difficult to be certain that no fracture will take place.

- Filling the cavern with solid residues is so costly a solution that it can only be considered in very specific cases.
- When creep closure is fast enough, allowing the cavern to close completely before abandonment is the simplest option (an outlet must be found for the relatively small brine rate that will be expelled from the cavern over a long period of time). The advantage of such an option is that possible negative consequences are not delayed (subsidence) or even are suppressed (brine seepage to the underground environment).
- When such a solution is not possible (for instance, because subsidence must be minimized), a waiting period must be managed to allow a temperature gap to reach a small value (injecting a small amount of a compressible fluid, e.g. nitrogen, can also be considered) and, as in the case of shallow caverns, a monitoring period must be managed.
- One can also try to prove that the amount of brine that can seep from the cavern through fractures or micro-fractures will remain confined in the salt formation. The recent Barradeel case (Duquesnoy et al., 2019) proves that such a demonstration is difficult.

- One should take care if cavities are built close to the top of a salt structure with a more significant amplitude, close to the lateral salt-sediment, or close to weak/strong layers within the salt such as stronger and dense anhydrite stringers or weak K-Mg-salt layers. For these cases, differential stresses tend to be higher and detailed computations (see salt-dome Report) are recommendable combined with microstructural analysis.

[6] A safety file including geological information, cavern history, *in situ* test results, results of numerical computation, and assessment of abandonment consequences for health and environmental protection should be prepared. It is likely that, in some cases, abandonment should be delayed (for instance, to allow the temperature gap to reach a small value). Monitoring will be mandatory for several years or decades before a final decision can be taken. In some cases, it will be difficult to avoid transferring monitoring and the abandonment decision to the state.

REFERENCES

Arnold C., Hak A.A. and Feldrappe H. (2014) Advanced exploration methods for dimensioning and optimizing of gas storage caverns at storage site Bernburg/Peissen (Central Germany). In: Proceedings SMRI Fall Meeting, Groningen, The Netherlands, 2014: 137-146.

Baar C.A. (1977) Applied salt-rock mechanics. Vol. I. Developments in Geotechnical Engineering. 16-A. Amsterdam: Elsevier Science.

Bahr H.A., Weiss H.J., Bahr U., Hoffmann M., Fischer G., Lamperscherf S. and Balke H. 2010) Scaling behavior of thermal shock crack patterns and tunneling cracks driven by cooling or drying. *J.M.P.S.* 58: 1411-1421.

Banach A. and Klafki M. (2009) Staβfurt Shallow Cavern Abandonment Field Tests. SMRI Research Report RR 2009-01.

Behr, A. (2001) Evaluation of Salt Permeability Tests, SMRI Project No. 01-0003, prepared by Wilsnack & Partners (IbeWa), Freiberg/Saxony, Germany, for the Solution Mining Research Institute.

Bérest P., Ledoux E., Legait P. and de Marsily G. (1979) Effets thermiques dans les cavités en couche saline. [Thermal effects in Cavities in Salt Rock], CR 4th Congrès SIMR, Montreux, Switzerland, Balkema, Vol.1, 31-35.

Bérest P. and Brouard B. (1995) Behavior of sealed solution-mined caverns. Proc. SMRI Spring Meeting, New Orleans.

Bérest P. (1998) Stability of a system whose boundary evolutions are governed by a standard constitutive law. Proc. IUTAM Symp. Kluwer Ac. Publ., 261-267.

Berest, P., J. Bergues, B. Brouard, V. de Greef, Y. Le Bras, J. G. Durup, and B. Guerber (1998) Long-Term Evolution of a Sealed Cavern, SMRI Project No. 98-0004, prepared by Laboratoire de Mécanique des Solides, Ecole Polytechnique, Palaiseau, France; and Gaz de France, La Plaine Sant Denis, France, for the Solution Mining Research Institute, 101 p.

Bérest P., Brouard B. and de Greef V. (2000a) Salt permeability testing - the influence of permeability and stress on spherical hollow salt samples. Technical Report RFP 98-1 for the Solution Mining Research Institute.

Bérest P., Brouard B. and Durup J.G. (2000b) Shut-in pressure tests - case studies. Proc. SMRI Fall Meeting, San Antonio, Texas, 105-125.

Bérest P., Bergues J., Brouard B., Durup J.G. and Guerber B. (2001a) A salt cavern abandonment test. Int. J. Rock Mech. & Mining Sci., 38:357-368.

Bérest P., Brouard B. and de Greef V. (2001b) Salt Permeability Testing. The Influence of Permeability and stress on Hollow Salt Samples. SMRI Research Project Report n° 2001-8.

Bérest P. and Brouard B. (2003) Safety of Salt Caverns Used for Underground Gas Storage. Oil Gas Sci. Technol.-Rev IFP 58, 361-384.

Bérest P., Diamond B., Duquesnoy A., Durup G., Feuga B. and Lohff L. (2004). Salt and Brine Production Methods in France: Main Conclusions of the International Group (IEG) commissioned by the French regulatory authorities. Proc. SMRI Fall Meeting, Berlin, 1-24.

Bérest P., Brouard B., Karimi-Jafari M. and Van Sambeek L. (2007) Transient behavior of salt caverns. Interpretation of Mechanical Integrity Tests. Int. J. rock Mech. Min. Sc. 44, 767-786.

Bérest P. (2010) Field testing issues relative to the long-term abandonment of salt caverns. Technical Class Book Fundamentals for the long-term abandonment of salt caverns, SMRI Fall Meeting, Leipzig, Germany, 31-49.

Bérest P., Brouard B. and Hévin G. (2011) A 12-year long pressure monitoring in an idle salt cavern – the 1997-1998 Etrez abandonment test revisited. Int. J. Rock Mech. Min. Sc., Vol. 45, Issue 7, 1025-1043.

Bérest P., Brouard B., Hertz E., Hévin G., de Laguérie P. and Hardy J.M. (2013) Cavern abandonment: three in situ tests. Proc. SMRI Fall Meeting, Avignon, France.

Bérest P., Brouard B. and Gharbi H. (2015) Rheological and geometrical reverse creep in salt caverns. Proc. 8th Conf. Mech. Beh. Salt, 199-208.

Bérest P., Brouard B. and Sicsic P. (2016) Thermomechanical effects of depressurization in a CAES. ARMA Conference, paper 16-632.

Bérest P. (2017) Cases, Causes and Classifications of Craters above Salt Caverns. Int. J. Rock Mech. Min. Sci. December 2017, 100, 318-329.

Bérest P., Brouard B., Brückner D., DeVries K., Gharbi H., Hévin G., Hofer G., Spiers C. and Urai J.L. (2019a) Very Slow Creep Tests on Salt Samples. Rock Mech Rock Eng. (2019) https://doi.org/10.1007/s00603-019-01778-9.

Bérest P. and Manivannan S. (2019b) Behavior of a salt cavern when creep law is modified to account for low deviatoric stresses. Proceedings ARMA 2019, New York, Paper 19- 477.

Bérest P., Réveillère A., Evans D. and Stöwer M. (2019c) Review and analysis of historical leakages from storage salt caverns wells. Proceedings SMRI Spring Meeting, New Orleans.

Bernhardt H. and Steijn J. (2013) Influence of Tubing Diameters on Lifting Methods During Gas First Fill of Gas Storage Caverns - A Practical Example in the Nüttermoor Cavern Field. Proc. SMRI Spring Meeting, La Fayette, Louisiana, 161-172.

Brouard B., Bérest P. and Durup J.G. (2001) In-situ salt permeability testing. Proc. SMRI Fall Meeting, Albuquerque, New Mexico, 139-157.

Brouard Consulting, Institute für Unterirdishches Bauen (IUB), Ecole Polytechnique, Total E&P France and Géostock (2006) Salt Cavern abandonment Field Test in Carresse. SMRI RFP 2003-2-B, Final Report.

Brouard B., Bérest P. and Karimi-Jafari M. (2007a) Deep salt cavern abandonment. Proc. 6th Conf. Mech. Beh. Salt, 445-452. London: Taylor & Francis Group.

Brouard B., Karimi-Jafari M. and Bérest P. (2007b) Onset of tensile effective stresses in gas storage caverns. Proc. SMRI Fall Meeting, Halifax, 119-135.

Brouard B., Lheur C., Hertz E., Bérest P., de Greef V. and Beraud JF. (2009) A brine-outflow test in a Gellenoncourt cavern. Proc. SMRI Spring Meeting, Krakow, Poland.

Brouard B., Bérest P., Staudtmeister K., de Laguérie P. and Réchède A. (2010) Update of the SMRI 2006 Carresse Research Report. SMRI Research Project Report 2010-S.

Brouard B., Bérest P., de Greef V. Beraud, J.F., Lheur C. and Hertz E. (2013) Creep closure rate of a shallow salt cavern at Gellenoncourt, France. Int. J. Rock Mech. Min. Sc., 2013.

Brouard B., Bérest P., Hertz E. and Lheur C. (2017) A Cavern Abandonment Test at Gellenoncourt, Lorraine − An Update − Proc. SMRI Fall Meeting, Münster, Germany.

Brückner D., Lindert A., Wiedemann M. (2003). The Bernburg Test Cavern – A Model Study of Cavern Abandonment. In: Proc. SMRI Fall Meeting, 5 – 8 October Chester, UK.

Brückner D. and Wekenborg H. (2006) Abandonment of Caverns at the Brine Field Stade-Süd, Germany, Geomechanical Concept, Geotechnical Procedures and the Proof of Long-term Safety by Numerical Modeling. Proc. SMRI Fall Meeting, Rapid City, South Dakota.

Bruno M.S. and Dusseault M.B. (2002) Geomechanical Analysis of Pressure Limits for Thin Bedded Salt Caverns. Proc. SMRI Spring Meeting, Banff, Alberta, 49-74.

Cartwright M.J., Ratigan J.L. (2005) Case History – Solution Mining a Cavern That Intersects a Plane of Preferred Dissolution. SMRI Fall Meeting, 2-5 October 2006, Nancy, France.

Chabannes C.R. (2005) Storage Pressure limits – Egan Facility. SMRI Spring Meeting, Syracuse, New York, in Ratigan et al., Panel discussion.

Colcombet B., Guerreiro V. and Lúcio J. (2008) An overview of the Carriço Gas Storage Project Development In: Proceedings SMRI Spring Meeting, Porto, Portugal, 2008: 1-18.

Coleman Hale P., Stroh G. and Osnes J. (2015) The Effects of Interbedded Salt & Potash on Cemented Casing at Dewdney Field. Proc. SMRI Fall Meeting, Santander, Spain.

Crossley N. G. (1992) Gas Storage in Saskatchewan Bedded Salt. Proc. SMRI Fall Meeting, Houston, 1992.

Crossley N.G. (1998) Sonar surveys used in gas-storage cavern analysis. Oil & Gas Journal, Vol-96, issue-18, 05/04/1998.

Crotogino F. (1995) External well mechanical integrity testing/performance, data evaluation and assessment. SMRI Research Project Report no. 95-0001-S.

Crotogino, F., Behrendt C. and Hackney J. (1997) Bibliography for Cavern Abandonment, SMRI Project No. 97-0002, prepared by KBB, Hannover, Germany; and PB-KBB Houston, TX, for the Solution Mining Research Institute, 158 p.

Crotogino F. and Kepplinger J. (2006) Cavern Well Abandonment Techniques. Guidelines Manual. SMRI Research Report 2006-3-SMRI, September.

de Laguérie P. and Durup G. (1994) Natural Gas Storage Cavities at Manosque, France. In: Proceedings SMRI Fall Meeting, Hannover, Germany.

de Laguérie P., Héas J.Y., Fourmaintraux D., You Th., Brouard B. and Bérest P. (2004) Decommissioning and Abandonment Procedure of LPG Caverns at Carresse (France) Proc. SMRI Fall Meeting, Berlin, 28-42.

de Lange E.R., Mulder L.P.T., Duquesnoy A.J.H.M. and Bakker T.W. (2012) Frisia Salt – Netherlands Deepest squeeze mining in the world. Proc. SMRI Spring Meeting, 23-24 April 2012, Regina, Saskatchewan, p. 103-120.

Djizanne H., Bérest P. and Brouard B. (2012) Tensile Effective Stresses in Hydrocarbon Storage Caverns. Proc. SMRI Fall 2012 Technical Conference, 1-2 October 2012. Bremen, Germany.

Duquesnoy A. (2011) Synthesis of SMRI-sponsored shallow cavern Abandonment Tests. SMRI Research Report RR2011-02.

Duquesnoy A. and de Lange B. (2015) Abandonment of Very Deep Brine-Filled Caverns at Frisia Salt Harlingen. Proc. SMRI Spring Meeting, Rochester, New York.

Duquesnoy A., Van El A. and Mastaler R. (2019) BAS-4 Cavern Abandonment Risk Analysis Frisia Salt Harlingen. SMRI Fall Meeting, Berlin, Germany, 71-96.

Durup J.G. (1990) Long term tests for tightness evaluations with brine and gas in salt (Field test n°1 with brine) Research Project Report n°90-2-SMRI.

Durup J.G. (1994) Long term tests for tightness evaluations with brine and gas in salt (Field test n°2 with gas) Research Project Report n°94-002-S.

Enterprise Products Operating L.L.C., PB Energy Storage Services, RESPEC 3824. (2009) Cavern Abandonment Field Tests in a Deep Cavern. March 2009. SMRI Research Report 2008-1.

Enterprise Products Operating L.L.C., PB Energy Storage Services, RESPEC 3824. (2015) SMRI Cavern abandonment field tests in deep caverns. August 2015. SMRI Research Report RR2015-02.

Fansheng B., Guangjie Y. and Ruichen S. (2010) Solution Mining and injection-production technology of gas storage in deep salt cavern. In: Proceedings SMRI Fall Meeting, Leipzig, Germany, 2010: 188-192.

Fawthrope R., Bonnier N., Bublak R., Schubert J., Jackson C. and Robb T. (2013) A First Completion Design in the UK to Use Welded Completions for a New Large Onshore Gas Storage Development in Salt Caverns. Proc. SMRI Spring Meeting, La Fayette, Louisiana, 255-270.

Fokker P.A. (1995) The behavior of salt and salt caverns. PhD Thesis Technical University Delft. Delft Geotechnics. P.O Box 69, 2600 AB Delft.

Fokker P.A., In't Veld C., Bakker T.W. and Jagt M. (2004) 10 years' experience in squeeze mining. Proc. SMRI Fall Meeting, Berlin, Germany.

Gaz de France (1990) Field Tests in Well EZ 58 – (Long-Term Tests for Tightness Evaluations) – Phase 1, prepared by Gas de France, Clichy, France, for the Solution Mining Research Institute, 41 p.

Gaz de France (1994) Long-Term Tests for Tightness Evaluations with Brine and Gas in Salt (Field Test No. 2 With GAS), prepared by Gas de France, Clichy, France, for the Solution Mining Research Institute, 36 p.

Gebhardt F., Eby D., Barnett D. (2001) Utilizing Coiled Tubing Technology to Control a Liquid Propane Storage Well Fire, A Case History. Proc. SMRI Spring Meeting, 301-306.

Guo F., Morgenstern N.R. and Scott J.D. (1993) Interpretation of hydraulic fracturing pressure: A comparison of eight methods used to identify shut-in pressure. Int. J. Rock Mech. Sci, Vol. 30, No.6, 627-631, 1993.

Hévin G. and Rousset E. (2013) Te02 salt cavern. 8 years of abandonment test. In: Proc. SMRI Fall Meeting, Avignon, France, 37-48.

Hévin G., Caligaris C. and Durup J.G. (2007) Deep salt cavern abandonment: a pilot experiment. SMRI Fall Meeting, Halifax, Canada, 16-25.

Hiltscher A. and Zwätz H. (2003) The research project “Bernburg Test Cavern”. Proc. SMRI Fall Meeting, Chester, England.

Hoelen Q., Dijk H., Wilke F. and Wippich M. (2010) Gas storage in salt caverns Zuidwending - The Netherlands. In: Proceedings SMRI Fall Meeting, Leipzig, Germany, 241-250.

Horvath P.L. and Wille S.E. (2009) Determination of Formation Pressures in Rock Salt with Regard to Cavern Storage. In: Proceedings SMRI Spring Meeting, Krakow, 83-90.

Igoshin A., Kazaryan V., Khloptsov V., Novenkov Y. and Salokhin V. (2010) Design, technology and experience of cavern construction at Kaliningrad UGS in Russia. Proceedings SMRI Fall Meeting, Leipzig, Germany, 2010:176-185.

Istvan J. A.; Evans L. J., Weber J. H. and Devine C. (1997) Rock Mechanics for Gas Storage in Bedded Salt Caverns: Int. J. Rock Mech. & Min. Sci. 34:3-4, Paper No. 142.

Istvan JA. (1998) Potential for Storage of Natural Gas in the Hutchinson Salt Member of the Wellington Formation of South-Central Kansas. Proc. SMRI Fall Meeting, Roma, Italy, 245-268.

Johansen J.I. (2010) 25 years of lifetime history for seven Energinet.dk gas caverns in the L.I. Torup Zechstein salt dome in Jutland, Denmark. Proc. SMRI Spring Meeting, Grand Junction, Colorado, 329-338.

Johnson D.O. (2003) Regulatory response to unanticipated geo-mechanical events effecting gas storage cavern operations in Texas. SMRI Spring Meeting, Houston, Texas, 205-2017.

Judgement by Thomas J. Kliebert, Jr. December 21, 2017. Division “B”, 23rd Judicial District Court, Parish of Assumption, State of Louisiana.

Karimi-Jafari M., Bérest P. and Brouard B. (2006) Transient behavior of salt caverns. Proc. SMRI Fall Meeting, Rapid City, 253-270.

Karimi-Jafari M., Bérest P. and Brouard B. (2007) Thermal Effects in Salt Caverns. Proc. SMRI Spring Meeting, Basel, Switzerland, 165-177.

Kelly S.L. and Fleninken J.A. (1999) Development of Cement Evaluation Quality Control Measures for Cavern Wells. Proc. SMRI Spring Meeting, Las Vegas, Nevada, 191-225.

Kenter C.J., Doig S.J., Rogaar H.P., Fokker P.A. and Davies D.R. (1990) Diffusion of brine through rock salt roof of caverns. SMRI Fall Meeting, October 14-19, Paris.

Klafki M., Bannach A. and Wagler T. (1998) Parameter Determination for Planning and Constructing of Gas Cavern Storage. In: Proceedings SMRI Fall Meeting, Roma, Italy, 269-289.

Kroon I.C., Orlic B. and Scheffers B.C. (2003). Abandonment of solution mined salt caverns in the Netherlands. Part 2. Best Practises and methods. NITG 03-172-B.

Langer, M.; Wallner, M. and Wassmann, H. (1984) Gebirgsmechanische Bearbeitung von Stabilitatsfragen bei Deponiekavernen im Deckgebirge. Kali und Steinsalz, Heft 2/1984, S. 66 - 76.

Langer M., Wallner M. and Wassmann H. (1996) Geoengineering with respect to stability of cavities used for disposal purposes, Kali und Steinsalz, 2, 66-76 [in German].

Lux K.H., Wermeling J. and Bannach (2003) Determination of allowable operating pressures for a gas storage cavern located close to a tectonic fault. Proc. SMRI Fall Meeting, Berlin.

Lux K.H., Düsterloh U. and Wolters R. (2006) Long-term Behaviour of Sealed Brine-filled Cavities in Rock Salt Mass – A new Approach for Physical Modelling and Numerical Simulation. Proc. SMRI Fall Meeting, 1-4 October, Rapid City, South Dakota.

Malinsky L. (2001) Evaluation of Salt Permeability Tests, SMRI Project No. 01-0004, prepared by G3S, Ecole Polytechnique, Palaiseau, France, for the Solution Mining Research Institute.

Manivannan S. and Bérest P. (2019) Transient closure of a cylindrical hole in a salt formation considered as a Norton-Hoff medium. Rock Mech. Rock Eng. https://doi.org/10.1007/s00603-018-1732-6

McCauley T.V., Ratigan J.L., Sydansk R.D. and Wilson S.D. (1998) Characterization of the Brine Loss Zone and Development of a Polymer Gel Plugging Agent to Repair Louisiana Offshore Oil Port (LOOP) Cavern 14. Proc. SMRI Fall Meeting, Roma, Italy.

McLeod R., Cooke D. and Slingsby J. (2011) The Repair of a Gas Storage Cavern Well after Failure of a Pre-operational Mechanical Integrity Test. In: Proceedings SMRI Fall Meeting, York, UK, 289-312.

Minkley W., Knauth M. and Wüste U. (2012) Integrity of salinar barriers under consideration of discontinuum-mechanical aspects. Mechanical Behavior of Salt VII, Paris, France, 16-19 April 2012, 469 – 478. Taylor & Francis Group, Lon-don, ISBN 978-0-415-62122-9.

Minkley W., Knauth M., Fabig T. and Farag N. (2015) Stability and integrity of salt caverns under consideration of hydro-mechanical loading. Minkley W., Knauth M., Fabig T., Farag N. DOI: 10.1201/b18393-29

Minkley W., Brückner D. and Lüdeling C. (2018a) Percolation in Salt Rocks. Paper 18652. WM2018 Conference, March 18 – 22, 2018, Phoenix, Arizona, USA.

Minkley W., Brückner D. and Lüdeling C. (2018b) Percolation in Salt Rocks. Proc. The Mechanical Behavior of Salt IX, September 12-14 2018, Hannover, Germany, 29-48.

Mullaly M.A.C. (1982) Underground storage in thin salt layers on Teesside. Proc. SMRI Fall Meeting, Manchester UK.

Nemat-Nasser S., Keer L.M. and Panhar K.S (1978) Unstable growth of thermally induced interacting cracks in brittle solids. Int. J. Solids Struct. 14: 409-430.

Nicot JP. (2009) A survey of oil and gas wells in the Texas Gulf Coast, U.S.A., and implications for geological sequestration of CO2. Environ Geol., 57:1625-1638.

Pellizzaro C., Bergeret G., Leadbetter A. and Charnavel Y. (2011) Thermomechanical behavior of Stublach gas storage caverns. Proc. SMRI Fall Meeting, York, UK, 161-178.

Pereira J.C. (2012) Common Practices – Gas Cavern Site Characterization, Design, Construction, Maintenance, and Operation. SMRI Project Report RR2012-03.

Pfeifle T. W., Mellegard K. D., Skaug N. T. and Bruno M. S. (2000) An Investigation of the Integrity of Cemented Casing Seals with Application Salt Cavern Sealing and Abandonment, SMRI Project No. 00-0002, prepared by RESPEC, Rapid City, SD; and Terralog Technologies USA Inc., Arcadia, CA, for the Solution Mining Research Institute, Encinitas, CA, 118 p.

Poyer C. and Cochran M. (2003) Kansas Underground Storage Regulations. Proc. SMRI Spring Meeting, Houston, Texas, 199-204.

Quintanilha de Menezes J.E., Guerreiro V.N. and Lúcio J.M. (2001) Natural Gas Underground Storage at Carriço in Portugal. Proc. SMRI Fall Meeting, Albuquerque, New Mexico, 97-103.

Ratigan J.L., Van Sambeek L.L., DeVries K.L. and Nieland J.D. (1991) The influence of Seal Design on the Development of the Disturbed Rock Zone in the WIPP Alcove Seal Tests. Report RSI-0400, prepared by RE/SPEC Inc., Rapid City, SD, for Sandia National Laboratories, Albuquerque, NM.

Ratigan J.L. (2003) Summary Report – The Solution Mining Research Institute Cavern Sealing and Abandonment Program, 1996 Through 2002, Research Project Report No. 2002-3- SMRI, prepared by J. L. Ratigan, Solution Mining Research Institute CS&A Project Manager and Research Coordinator, for the Solution Mining Research Institute, Encinitas, CA.

Réveillère A., Bérest P., Evans DJR., Stöwer M., Bolt R., Chabannes C. and Koopmans T. (2017) Past salt caverns incidents database Part 1: blow-out, leakage and overfilling. SMRI Research Report RR2014-1.

Rokahr R., Staudtmeister K. and Zander-Schiebenhöfer D. (1998) Rock Mechanical Determination of the Maximum Internal Pressure for Gas Storage Caverns in Rock Salt. Proc. SMRI Fall Meeting, 4-7 October 1998, Roma, Italy.

Rokahr R.B., Hauck R., Staudtmeister K., Zander-Schiebenhöfer D., Crotogino F. and Rolf O. (2002) High Pressure Cavern Analysis. SMRI Research Project Report 2002-2, 314 pages.

Rokahr R.B., Staudtmeister K. and Zander-Schiebenhöfer D. (2003) High Pressure Cavern Analysis: Proceedings of the SMRI Spring Meeting, Houston, pp. 88-113.

Rokahr R.B., Hauck R., Staudtmeister K. and Zander-Schiebenhöfer D.Z. (2000). The results of the pressure Build-up test in the brine filled cavern Etzel K102: Proceeding of the SMRI Fall Meeting, San Antonio, Texas, USA, pp 89-104.

Rummel F., Benke K. and Denzau H. (1996) Hydraulic Fracturing Stress Measurements in the Krummhörn Gas Storage Field, North-western Germany. Proc. SMRI Spring Meeting, Houston.

Schmidt T. (1993) Fracture Tests for Determining Primary Stress Conditions in Salt Deposits Provide Clues to the Rock Mechanics of Salt Caverns, Proc. 7th Symp. on Salt, Vol I, Elsevier, 135-40.

Schreiner W., Japël G. and Popp T. (2004) Pneumatic fracture tests and numerical modeling for evaluation of the maximum gas pressure capacity and the effective stress conditions in the leaching horizon of storage caverns in salt diapirs. Proc. SMRI Fall Meeting, Berlin, 129-142.

Schreiner W., Lindert A. and Brückner D. (2010) IfG Cavern Design Concept. Rock mechanical aspects for the development and operation of rock salt caverns. Proc. SMRI Fall Meeting, Leipzig, Germany, 67-82.

Schulte B. and Stilson D. (2019). Plugging and abandonment of West Texas Salt Cavern Wells. Proc. SMRI Spring Meeting, New Orleans, Louisiana. p.139-154.

Schweinsburg H.J. and Schneider R. (2010) Etzel Cavern Storage – Rock Mechanical and Solution Mining aspects relating to Cavern Field Expansion. Proc. SMRI Spring Meeting, Grand Junction, Colorado, 291-302.

Sicsic P. and Bérest P. (2014) Thermal cracking following a blowout in a gas storage cavern. Int. J. Rock Mech. & Min. Sci. 71: 320-329. 10.1016/j.ijrmms.2014.07.014.

Slingsby J., Melody A. and McLeod A. (2011) The Removal of Damaged Dewatering Tubing from a High-Pressure Storage Well. Proc. SMRI Fall Meeting, York, UK, 2011.

Smit A.J., Vissert J., Fokker P. and Barth A. (2019) Sudden Pressure Drop in Nedmag Cavern Cluster. Proc. SMRI Fall Meeting, Berlin, 117-130.

SMRI (2010) Fundamentals for the Long-term abandonment of Salt Caverns. Technical Class Book, SMRI Fall Meeting, Leipzig.

Sobolik S.R. and Lord A.S. (2014) Case study of the Impact of Prior Cavern Abandonment on Long-Term Oil Storage at a Strategic Petroleum Reserve Site. 48th US Rock Mechanics/Geomechanics Symposium Minneapolis, MN, 1-4 June 2014, ARMA paper 14-7002.

Staudtmeister K. and Rokahr R.B. (1998) Pressure Build-Up Test in the Etzel K 102 Cavern, SMRI Project No. 98-0005, Institut für Unterirdisches Bauen University of Hannover, Germany, for the Solution Mining Research Institute, 176 p.

Staudtmeister K. and Schmidt T. (2000) Comparison of Different Methods for the Estimation of Primary Stresses in Rock Salt Mass with Respect to Cavern Design. Proc. 8th World Salt Symposium, Vol. I, Elsevier, 331-35.

Stormont J. C. (2001) Evaluation of Salt Permeability Tests, SMRI Project No. 01-0002, prepared by Department of Civil Engineering, University of New Mexico, Albuquerque, NM, for the Solution Mining Research Institute.

Thiel W.R. (1993) Precision Methods for Testing the Integrity of Solution Mined Underground Storage Caverns. In: Kakihana H., Hardy. R. Jr, Hoshi T., Toyokura K. eds. Proc. 7th Symp on Salt. Amsterdam: Elsevier, I:377-383.

Thoraval A., Daupley X., Lahaie F., Richard T. and Quental P. (2018) Long-term Behavior of Salt Caverns in the Matacães Solution Mining Concession in Portugal. In Situ Measurements and Numerical Modeling. In: Proc. SMRI Fall Conference, 24-25 September 2018, Belfast, Northern Ireland, UK.

Thoraval A., Lahaie F., Bérest P. and Brouard B. (2015) A generic model for predicting the behaviour of storage caverns in salt to help evaluate and prevent the risks associated with their abandonment. Int. J. Rock Mech. Min. Sci., 77:44-59.

Van Heekeren H., Bakker T., Duquesnoy T., de Ruiter V. and Mulder L. (2009) Abandonment of an extremely deep Cavern at Frisia Salt. In: Proc. SMRI Fall Meeting, 27-28 April 2009, Krakow, Poland.

Van Sambeek L., Bérest P. and Brouard B. (2005) Improvements in Mechanical Integrity Tests for Solution-Mined Caverns Used for Mineral Production or Liquid-Product Storage. Report for The Solution Mining Research Institute, Topical Report RSI-1799, 142 pages.

Wang L., Bérest P. and Brouard B. (2015) Mechanical Behavior of Salt Caverns: Closed-Form Solutions vs Numerical Computations. Rock Mechanics and Rock Engineering. Vol. 48, (6), 2369-2382.

Wang T., Yang C., Chen J. and Daemen J.J.K. (2018) Geomechanical investigation of roof failure of China's first gas storage salt cavern Engineering Geology Volume 243, 4 September 2018, 59-69 https://doi.org/10.1016/j.enggeo.2018.06.013.

Wagler T. and Draijer A. (2013) Nitrogen buffer for large scale conditioning of H- to L-Gas. How to fit an existing cavern to capacity and performance requirements? Proc. SMRI Fall Meeting, Avignon, France, 164-174.

Wallner M. (1986) Frac-pressure risk in rock salt. SMRI Fall Meeting, Amsterdam, 21-24 September 1986.

Wallner M. (1988) Frac-pressure risk for cavities in rock salt. H. Reginald Hardy, Jr. & Michael Langer (Eds.), Proc. 2nd Conf. Mech. Beh. of Salt, 645-658. Clausthal-Zellerfeld: Trans Tech Pub.

Wallner M. and Paar W.A. (1997) Risk of progressive pressure build up in a sealed cavity. Proc. SMRI Fall Meeting, El Paso, Texas, 177-188.

Wallner M. and Eickemeier R. (2001) Subsidence and fractures caused by thermo-mechanical effects. In Proc. SMRI Spring Meeting, Orlando, Florida, 363-371.

Warren J.K. (2006) Evaporites: Sediments, Resources and Hydrocarbons, Springer-Verlag Berlin Heidelberg, Chapter 12, p.935.

Wawersik W. and Stone C.M. (1989) A characterization of pressure records in inelastic rock demonstrated by hydraulic fracturing measurements in salt. Int. J. Rock Mech. Min. Sci,1989, 613-627.

Wolters R., Lux K.H. and Düsterloh U. (2012) Evaluation of rock salt barriers with respect to tightness: Influence of thermomechanical damage, fluid infiltration and sealing/healing. In: Proc. Mechanical Behavior of Salt VII, Taylor & Francis Group, London, 425-434.

Yang H., Guo K. and Li J. (2015) Analysis on long-term operation and interval optimization of pressure for single cavity injection/production in underground salt cavern gas storage – Taking the cavity of Well Xi-2 in salt cavern gas storage in Jintan as an example. Oil & Gas Storage and Transportation,34(9): 945-950.

You Th., Maisons C. and Valette M. (1994) Experimental Procedure for the Closure of the Brine Production Caverns on the “Saline de Vauvert” Site. SMRI Fall Meeting, Hannover, Germany.

Zander-Schiebenhöfer D. (2002) High Pressure Cavern Analysis, SMRI Project No. 02-0002, prepared by Institut für Unterirdisches Bauen (IUB), Hannover University, Germany, and Kavernen Bau und Betriebs GmbH, Hannover, Germany, for the Solution Mining Research Institute.

Zhao Y., Ma J., Zheng Y., Wang Z. and Zhang H. (2013) Determination of operation pressure limit for injection-production cycle of salt-cavern gas storage in Huai’an City. Oil & Gas Storage and Transportation. 2013, 32(5):526-531.

LIST OF FIGURES

LIST OF TABLES